THE UNIVERSITY OF CHICAGO

REGULATION OF HIPPO SIGNALING VIA PROTEOLYTIC DEGRADATION AND ACTOMYOSIN DYNAMICS

A DISSERTATION SUBMITTED TO
THE FACULTY OF THE DIVISION OF THE BIOLOGICAL SCIENCES
AND THE PRITZKER SCHOOL OF MEDICINE
IN CANDIDACY FOR THE DEGREE OF
DOCTOR OF PHILOSOPHY

COMMITTEE ON DEVELOPMENT, REGENERATION, AND STEM CELL BIOLOGY

BY

SHERZOD A. TOKAMOV

CHICAGO, ILLINOIS

DECEMBER 2022

Copyright © 2022 by Sherzod A. Tokamov

All Rights Reserved

TABLE OF CONTENTS

LIST OF FIGURES……v

LIST OF TABLES……..viii

ACKNOWLEDGEMENTS……ix

STATEMENT OF CONTRIBUTIONS……...x

ABSTRACT……...xi

CHAPTER 1: Introduction……...1

1.1 Overview……....1

1.2 The robustness of organ growth control……1

1.3 Signaling pathways regulating tissue growth and patterning……..4

1.4 The Hippo pathway……..12

1.5 Regulation of Hippo signaling via ubiquitin-mediated proteolytic degradation……...22

1.6 Non-transcriptional roles of the Hippo pathway components……..28

1.7 Polarity and Hippo signaling……38

1.8 Regulation of the Hippo pathway by the cortical cytoskeleton and mechanical forces……..…42

1.9 Concluding remarks and dissertation outline……51

CHAPTER 2: Negative feedback couples Hippo pathway activation with Kibra degradation independently of Yorkie-mediated transcription……53

2.1 Introduction……..53

2.2 Results.……56

2.3 Discussion……91

2.4 Methods……95

CHAPTER 3: Tension regulates Kibra abundance via Par-1……...108

3.1 Introduction……108

3.2 Results……111

3.3 Discussion……..138

3.4 Methods……..141

CHAPTER 4: Kibra organization at the apical cortex is regulated via actomyosin dynamics.……146

4.1 Introduction……146

4.2 Results……149

4.3 Discussion……..169

4.4 Methods……..171

CHAPTER 5: Discussion: conclusions and future questions……..174

APPENDIX A: Apical polarity network tethers Kibra at the junctional cortex……185

APPENDIX B: Kibra accumulates in the Z-disc in the larval body wall muscle……200

APPENDIX C: Kibra and myosin dynamics in the *Drosophila* mesoderm invagination...206

REFERENCES……...211

LIST OF FIGURES

Figure 1.1 Autonomous organ growth requires communication between tissue size and growth rate……2

Figure 1.2 The activity of major signaling pathway involved in wing imaginal growth and patterning is concentrated at the center of the tissue……...6

Figure 1.3 A simplified schematic of the mechanical feedback model…….11

Figure 1.4 A simplified schematic of the core kinase cassette of the Hippo pathway and some of its regulators……...16

Figure 1.5 A simplified diagram of the regulation and function of the budding yeast core Hippo pathway components……..31

Figure 1.6 Hippo signaling in the neuroblast asymmetric cell division……35

Figure 1.7 A simplified schematic of epithelial polarity regulators……..39

Figure 1.8 A simplified cartoon illustrating the regulation of Yki/YAP/TAZ activity by mechanical forces and cytoskeletal components……...44

Figure 1.9 Hippo signaling as a mediator of mechanical feedback and tissue growth……..49

Figure 2.1 Transcriptional feedback alone does not explain Kib upregulation in *Mer* clones.....57

Figure 2.2 Ubi>Kib-GFP is a functional protein……...60

Figure 2.3 The Hippo pathway regulates Kib levels independently from Yki-mediated transcription……...62

Figure 2.4 The Hippo pathway regulates Kib levels independently from Yki-mediated transcription……...63

Figure 2.5 Effect of different E3 ubiquitin ligases on Kib levels……..67

Figure 2.6 Slimb regulates Kib abundance via a consensus degron…….....70

Figure 2.7 The Hippo pathway regulates Kib abundance via a putative degron motif…….73

Figure 2.8 Kib abundance is regulated independently of Expanded or other upstream Hippo components……77

Figure 2.9 Truncation analysis to identify Kib domains responsible for pathway mediated degradation…….80

Figure 2.10 The WW domains of Kib are required for Hippo pathway- and Slimb-mediated degradation…….83

Figure 2.11 Kib degradation is patterned by mechanical tension in the wing pouch to control proportional growth……...87

Figure 3.1 RhoGEF2 overexpression promotes Kib degradation……112

Figure 3.2 myr-Yki overexpression promotes Kib degradation……..115

Figure 3.3 Changes in osmotic conditions affect myosin activity and junctional tension……...117

Figure 3.4 Effect of osmotic shifts on nuclear Yki localization……..120

Figure 3.5 Osmotic changes alter Kib abundance……...123

Figure 3.6 Treatment with Y-27632 raises Kib abundance and reverses the effect of hypotonic shift……..124

Figure 3.7 aPKC inhibition does not affect Kib levels……126

Figure 3.8 Tension-mediated Kib degradation is independent of Jub-Wts mechanism……..128

Figure 3.9 Par-1 regulates Kib abundance independently of Hpo phosphorylation……130

Figure 3.10 Tension promotes Par-1 association with the cell cortex…….132

Figure 3.11 Par-1 levels are downregulated in *bantam* colones……..134

Figure 3.12 Par-1 regulates Kib abundance in tension dependent manner……..136

Figure 4.1 Kib decorates apical F-actin network…….150

Figure 4.2 Kib is associated with actomyosin dynamics……151

Figure 4.3 Osmotic shifts modulate junctional-apicomedial actomyosin organization……...153

Figure 4.4 Osmotic changes modulate Kib localization……..156

Figure 4.5 The effect of osmotic shifts on Kib localization is specific……...158

Figure 4.6 Treatment with Jasp acutely stabilizes F-actin……...159

Figure 4.7 Kib apicomedial localization is dependent of F-actin dynamics……161

Figure 4.8 Kib apicomedial localization is dependent of myosin dynamics……...163

Figure 4.9 Mer and Hpo are recruited to Kib punctae via actomyosin dynamics……...167

Figure 5.1 Ectopic Wts expression promotes medial Kib recruitment and Hippo complex formation without promoting Kib degradation……176

Figure 5.2 Deletion of the first 483 amino acids of Kib prevents the formation of Kib assemblies at the apicomedial cortex……180

Figure A.1 Loss of Crb leads to the loss of Kib at the junctional cortex without significantly affecting Kib abundance……..……186

Figure A.2 Loss of Crb disrupts junctional actomyosin organization……188

Figure A.3 Crb is necessary to tether Kib at the junctional cortex……..189

Figure A.4 Crb does not regulate Kib localization via Patj, Sdt, Ex, Yurt, or Moe……191

Figure A.5 aPKC tethers Kib at the junctional cortex……192

Figure A.6 Kib forms an apical crescent in mitotic Drosophila larval neuroblasts…….196

Figure B.1 Kib is associated with the Z-disc in the Drosophila larval sarcomere……...201

Figure B.2 Loss of the capping protein A or alpha-actinin has no detectible effect on Kib abundance or localization……203

Figure C.1 Kib dynamics in the Drosophila ventral furrow correlate with myosin……207

LIST OF TABLES

Table 2.1 Reagents…….....96

Table 2.2 List of primers……..107

Table 3.1 Reagents……...141

Table 4.1 Reagents……...171

Table A.1 Reagents...……...197

Table B.1 Reagents...……...204

Table C.1 Reagents...……...209

ACKNOWLEDGEMENTS

I would like to thank my advisor, Rick Fehon, for being a terrific mentor and colleague. Throughout my time in the lab, Rick has been both the most challenging critic and the strongest advocate of my research. Through his ability to carefully maintain this balance, Rick has always motivated me to do rigorous and interesting science. I will always cherish our one-on-one weekly meetings and Saturday chats, which were often productive and, at times, therapeutic. Rick's patience, remarkably positive outlook, and ability to draw lessons from seemingly uninteresting results has taught me to approach science as a journey rather than a job.

I also want to thank the former and current Fehon lab members Jiajie, Will, Ting, Hitoshi, Stephan, Annie U., Arden, Niranjan, Nicki, Annie G., and KathyAnn; the 9th floor, especially Ashley (Glotzer lab), Audrey and Allison (Horne-Badovinac lab); the Munro lab; my thesis committee members Sally, Ed, and Michael for their guidance. I also want to thank the NSF-REU organizers, and especially Ilaria Rebay. The REU experience in Ilaria's lab and Ilaria's continued support after the REU made me choose UChicago for my PhD.

I want to thank my undergraduate mentor William Sanders, who has been the dearest friend throughout my undergraduate and graduate years and helped me grow academically and personally. I am fortunate to have a met him and have his continued support to this day.

Finally, I thank my family. I am very grateful to my mother, who cared for my baby daughter, Valentina, for a year while I was collecting data for Chapter 2. I thank my big brother, Anvar, who I can always rely on. My stepdaughter, Anabela, who makes parenting easy by being a responsible and hard-working child. My daughter, Valentina, for making me more efficient at everything I do. And, most importantly, my wife, Paquita, for her infinite love, support, and faith in me. I would not be where I am now without her in my life.

STATEMENT OF CONTRIBUTIONS

Although most of the work described in this dissertation is my own, several people deserve credit for their contributions. Dr. Ting Su made the initial observations of the changes in Kib abundance under the loss of Hippo pathway components and Slimb. Dr. Su also generated plasmids carrying Kib truncations under UASt promoter, which I later cloned into Ubi promoter plasmids and generated transgenes for the work in Chapter 2. Annie Ullyot performed the ubiquitination assays. Annie Ullyot also performed an F-box protein RNAi screen; only the results of SCF component knockdown are shown from this screen in Chapter 2. Stephan Buiter helped generate Ubi>Kib-GFP-Flag on 86Fb and UASp-Kib-GFP-Flag transgenes. Arden Feil made Ubi>Kib-Halo and Ubi>Mer-Halo transgenes. The laser ablation experiments in Chapter 3 were done in the lab of Dr. Rodrigo Fernandez-Gonzalez at the University of Toronto. A graduate student in the Fernandez-Gonzalez lab, Gordana Scepanovic, trained me on the microscope and helped with the data analysis. Audrey Williams from Dr. Sally Horne-Badovinac's lab performed the segmentation, tracking, and area measurements of cells under osmotic shifts shown in Chapter 3. To track cells, Audrey used a tracking algorithm that she co-wrote with Dr. Seth Donoughe. The larval fillet and muscle staining was done with the help of Meike Lobb-Rabe in Dr. Robert Carillo's lab. The rest of the work was done by me under the guidance and supervision of Dr. Richard Fehon.

ABSTRACT

The Hippo pathway is an evolutionarily conserved regulator of tissue growth. At the core of the Hippo pathway, a kinase cascade represses the activity of a transcriptional effector, an oncoprotein called Yorkie. Multiple upstream inputs synergistically promote the activity of the kinase cascade from the apical cortex of polarized epithelial cells. How these upstream components organized and regulated at the cell cortex is poorly understood. One of the key upstream components, Kibra, localizes at the junctional and apicomedial cortex. In the absence of a conventional receptor/ligand pair, it remains unknown what controls the organization of Kibra, how its activity is regulated, and whether Kib-mediated signaling is modulated by any stimuli.

In this dissertation, I investigate the upstream components of the Hippo pathway, focusing on the regulation and organization of Kibra. I will first demonstrate that ubiquitin-mediated degradation is a major mechanism that regulates Kibra-mediated Hippo signaling. Specifically, upon Hippo complex assembly, Kibra is ubiquitinated via the SCF^{Slimb} E3 ubiquitin ligase machinery and subsequently degraded. Next, I will show that actomyosin generated tension promotes Kibra degradation. Mechanistically, tension promotes cortical association of the Ser/Thr kinase Par-1, and Par-1 promotes Kibra degradation. Finally, I examine the subcellular association of Kibra with the actomyosin network. I find that Kibra organization at the cell cortex is modulated by actomyosin dynamics, whereby apicomedial actomyosin flows promote medial Kibra accumulation and Hippo signaling activity. Additionally, I provide evidence that Kibra is tethered via the apical polarity network at the junctional cortex.

Collectively, these findings expand our understanding of upstream Hippo signaling organization and regulation and how actomyosin dynamics can modulate these processes.

CHAPTER 1

Introduction

1.1 Overview

How organs "know" when they reach their optimal size is a fundamental question in developmental biology. Although this question has been studied experimentally for over a century, we still lack a mechanistic understanding of how this process works. The discovery of the Hippo pathway, a key signaling pathway that regulates tissue growth, has led to numerous studies to tackle the molecular underpinnings of tissue growth control. In this introductory chapter, I will provide a brief overview of the key findings that have guided our thinking about the biology of organ growth control, up to the discovery of the Hippo pathway and the emergence of mechanical forces as a major contributor in this process. I will review the composition, organization, and regulation of the Hippo pathway and its components, mostly focusing on the work in *Drosophila*, where the pathway was discovered and characterized, but also including key studies in mammalian systems.

1.2 The robustness of organ growth control

Despite the vast diversity of species, all animals develop with organs that are proportional to their body size. Although taken for granted and unsurprising on the surface, the consistency in organ growth poses interesting biological questions that have captivated human minds for centuries. How do organs "know" what their final size should be? Can organs sense the size of the body that they occupy and scale to the right proportions? Experimentally, these questions were first approached by Harrison (1924) and later by Twitty and Schwind (1931) who performed heteroplastic transplantations of limb buds between closely related Ambystoma

Figure 1.1: Autonomous organ growth requires communication between tissue size and growth rate.

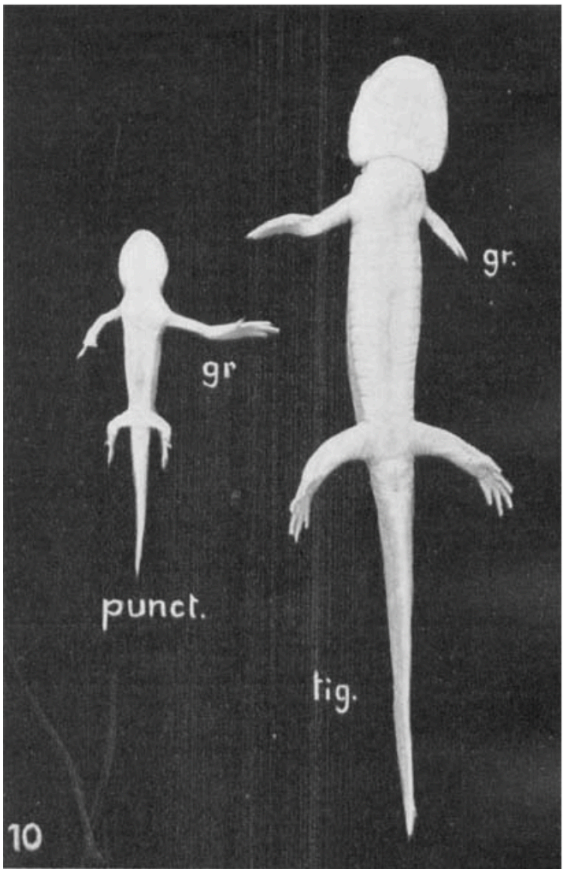

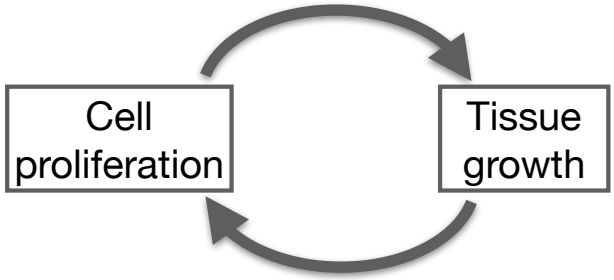

Reproduced with permission from Twitty & Schwind (1931). Copyright © 1931 John Wiley and Sons.

Left: A photograph from the classic study by Twitty & Schwind (1931) showing that when limb buds are exchanged between the species of salamanders that differ greatly in size as adults, the transplanted limbs grow to the size of the original donor.

Right: The autonomous nature of organ growth suggests that while tissue growth depends on cell proliferation, cell proliferation must also adjust with respect to tissue size.

salamander species, *A. punctatum* and *A. tigrinum*, that grow to drastically different sizes as adults. These authors asked a simple question: if limb buds between the salamanders were exchanged, would the transplanted limbs grow to the size of the new host or the original donor? The results from Twitty and Schwind, who adapted a maximum feeding strategy to eliminate nutrition-related growth inconsistencies encountered by Harrison, showed that the transplanted limbs grow to the size of the original donor irrespective of the size of the new host (Fig. 1.1). Thus, the smaller *A. punctatum* salamander developed with the large limb from *A. tigrinum*, and vice versa. Twitty and Schwind also observed similar results from eye transplantation experiments between *A. punctatum* and *A. tigrinum*. These results provided the first evidence of organ-intrinsic regulation of growth.

Since the publication of the work by Twitty and Schwind, the autonomy of organ growth control has been observed in other animals. Some examples include mouse thymus transplantation studies, where over twenty thymus grafts transplanted into thymectomised mouse hosts grew to their normal size (Metcalf, 1963), and the *Drosophila* larval wing imaginal discs, which reach their normal size when cultured in the abdomen of an adult female fly for up to two weeks (Bryant and Levinson, 1985). It should be noted that not all organs employ organ-intrinsic mechanisms in growth control. For example, when multiple spleen grafts are transplanted into a splenectomized mouse host, each transplanted spleen develops smaller but collectively they attain a final combined mass equivalent to a single normal spleen (Metcalf, 1964), indicating that spleen growth is regulated by extrinsic factors (e.g. by feedback from hormones produced by each spleen). Regardless of the mechanisms employed, collectively these studies demonstrate that organ growth regulation is remarkably robust and raise the question of how such precision is achieved at the molecular level.

In this introduction, I will focus mainly on organ-intrinsic growth control, drawing largely from studies in *Drosophila* from which most of our mechanistic understanding of this process has come. In particular, the *Drosophila* wing imaginal disc, a precursor for the adult wing, has been most widely used to study tissue growth control for several reasons. First, the wing disc undergoes exponential growth during four days of larval development, starting from a primordium of ~50 cells in the embryo and growing into a tissue of ~50,000 cells at the end of larval development (Bryant and Levinson, 1985). Second, the growth of the wing imaginal disc is largely completed at the onset of pupariation, at which point the tissue begins to undergo a series of dramatic morphogenetic events to produce an adult wing. Thus, any perturbations of growth-controlling components in the larval stages will affect the final size of the adult wing. Third, the availability of the powerful genetic toolkit in *Drosophila*, in particular the use of somatic mosaic genetics, has allowed for rigorous genetic manipulations of growth control genes that would be embryonic lethal in a mutant organism. Finally, because many *Drosophila* genes involved in tissue growth are strongly conserved in vertebrates, studies in *Drosophila* have been highly informative for parallel studies in vertebrate systems, including mammals.

1.3 Signaling pathways regulating tissue growth and patterning

The studies described above revealed that developing organs are endowed with the information necessary for proper growth and patterning. Intuitively, tissue size must depend on the growth and/or proliferation of individual cells. However, the autonomous nature of organ growth suggests that cell growth and proliferation is also dependent on tissue size (Fig. 1.1). Although our understanding of how growth rate is adjusted with tissue size is still in its early stages, studies over the past several decades have uncovered several key signaling pathways involved in

growth regulation, providing the framework for tissue-intrinsic control of growth. Additionally, physical forces, such as actomyosin-generated tension within cells, have gained attention as a potential point of communication between tissue size and cell proliferation.

Morphogens and signaling pathways that regulate tissue patterning and growth

Our initial molecular understanding of tissue growth control came from the discovery of morphogens and their role in both tissue patterning and promoting cell proliferation (Schwank and Basler, 2010). The *Drosophila* wing imaginal epithelium has been most widely used as a system to study tissue growth control due to the availability of powerful genetic tools and the fact that the wing disc is patterned by multiple evolutionarily conserved signaling pathways, including Decapentaplegic (Dpp, a BMP2 homolog), Wingless (Wg, a Wnt homolog), Hedgehog (Hh, a Shh homolog), and Notch. These signaling pathways exert their activity in narrow stripes of cells that run across the center of the wing blade-forming portion of the wing imaginal disc, called the disc proper or disc pouch (Fig1.2). For example, Dpp expressing cells are positioned immediately anterior of the anterior-posterior (A-P) boundary (Affolter and Basler, 2007), while the Wg stripe lines the dorsal-ventral (D-V) boundary (Swarup and Verheyen, 2012). Both Dpp and Wg diffuse from the source in a gradient toward tissue periphery. In the case of Dpp, the transmembrane receptors Thickvein (Tkv), Saxaphone (Sax), and Punt (Put) transduce the signal to the transcriptional effector Mad in the receiving cells (Ruberte et al., 1995; Wiersdorff et al., 1996). Wg, on the other hand, mediates its signaling via a transmembrane protein Frizzled (Fz) and a transcriptional co-factor Armadillo (Arm), a β-catenin homolog (Swarup and Verheyen, 2012). Similarly, while Hh is produced in the entire posterior compartment of the wing disc, it diffuses anteriorly and is received in a narrow stripe just anterior of the A-P boundary, where the

Figure 1.2: The activity of major signaling pathway involved in wing imaginal growth and patterning is concentrated at the center of the tissue.

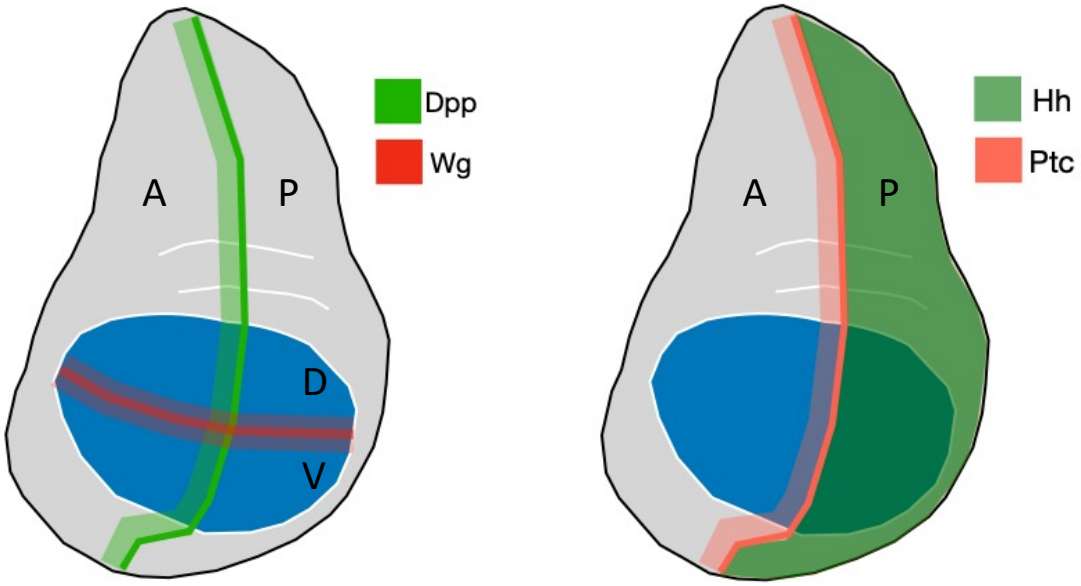

Left: Wg and Dpp morphogens are expressed in narrow stripes along the anterior-posterior (A-P) boundary (Dpp) or dorso-ventral (D-V) boundary (Wg).

Right: Hh ligand is expressed in the entire posterior compartment of the wing imaginal disc, but as it diffuses anteriorly, it is received by its receptor Ptc in a narrow region just anterior of the A-P boundary.

Hh receptor, Patched (Ptc), is highly enriched (Basler, 1994; Tabata and Kornberg, 1994; Ingham, 1998). Binding of Hh to Ptc leads to Ptc inhibition and derepression of another transmembrane protein Smoothened (Smo), which in turn activates the downstream transcription factor Ci (Ingham, 1998). Finally, Notch is a transmembrane receptor that is activated in a narrow stripe along the D-V boundary by its ligands Delta and Serrate. Notch signaling is critical for D-V patterning of the wing imaginal tissue and is also important for inducing expression of Wg and a wing identity selector gene *vestigial* (Vg, Fehon et al., 1990; Rebay et al., 1991; Lai, 2004).

All of the signaling pathway listed above have been implicated in the control of cell survival and/or proliferation. For example, although high Wg signaling leads to growth suppression, mild Wg signaling can promote cell proliferation in a gradient-independent manner, and loss of Wg leads to cell death (Giraldez and Cohen, 2003; Baena-Lopez et al., 2009; Alexandre et al., 2014). Notch signaling has also been shown to promote cell proliferation, though it seems to do so via both cell-autonomous and non-autonomous mechanisms (Go et al., 1998; Baonza and Garcia-Bellido, 2000; Giraldez and Cohen, 2003; Baonza and Freeman, 2005). The cell-autonomous mechanism involves the regulation of E2F1 and Cyclin A expression (Baonza and Freeman, 2005), whereas the non-autonomous mechanism relies, at least partly, on the induction of Wg expression (Giraldez and Cohen, 2003). Similarly, Hh signaling was shown to regulate growth by promoting the expression of Cyclin E and Cyclin D, both of which inhibit RBF, thereby relieving the inhibition of the growth promoting transcription factor E2F1 (Duman-Scheel et al., 2002). However, while loss of E2F1 or overexpression of RBF blocks cell proliferation, wing imaginal discs still reach their normal size due to increased cell growth

(Neufeld et al., 1998), suggesting that regulation of cell cycle components by Notch and Hh signaling is unlikely to contribute to final tissue size.

Most studies to date have focused on the morphogen Dpp as a key regulator of cell proliferation and tissue size. Loss of Dpp leads to dramatic tissue undergrowth, while ectopic Dpp expression results in increased cell proliferation and tissue overgrowth (Affolter and Basler, 2007; Vollmer et al., 2017). Interestingly, the function of Dpp in promoting cell proliferation depends solely on the inhibition of a transcriptional repressor Brinker (Brk), which is mostly expressed in the lateral cells of the wing imaginal disc where Dpp levels are low (Schwank et al., 2008). Indeed, loss of Brk leads to similar overgrowth phenotype as gain of Dpp, and while loss of Dpp results in severe tissue undergrowth, this effect is suppressed by the loss of Brk (Schwank et al., 2008; Barrio and Milán, 2017). Thus, wings lacking both Brk and Dpp can grow almost to their normal size, albeit with severe patterning defects (Barrio and Milán, 2017). These observations argue that Dpp has a permissive rather than instructive role in promoting cell proliferation and determining final tissue size (Vollmer et al., 2017).

The enrichment of the growth promoting morphogens, such as Dpp and Wg, in the medial region of the wing disc suggests that more growth should occur at the center of the tissue than the periphery, where morphogen concentration is relatively low. However, it was shown that cell proliferation occurs uniformly across the wing disc (Milán et al., 1996). How can non-uniform morphogen distribution generate uniform growth? Several models have been proposed to resolve this paradox (reviewed in Hariharan, 2015; Vollmer et al., 2017). Here, I will briefly discuss one of these models – the mechanical feedback model – which has gained significant experimental support in the past several years and is relevant to the rest of my thesis work.

The mechanical feedback model of tissue growth

The paradox of how uniform growth is achieved with non-uniform morphogen distribution has led to a hypothesis that physical forces could modulate growth to balance the heterogeneous morphogen concentration. The initial model postulated that if a somatic mosaic clone of fast-growing cells was generated in a tissue of slower dividing cells, the faster-growing clone would experience compressive forces which will counteract cell proliferation (Shraiman, 2005). This model was later extended to the wing imaginal disc, where the authors proposed that because the peripheral cells divide more slowly due to the lack of morphogens, this will result in increased pressure in the central portion of the wing disc, leading to the overall growth arrest in the mature wing imaginal tissue (Hufnagel et al., 2007). However, the underlying assumption in this model was that the length scale of the Dpp gradient remains constant throughout tissue growth, which was challenged by studies showing that the Dpp gradient scales with tissue size (Wartlick et al., 2011; Romanova-Michaelides et al., 2022).

Alternative models have been proposed to account for the scaling of Dpp gradient and incorporate a second growth factor akin to Wg morphogen (Aegerter-Wilmsen et al., 2007, 2012). These models incorporated the original assumption that at early stages of development, morphogens will stimulate more growth at the center of the tissue than the periphery, but also assumed that this heterogeneity in growth would cause cells in the center of the tissue to push against and induce stretching of the peripheral cells. Conversely, the stretching at the periphery would induce compression at the center (Fig. 1.3). As a result, stretching could promote growth at the periphery to compensate for lower morphogen concentration, while compression in the center could counteract the growth induced by morphogens. This model explains not only how mechanical feedback can generate uniform growth with non-uniform morphogen distribution,

but also how tissue growth ultimately ceases: lack of growth in the center would eventually relieve the stretching at the periphery, thereby leading to growth arrest across the tissue.

Several studies have found experimental support for the mechanical feedback model. Analysis of growth in the wing imaginal disc across different developmental stages revealed that cell proliferation indeed occurs mostly in the center at early stages, and becomes uniform across the wing disc as the tissue grows (Mao et al., 2013). Additionally, measurements of junctional forces using laser ablation experiments demonstrated that cells at the periphery of the third instar wing imaginal disc experience significantly higher tension than cells in the center (LeGoff et al., 2013; Mao et al., 2013). Together, these studies supported the hypothesis that heterogeneous growth could lead to mechanical heterogeneity across a tissue in normal development.

When the mechanical feedback model was proposed, the idea that physical forces could promote cell proliferation was largely an assumption. However, studies investigating the relationship between mechanical inputs and growth were beginning to emerge. For example, mammary epithelial cell acini were shown to grow proportionally to the ECM matrix stiffness (Paszek et al., 2005). Additionally, molecular studies of contact inhibition of growth began to uncover cytoskeletal components critical for growth inhibition induced by cell-cell adhesion (Okada et al., 2005; Zhao et al., 2007), suggesting a potential mechanism by which compressive forces generated by cell crowding could suppress growth. Ultimately, the discovery of the Hippo pathway as a major regulator of cell proliferation and growth and its sensitivity to mechanical stimuli has paved the way for more mechanistic studies of how physical forces modulate growth in *Drosophila* and vertebrate systems. In the rest of this chapter, I will provide an overview of the Hippo pathway and its main regulators, ending with how mechanical stimuli regulate Hippo signaling.

Figure 1.3: A simplified schematic of the mechanical feedback model.

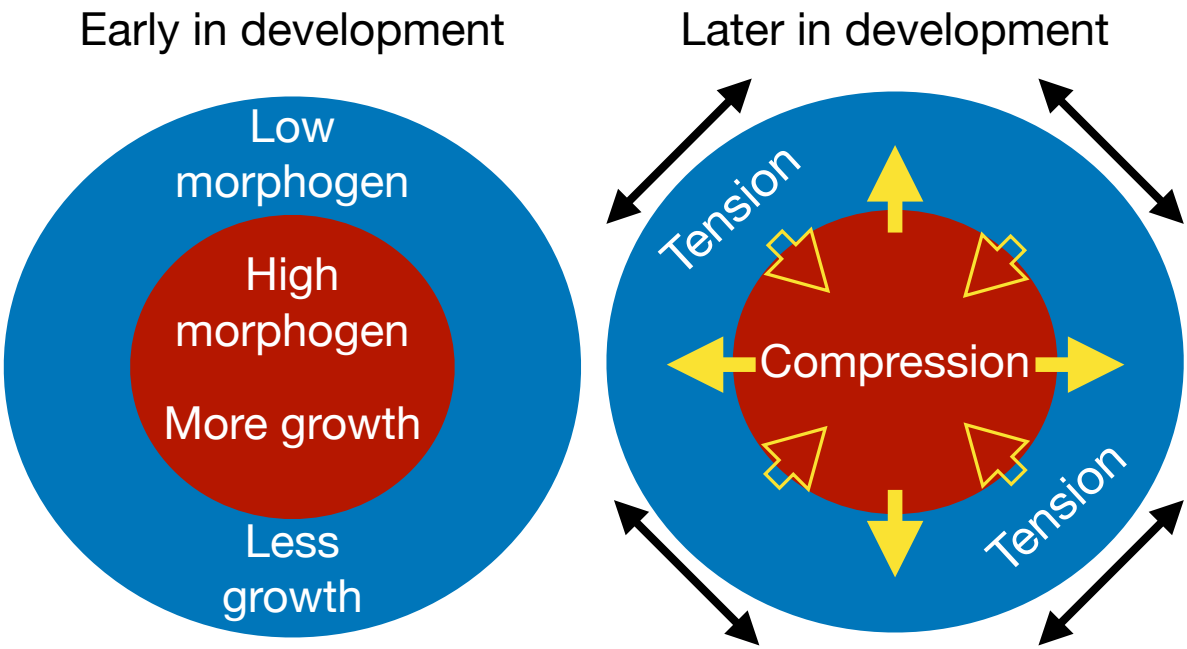

Adapted from Aegerter-Wilmsen et al., 2007

Left: Earlier in development, more growth will occur in the center of the wing imaginal disc due to higher morphogen concentration.

Right: As a result of the heterogeneous growth, the faster growing central region of the tissue will push against the slower growing peripheral tissue, thereby inducing stretching of the peripheral cells. In turn, the peripheral cells will induce crowding and compression of the central cells. Tension at the tissue periphery could promote growth and compensate for the lack of morphogens, whereas compression in the center of the tissue could suppress growth to counteract the effect of morphogens.

1.4 The Hippo pathway

The core components of the Hippo pathway

The Hippo pathway is a key regulator of cell proliferation and survival. Initially discovered in *Drosophila*, the Hippo pathway is now recognized as a key tissue growth regulator in vertebrates, including mammals. The components of the Hippo pathway were discovered in somatic mosaic genetic screens for tumor suppressor genes. The first identified component, a Nuclear Dbf2-Related (NDR) family kinase Warts (Wts), when mutated via somatic mosaic recombination produced rounded and severely overgrown clones (Justice et al., 1995; Xu et al., 1995). Other components, including Salvador (Sav), Hippo (Hpo), and Mob as tumor suppressor (Mats), produced similar overgrowth phenotypes and were placed upstream of Wts via epistasis analyses. Together, Sav, Mats, Hpo, and Wts form the core kinase cassette of the Hippo pathway. Hpo is a sterile-20 (Ste20) family kinase that phosphorylates and activates Wts (Harvey et al., 2003; Jia et al., 2003; Udan et al., 2003; Wu et al., 2003). Sav is a WW domain containing scaffold protein that binds Hpo and promotes Wts phosphorylation (Kango-Singh, 2002; Tapon et al., 2002; Wu et al., 2003). Mats is a mob-superfamily protein that associates with Wts and links it to Hpo-Sav complex for Wts activation (Lai et al., 2005; Wei et al., 2007).

The downstream target of the Hippo kinase cascade is a transcriptional co-factor Yorkie (Yki), which binds directly to and is phosphorylated by active Wts (Huang et al., 2005). Phosphorylation of Yki by Wts leads to the inhibition of Yki nuclear translocation and subsequent inactivation via a protein 14-3-3 (Oh and Irvine, 2008), though the exact details of Yki inactivation remain unclear (reviewed in Manning et al., 2020). Conversely, blocking the kinase cascade activity leads to the accumulation of Yki in the nucleus, where it promotes transcription of pro-growth genes, including *Death-associated inhibitor of apoptosis 1* (*Diap1*),

Cyclin E, and the oncogenic microRNA *bantam* (Tapon et al., 2002; Wu et al., 2003; Nolo et al., 2006).

As a transcriptional co-factor, Yki is unable to bind DNA by itself. Instead, it partners with other transcription factors. A key component that mediates Yki output downstream of the Hippo pathway is Scalloped (Sd), a TEAD-family protein that can function as either a transcriptional activator or repressor (Wu et al., 2008; Koontz et al., 2013). In its default capacity, Sd associates with the Tondu-domain-containing growth inhibitor (Tgi) and represses transcription of Yki target genes; Yki competes with Tgi for binding to Sd, and the Yki-Sd complex functions as a transcriptional activator (Koontz et al., 2013).

The overall organization and function of the Hippo pathway and its various regulators is remarkably conserved in evolution (Zheng and Pan, 2019). This strong conservation is illustrated by the fact that *Drosophila* Hippo pathway components, including Hpo, Mats, and Wts, can be functionally replaced by their human orthologs (Tao et al., 1999a; Wu et al., 2003; Lai et al., 2005; Gavilan et al., 2014). In the future sections, I will refer to the Hippo pathway components by their *Drosophila* designated names, but when appropriate, I will also highlight examples from mammalian literature using the following names for the mammalian counterparts of the Hippo pathway components: Mst1/2 (Hpo), Mob (Mats), LATS1/2 (Wts), YAP/TAZ (Yki), and TEAD (Sd).

Regulation of the Hippo kinase cascade

At a basic level, the activity of the Hippo kinase cascade is determined by the phosphorylation status of its core kinases, Hpo and Wts. To date, two important kinases have been found to regulate Hpo activity. The Ste20-family kinase Tao-1 was found to phosphorylate Hpo at Thr195

in the kinase activation loop, which activates Hpo, promotes Wts phosphorylation, and inhibits Yki-mediated transcription (Boggiano et al., 2011; Poon et al., 2011). In contrast, the Ser/Thr kinase Par-1 inhibits Hpo activity by phosphorylating Hpo on Ser30, which prevents Hpo-Sav complex formation and blocks Tao-1 mediated phosphorylation of Hpo on Thr195 (Huang et al., 2013). Thus, in a canonical sense, Tao-1 and Par-1 are the most upstream modulators of the Hippo kinase cascade. Interestingly, both Tao-1 and Par-1 have been implicated in the regulation of microtubule (MT) stability (Doerflinger et al., 2003; Liu et al., 2010b), suggesting a potential role for MT dynamics as an upstream stimulus regulating the Hippo pathway activity. However, the role of MTs in the Hippo pathway regulation remains an untouched territory.

Another major way by which the core kinase cascade is regulated is via Hpo dephosphorylation A combination of yeast two-hybrid, proteomic, and genome-wide RNAi screens in *Drosophila* uncovered dSTRIPAK PP2A phosphatase complex as an inhibitor of Hpo activity (Formstecher et al., 2005; Ribeiro et al., 2010; Guruharsha et al., 2011). Biochemical and genetic experiments determined that Hpo autophosphorylates its own linker region between the kinase and SARAH (Salvador-Rassf-Hippo) domains, which leads to dSTRIPAK PP2A binding to the linker and dephosphorylation of Hpo on T195 (Zheng et al., 2017).

Besides control of phosphorylation status of the core kinases, multiple other mechanisms regulate the core Hippo kinase cassette. For example, Rassf competes with Sav for direct binding to Hpo, thereby blocking Hpo activity (Polesello et al., 2006). Wts is also known to be inhibited by at least two different mechanisms. An unconventional myosin Dachs, which functions downstream of Fat (Ft)/Dachsous (Ds) signaling (discussed later in this introduction), inhibits Wts activity (Cho et al., 2006; Mao, 2006; Vrabioiu and Struhl, 2015). Additionally, a LIM domain protein Ajuba (Jub, discussed later in this introduction) can sequester and inhibit Wts at

the adherens junctions in response to tension (Rauskolb et al., 2014). With such a complex network of activators and inhibitors, the main challenge is to understand when and how the regulation of the core Hippo kinase cascade occurs during tissue growth and what external and/or internal cue govern this regulation.

Upstream regulation of the Hippo pathway: Crumbs, Expanded, Merlin, and Kibra

A unique feature of the Hippo pathway is that it is regulated by multiple upstream components that form distinct modules at the apical cortex of epithelial cells (Fig. 1.4). Among them, a FERM-domain protein Expanded (Ex) binds to the transmembrane polarity protein Crumbs (Crb) at the apical junctional cortex, where it recruits and activates the core kinase cassette (Boedigheimer et al., 1997; Hamaratoglu et al., 2006; Ling et al., 2010; Sun et al., 2015). The junctional localization and activity of Ex also depends on another transmembrane component of the Hippo pathway, an atypical cadherin Ft (Silva et al., 2006). Additionally, Ex can directly sequester and inactivate Yki at the junctional cortex (Badouel et al., 2009), though it remains unclear whether this function of Ex relies on binding to Ft or Crb or is irrespective of the binding partner.

In parallel to Ex, a WW-domain containing protein Kibra (Kib) together with its binding partner, a FERM-domain protein Merlin (Mer), assembles a signaling complex that activates the kinase cascade from the apicomedial cortex (Hamaratoglu et al., 2006; Baumgartner et al., 2010; Genevet et al., 2010; Yu et al., 2010; Su et al., 2017). Another component, a tyrosine phosphatase called Pez, is known to regulate Hippo signaling in complex with Kib, though this regulation does not require Pez phosphatase activity (Poernbacher et al., 2012).

Figure 1.4: A simplified schematic of the core kinase cassette of the Hippo pathway and some of its regulators.

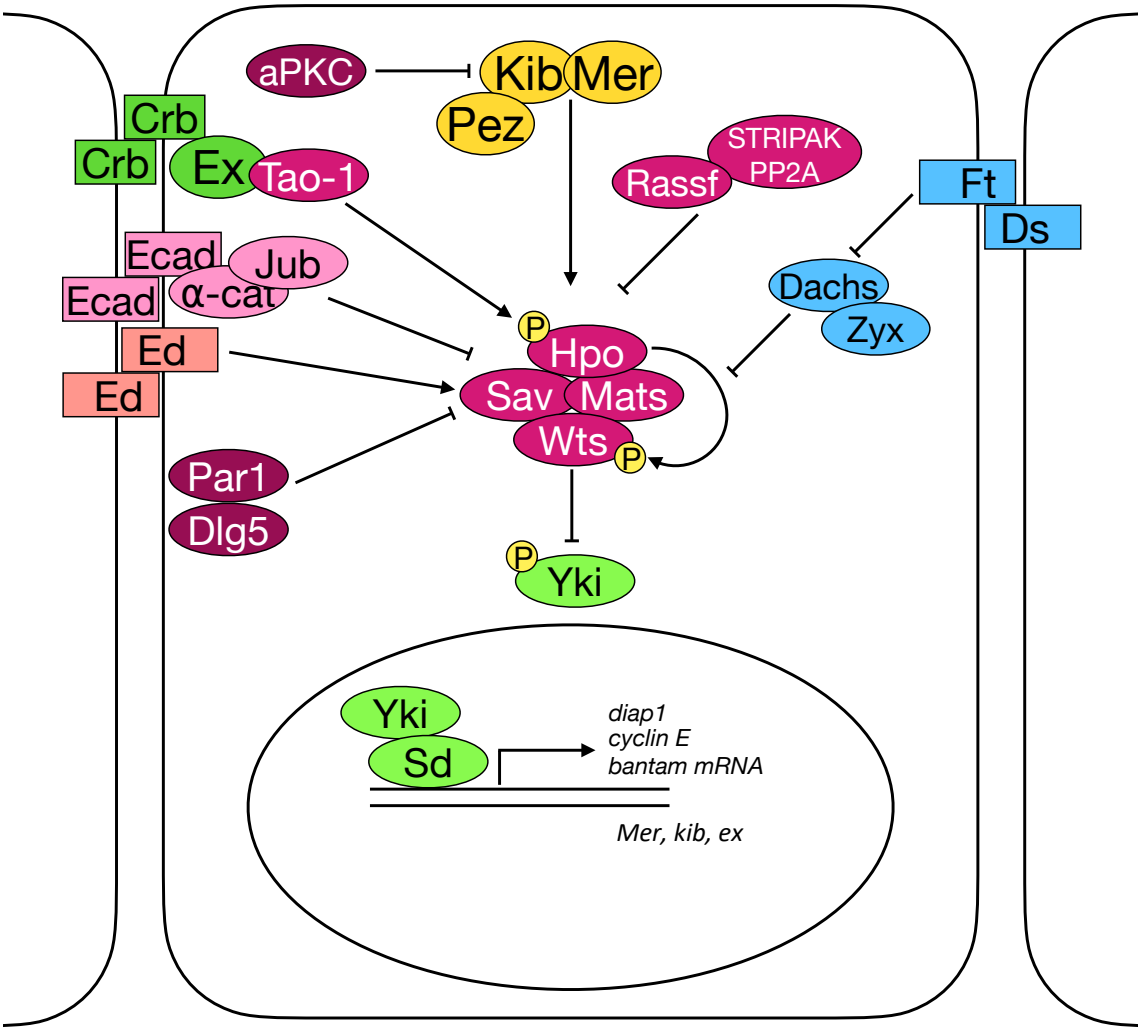

The core Hippo kinase cassette consists of Hpo and Wts kinases linked together by scaffolding proteins Sav and Mats. When active, the kinase cascade culminates in the phosphorylation of Yki and its retention in the cytoplasm. Dephosphorylated Yki is active in the nucleus where, together with its binding partner Sd, it promotes transcription of pro-growth genes. Yki also regulates the expression of its upstream inhibitors Mer, Kib, and Ex in a transcriptional negative feedback loop.

The relationship between Kib, Ex, and Mer has been one of the most confounding aspects of Hippo pathway regulation. All three components were found to localize at the junctional cortex of epithelial cells (McCartney et al., 2000; Genevet et al., 2010; Sun et al., 2015; Su et al., 2017) and were thought to function as a trimeric complex in Hippo pathway activation. Indeed, Mer interacts directly with both Ex and Kib (McCartney et al., 2000; Formstecher et al., 2005), and the WW domains of Kib are thought to bind a PPXY motif in Ex (Genevet et al., 2010). However, several results challenged the idea of a trimeric complex. First, all three components can localize at the apical cortex independently of one another (McCartney et al., 2000; Genevet et al., 2010; Su et al., 2017). Second, genetic experiments suggest that Mer, Ex, and Kib act synergistically in growth control (McCartney et al., 2000; Hamaratoglu et al., 2006; Maitra et al., 2006; Baumgartner et al., 2010; Yu et al., 2010). Third, while Ex localizes exclusively at the junctional cortex, Kib and Mer localize both at the junctional and apicomedial (medial) cortex separately from Ex (Su et al., 2017). Though its function at the junctional cortex remains unknown, Kib requires Mer to recruit Sav and Wts and activate Hippo signaling at the medial cortex, suggesting that Kib and Mer can function together. It is possible that multiple functional complexes with different combinations of these three proteins may exist, which would explain their genetic synergism.

While Ex is known to localize at the junctional cortex by binding to the intracellular region of Crb, what controls Kib and Mer localization remains unknown. Like Ex, Mer is a FERM domain protein, a family of proteins that anchor the actin cytoskeleton to the plasma membrane (Bretscher et al., 2002). Indeed, the mammalian homolog of Mer, NF2, is known to bind phosphatidylinositol 4,5-bisphosphate (PIP_2), which is thought to promote its activity (Chinthalapudi et al., 2018). In the *Drosophila* follicular epithelium, Mer fails to localize to the

apical membrane in cells lacking phosphatidylinositol 4-kinase, a kinase involved in the production of PIP_4, a precursor of PIP_2.(Yan et al., 2011). However, the role of membrane binding by Mer in the regulation of the Hippo pathway remains unknown.

Kib is a multivalent protein that can, in theory, localize to the cell membrane via multiple direct or indirect ways. For example, Kib could associate with the plasma membrane via its C2 domain, a domain that can mediate protein binding to membrane in a Ca^{2+}-dependent manner (Yu et al., 2010; Corbalan-Garcia and Gómez-Fernández, 2014). Alternatively, three coiled-coil (CC) motifs, two WW domains, or a putative PDZ-binding motif also could mediate Kib membrane recruitment. Kib can also interact with the apical polarity protein aPKC via its putative aPKC-binding domain (Yoshihama et al., 2011; Jin et al., 2015), which could mediate Kib membrane recruitment by the apical polarity network. Interestingly, to date, the only protein known to be required for Kib localization at the junctional cortex is Crb. Loss of Crb leads to the loss of Kib at the junctional cortex and more pronounced accumulation at the medial cortex (Su et al., 2017). When untethered from the junctional cortex by Crb removal, Kib becomes a more potent activator of the Hippo pathway, as seen by enhanced repression of nuclear Yki localization and tissue undergrowth (Su et al., 2017). This suggests an intriguing possibility that the apical polarity network, stabilized by Crb, could suppress Kib activity by tethering it at the junctional cortex.

An intriguing difference between the regulation of Ex and Kib by Crb is that in the absence of Crb, Ex simply becomes diffuse throughout the cytoplasm (Ling et al., 2010; Su et al., 2017). In sharp contrast, Kib does not diffuse but rather accumulates at the apicomedial domain in *crb* mutant cells (Su et al., 2017), suggesting that the junctional and medial cortex represent two distinct subcellular compartments that may compete for Kib binding and raising

several important questions about how Kib localization between the junctional and medial cortex is regulated. Are there different binding partners that recruit Kib to these distinct subcellular regions? Is Kib localization regulated via distinct posttranslational modifications? Does Kib interact with the cytoskeletal components at the medial or junctional cortex, such the actomyosin or spectrin cytoskeletons? Indeed, Mer displays partial co-localization with myosin at the apicomedial cortex (Su et al., 2017), and loss of Crb can lead to increased apicomedial actomyosin dynamics in the embryo and the developing fly wing (Flores-Benitez and Knust, 2015; Salis et al., 2017). One intriguing possibility is that while apical polarity network could tether Kib at the junctional cortex, apicomedial actomyosin dynamics could displace Kib from the junctions and promote its coalescence and activity at the medial cortex. To date, however, no study has looked at the link between apical polarity, actomyosin dynamics, and Kib localization, as well as the functional significance of this interaction.

The Fat/Dachsous module

The tumor suppressor function of Ft was known long before the discovery of the Hippo pathway (Bryant et al., 1988). In planar polarized cells, Ft and Ds occupy the opposing cell membranes and bind each other in trans, with Ds serving as a ligand for Ft. Together Ft and Ds regulate growth, planar cell polarity (PCP), and planar MT alignment (Matakatsu and Blair, 2004; Bennett and Harvey, 2006; Harumoto et al., 2010; Brittle et al., 2012). The regulation of tissue growth by Ft/Ds, however, appears to be independent of the regulation of PCP and MT organization (Harumoto et al., 2010; Matakatsu and Blair, 2012; Singh et al., 2018). At the center of Ft/Ds mediated growth control is an unconventional myosin Dachs (Mao, 2006). When Dachs localizes at the junctional cortex, it promotes growth by binding and changing Wts

conformation into an inactive state and/or by promoting Wts degradation (Cho et al., 2006; Vrabioiu and Struhl, 2015).

The activity of Dachs is strongly correlated with its cortical localization, which is inhibited by Ft and promoted by two other components, Approximated (App) and Dachs ligand with SH3s (Dlish). App is a conserved DHHC-family palmitoyltransferase that can palmitoylate Dlish, thereby promoting its membrane localization (Misra and Irvine, 2016; Zhang et al., 2016). Cortical localization of Dachs depends on Dlish, so App-mediated membrane recruitment of Dlish is thought to promote Dachs activity (Misra and Irvine, 2016; Zhang et al., 2016). App can also promote Dachs activity via palmitoylation of the Ft intracellular domain (ICD), which inhibits Ft activity (Matakatsu et al., 2017). Discs-overgrown (Dco), the *Drosophila* Casein kinase I ε, phosphorylates the Ft ICD near the inhibitory sites palmitoylated by App, which is thought to antagonize Ft inhibition by App (Feng and Irvine, 2009; Sopko et al., 2009; Matakatsu et al., 2017). The significance of Ft regulation via the opposing functions of Dco and App is best illustrated by the observations that while homozygous *dco* mutation is lethal, flies double mutant for *dco* and *app* survive to adulthood without significant growth defects (Matakatsu et al., 2017).

Another growth regulator that functions downstream of Ft is Ex. As mentioned above, Ex localization at the junctional cortex depends partly on Ft (Silva et al., 2006), and loss of both Ft and Ex does not result in additive overgrowth phenotype. However, it remains unclear whether Ft-mediated recruitment of Ex is completely independent of Crb. Because Ex can repress Yki activity both via direct recruitment and through Hippo complex assembly (Badouel et al., 2009; Sun et al., 2015), one intriguing possibility is that these distinct functions of Ex could depend on its association with Ft or Crb.

Regulation of Hippo signaling by cell-cell adhesion components

The junctional cortex of epithelial cells appears to be a critical hub for Hippo pathway regulation. All of the upstream Hippo pathway regulators form signaling modules at the cell-cell contacts (Fulford et al., 2018). The transmembrane components described so far – Crb, Ft, and Ds – play a crucial role in organizing their signaling complexes. However, other junctional components such as E-Cadherin (Ecad), α-catenin, and Echinoid can regulate Hippo signaling as well. For example, the adherens junction (AJ) components Ecad and α-catenin mediate junctional recruitment of a LIM domain protein Jub, and junctional Jub sequesters and inactivates Wts (Rauskolb et al., 2014; Alégot et al., 2019; Sarpal et al., 2019). The recruitment of Jub to the AJ is stimulated by tension, whereby high tension is thought to induce changes in α-catenin conformation and allows for Jub binding (Alégot et al., 2019). Jub can also stabilize AJ regions under high tension (Razzell et al., 2018), suggesting that tension may induce a positive feedback that could amplify Hippo signaling repression.

Echinoid (Ed) is another transmembrane protein that inhibits Yki activity by positively regulating Hippo signaling. Ed is an immunoglobulin domain-containing protein that cooperates with Ecad in stabilizing the adherens junctions (Wei et al., 2005). In a genetic modifier screen, loss of Ed was found to enhance Yki-mediated tissue overgrowth (Yue et al., 2012). Biochemical and genetic experiments showed that Ed stabilizes Sav at the junctional cortex, as Sav is degraded more rapidly in the absence of Ed (Yue et al., 2012). However, the exact nature of Ed-mediated positive regulation of Sav is unclear. On one hand, the stabilization of Sav by Ed could simply serve as a mechanism to increase Sav abundance, while on the other hand Ed could also facilitate physical association of Sav with junctional Hippo complexes, such as those assembled

by Crb and Ex. While there is some evidence for the former scenario, evidence for the latter case is currently lacking.

1.5 Regulation of Hippo signaling via ubiquitin-mediated proteolytic degradation

Having a complex network of parallel upstream modules regulating a single signaling pathway presents an interesting challenge for a cell – somehow the activity of these inputs must be controlled. The activity of signaling networks depends on the abundance of individual signaling proteins, which can be controlled at the transcriptional, translational, or posttranslational level. At the transcriptional level, Yki promotes expression of the upstream Hippo pathway components Ex, Kib, and Mer (Genevet et al., 2010; Hamaratoglu et al., 2006; Yee et al., 2019). This results in a transcriptional negative feedback loop since all three targets activate the Hippo pathway to repress Yki activity (Fig. 1.4). However, this transcriptional feedback acts on both Ex- and Kib-mediated signaling and can be modulated by the overall state of Hippo pathway activity regardless of the input. To understand how individual upstream inputs into the Hippo pathway are regulated, we must identify the mechanisms that function locally within the distinct signaling modules.

Ubiquitin-mediated protein degradation is a major way by which cells can regulate protein abundance at the posttranslational level and is critical for many cellular processes, including the control of fate specification and proliferation (Rape, 2018). Protein ubiquitination is achieved via an enzymatic cascade that culminates in the attachment of ubiquitin molecules to substrates by E3 ubiquitin ligases and targets the substrates for proteasomal degradation (Zheng and Shabek, 2017). In contrast to transcriptional regulation, ubiquitination allows cells to rapidly adjust signaling output in response to a particular stimulus or sudden changes in environmental

conditions (Rape, 2018). For example, the transcription factors downstream of Wg and Hh signaling, Arm and Ci, respectively, are ubiquitinated via Skp/Cullin/F-box^{Slimb} (SCF^{Slimb} or Slimb) E3 ubiquitin ligase and degraded in the absence of the ligands. Binding of Wg or Hh to their receptors rapidly inhibits Slimb-mediated ubiquitination, leading to the accumulation of Arm and Ci and their increased nuclear activity (Jiang and Struhl, 1998). Ubiquitin-mediated degradation can also be modulated by extrinsic cues. For example, ubiquitination of Arm/β-catenin by Slimb is regulated by intracellular pH, whereby higher pH promotes Arm/β-catenin ubiquitination and degradation (White et al., 2018).

In the past several years, multiple Hippo pathway components were shown to be regulated via ubiquitin-mediated degradation. Importantly, the turnover of Hippo pathway components appears to be tightly associated with protein-protein interactions within the distinct signaling modules, suggesting that protein degradation may be more than a simple quality control mechanism. The current challenge is to understand how these various degradation mechanisms within the Hippo pathway are regulated during development.

Regulation of Ex abundance

As mentioned earlier, Crb recruits Ex to the junctional cortex to promote Hippo pathway activation, as loss of Crb leads to the loss of Ex from the apical cortex and its basolateral and cytoplasmic re-localization, as well as upregulation of Yki activity (Ling et al., 2010; Robinson et al., 2010). Paradoxically, overexpression of the intracellular domain of Crb (Crb^{i}) also leads to the loss of cortical Ex and upregulation of Yki activity (Chen et al., 2010; Grzeschik et al., 2010; Ling et al., 2010; Robinson et al., 2010). This dual oncogenic and tumor-suppressive function of Crb is now known to be mediated via the ability of Crb to simultaneously recruit Ex to the cortex

and promote Ex degradation via Slimb (Ribeiro et al., 2014). Ex contains a consensus motif recognized by Slimb, called a degron. Upon binding to Crb, Ex is recognized by Slimb via the degron and Slimb promotes Ex ubiquitination and subsequent degradation (Ribeiro et al., 2014). This regulation also involves casein kinase 1 (CK1) family kinases, which phosphorylate Ex on a crucial Ser within the degron and promote Ex recognition by Slimb (Fulford et al., 2019). Recently, it was shown that Dlish (a Dachs-binding protein that is inhibited by Ft) can bridge Slimb and Ex via direct interactions with both proteins to promote Ex ubiquitination and degradation, thereby providing a potential crosstalk between Ft- and Crb-mediated signaling (Wang et al., 2019).

Ex levels are also controlled by Plenty of SH3 (POSH), a RING family E3 ubiquitin ligase (Ma et al., 2018). In vitro, POSH binds Ex directly and promotes Ex ubiquitination. Ectopic POSH expression in vivo can promote Ex turnover and loss of POSH suppresses Crb^{i}-induced Ex degradation (Ma et al., 2018), suggesting that POSH regulates Ex stability downstream of Crb. This mechanism seems to function in parallel to Slimb-mediated Ex degradation, and it remains unclear whether Slimb and POSH compete for Ex regulation or whether they function in different contexts.

Ubiquitin-mediated degradation downstream of Ft/Ds signaling

Two ubiquitin-mediated mechanisms have been discovered in the Ft/Ds branch of the Hippo pathway. One of them involves an F-box protein Fbxl7, the target recognizing component of the SCF E3 ubiquitin ligase machinery that localizes to the proximal side of planar polarized cells where it is recruited by Ft (Bosch et al., 2014). In turn, Fbxl7 stabilizes Ft and is thought to prevent Dachs and Ds accumulation on the proximal side. Indeed, Dachs and Ds are less

polarized and their cortical levels are elevated in cells lacking Fbxl7 (Bosch et al., 2014; Rodrigues-Campos and Thompson, 2014). However, while one study hypothesized that Dachs is a direct target of Fbxl7, the authors did not find any changes in Dachs ubiquitination under the gain or loss of Fbxl7 function using in vitro ubiquitination assays (Bosch et al., 2014). In polar contrast, a separate study found that Fbxl7 promotes ubiquitination of both Dachs and Ds (Rodrigues-Campos and Thompson, 2014). It should be noted that these two studies used different experimental approaches to detect protein ubiquitination, which was likely the cause of the difference in their results. Nevertheless, these studies provided a potential mechanism by which Ft antagonizes Dachs activity and highlighted the importance of ubiquitin-mediated protein turnover in controlling subcellular organization of signaling components.

Another protein implicated in modulating Ft/Ds signaling output is a RING family ubiquitin ligase called Early girl (Elgi). Loss of Elgi leads to a significant increase in Dachs and Dlish levels. In biochemical assays, Elgi was found to physically interact with Dachs and Ft ICD, suggesting Elgi could antagonize Dachs activity in a similar manner to Fbxl7. However, neither Dachs nor Dlish ubiquitination was affected under the loss or gain of Elgi function (Misra and Irvine, 2019). Additionally, unlike Fbxl7, loss of Elgi does not affect Dachs planar polarity (Misra and Irvine, 2019), suggesting that Elgi may regulate Dachs differently from Fbxl7.

Ubiquitin-mediated degradation of the core Hippo pathway components

Although relatively less is known about the regulation of the core pathway kinase cassette by ubiquitin-mediated degradation, some studies have shown that such regulation exists. For example, Sav turnover was shown to be regulated by a HECT-family E3 ubiquitin ligase Herc4. Herc4 promotes Sav ubiquitination in vitro, and ectopic Herc4 expression reduces Sav levels in

vivo (Aerne et al., 2015). Interestingly, Hpo competes with Herc4 for Sav binding and antagonizes Herc4-mediated ubiquitination of Sav (Aerne et al., 2015). Additionally, coexpression of Kib and Ed in S2 cells stabilizes Sav (Aerne et al., 2015). This is consistent with a previous study that showed that Ed stabilizes Sav at the cell cortex in vivo (Yue et al., 2012), and suggests that Sav is protected from degradation when it is in a signaling complex.

To date, no study in *Drosophila* has shown that Hpo is regulated via degradation. However, a recent study done in malignant and non-malignant human breast epithelial cells showed that a mammalian homolog of Hpo, Mst2, is regulated via proteosomal degradation (Fiore et al., 2022). Mass spectrometry analysis revealed that Mst2 interacts with βTrCP, the mammalian homolog of Slimb. Interestingly, βTrCP-driven degradation of Mst2 is dependent on the matrix stiffness and mediated via a focal adhesion kinase ILK (Fiore et al., 2022), suggesting that mechanical forces can modulate Mst2 turnover.

Finally, Wts stability was shown to be regulated by a HECT-family E3 ubiquitin ligase called dSmurf. In S2 cells, dSmurf depletion leads to increased Wts stability and Yki phosphorylation, and loss of dSmurf enhances the defects caused by Wts overexpression in the *Drosophila* eye (Cao et al., 2014). However, it is unclear if dSmurf regulates Wts directly via ubiquitination as biochemical and in vivo studies of this interaction are lacking. In contrast, Wts was shown to be ubiquitinated by another E3 ubiquitin ligase called Cullin-RING4 (CRL4) and its substrate receptor Mahjong (Mahj). In the *Drosophila* larval central nervous system, Wts inhibits neural stem cell (known as neuroblasts) exit from quiescence (Ding et al., 2016; Ly et al., 2019). $CRL4^{Mahj}$ promotes Wts ubiquitination and degradation, thereby reactivating neuroblasts (Ly et al., 2019). Loss of Wts activity in the *Drosophila* larval CNS was previously

shown to increase brain size (Poon et al., 2016). However, it is unknown whether $CRL4^{Mahj}$ controls Wts stability in epithelia and whether this regulation plays a role in tissue growth.

Ubiquitin-mediated degradation of Yki/YAP/TAZ

The transcriptional effectors of the Hippo pathway – Yorkie, YAP, and TAZ – are negatively regulated via direct phosphorylation by Wts/LATS on multiple residues (Zhao et al., 2007; Lei et al., 2008; Oh and Irvine, 2008, 2009). One of the residues phosphorylated by Wts/LATS, Ser168 on Yki (Ser127 on YAP and Ser 89 on TAZ) promotes Yki association with 14-3-3 and is crucial for inhibiting Yki nuclear accumulation. However, other residues phosphorylated by Wts/LATS are also thought to be important for Yki/YAP/TAZ activity, including the regulation of protein stability. For example, LATS also phosphorylates YAP on Ser381 and TAZ on Ser311, and these phosphorylation sites are near the consensus phosphodegron motif recognized by $SCF^{\beta TrCP}$ E3 ubiquitin ligase (Slimb homolog). Phosphorylation by LATS primes YAP and TAZ phosphodegrons for phosphorylation by CK1ε on the Ser384 and Ser314, respectively, which leads to YAP/TAZ ubiquitination and degradation (Liu et al., 2010a; Zhao et al., 2010). The phosphodegron residues found in YAP/TAZ are not precent in Yki, but a recent study found that a kinase CDK7 and an E3 ubiquitin ligase $CRL4^{DCAF12}$ regulate Yki stability in the nucleus (Cho et al., 2020). CDK7 phosphorylates Yki on Ser169, which is adjacent to Ser168 phosphorylated by Wts, which leads to $CRL4^{DCAF12}$-mediated ubiquitination and degradation of Yki. The regulation of Yki by CDK7 appears to be independent of Wts-mediated Yki regulation but is conserved in YAP/TAZ (Cho et al., 2020).

1.6 Non-transcriptional roles of the Hippo pathway components

An important and frequently overlooked aspect of the Hippo pathway is that the core Hippo signaling components have functions that do not rely on Yki activity. The relative scarcity of studies on transcription-independent functions of the Hippo pathway has historical and practical explanations. First, while the genetic screens that led to Hippo pathway discovery were genotypically unbiased, they were biased phenotypically as they focused only on the isolation of the mutations that produced overgrowth phenotypes. Therefore, it is not surprising that most of the work on the Hippo pathway focuses on the transcriptional output via Yorkie/YAP/TAZ. Second, because a significant part of the Hippo pathway output is mediated via Yki/YAP/TAZ transcriptional activity, uncoupling the transcriptional and non-transcriptional functions of the Hippo pathway can be difficult. Thus, development of approaches to specifically study transcription-independent roles of Hippo signaling components is paramount to uncovering the novel biological functions of the Hippo pathway.

Another critical challenge of identifying transcription-independent roles of Hippo signaling components is knowing what these functions might be. The homologs of the core Hippo pathway components Hpo, Mats, and Wts are thought to have first evolved in the opisthokonts, a broad phylogenetic group that includes both fungi and animals (Sebé-Pedrós et al., 2012). However, the transcriptional effector Yki only appears in holozoans, the branch of opisthokonts that includes unicellular animal ancestors and metazoans but excludes fungi and other eukaryotes (Sebé-Pedrós et al., 2012; Phillips et al., 2022). Thus, investigating the function of Hippo signaling components in fungi and organisms that predate them could provide potential clues about Yki-independent functions of the core Hippo pathway proteins.

The core Hippo pathway components in yeast

Cell proliferation requires successful cell cycle progression, mitotic spindle alignment, and proper segregation of chromosomes. However, despite the established role of Hippo signaling in the control of cell proliferation and tissue growth, the link between Hippo pathway components and the control of cell division has not been extensively studied in animals. On the other hand, the homologs of the core Hippo pathway components have been studied in the budding and fission yeast, where these proteins function in a kinase cascade similar to the canonical Hippo pathway and are required for cell cycle progression (Fig. 1.5, Hergovich and Hemmings, 2012). In the budding yeast Cdc15 (Hpo), Mob1 (Mats), and Dbf2 (Wts) are part of the mitotic exit network (MEN), which also includes an upstream activator, a Ras-like GTPase called Tem1, and a downstream phosphatase Cdc14. Tem1 activates the Cdc15-Mob1-Dbf2 kinase cascade, which culminates in the phosphorylation and derepression of Cdc14 by Wts (Mah et al., 2001; Visintin and Amon, 2001; Mohl et al., 2009). Cdc14 then drives exit from mitosis by promoting the degradation of mitotic Cdk1-Cyclin B complexes via the anaphase promoting complex (APC) E3 ubiquitin ligase and by dephosphorylating Cdk1 targets (Jaspersen et al., 1998; Visintin et al., 1998). Thus, loss of the MEN components leads to the arrest of cells in anaphase due to ectopic Cdk1-cyclin activity (Jaspersen et al., 1998).

The activation of the MEN network in the budding yeast is coordinated by cell polarity and spindle position checkpoint (SPOC). Budding yeast cells divide asymmetrically, with the mother cell producing a bud, which after cell division becomes a smaller daughter cell with a distinct fate. The two spindle pole bodies (SPBs, the yeast centrosomes) are initially situated in the mother cell, but as the bud grows, the old SPB associates with the bud via a protein Kar9, which is critical for proper spindle orientation and SPB inheritance (Korinek et al., 2000; Lee et

al., 2000). The MEN components, including Tem1 and the Hippo kinase cascade, accumulate preferentially on the daughter/old SPB (Visintin and Amon, 2001). Because the MEN cascade is triggered by the GTPase Tem1 and the initiation of the cascade has to occur only after the spindle is properly aligned (Visintin and Amon, 2001), Tem1 regulation must be mediated through polarity and SPOC cues. The activator of Tem1, a guanine exchange factor (GEF) called Lte1, localizes asymmetrically through Cdk1 and Cdc42 activity, which also establishes polarity (Johnson, 1999; Jensen et al., 2002). Polarization of Lte1 to the bud leads to the inhibition of Bub2-Bfa1 complex, a SPOC component and a GTP activating protein (GAP) complex that inhibits Tem1, in the bud (Bardin et al., 2000). Meanwhile, another SPOC component Kin4 phosphorylates and activates Bub2-Bfa1 GAP in the mother cell (Pereira and Schiebel, 2005). This asymmetric distribution of Tem1 regulators ensures that the MEN cascade is activated only after the spindle is properly aligned and the daughter SPB is positioned in the bud. Additionally, the preferential accumulation of the MEN components on the daughter SPB is necessary for spindle alignment as the MEN cascade leads to the phosphorylation of Kar9, which promotes Kar9 association with the old SPB and proper spindle orientation (Hotz et al., 2012).

Non-transcriptional regulation of cell division by the Hippo pathway in animals

Although the role of Hippo pathway components in cell division and cell cycle control in *Drosophila* and mammalian cells is not well understood, several lines of evidence suggest that some aspects of their function in the budding yeast may also be conserved in metazoans. For example, similar to Dbf2 (the yeast homolog of Wts), Wts is known to accumulate at the spindle poles, as well as along the spindle, in *Drosophila* and human mitotic cells (Nishiyama et al., 1999; Dewey et al., 2015). However, unlike Dbf2, which is thought to inhibit Cdk activity

Figure 1.5: A simplified diagram of the regulation and function of the budding yeast core Hippo pathway components

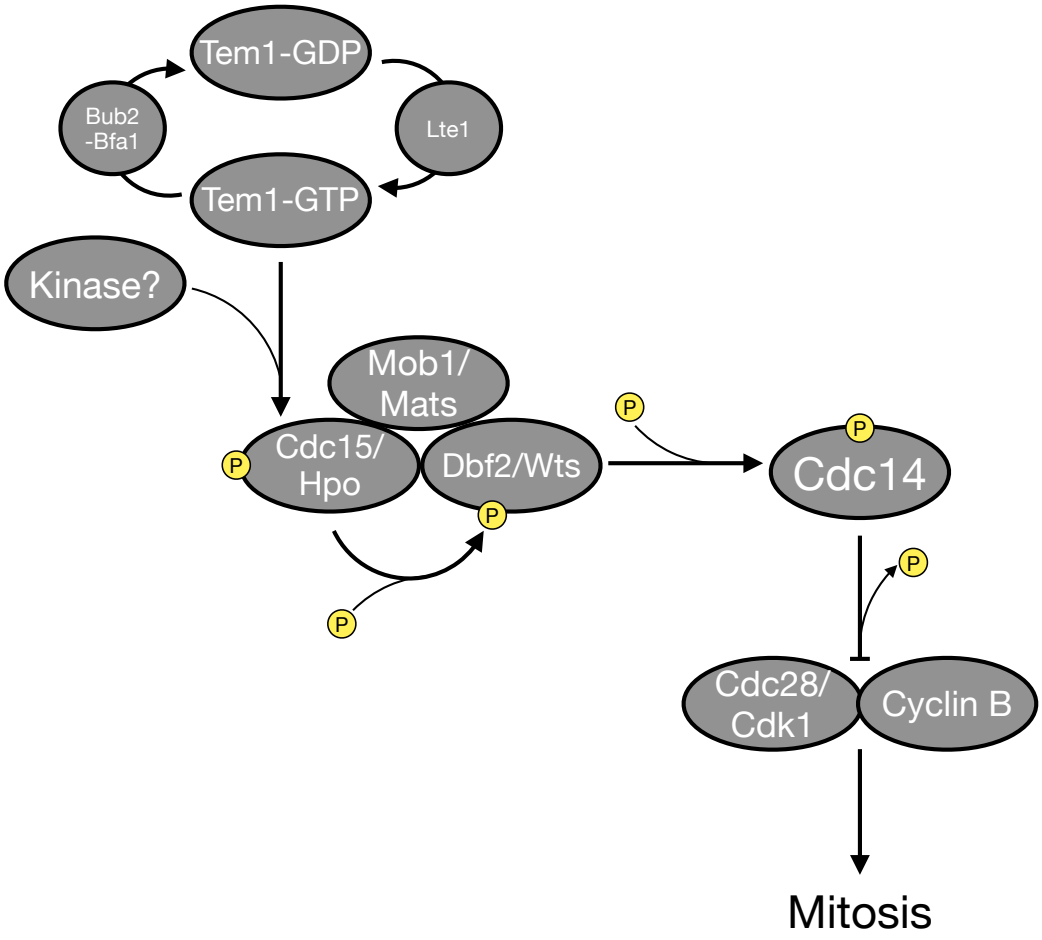

The core Hippo pathway components Hpo (Cdc15), Mats (Mob1), and Wts (Dbf2) form a kinase cassette that promotes exit from mitosis in the budding yeast. The Hippo kinase cascade phosphorylates and derepresses Cdc14, and Cdc14 dephosphorylates mitotic cyclins and promotes their degradation, thereby ending mitosis. A GTPase Tem1 acts upstream of the Hippo kinase cascade and promotes its activity.

primarily through the activation of the downstream phosphatase Cdc14, Wts directly binds Cdk1 in early mitosis, thereby preventing Cdk1 association with cyclins and inhibiting Cdk1 kinase activity (Tao et al., 1999b). Although it is unclear whether Wts phosphorylates Cdk1, it has been shown that Cdk1 can phosphorylate Wts in early mitosis, though the biological significance of this regulation is not understood (Nishiyama et al., 1999; Tao et al., 1999b; Morisaki et al., 2002). Furthermore, removing a single copy of *cdk1* in *Drosophila* suppresses the lethality and tissue overgrowth induced by homozygous *wts* mutation (Tao et al., 1999b). These results suggest that in animals, Wts could suppress cell proliferation via transcriptional (by regulating Yki/YAP/TAZ) and non-transcriptional (by inhibiting the mitotic Cdk1 activity) mechanisms. Future work is needed to understand whether other core Hippo pathway components are involved in Wts-mediated regulation of the mitotic Cdk1/cyclin activity.

It should also be noted that unlike the loss of Dbf2 in the budding yeast, there are no reports that loss of Wts causes cell cycle arrest in animal cells. However, in the *Drosophila* eye imaginal tissue, cells mutant for Wts ectopically accumulate Cyclin A, the main cyclin involved in S phase and G2-M transition (Lehner and O'Farrell, 1989). It is possible that Wts can also associate with Cyclin A and promote its degradation (akin to Kib regulation described in Chapter 2), though the potential role of Yki-mediated transcription in the upregulation of Cyclin A has not been eliminated.

The association with the spindle and Cdk1 is not unique to Wts. All of the core Hippo pathway components, including YAP, have so far been found to associate with the spindle and most are phosphorylated by Cdk1 during mitosis (Guo et al., 2007; Yang et al., 2013; Bui et al., 2016; Chen et al., 2016). The significance of the regulation of Hippo pathway components by Cdk1 is still poorly understood. However, in human cells, YAP was found to be required for

proper localization of actomyosin machinery, including the GTPase RhoA and its GEF Ect2, to the cytokinetic furrow, and phosphorylation by Cdk1 enables this non-transcriptional function of YAP (Bui et al., 2016). However, unlike the situation in *Drosophila*, where Yorkie promotes myosin activity, YAP seems to attenuate myosin activation, as loss of YAP leads to significantly elevated phosphorylation of the myosin regulatory light chain (Bui et al., 2016; Xu et al., 2018). It is unclear whether the non-transcriptional function of YAP in cytokinesis requires other Hippo pathway components. This question is particularly interesting since, as mentioned earlier, the evolution of the core Hippo pathway components predates YAP. Thus, the function of YAP in cytokinesis could have been co-opted by the core Hippo kinase cassette.

What is the significance of the association of Hippo pathway components with the spindle and centrosomes? As mentioned above, all core Hippo pathway components localize to centrosomes in mammalian cells, suggesting that the entire Hippo pathway kinase cassette may assemble and function at centrosomes. Interestingly, the activity of the Hippo kinase cascade is important for centrosome duplication, and Mst2 and Sav have been shown to directly recruit and activate Nek2A kinase at centrosomes, which is required for successful centrosome disjunction (Hergovich et al., 2009; Mardin et al., 2010). Because centrosome duplication and segregation is tightly linked to cell cycle control (Lacey et al., 1999), it is likely that the Hippo pathway can also influence these processes indirectly via the regulation of Cdk activity.

Non-transcriptional function of the Hippo pathway in spindle alignment and asymmetric cell division

The *Drosophila* neural stem cells, known as neuroblasts (NBs), have recently emerged as an intriguing system to study the association of Hippo signaling components with cell polarity,

spindle positioning, and cell cycle. NBs are born and proliferate during embryogenesis and become temporarily quiescent in the late embryo, before reactivating in the early larva (Chia et al., 2008). During development, NBs divide asymmetrically whereby the mother cell self-renews to retain the NB fate, while the daughter cell, known as a ganglion mother cell (GMC), differentiates into neurons and glia that populate the central nervous system (Prehoda, 2009). The asymmetric cell division (ACD) of NBs is regulated by the conserved polarity network including Bazooka (Par3), Cdc42, Par6, aPKC, Disc large (Dlg) and Canoe (Cno) in concert with the spindle positioning machinery consisting of proteins Inscuteable (Insc), Partner of inscuteable (Pins), Mud (NuMA), the Dynein/Dynactin complex, a kinesin motor Khc73, and mitotic kinases Aurora A and Polo. The polarity and spindle positioning complexes are physically linked at the apical side of NBs via Baz-Insc-Pins interaction, and together they restrict GMC fate determinants to the basal side (Fig. 1.6A, Doe, 2008; Wodarz et al., 1999).

Pins regulates spindle positioning via two mechanisms (Fig. 1.6B). On the one hand, the TPR domain of Pins can recruit Mud and Dynein/Dynactin complex, which is critical for Dynein-mediated force generation and microtubule shortening (Johnston et al., 2009). On the other hand, Pins contains a linker region that can recruit the Dlg/Khc73 complex and mediate microtubule attachment to the cell cortex (Johnston et al., 2009). However, like Mud, Insc and Cno bind to Pins TPR domain, and Insc competes with Mud for Pins binding (Yu et al., 2000; Wee et al., 2011), suggesting that Insc, Cno, and Mud interaction with Pins has to be regulated throughout mitosis.

Recent studies have shown that Hippo pathway components are required for ACD. In genetic interaction experiments, loss of Hippo signaling components significantly enhances the

Figure 1.6: Hippo signaling in the neuroblast asymmetric cell division

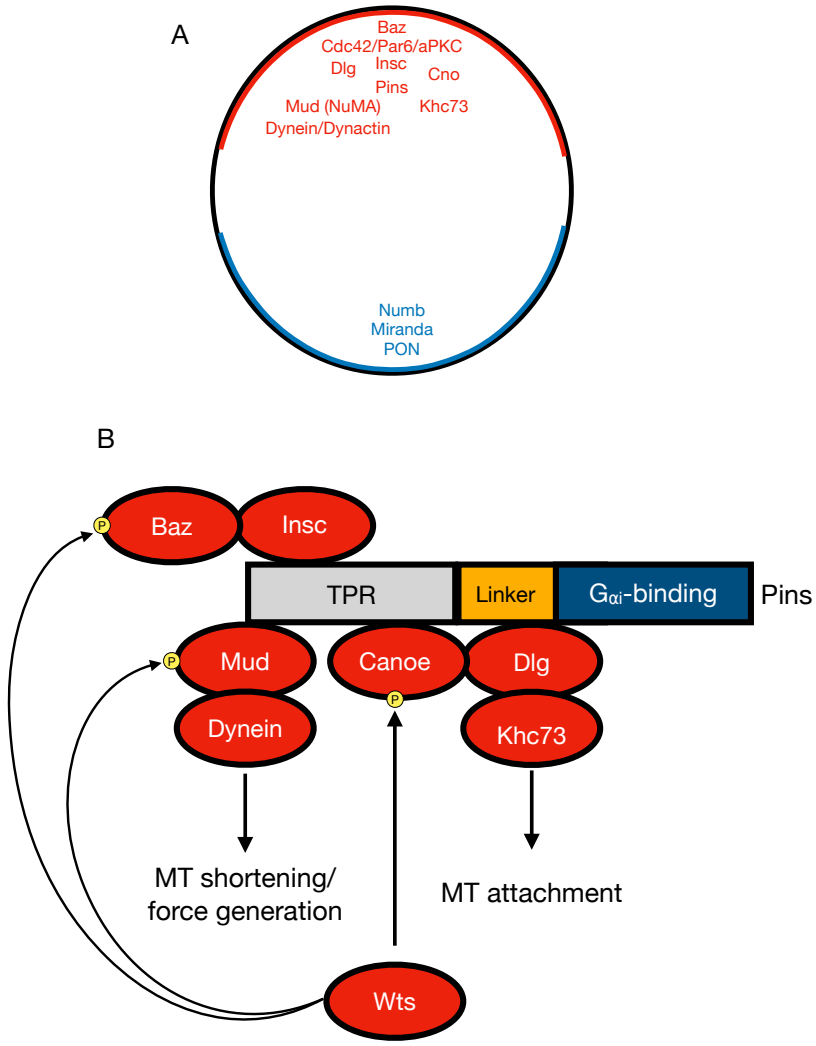

Adapted from Johnston et al., 2009.

A) A simplified cartoon of a mitotic *Drosophila* neuroblast. The apical polarity determinants (red) localize to the apical side of the cell where they restrict the localization of the basal components (blue) to the opposite side.
B) A cartoon of Pins and its interacting partners. Insc, Mud, and Canoe all bind to the TPR domain of Pins to couple spindle alignment to cell polarity. Wts promotes Baz, Mud, and Canoe phosphorylation, thereby potentially regulating the dynamics between the spindle alignment machinery and apical polarity.

ACD defects caused by the loss of apical polarity and spindle positioning proteins (Keder et al., 2015). These defects were shown to be mediated through Wts but are independent of Yki transcriptional activity (Dewey et al., 2015; Keder et al., 2015). Specifically, Wts seems to control the dynamics within the spindle positioning machinery and, possibly, its linkage to the apical polarity component Baz. For example, Wts was shown to phosphorylate Cno, which promotes Cno association with Pins and is required for Dlg recruitment (Keder et al., 2015). However, Wts also phosphorylates Mud and promotes its interaction with Pins, whereby under Wts depletion Mud still localizes to the spindle poles but is no longer recruited to the cell cortex by Pins (Dewey et al., 2015). Additionally, Wts also physically interacts with Baz and promotes its phosphorylation, although the biological role of Baz regulation by Wts is unclear. These studies suggest that Wts may be a key component that regulates the dynamics within the spindle positioning machinery, possibly by sequentially regulating interactions of Baz, Cno, and Mud with Pins throughout mitosis or by providing robustness to the coupling of the spindle machinery to the polarity network.

Work on *Drosophila* NBs and sensory organ precursor cells has also linked Hippo signaling components to the regulation of cell cycle, though it is unclear whether pathway components contribute non-transcriptionally in this process. Loss of Hippo pathway components was shown to promote NB exit from quiescence and cause larval brain overgrowth (Ding et al., 2016; Poon et al., 2016; Ly et al., 2019). This effect is mediated at least in part via Hippo pathway-mediated Yki inhibition, and Yki was shown to be both necessary and sufficient for NB reactivation (Ding et al., 2016). Specifically, the downstream targets of Yki, the oncogenic micro RNA *bantam* and the cell cycle regulator *cyclin E* are thought to regulate Yki-mediated exit from quiescence in NBs (Ding et al., 2016). However, as discussed earlier in this chapter, the

importance of Yki as a downstream transcriptional effector has hindered the investigation of the potential non-transcriptional contribution of the core Hippo kinase cassette to cell cycle regulation in NBs.

An surprising revelation came from a recent study that found that Cyclin A is polarized at the cell cortex of mitotic primary sensory organ precursor cells, or pI cells. Similar to NBs, a pI cell undergoes asymmetric cell division that is regulated by apical polarity components such as aPKC and spindle alignment machinery. Interestingly, endogenous Cyclin A forms a cortical crescent with aPKC on the apical posterior side of dividing pI cell (Darnat et al., 2022). Furthermore, cortically localized Cyclin A is required for Mud recruitment to the cortex and proper spindle alignment. This study raises an intriguing possibility of a direct link between cell polarity, spindle alignment, and cell cycle control. Additionally, given the direct interaction between Wts and Cdk1, the potential regulation of Cyclin A levels by Wts, and the role of Wts in the regulation of Mud recruitment to the cell cortex, this study provides a potential pathway to explore the role of Wts in Cyclin A regulation at the cell cortex. For example, is Wts necessary for Cyclin A cortical localization? Does Wts-mediated regulation of Cdk1 influence cortical Cyclin A recruitment? Does Wts interact with Cyclin A and promote its phosphorylation? Is cortical Cyclin A pool distinct from Cdk1-associated Cyclin A, and if so, does Wts play a role in the spatial separation of these pools? Finally, is Cyclin A also polarized at the cell cortex of mitotic NBs? Answering these questions could provide interesting insights into the non-transcriptional role of the Hippo pathway in coordinating critical processes during cell division.

1.7 Polarity and Hippo signaling

Epithelial tissues are comprised of cells that display distinct polarity. Generally, the polarity of epithelial cells can be roughly segregated into two domains – the apical domain, which faces the external environment, such as the lumen of a developing tissue, and the basal domain, which mediates the attachment of cells to the extracellular matrix, such as the basement membrane (Tepass, 2012). Such organization of epithelial cells is achieved via mutual antagonism between the apical and basal polarity determinants (Fig. 1.7). The apical polarity network is comprised of multiple components, including Crb, Patj, Stardust (Sdt), aPKC, Par6, and Bazooka (Baz, a fly homolog of Par3). These components can be further subdivided into distinct apical polarity modules consisting of Crb/Patj/Sdt, aPKC/Par6, and Baz, which can interact with one another and occupy distinct subdomains of the apical membrane (Morais-de-Sá et al., 2010; Tepass, 2012). These proteins localize at the marginal zone of epithelial cells (Tepass, 2012), a subcellular region below the apical surface and above the adherens junctions (throughout this dissertation, I refer to this subcellular region as the junctional cortex). The basolateral polarity network includes Scrib, Lgl, Dlg, and Par-1. These proteins localize below the adherens junctions and display complementary localization to the apical polarity proteins along the apico-basal axis of the cell cortex.

The role of polarity in growth control has long been recognized. Intact polarity is thought to be a barrier to tumorigenesis, and disrupted cell polarity is a defining feature of neoplastic tumors (Halaoui and McCaffrey, 2015). However, studies over the years have identified both oncogenic and tumor suppressor roles of polarity (e.g. the dual function of Crb described earlier), and few studies have focused on the mechanistic interactions of individual polarity components with growth-regulating pathways (Fomicheva et al., 2020). Therefore, mechanistic understanding

Figure 1.7: A simplified schematic of epithelial polarity regulators.

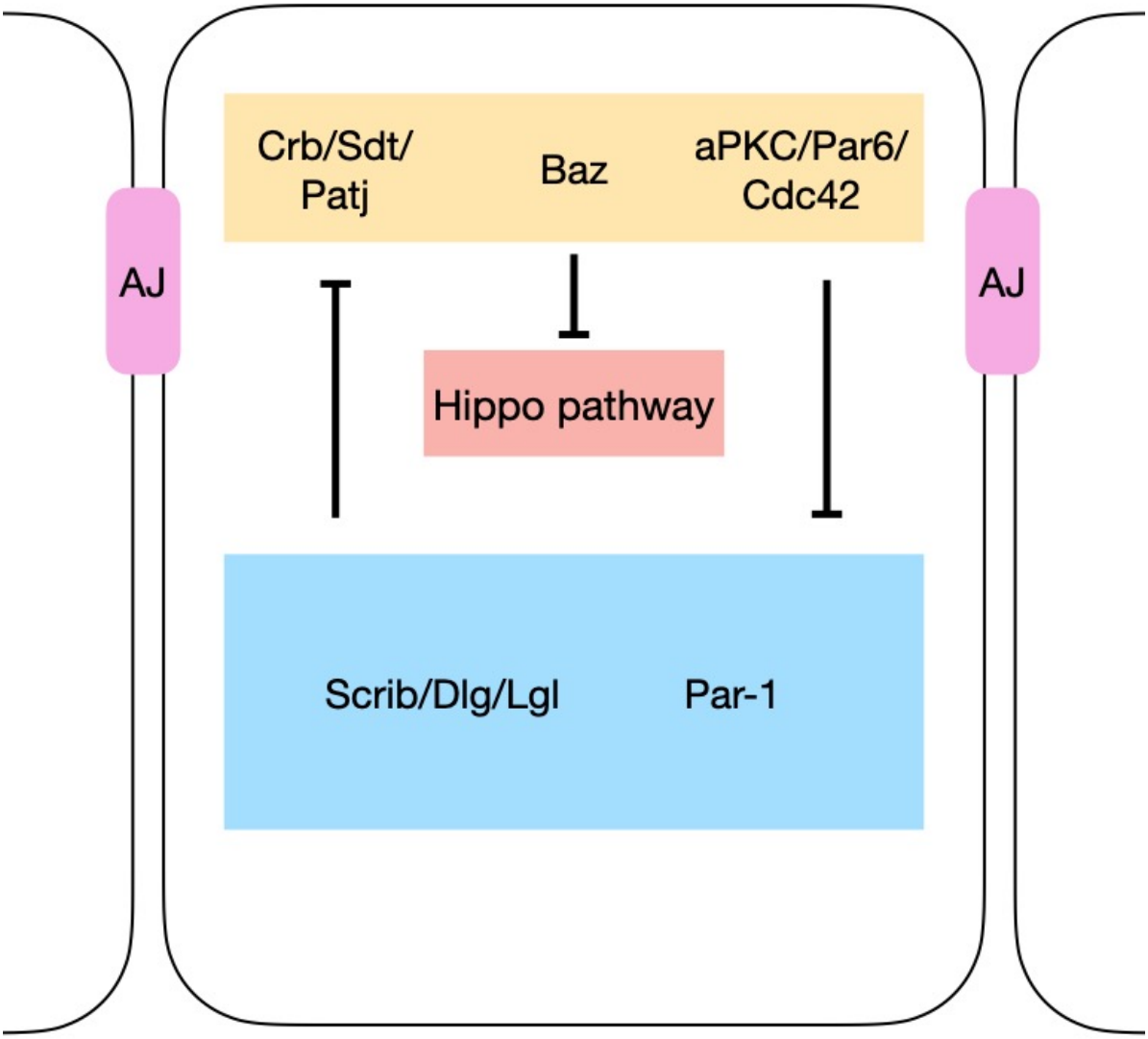

Epithelial polarity is achieved via antagonistic relationship between the apical and basal polarity modules. The apical polarity components localize above the adherens junctions (AJ), where they antagonize the basolateral components to restrict their localization below the AJs.

The apical polarity components are thought to inhibit Hippo signaling and promote Yki activity, whereas basolateral components regulate Hippo signaling in part by antagonizing the apical polarity network.

of how individual polarity components regulate Hippo signaling is still lacking. Below, I will briefly describe some of the studies that link polarity regulators to the Hippo pathway.

Apical polarity and Hippo signaling

The most mechanistically understood interaction between apical polarity and Hippo signaling is the regulation of Ex by Crb. As described earlier in this chapter, the recruitment of Ex by Crb promotes Ex-mediated inhibition of Yki both via Hippo pathway activation and direct sequestration of Yki at the junctional cortex. Mammalian Crb3 also inhibits YAP at the apical cortex (Szymaniak et al., 2015). Although Ex is not conserved in mammals, a functional homolog of Ex, Angiomotin (AMOT) can sequester YAP at the junctional cortex by associating with NF2 (Merlin homolog) and Crb-binding partners Pals1 (Sdt homolog) and Patj (Yi et al., 2011; Moleirinho et al., 2017).

The activity of aPKC has also been reported to promote Yki activity (Grzeschik et al., 2010). Somatic mosaic clones expressing an active, membrane-tethered version of aPKC ($aPKC^{CAAX}$) upregulate the expression of Yki target genes (Grzeschik et al., 2010). This effect is thought to be mediated, at least in part, via $aPKC^{CAAX}$-induced mislocalization of Hpo (Grzeschik et al., 2010). Alternatively, reports from both mammalian and *Drosophila* studies suggest that apical polarity components, including aPKC, may antagonize Hippo complex formation. For example, in human cancer cell lines, apical polarity components sequester Kib from functional Hippo complex formation, which prevents Hippo pathway activation and is thought to promote cancer metastasis (Zhou et al., 2017). Additionally, Kib contains an aPKC-binding domain and was shown to be an aPKC substrate (Büther et al., 2004). Kib physically interacts with aPKC in both mammalian and *Drosophila* cells, and aPKC was found to inhibit

Kib function in autophagy in *Drosophila* (Yoshihama et al., 2011; Jin et al., 2015). To date, however, mechanistic understanding of the molecular interactions between apical polarity and Hippo pathway components in growth control or other contexts is lacking.

Basolateral polarity and Hippo signaling

Studies in both *Drosophila* and mammals have found that basolateral polarity components act as tumor suppressors (Halaoui and McCaffrey, 2015). Somatic mosaic clones mutant for Scrb, Lgl, or Dlg display elevated Yki activity. The basolateral components appear to regulate Yki activity via multiple mechanisms (reviewed in Stephens et al., 2018). Notably, overexpression of a dominant-negative form of aPKC in *lgl*-mutant clones suppresses Yki hyperactivation induced by the loss of Lgl (Grzeschik et al., 2010), suggesting that loss of basolateral polarity upregulates Yki at least in part via increased activity of apical polarity regulators.

A more direct mechanism of Hippo pathway regulation by basolateral components is mediated via Par-1 and Dlg5. Par-1 is widely recognized as basolateral polarity protein, whereas the role of Dlg5 in cell polarity has not been clear. Loss of Dlg5 disrupts normal localization of apical components, including aPKC and Crb, and Dlg5 can localize to both the apical and basolateral domains of epithelial cells (Nechiporuk et al., 2013; Luo et al., 2016). As mentioned earlier in this chapter, Par-1 promotes Hpo phosphorylation on Ser30, which blocks Sav-Hpo association and Tao-1-mediated phosphorylation of Hpo on Thr195 and, therefore, blocks Hpo activity (Huang et al., 2013). A mechanistic understanding of Par-1-mediated inhibition of Hpo is now beginning to emerge with the identification of additional components involved in Hpo inhibition. For example, a scaffold protein Dlg5 links Par-1 (MARK3) to Hpo (Mst1/2), thus promoting Par-1-mediated inhibition of Hpo in *Drosophila* and mammals (Kwan et al., 2016).

Interestingly, Dlg5 also associates with Slmap, a key component of the STRIPAK phosphatase complex that inactivates Hpo by dephosphorylating it on Thr195 (Zheng et al., 2017; Ribeiro et al., 2010; Kaya-Çopur et al., 2021). Thus, one possible mechanism is that Dlg5 could bring Par-1 to Hpo, and phosphorylation of Hpo on Ser30 by Par-1 could recruit the STRIPAK phosphatase complex. Rassf, a component of the STRIPAK complex, is known to compete with Sav for binding to Hpo and could therefore block Hpo-Sav complex formation (Polesello et al., 2006). In the meantime, PP2A, the protein phosphatase component of the STRIPAK complex, could dephosphorylate Hpo on Thr195. This mechanism could provide a means by which Hpo activity is restricted apically in epithelial cells, where the rest of the Hippo signaling components are enriched.

1.8 Regulation of the Hippo pathway by the cortical cytoskeleton and mechanical forces

Unlike other signaling pathways, such as Notch or Hh, the Hippo pathway does not contain a conventional ligand/receptor pair. Instead, the activity of the Hippo pathway is modulated via actomyosin cytoskeleton and mechanical stimuli (Fig. 1.8). Studies from both *Drosophila* and mammalian systems have found the activity of Yki/YAP/TAZ is regulated by physical forces transmitted at cell-cell junctions, focal adhesions, and nuclear envelope (reviewed in Misra and Irvine, 2018). Below, I describe a few relevant examples that link cortical cytoskeleton and mechanical cues to the regulation of Hippo signaling.

Regulation of Hippo signaling by the actin cytoskeleton

The activity of Hippo signaling is negatively regulated by the actin cytoskeleton. For example, ectopic activity of the *Drosophila* formin, Diaphanous (Dia) leads to the upregulation of Yki

transcriptional targets and significant tissue overgrowth, and this effect is conserved in mammalian cells (Sansores-Garcia et al., 2011). The effect of Dia activity on growth is, at least in part, mediated via increased F-actin polymerization, as the loss of actin capping proteins also leads to Yki-dependent tissue overgrowth (Fernandez et al., 2011; Sansores-Garcia et al., 2011), whereas F-actin depolymerization leads to hyperactivation of the Hippo pathway and reduced Yorkie/YAP activity (Dupont et al., 2011; Sansores-Garcia et al., 2011; Wada et al., 2011). However, Dia also positively regulates myosin stability and/or activity (Homem and Peifer, 2008), which can also promote Yki activation.

The regulation of Yorkie/YAP activity by the actin cytoskeleton occurs through multiple mechanisms. First, F-actin depolymerization enhances Mer-Wts interaction, suggesting that F-actin can promote nuclear Yorkie/YAP by inhibiting Hippo complex formation (Yin et al., 2013). Second, in mammalian cultured cells, AMOT sequesters YAP in the cytoplasm, and binding of F-actin to AMOT releases YAP from this inhibition (Mana-Capelli et al., 2014; Moleirinho et al., 2017). Finally, LATS phosphorylates AMOT and blocks its interaction with F-actin, thereby promoting AMOT-mediated cytoplasmic retention of YAP (Mana-Capelli et al., 2014). AMOT can also promote LATS activity (Hirate et al., 2013; Leung and Zernicka-Goetz, 2013), suggesting that positive feedback between AMOT and LATS may robustly drive YAP inhibition. Although AMOT is not present in *Drosophila*, Ex functions similarly to AMOT in that it can inhibit Yki both via both Wts activation and direct sequestration of Yki at the cell cortex (Hamaratoglu et al., 2006; Badouel et al., 2009; Sun et al., 2015). Additionally, as a FERM domain protein, Ex could potentially interact with F-actin. However, it remains unknown whether Ex-mediated Yki sequestration is regulated by F-actin.

Figure 1.8: A simplified cartoon illustrating the regulation of Yki/YAP/TAZ activity by mechanical forces and cytoskeletal components.

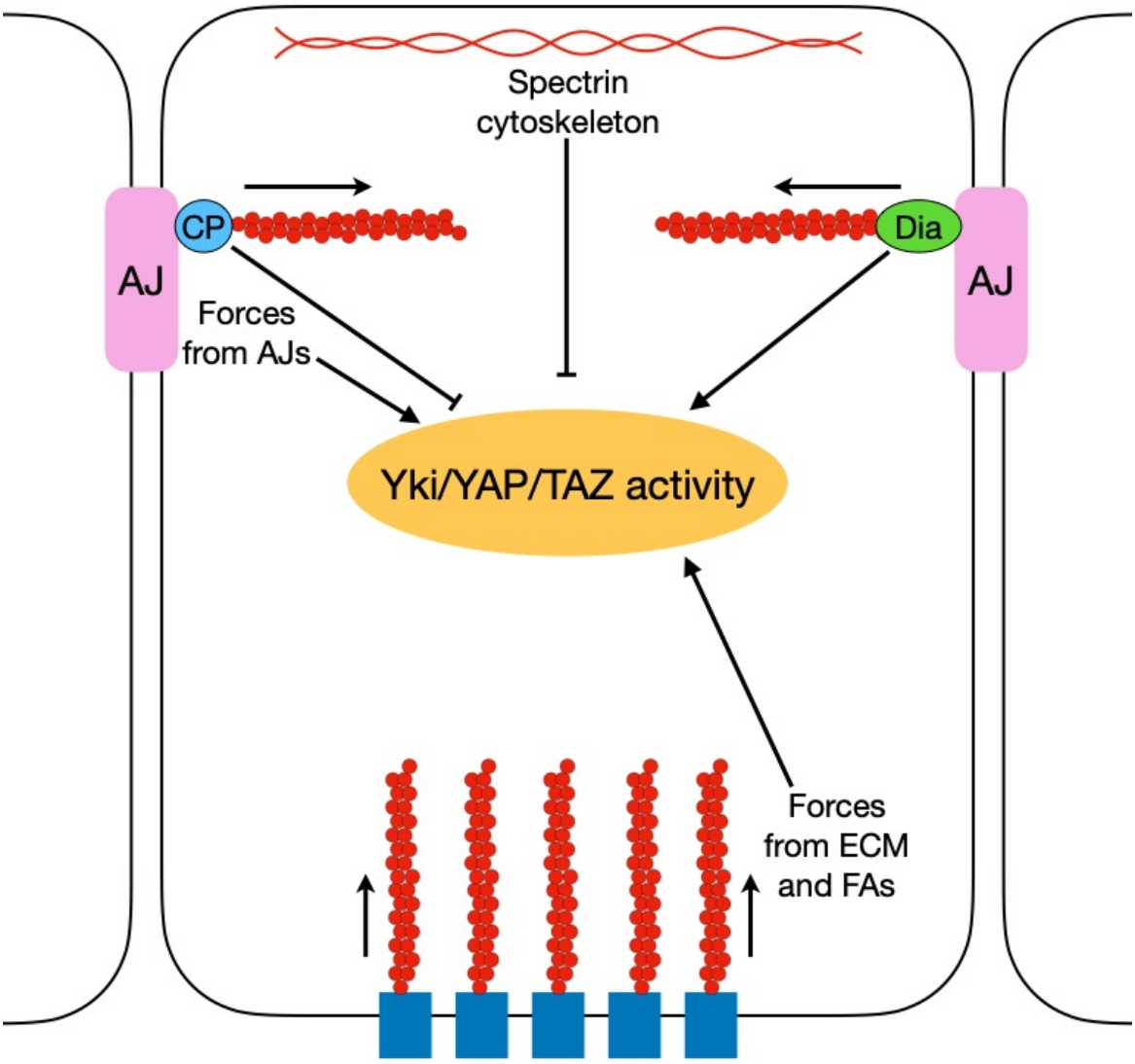

The activity of Yki/YAP/TAZ is promoted by F-actin nucleator Dia and forces transmitted at the adherens junctions (AJs) and focal adhesions (FAs).

Capping proteins (CP) and the spectrin cytoskeleton repress Yki/YAP/TAZ activity.

Regulation of Hippo signaling by the spectrin cytoskeleton

Underlying the plasma membrane, the spectrin cytoskeleton (SC) plays a critical role in cell shape and mechanical properties (Leterrier and Pullarkat, 2022). Previous studies identified the SC as a positive regulator of the Hippo pathway (Deng et al., 2015; Fletcher et al., 2015). Loss of individual spectrin components α-spectrin, β-spectrin, or βHeavy spectrin (Kst in flies), leads to increased expression of Yki-target genes and tissue overgrowth (Deng et al., 2015; Fletcher et al., 2015).

Two models that are not mutually exclusive have been proposed to explain how the SC regulates Hippo signaling. First, the SC modulates myosin activity and cortical tension, which is known to inhibit the Hippo pathway (Rauskolb et al., 2014; Deng et al., 2015, 2020). How the SC regulates myosin activity is still unknown, but it involves the regulation of the Spaghetti squash (Sqh), a myosin regulatory light chain in *Drosophila*. A scaffold protein called Big bang (Bbg) forms a complex with both the SC and Sqh and promotes myosin activity (Forest et al., 2018; Tsoumpekos et al., 2018). If Bbg were the only component downstream of the SC to regulate myosin activity, then one would predict a decrease in Sqh phosphorylation in cells lacking the SC. However, the opposite is true: MRLC phosphorylation is significantly increased in spectrin mutant cells (Deng et al., 2015, 2020). These findings suggest that in addition to promoting Sqh phosphorylation via Bbg recruitment to the cell cortex, the SC directly or indirectly inhibits Sqh activity independently of Bbg.

A second possibility is that the SC could function as a scaffold for Hippo signaling complex assembly. In support of this idea, upstream Hippo pathway components Kib, Mer, and Ex can form a complex with Kst (Fletcher et al., 2015). However, the observation that loss of Kst has no effect on Ex localization argues against this model (Fletcher et al., 2015). Whether Kst is

required for Kib and Mer localization at the junctional and/or apicomedial cortex remains to be tested. Intriguingly, Mer displays partial co-localization with apicomedial myosin in the wing imaginal disc cells, and Kst was recently shown to associate with apicomedial myosin during *Drosophila* mesoderm invagination (Su et al., 2017; Krueger et al., 2020), raising the possibility that the SC could regulate Kib and Mer apicomedial localization.

Regulation of Hippo signaling by mechanical forces

To date, most studies examining how mechanical forces modulate Hippo signaling have focused on Yorkie/YAP/TAZ activity. In mammalian cells, YAP/TAZ localization is regulated by cell-cell and cell-ECM contacts (Misra and Irvine, 2018). The mechanosensitivity of YAP/TAZ is supported by the observations that YAP/TAZ nuclear-cytoplasmic localization changes with cell culture density, ECM stiffness, cell geometry, and physical forces applied to cells (Dupont et al., 2011; Aragona et al., 2013). Generally, under conditions associated with higher tension (e.g. low cell culture density, higher ECM stiffness, or stretching of cells), YAP/TAZ becomes predominantly nuclear (Zhao et al., 2007; Dupont et al., 2011; Aragona et al., 2013). Similarly, actomyosin-generated tension at cell-cell junctions promotes Yki/YAP/TAZ nuclear activity (Rauskolb et al., 2014; Ibar et al., 2018).

The biomechanical regulation of Yki/YAP/TAZ activity involves multiple mechanisms and not all of them are yet understood. The ECM-mediated regulation of YAP occurs via both Hippo pathway dependent and independent mechanisms (Dupont et al., 2011; Aragona et al., 2013; Chakraborty et al., 2017). ECM stiffness can regulate Hippo pathway activity via focal adhesion-mediated signaling. For example, a proteoglycan called Agrin, which is involved in the transduction of mechanical signals from the ECM via focal adhesions, can inhibit Hippo pathway

activity via the focal adhesion kinase, FAK (Chakraborty et al., 2017). Depletion of Agrin or FAK leads to increased phosphorylation of Mst1/2, LATS1/2, and AMOT and blocks nuclear translocation of YAP (Chakraborty et al., 2017). Mechanistically, Agrin-FAK signaling is thought to promote complex formation between Mer, p21-associated kinase (PAK1), and integrin-linked kinase (ILK), which inactivates Mer via PAK1-mdiated phosphorylation of Mer on Ser581 (Kissil et al., 2002; Xiao et al., 2002; Chakraborty et al., 2017). Interestingly, while loss of Agrin does not affect the enrichment of bona fide focal adhesion complexes, it dramatically reduces the enrichment of Hippo pathway components at focal adhesions (Chakraborty et al., 2017). Recently, it was shown ECM stiffness can promote Mst2 degradation via ILK activity and βTrCP-mediated ubiquitination (Fiore et al., 2022), suggesting that protein turnover may be one way by which mechanical stimuli can locally regulate abundance of signaling components.

Tension at cell-cell junctions also regulates Hippo signaling. As described ealier, the most mechanistically understood process involves a LIM-domain protein Ajuba (Jub), which inactivates Wts by sequestering it at the adherens junctions in a tension-dependent manner (Rauskolb et al., 2014; Alégot et al., 2019; Sarpal et al., 2019). This mechanism is conserved in mammalian cells, where LIM domain proteins LIMD1 (Jub homolog) and TRIP6 accumulate at the adherens junctions in response to tension and sequester LATS1/2 (Dutta et al., 2017; Ibar et al., 2018). Another LIM domain protein, Zyxin (Zyx) also sequesters and inhibits Wts downstream of Ft/Ds signaling (Rauskolb et al., 2011), though it is not known whether this mechanism is modulated by mechanical forces. Nonetheless, the involvement of several LIM domain proteins in Hippo signaling is intriguing, since LIM domains are known for their mechanosensitivity. For example, some LIM domains are thought to bind to strained F-actin

bundles (Winkelman et al., 2020; Anderson et al., 2021; Germain et al., 2022). In vitro, purified LIM domains of some proteins, such as Zyx and Paxillin, display increased association with F-actin in the presence of myosin II and accumulate to F-actin regions that are under high stress (Winkelman et al., 2020). Future investigation of LIM domain proteins, such as through proteomic analyses followed by genetic manipulations, could provide a better mechanistic understanding of how mechanical forces influence Hippo signaling and growth.

While the role of mechanical stimuli in the regulation of Hippo signaling are now widely recognized, we still know very little about how upstream components of the Hippo pathway are affected by forces. Among the upstream Hippo pathway regulators, only mammalian Mer was found to be regulated by cell-cell or cell-ECM transmitted forces. A study mentioned above suggested that force generation at focal adhesions can silence Mer via PAK1/ILK mediated mechanism (Chakraborty et al., 2017). PAK1-mediated inhibition of Mer is also important for contact inhibition of growth, where Mer is thought to interact with CD44 and suppress growth by inhibiting Rac activity (Morrison et al., 2001; Okada et al., 2005). How mechanical forces regulate other upstream components such as Crb, Ft, Ds, Ex, or Kib remains unknown.

Mechanical feedback, Hippo signaling, tissue growth control

As discussed earlier, the mechanical feedback model proposes that mechanical heterogeneity due to differential growth could regulate cell proliferation, thus requiring a mechanism by which tension promotes and compression inhibits growth (Shraiman, 2005; Aegerter-Wilmsen et al., 2007, 2012). Specifically, the model predicts that a somatic mosaic clone that proliferates faster than the surrounding tissue would be compressed, and the compressive forces could inhibit growth (Shraiman, 2005). The negative regulation of Hippo signaling (and therefore, positive

Figure 1.9: Hippo signaling as a mediator of mechanical feedback and tissue growth.

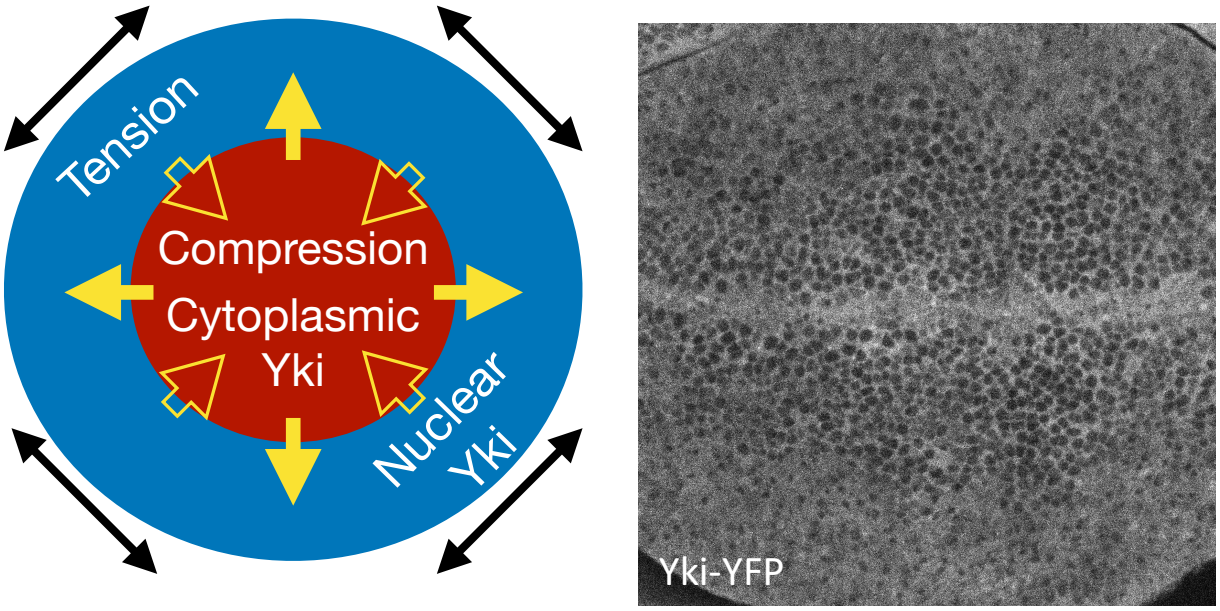

Left: The mechanical feedback model predicts that tension at the tissue periphery can promote growth and compensate for the lack of morphogens, whereas compression at the center of the tissue could suppress growth. If Hippo signaling mediates the crosstalk between mechanical forces and growth, then Yki should be more nuclear at the tissue periphery and more cytoplasmic at the center.

Right: A live image of a third instar larval wing imaginal disc pouch endogenously expressing Yki-YFP. Consistent with the mechanical feedback model, Yki is predominantly nuclear at the tissue periphery and more cytoplasmic at the center (as seen by the darker nuclei in the center of the pouch).

regulation of Yorkie/YAP/TAZ and growth) by tension provides a potential mechanism linking mechanical forces to tissue growth. A study in *Drosophila* tested the potential role of Yki in the regulation of growth via mechanical feedback by examining the effect of differential growth on Yki activity in somatic mosaic clones ectopically expressing an oncogenic micro-RNA *bantam* (bantam clones). Consistent with the model, the fast growing bantam clones were compressed by the surrounding wild-type cells and displayed decreased cortical myosin and Jub accumulation as well as lower junctional tension (Pan et al., 2016). Strikingly, the compressive forces generated by the differential growth were sufficient to suppress nuclear Yki localization and downregulate the expression of Yki target genes (Pan et al., 2016).

Another prediction of the mechanical feedback model, as was discussed earlier, is that early in development growth should be higher in the center of the wing imaginal disc (due to higher morphogen concentration). However, as the wing disc grows, tension at tissue periphery will promote growth to compensate for the lack of morphogens, whereas compression in the center of the wing disc will counteract the growth induced by morphogens. This prediction suggests that nuclear Yki localization may also change throughout the wing disc growth (Fig. 1.9). Consistent with the model, analysis of Yki localization during wing disc development revealed that Yki is nuclear across the tissue in the early stages of wing disc growth, but as the tissue becomes larger, Yki gradually becomes predominantly nuclear at the periphery and mostly cytoplasmic at the center of the tissue (Pan et al., 2018, and Fig. 1.9).

A recent study also found that Yki can localize at the cell cortex in a tension-dependent manner, where it promotes myosin activity via a myosin light chain kinase called Stretchin-MLCK (Xu et al., 2018). This suggests a feed-forward mechanism, whereby Yki could amplify its own activity under higher tension, such as at the wing disc periphery. Together, these studies

strongly support the role of Hippo signaling in mediating tissue growth via the mechanical feedback. Future challenges will be to identify additional mechanisms by which tissue mechanics can regulates Hippo signaling and how such mechanisms could pattern growth across developing epithelia.

1.9 Concluding remarks and dissertation outline

Since the discovery of the Hippo pathway, much progress has been made in understanding the molecular mechanisms that govern the regulation of the core Hippo kinase cassette and its downstream transcriptional effector Yki/YAP/TAZ. We are also now beginning to understand that unlike other signaling pathways that contain a dedicated receptor/ligand pair, the Hippo pathway is regulated by the features of epithelial architecture, including the polarized cortex, cell-cell adhesion, and mechanotransduction. However, how these features ultimately regulate the subcellular organization and activity of the upstream Hippo pathway components remains poorly understood. Specifically, how can a cell dynamically regulate multiple parallel upstream inputs into the same signaling pathway in a distinct manner? Ultimately, such regulation must be achieved via basic cell biological means, such as control of protein localization, posttranslational modifications, and abundance.

In this dissertation, I will focus on the regulation of Kib, a key upstream activator of the Hippo pathway. In Chapter 2, which has already been published (Tokamov et al., 2021), I will describe a mechanism whereby Kib is targeted for ubiquitin-mediated degradation when it assembles a signaling complex. In Chapter 3, I will demonstrate that the degradation mechanism described in Chapter 2 is regulated by actomyosin-generated tension. In Chapter 4, I further investigate the subcellular relationship between Kib and actomyosin organization and show that

actomyosin dynamics promote apicomedial Kib localization. In the appendices, I provide supportive evidence that Kib associates with the actomyosin cytoskeleton in other contexts, including the *Drosophila* embryonic ventral furrow and larval body wall muscles, and that the apical polarity network tethers Kib at the junctional cortex of wing imaginal disc cells. Collectively, my work reveals the mechanisms that govern the regulation and organization of a key upstream inputs into the Hippo pathway and provide a framework for future investigations of cell signaling by actomyosin dynamics, mechanical cues, and polarity.

CHAPTER 2

Negative feedback couples Hippo pathway activation with Kibra degradation independently of Yorkie-mediated transcription

2.1 Introduction

How organs achieve and maintain optimal size is a fundamental question in developmental biology. The Hippo signaling pathway is an evolutionarily conserved inhibitor of tissue growth that was first identified in *Drosophila* in somatic mosaic screens for tumor-suppressor genes (Xu et al., 1995; Tapon et al., 2002; Harvey et al., 2003; Wu et al., 2003). Central to the Hippo pathway activity is a kinase cassette that includes serine/threonine kinases Tao-1, Hippo (Hpo), and Warts (Wts), as well as two scaffolding proteins Salvador (Sav) and Mob as tumor suppressor (Mats). Activation of the Hippo pathway results in a kinase cascade that culminates in the phosphorylation of a transcriptional co-activator Yorkie (Yki) by Wts, which inhibits Yki nuclear accumulation. Conversely, inactivation of the Hippo pathway allows Yki to translocate into the nucleus where, together with its DNA-binding partners such as Scalloped (Sd), it promotes transcription of pro-growth genes. As a result, inactivation of the Hippo pathway is characterized by excessive tissue growth. Mutations that disrupt Hippo pathway activity can lead to various human disorders including benign tumors and carcinomas (Zheng and Pan, 2019).

A distinct feature of the Hippo pathway is the remarkably complex organization of its upstream regulatory modules (Fulford et al., 2018). The core Hippo kinase cascade is regulated from the cell cortex by multiple upstream components, including Fat (Ft), Dachsous (Ds), Echinoid (Ed), Expanded (Ex), Crumbs (Crb), Kibra (Kib) and Merlin (Mer). Broadly speaking, these components localize either exclusively junctionally (a term that we use to include both the

adherens junctions and the marginal zone; Tepass, 2012) or both junctionally and at the apical medial cortex (Su et al., 2017). Ft and Ds are protocadherins that promote Hippo pathway activity from the junctions by restricting the activity of Dachs, an atypical myosin that inhibits Wts (Bennett and Harvey, 2006; Cho et al., 2006; Mao, 2006; Matakatsu and Blair, 2012; Vrabioiu and Struhl, 2015). Ed is a cell-cell adhesion protein that binds and stabilizes Sav at the junctional cortex, thereby enabling Sav to promote Hippo pathway activity (Yue et al., 2012). Ex is a FERM-domain protein that also localizes at the junctional cortex where it binds to the transmembrane protein Crb and activates the Hippo pathway by recruiting the core kinase cassette (Hamaratoglu et al., 2006; Ling et al., 2010; Robinson et al., 2010; Sun et al., 2015). The WW-domain protein Kib and FERM-domain protein Mer localize both at the junctional and apical medial cortex and promote Hippo pathway activity by recruiting the core kinase cassette independently of Ex (Yu et al., 2010; Baumgartner et al., 2010; Genevet et al., 2010; Hamaratoglu et al., 2006; Su et al., 2017). The existence of multiple upstream regulatory modules that converge to control the activity of a single downstream effector, Yki, raises a question of whether and how these parallel inputs are regulated and to what extent they are distinct from one another.

One way that cells modulate signaling output is by controlling the levels of signaling components. Within the Hippo pathway, transcription of Ex, Kib, and Mer is positively regulated by Yki activity in a negative feedback loop (Hamaratoglu et al., 2006; Genevet et al., 2010; Yee et al., 2019). Multiple Hippo pathway components are also regulated post-translationally. For example, Crb promotes Ex ubiquitination via Skip/Cullin/F-box^{Slimb} (SCF^{Slimb}) E3 ubiquitin ligase complex, which leads to Ex degradation (Ribeiro et al., 2014; Fulford et al., 2019). Similarly, Ds and Dachs levels are downregulated by the SCF^{Fbxl-7} E3 ubiquitin ligase, and Dachs

stability is also influenced by an E3 ubiquitin ligase called Early girl (Rodrigues-Campos and Thompson, 2014; Misra and Irvine, 2019). Sav stability is also inhibited by the HECT ubiquitin ligase Herc4 (Aerne et al., 2015). These studies underscore the importance of post-translational regulation of Hippo pathway components and suggest that individual signaling branches of the Hippo pathway might be regulated in a distinct manner from one another.

In this study, we reveal that the Hippo pathway negatively regulates Kib levels via post-translational negative feedback. We show that the regulation of Kib levels by the Hippo pathway is independent of Yki- and Sd-mediated transcriptional output and is instead mediated by SCF^{Slimb}. We find that this mechanism operates independently of other upstream inputs, such as Ex/Crb or Ft/Ds, and requires Kib-mediated complex formation. Intriguingly, our data suggest that Kib degradation is regulated by mechanical tension across the wing imaginal tissue. We propose a model in which Kib-mediated Hippo pathway complex formation results in Kib degradation in isolation from other upstream inputs, thereby forming a tightly compartmentalized negative feedback loop. Such feedback may function as a homeostatic mechanism to tightly control signaling output specifically downstream of Kib and ensure proper tissue growth during development.

2.2 Results

Transcriptional feedback is insufficient to explain the increase in Kibra abundance upon pathway inactivation

A notable feature of the Hippo pathway is that its upstream components Kib, Ex, and Mer are upregulated by Yki transcriptional activity in a negative feedback loop (Hamaratoglu et al., 2006; Genevet et al., 2010; Yee et al., 2019). In particular, Kib levels were previously shown to be significantly elevated in double-mutant *Mer; ex* somatic mosaic clones, consistent with the transcriptional feedback regulation of *kibra* by Yki (Genevet et al., 2010). However, when we examined endogenous Kib::GFP in live wing imaginal discs containing either *Mer* or *ex* mutant clones individually, we found that Kib abundance was significantly higher in *Mer* mutant clones than in *ex* mutant clones (Figure 2.1A-C). These results suggest that loss of Mer has a greater effect on Yki transcriptional activity than loss of Ex, which has not been reported previously.

To directly assess the relative contribution of Mer and Ex to Yki activity, we examined the nuclear localization of endogenously expressed Yki-YFP, a biosensor for Yki activity (Su et al., 2017; Xu et al., 2018). In sharp contrast to what we observed with Kib levels, Yki strongly accumulated in the nuclei of *ex* mutant clones, whereas Yki was mostly cytoplasmic and indistinguishable from wild-type cells in *Mer* clones (Figure 2.1D-E’’’). These results indicate that Ex is more potent at inhibiting Yki nuclear translocation than Mer, consistent with Ex’s ability to limit Yki activity by direct sequestration at the junctional cortex (Badouel et al., 2009) and suggesting that loss of *ex* should have a greater effect on pathway target gene expression than loss of *Mer*.

To compare the effects of *Mer* and *ex* loss on target gene expression, we examined the expression of *ban3>GFP* (Matakatsu and Blair, 2012), a reporter for one of Yki’s target genes

Figure 2.1: Transcriptional feedback alone does not explain Kib upregulation in *Mer* clones

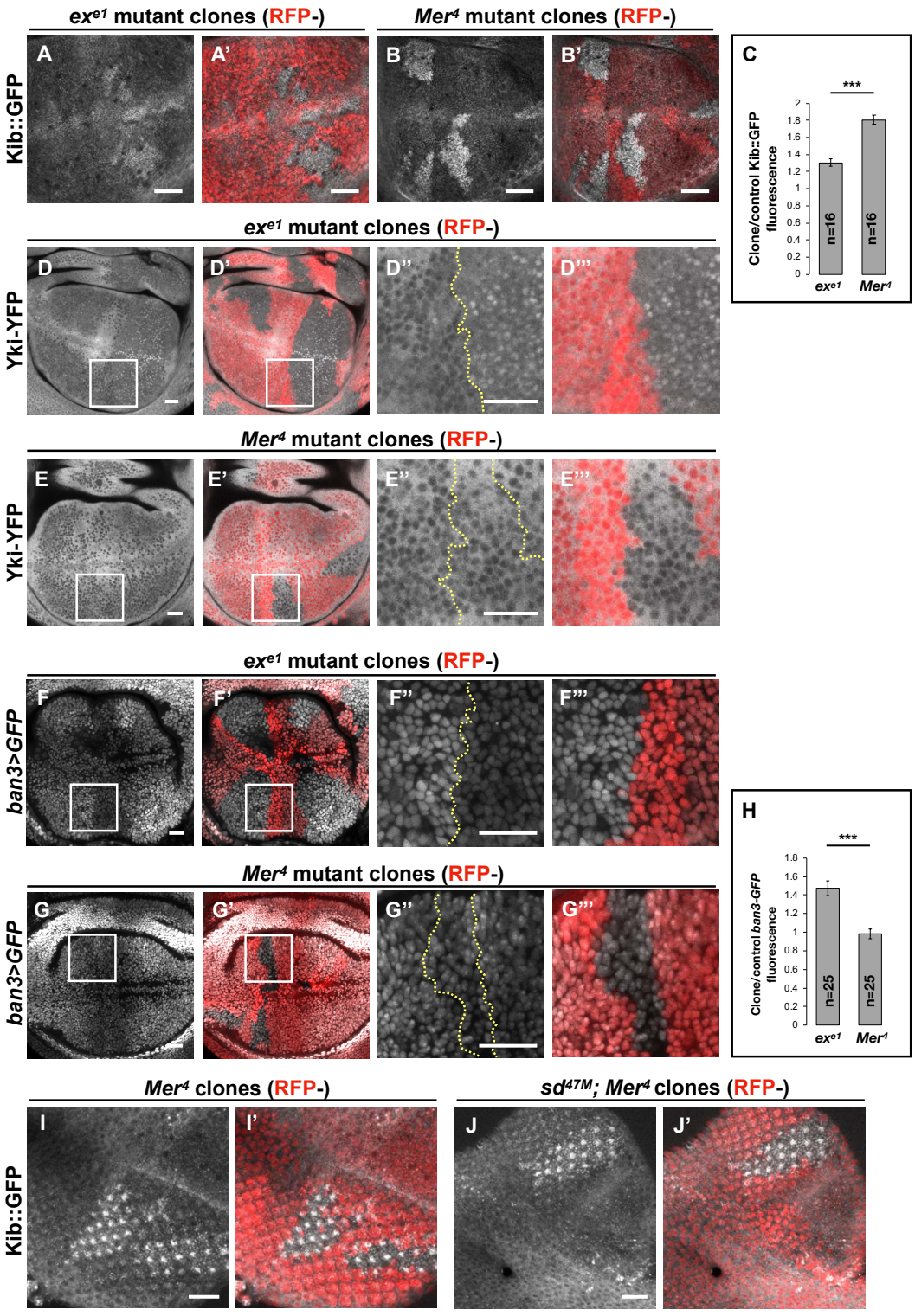

Figure 2.1 continued

(A-G’’’) All tissues shown are living late third instar wing imaginal discs expressing the indicated fluorescent proteins.

(A-C) Endogenous Kib::GFP in *ex* (A and A’) or *Mer* (B and B’) somatic mosaic clones (indicated by loss of RFP). Loss of Mer leads to a greater increase in Kib levels than loss of Ex. Quantification is shown in (C).

(D-E’’’) Endogenously expressed Yki-YFP is strongly nuclear in *ex* mutant clones (D-D’’’) but is mostly cytoplasmic in *Mer* mutant clones (E-E’’’).

(F-H) Expression *ban3>GFP*, a reporter of Yki activity, is elevated in *ex* mutant clones (F-F’’’) but is not detectably affected in *Mer* mutant clones (G-G’’’). Quantification is shown in (H).

I-J’) Endogenous Kib:GFP levels are elevated in single *Mer* somatic mosaic clones (I & I’) and in double *sd; Mer* clones (J & J’). Yellow dashed lines indicate clone boundaries. All scale bars = 20°µm. Quantification in C & H is represented as the mean ± SEM; n = number of clones (no more than two clones per wing disc were used for quantification). Statistical analysis was performed using non-parametric Mann-Whitney U test. Throughout the study, statistical significance is reported as follows: ***$p \leq 0.001$, **$p \leq 0.01$, *$p \leq 0.05$, ns (not significant, $p > 0.05$).

bantam (Thompson and Cohen, 2006; Nolo et al., 2006). *ban3>GFP* expression was significantly upregulated in *ex* mutant clones, whereas no detectible difference was observed in *Mer* clones relative to control tissue (Figure 2.1F-H), indicating that Yki is more active in *ex* clones than in *Mer* clones. Together, these results suggest that the dramatic increase in Kib levels in *Mer* clones cannot be explained strictly by Yki-mediated transcriptional feedback and that Kib is also regulated via a previously unrecognized non-transcriptional mechanism.

Hippo pathway components regulate Kibra abundance non-transcriptionally

If a Yki-independent mechanism is responsible for Kib upregulation in *Mer* clones, then Kib levels should be elevated in *Mer* clones in the absence of Yki activity. To test this hypothesis, we took advantage of a previously published method of blocking Yki-mediated transcription downstream of the Hippo pathway by removing Yki's DNA binding partner, Sd, in the eye imaginal disc, where Sd is dispensable for cell viability (Koontz et al., 2013; Yu and Pan, 2018). Endogenous Kib::GFP was upregulated in *sd; Mer* double mutant clones to a similar degree as in *Mer* single mutant clones (Figure 2.1I-J'), suggesting that Mer regulates Kib levels independently of Yki activity.

To understand how Mer regulates Kib levels, we set out to develop a simpler approach to uncouple Kib protein abundance from its transcriptional regulation. Recently, the *ubiquitin 63E* promoter was used to drive expression of other Hippo pathway components to study their post-translational regulation (Aerne et al., 2015; Fulford et al., 2019), based on the assumption that the ubiquitin promoter is not regulated by Yki activity. Therefore, we made a transgenic fly line ectopically expressing Kibra-GFP-FLAG under control of the ubiquitin promoter (Ubi>Kib-GFP) (Figure 2.2A). Similar to endogenous Kib::GFP, Ubi>Kib-GFP localized both at the

Figure 2.2: Ubi>Kib-GFP is a functional protein

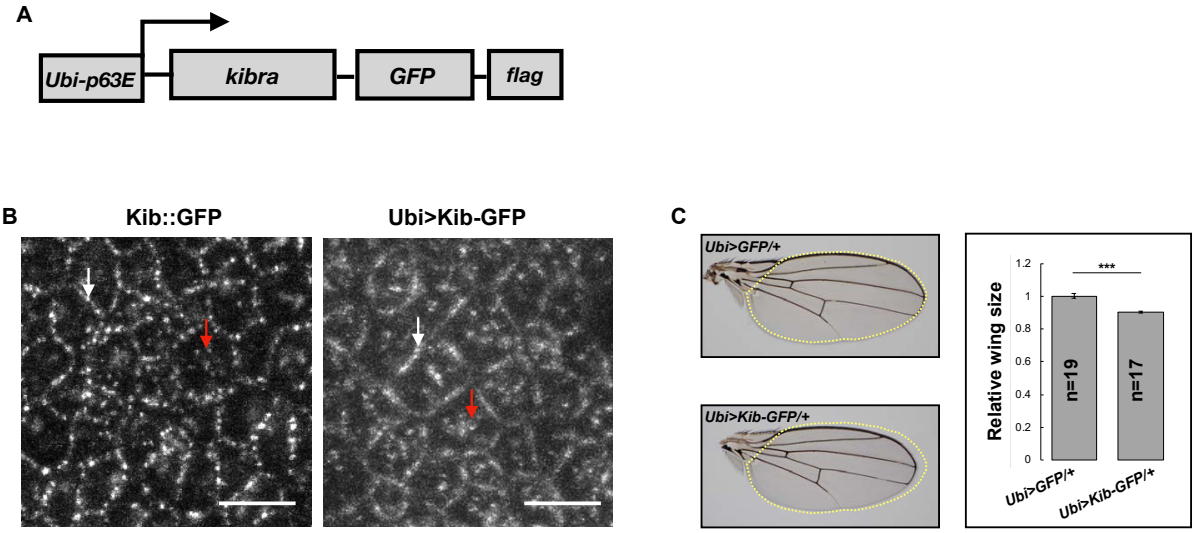

A) A cartoon of the DNA construct used to generate the *Ubi>Kib-GFP* transgenic fly line.
B) Similar to endogenous Kib:GFP (left), Ubi>Kib-GFP (right) accumulates both at the junctional (white arrows) and apical medial cortex (red arrows). Scale bars = 5µm.
C) Size comparison of adult wings from flies expressing *Ubi>GFP* or *Ubi>Kib-GFP*; quantification is shown as the mean ± SEM relative to the control; n = number of wings. Statistical comparison was performed using Mann-Whitney U test.

junctional and medial cortex (Figure 2.2B). Flies expressing Ubi>Kib-GFP had slightly undergrown wings compared to control flies expressing Ubi>GFP (Figure 2.2C), suggesting that Ubi>Kib-GFP promotes Hippo pathway activity. Although wild-type flies expressing Ubi>Kib-GFP were viable, Ubi>Kib-GFP only partially rescued the *kibra*^{del} null allele (not shown, Yu et al., 2010), suggesting that expression from the *Ubiquitin* promoter may not be sufficient in some tissues that require Kib for viability.

Consistent with the hypothesis that Mer negatively regulates Kib levels non-transcriptionally, depletion of Mer in the posterior compartment of the wing disc using the *hh>Gal4* driver led to a substantial increase in Ubi>Kib-GFP levels across the entire compartment (Figure 2.3A). Knockdown of Sav, Hpo, and Wts also dramatically increased Ubi>Kib-GFP levels (Figure 2.3B-D), suggesting that regulation of Kib abundance is not mediated uniquely by Mer but is Hippo pathway dependent. In contrast, expression of a Ubi>RFP control transgene was not affected by depletion of Hpo, confirming that Yki does not regulate expression at the ubiquitin promoter (Figure 2.3E-E''). Ex is also upregulated upon Hippo pathway inactivation, with a particularly strong increase when Hpo or Wts is depleted (Hamaratoglu et al., 2006, and Figure 2.3F-I). Ex and Kib also form a complex in cultured cells (Genevet et al., 2010; Yu et al., 2010), raising the possibility that the increase in Ubi>Kib-GFP levels upon Hpo or Wts depletion is caused by increased interaction with Ex resulting in greater Kib stability. To test this possibility, we compared Ex and Ubi>Kib-GFP levels in *hpo* or *sd; hpo* double mutant clones. While Ubi>Kib-GFP levels were similarly elevated in both *hpo* and *sd; hpo* double mutant clones (Figure 2.4A-A'''), Ex levels were upregulated only in *hpo* single mutant clones but not in *sd; hpo* double mutant clones (Figure 2.4B-B'''), indicating that the increase in Kib levels upon Hippo pathway inactivation is not mediated via Ex. We confirmed

Figure 2.3: The Hippo pathway regulates Kib levels independently from Yki-mediated transcription

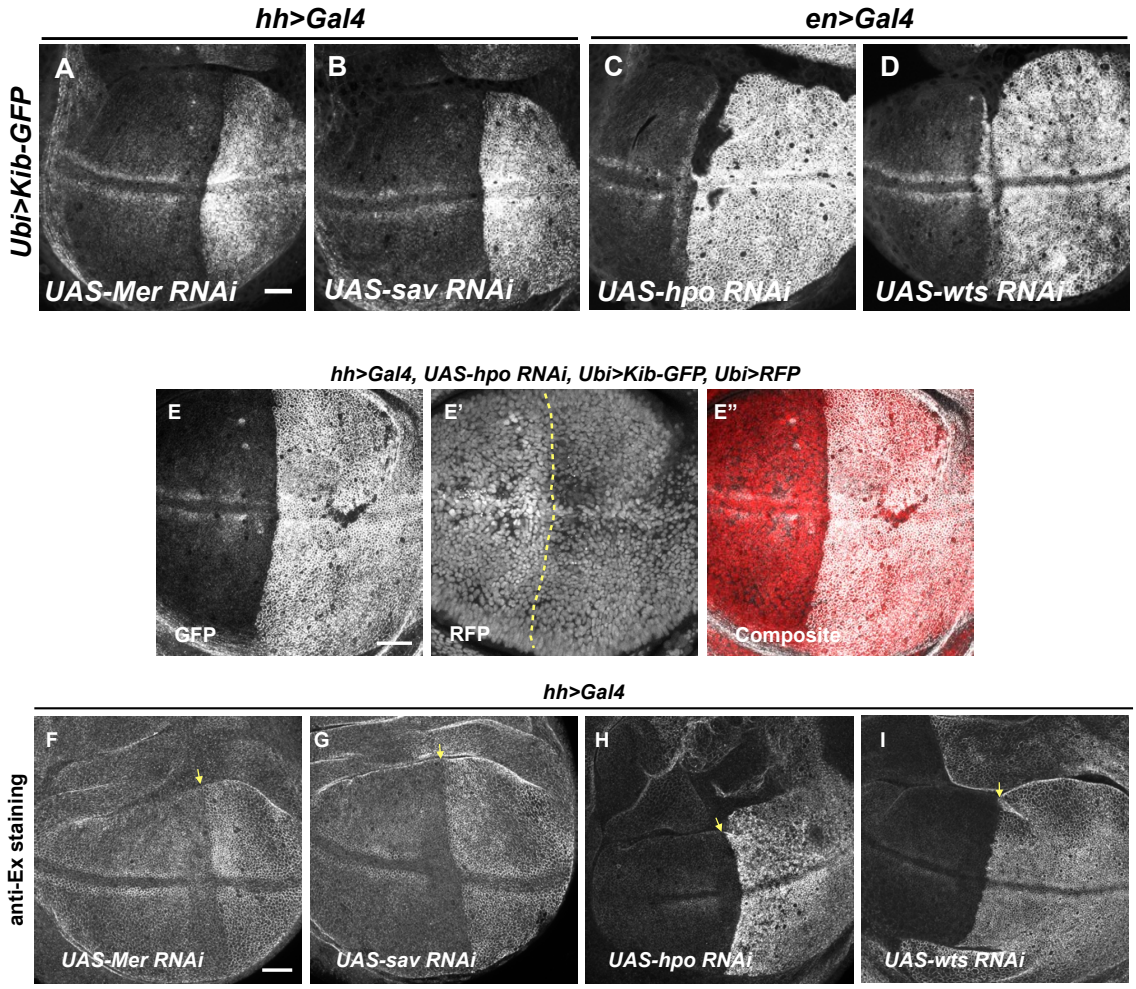

A-D) Depletion of Hippo pathway components Mer, Sav, Hpo and Wts by RNAi in the posterior compartment of the wing results in elevated Kib-GFP levels. Scale bars = 20µm. Throughout the paper, wing imaginal discs are oriented with posterior side to the right and dorsal side up.

E-E'') Depletion of Hpo in the posterior compartment of the wing does not cause increased Ubi>RFP expression. Yellow dashed line indicates the anterior-posterior (A-P) boundary.

F-I) Ex levels are elevated upon Hippo pathway inactivation, with a particularly strong increase upon Hpo or Wts depletion (H & I, respectively).

Figure 2.4: The Hippo pathway regulates Kib levels independently from Yki-mediated transcription

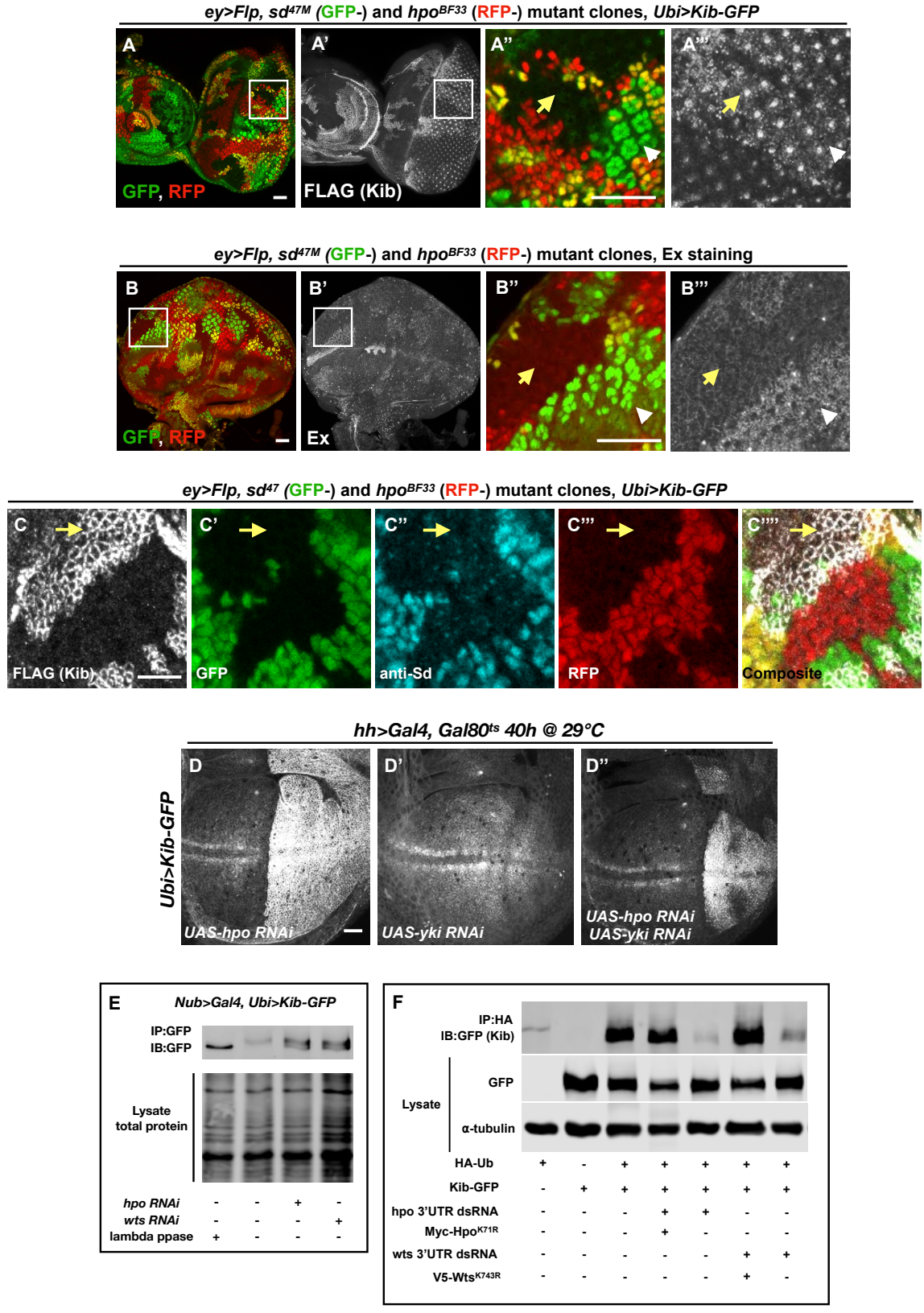

Figure 2.4 continued

A-A’’’) In the eye imaginal disc, Kib-GFP is upregulated both in *hpo* mutant clones and *sd; hpo* double mutant clones, indicating that Hippo pathway activity controls Kib levels independently of Yki/Sd-mediated transcription. White arrowheads indicate *hpo* single mutant clones; yellow arrows indicate *sd; hpo* double mutant clones. Note: the clonal GFP marker (sd^{+}), which is nuclear, is readily distinguishable from Kib-GFP which is apical.

B-B’’’) Ex levels are also upregulated in *hpo* mutant clones; but in contrast to Kib, Ex upregulation is not observed in *sd; hpo* double mutant clones. Scale bars in A-B’’’ = 20µm.

C-C’’’’) Single *sd* (GFP-) or *hpo* (RFP-) somatic mosaic clones or double *sd; hpo* clones (GFP- and RFP-, yellow arrow) induced in the eye imaginal disc using *ey>Flp.* Ubi>Kib-GFP (FLAG staining) is upregulated in *sd; hpo* double mutant clones; loss of *sd* was confirmed by anti-sd staining (cyan). Scale bar = 10µm.

D-D’’) Effect of transient depletion of Hpo (D), Yki (D’), or Hpo and Yki (D’’) on Ubi>Kib-GFP levels in the posterior compartment of the wing using $Gal80^{ts}$. Scale bar = 20µm.

E) Kib is phosphorylated in wing discs, and depletion of Hpo or Wts leads to decreased Kib phosphorylation.

F) Kib is ubiquitinated in S2 cells. Depletion of Hpo or Wts with dsRNA targeting 3’-UTR of each kinase leads to decreased Kib ubiquitination; the effect of Hpo or Wts knockdown is rescued by addition of kinase-dead Hpo^{K71R} or Wts^{K743R}. Throughout this chapter, all immunoblot data are representative of at least three replicates.

via immunostaining that the double-mutant clones completely lacked Sd (Figure 2.4C-C’’’’). Furthermore, transient co-depletion of Hpo and Yki in the wing disc posterior compartment using Gal80^{ts} did not suppress the increase in Kib abundance observed when Hpo alone was depleted, even though Yki was sufficiently depleted to suppress tissue overgrowth induced by Hpo depletion (Figure 2.4D-D’’). Together, these results provide strong evidence that the Hippo pathway regulates Kib levels independently of Yki transcriptional output.

The Hippo pathway promotes Kibra phosphorylation and ubiquitination

Our observation that Hippo pathway activity controls Kib levels in a Yki-independent manner suggests that Kib could be regulated post-translationally. Protein abundance is commonly regulated by phosphorylation-dependent ubiquitination, and multiple Hippo pathway components are regulated via ubiquitin-mediated proteasomal degradation (Ribeiro et al., 2014; Rodrigues-Campos and Thompson, 2014; Cao et al., 2014; Aerne et al., 2015; Ma et al., 2018; Ly et al., 2019). Therefore, we hypothesized that the Hippo pathway could promote Kib phosphorylation and target it for ubiquitination and subsequent degradation.

We first asked whether Kib is phosphorylated in a pathway dependent manner *in vivo*. To this end, we examined the phosphorylation state of Kib-GFP in wing imaginal discs depleted for either Hpo or Wts using a gel shift assay. In wild-type controls, phosphatase treatment of immunoprecipitated Kib-GFP resulted in increased mobility and coalescence into a single band, suggesting that Kib is normally phosphorylated (Figure 2.4E). Depletion of either Hpo or Wts resulted in a faster migrating Kib band that aligned with phosphatase-treated Kib (Figure 2.4E), suggesting that Kib is phosphorylated in a pathway-dependent manner *in vivo*.

Next, we asked if Kib is ubiquitinated and, if so, whether this depends on Hippo pathway activity. To address this question, we expressed Kib-GFP and HA-tagged ubiquitin in cultured Drosophila S2 cells. We found that Kib was ubiquitinated and that depletion of the core pathway kinases Hpo or Wts resulted in dramatically decreased Kib ubiquitination (Figure 2.4F). Taken together, these results suggest that Kib is phosphorylated and ubiquitinated in a Hippo pathway dependent manner and that these posttranslational modifications promote its degradation.

Slimb regulates Kibra levels via a consensus degron motif

To better understand how the Hippo pathway controls Kib levels via ubiquitination, we sought to identify the machinery that mediates this process. Protein ubiquitination occurs via an enzymatic cascade that culminates in the covalent attachment of ubiquitin molecules to substrates by E3 ubiquitin ligases (Zheng and Shabek, 2017). We first tested the effects of depletion or overexpression of E3 ubiquitin ligases previously reported to act within the Hippo pathway on Ubi>Kib-GFP abundance (Figure 2.5A-D). Of these, only depletion of the F-box protein Slimb, and its partners SkpA and Cul1, increased Ubi>Kib-GFP levels (Figure 2.5B-D). Importantly, increased Ubi>Kib-GFP was evident throughout the affected cells in comparison to control tissue (Figure 2.5B & B'), suggesting that overall Kib abundance was increased. Because loss of Slimb increases Ex levels (Ribeiro et al., 2014) and Ex interacts with Kib in cultured cells (Genevet et al., 2010; Yu et al., 2010), we considered the possibility that increased Ubi>Kib-GFP upon Slimb depletion could result indirectly from ectopic interactions with increased Ex. However, co-depletion of Ex and Slimb did not suppress the increase in Ubi>Kib-GFP levels (Figure 2.5E-G'), suggesting that Slimb directly regulates Kib abundance.

Figure 2.5: Effect of different E3 ubiquitin ligases on Kib levels

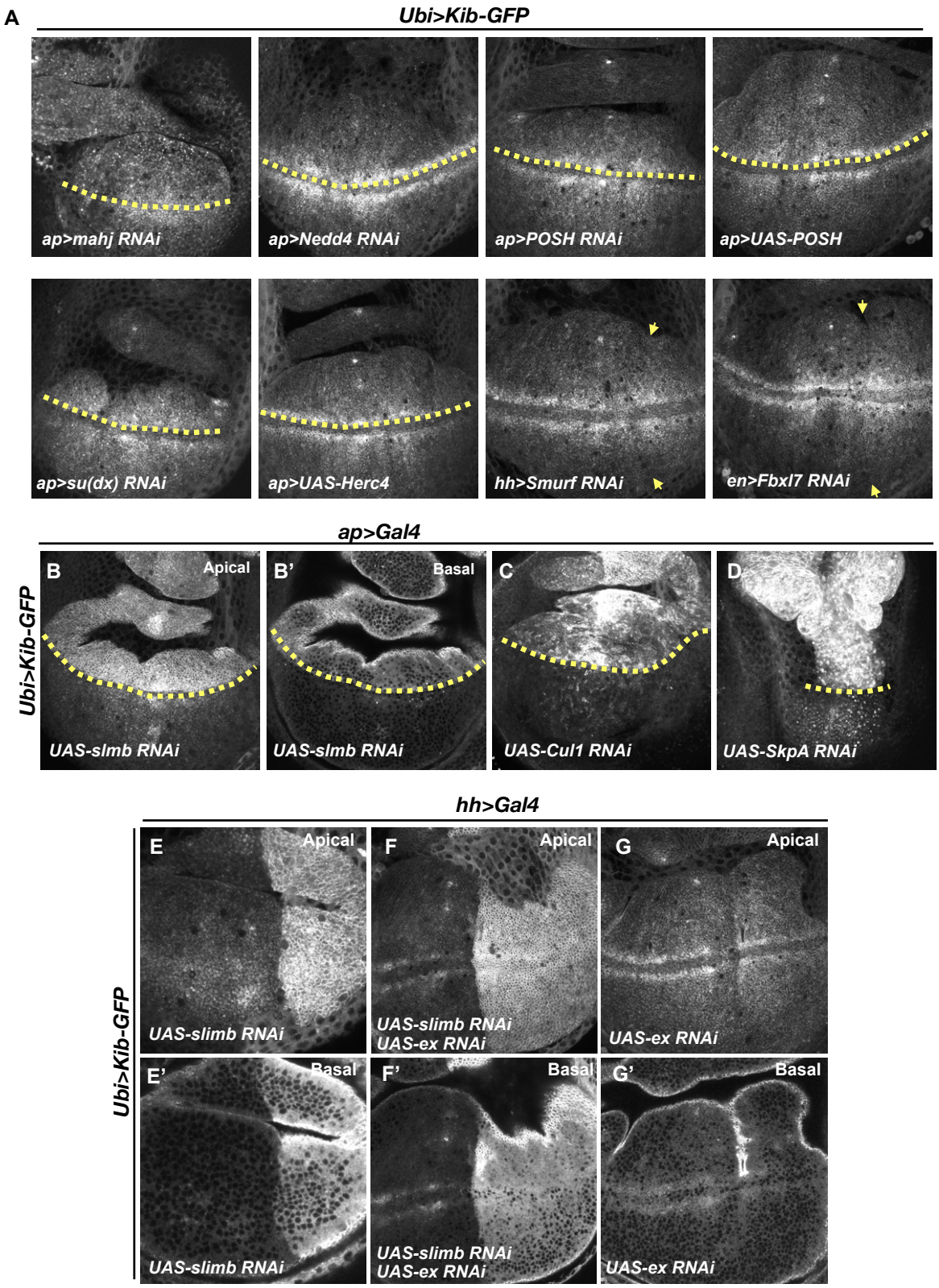

Figure 2.5 continued

A) Depletion or overexpression of other E3 ubiquitin ligases known to regulate Hippo pathway components has no effect on Ubi>Kib-GFP levels. Yellow dashed line represents the dorsal-ventral boundary, with dorsal side up (for ap>Gal4); yellow arrows indicate the anterior-posterior boundary, with posterior to the right (for hh and en>Gal4).

B-D) Depletion of SCF^{Slimb} E3 ubiquitin ligase components Slimb (B), Cul1 (C), or SkpA (D) in the dorsal compartment of the wing imaginal disc results in increased Ubi>Kib-GFP levels.

E-G') Ubi>Kib-GFP levels are elevated upon depletion of Slimb alone or co-depletion of Slimb and Ex, but not when Ex alone is depleted in the posterior compartment of the wing imaginal disc.

Slimb is a homolog of the mammalian β-TrCP that functions as a substrate-targeting component of the SCF E3 ubiquitin ligase complex by recognizing a consensus degron motif on target proteins (Skaar et al., 2013). Kib contains a conserved single stretch of amino acids ^{676}DSGVFE^{681} that matches the consensus Slimb degron (Figure 2.6A). If Slimb regulates Kib stability via the degron, then we predict that 1) Kib ubiquitination should be Slimb-dependent, 2) Slimb should physically interact with Kib via the degron, 3) mutation of the degron site should diminish Kib ubiquitination, and 4) the degron mutant Kib should display greater stability than wild-type Kib. Using S2 cells, we found that depletion of Slimb severely reduces Kib ubiquitination and that Kib and Slimb formed a complex (Figure 2.6B-C). Additionally, mutating a serine residue in Kib (Kib^{S677A}) known to be important for proper substrate recognition by Slimb (Hart et al., 1999; Rogers et al., 2009; Morais-de-Sá et al., 2013; Ribeiro et al., 2014) significantly reduced both Slimb-Kib interaction (Figure 2.6C) and Kib ubiquitination (Figure 2.6D).

To assess the effects of the degron mutation on protein stability *in vivo*, we generated wild-type and Kib^{S677A} transgenes inserted at identical genomic positions. For these experiments we used the UASp promoter (Rørth, 1998), which expresses at lower levels in somatic tissues than UASt (attempts to generate a transgenic line expressing Kib^{S677A} under the ubiquitin promoter were unsuccessful, presumably because ubiquitous expression of a stabilized form of Kib is lethal). Kib^{S677A}-GFP accumulated to much greater levels than wild-type Kib-GFP when expressed in the wing disc pouch using the *nub>Gal4* driver (Figure 2.6E-G). Confocal imaging revealed that while Kib-GFP and Kib^{S677A}-GFP had similar localizations apically, Kib^{S677A}-GFP displayed bright foci in basal tissue sections (Figure 2.6H-I'), presumably due to protein aggregation caused by higher Kib levels. Consistent with the observed increased protein

Figure 2.6: Slimb regulates Kib abundance via a consensus degron

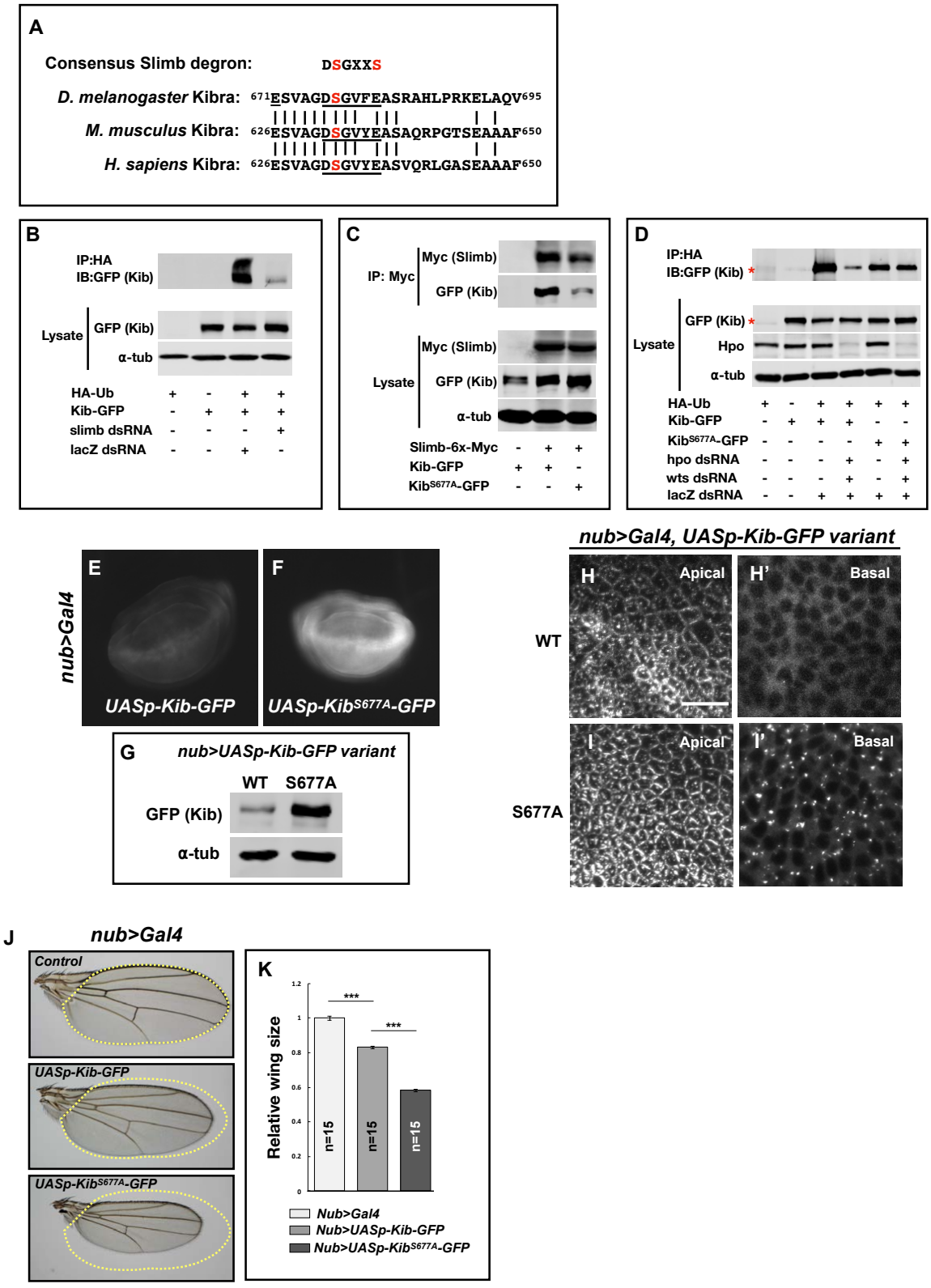

Figure 2.6 continued

A) Alignment of the fly, mouse, and human Kib protein sequences showing the conservation of the putative Slimb degron motif DSGXXS (underlined). The vertical lines indicate conserved residues.

B) Immunoblot showing that depletion of Slimb in S2 cells decreases Kib ubiquitination.

C) Co-IP experiments showing that Kib forms a complex with Slimb in S2 cell lysates in a degron-dependent manner.

D) Ubiquitination of the degron mutant, Kib^{S677A}, is diminished and is insensitive to Hippo pathway inactivation. Asterisks indicate non-specific bands.

E-F) Widefield fluorescence images of wing discs expressing either *UASp-Kib-GFP* (E) or *UASp-Kib^{S677A}-GFP* (F) with the *nub>Gal4* driver; images were taken using identical settings.

G) Immunoblot of wing disc cell lysates (20 discs each) of *UASp-Kib-GFP* or *UASp-Kib^{S677A}-GFP* expressed with the *nub>Gal4* driver.

H-I') Confocal images of Kib-GFP or Kib^{S677A}-GFP expressed under UASp control with nub>Gal4. Kib^{S677A}-GFP shows similar localization to Kib-GFP apically but Kib^{S677A}-GFP forms foci basally. Note that images in I and I' were taken at lower gain than images in H and H' to avoid saturation. Scale bars = 10μm.

J-K) Ectopic expression of Kib^{S677A}-GFP in the wing results in stronger growth suppression than expression of wild-type Kib-GFP. Quantification of wing sizes in (I) is represented as mean ± SEM relative to the control; n = number of wings (one wing per fly). Statistical comparison was performed using the One-way ANOVA test followed by Tukey's HSD test.

abundance, expression of Kib^{S677A}-GFP under the *nub>Gal4* driver led to significantly smaller adult wings than did wild-type Kib-GFP (Figure 2.6J-K). We presume this was because of increased Kib-driven upstream pathway activity, though we have not demonstrated this directly. Collectively, these results indicate that Slimb regulates Kib stability *in vivo*.

The Hippo pathway regulates Kibra abundance via Slimb

To this point, our results identify both the Hippo pathway and Slimb as regulators of Kib abundance, but they do not resolve whether the two mechanisms act in parallel or together. We reasoned that if Slimb regulates Kib levels in parallel to the Hippo pathway, then loss of pathway components in tissue expressing Kib^{S677A} would have an additive effect on Kib levels. Conversely, if Hippo pathway components regulate Kib abundance via Slimb, then Kib^{S677A} should be insensitive to pathway inactivation. We first tested the effect of depleting Hippo pathway components on ubiquitination of Kib^{S677A}. In striking contrast to wild-type Kib, ubiquitination of Kib^{S677A} was not sensitive to depletion of Hpo and Wts (Figure 2.6D), suggesting that the Hippo pathway promotes Kib degradation via Slimb-mediated ubiquitination.

To test if the Hippo pathway promotes Kib degradation via Slimb *in vivo*, we induced *Mer* mutant clones in wing imaginal discs expressing either wild-type Kib-GFP or Kib^{S677A}-GFP under the *nub>Gal4* driver. Similar to endogenous Kib (Figure 2.1B) or Kib expressed by the ubiquitin promoter (Figure 2.3A), UASp-Kib-GFP was dramatically upregulated apically and basally in *Mer* clones relative to control cells (Figure 2.7A-C', G). In contrast, Kib^{S677A}-GFP appeared only mildly apically stabilized in *Mer* clones (Figure 2.7D-E'), with no detectible difference in basal Kib^{S677A}-GFP levels between the clone and control cells (Figure 2.7F-F', H). Taken together, these results indicate that the Hippo pathway regulates Kib levels via the degron

Figure 2.7: The Hippo pathway regulates Kib abundance via a putative degron motif

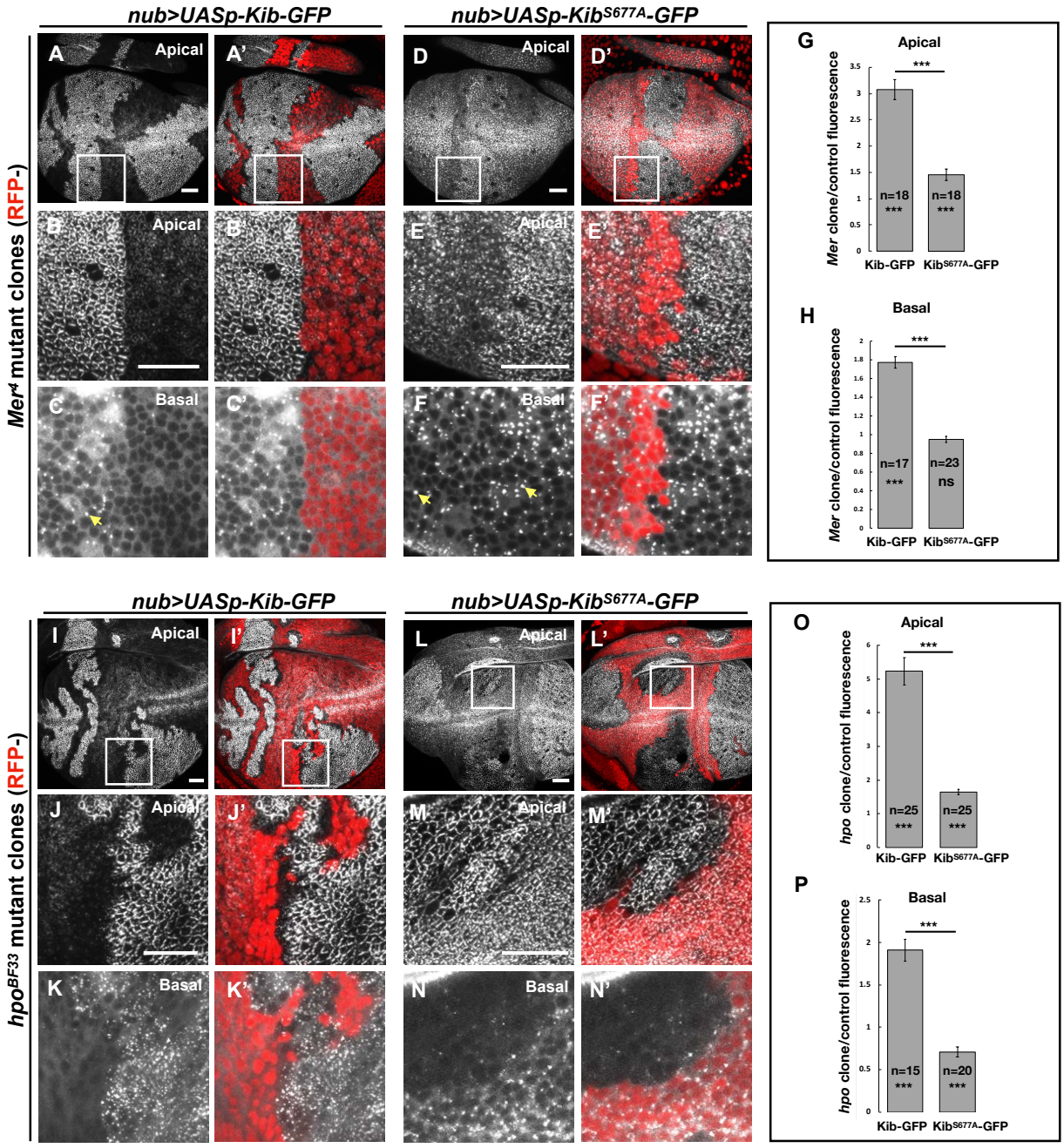

Figure 2.7 continued

A-F') *Mer* somatic mosaic clones in wing discs expressing either *UASp-Kib-GFP* (A - C') or *UASp-Kib^{S677A}-GFP* (D-F') with the *nub>Gal4* driver. Note that wild-type Kib-GFP is significantly elevated in *Mer* clones both apically and basally, while Kib^{S677A}-GFP is only slightly stabilized apically and is not affected basally. Yellow arrows in C and F point to presumed Kib aggregates due to increased abundance. All scale bars = 20□m.

G-H) Quantification of clone/control ratio of apical (G) and basal (H) Kib-GFP fluorescence. All quantification is represented as the mean ± SEM; asterisks above the plots show p-values between the transgenes; asterisks inside each bar show p-values for each transgene with respect to 1; n = number of clones (no more than two clones per wing disc were used for quantification). Statistical comparison was performed using Mann-Whitney U test.

I-N') *hpo* somatic mosaic clones in wing discs expressing either *UASp-Kib-GFP* (I-K') or *UASp-Kib^{S677A}-GFP* (L-N') with the *nub>Gal4* driver. Note that wild-type Kib-GFP levels are significantly elevated in *hpo* clones both apically and basally, while Kib^{S677A}-GFP is stabilized apically but depleted basally in *hpo* clones.

O-P) Quantification of clone/control ratio of apical (O) and basal (P) Kib-GFP fluorescence.

motif. Interestingly, in *Mer* clones but not in control cells, Kib-GFP also formed bright aggregate-like foci basally (Figure 2.7C), similar to Kib^{S677A}-GFP (Figure 2.6I'), suggesting these foci form as a result of high Kib levels.

The slight apical stabilization of Kib^{S677A}-GFP in *Mer* clones could be caused by two possibilities that are not mutually exclusive: 1) Slimb could still weakly bind Kib^{S677A}-GFP and promote its degradation, albeit with reduced efficiency, and 2) loss of Hippo pathway activity could lead to greater cortical Kib accumulation at the expense of the total cytoplasmic pool. In support of the first possibility, Kib^{S677A}-GFP weakly associated with Slimb (Figure 2.6C) and was still slightly ubiquitinated in S2 cells (Figure 2.6D). To ask whether the mild apical accumulation of Kib^{S677A}-GFP in *Mer* clones could also be caused by cortical recruitment, we examined Kib in tissues lacking Hpo, which resulted in stronger junctional accumulation of Ubi>Kib-GFP than loss of Mer (Figure 2.3C). Strikingly, whereas wild-type Kib-GFP increased both apically and basally in *hpo* clones (Figure 2.7I-K' , O), Kib^{S677A}-GFP increased apically but decreased basally in *hpo* clones (Figure 2.7L-N', P). These results suggest that the stabilization of Kib^{S677A}-GFP observed upon Hippo pathway inactivation is, at least in part, due to the recruitment of Kib apically, where it might be stabilized in a protein complex.

The Hippo pathway promotes Kibra degradation in a highly compartmentalized manner and independently of pathway activation by Expanded

Previous work showed that Ex interacts with Kib in S2 cells and suggested that Kib and Ex function in a complex to regulate the Hippo pathway (Yu et al., 2010; Genevet et al., 2010). In contrast, *in vivo* studies suggest that Kib functions in parallel to Ex and its partner Crb to regulate activity of the downstream kinase cascade (Baumgartner et al., 2010; Yu et al., 2010; Su et al.,

2017). Given these observations, we wondered whether loss of Ex or Crb would result in elevated Ubi>Kib-GFP abundance similar to the loss of Mer, Sav, Hpo, or Wts. To our surprise, depletion of Ex and Crb, either individually or together, had no detectable effect on Ubi>Kib-GFP levels (Figure 2.8A-C'). Moreover, reducing Hippo pathway activity by other means, such as by overexpressing Dachs or depleting Fat, Ds, or the Hpo activator Tao-1 (Boggiano et al., 2011), similarly had no effect on Ubi>Kib-GFP levels (Figure 2.8D-G). On the other hand, knockdown of Mats or Kib's binding partner, Pez (Poernbacher et al., 2012), increased Ubi>Kib-GFP levels (Figure 2.8H-I). These results suggest that upstream regulation of the Hippo pathway is highly compartmentalized and that Kib degradation is promoted specifically via the pathway components it associates with during Hippo pathway activation.

This parallel behavior of Hippo pathway regulation prompted us to ask whether increasing the activity of one upstream branch of the pathway can substitute for the loss of another. To test this idea, we asked if the Ubi>Kib-GFP transgene, which causes mild undergrowth in a wild-type background (Figure 2.2C), can suppress the lethality of ex^{e1}, a null allele (Boedigheimer and Laughon, 1993). Ubi>Kib-GFP strongly suppressed ex^{e1} lethality, producing viable and fertile adult flies at expected frequencies (Figure 2.8J) that completely lacked Ex protein (Figure 2.8K-L'). Homozygous *ex^{e1}; Ubi>-Kib-GFP/+* flies had significantly larger wings than heterozygotes (Figure 2.8M-N), but otherwise were phenotypically normal. Together, these results establish that Kib and Ex signal in parallel to regulate at least some aspects of pathway activity.

Figure 2.8: Kib abundance is regulated independently of Expanded or other upstream Hippo components

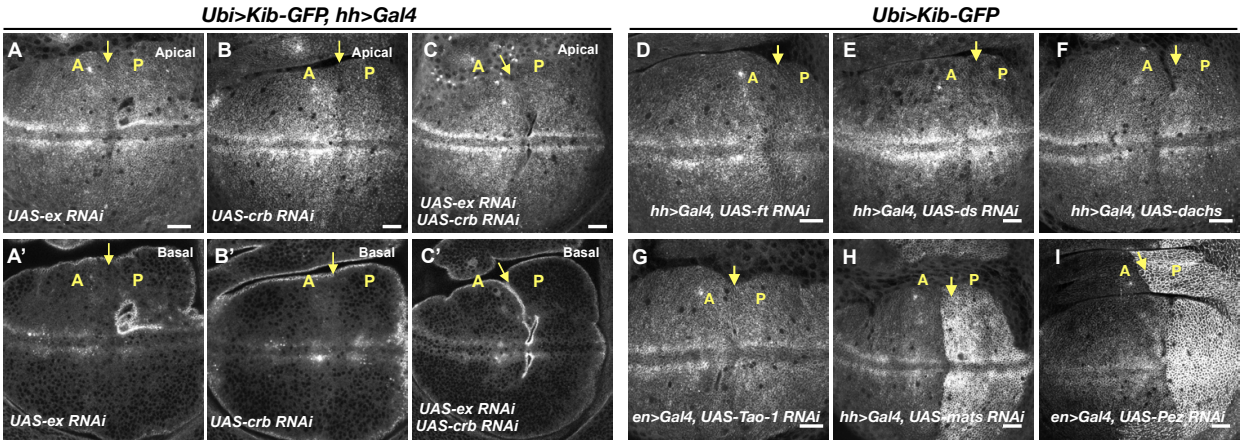

J

ex^{e1}/CyO; Ubi>Kib-GFP/TM6 X ex^{e1}/CyO; Ubi>Kib-GFP/TM6

F_1 progeny	Observed	Expected
ex^{e1}/CyO; Ubi>Kib-GFP/TM6	55	51
ex^{e1}/ex^{e1}; Ubi>Kib-GFP/TM6	21	25

$X^2 = 0.95$

$p = 0.31$

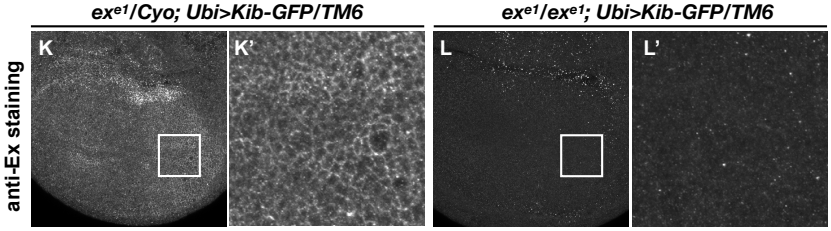

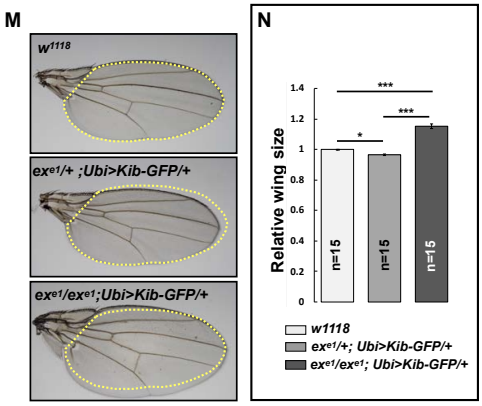

Figure 2.8 continued

A-C') Depletion of Ex (A & A'), Crb (B & B'), or both Ex and Crb (C & C') in the posterior wing imaginal disc does not affect Ubi>Kib-GFP abundance. Yellow arrows indicate the anterior-posterior (A-P) boundary. Scale bars = 20μm.

D-I) Inactivation of the Hippo pathway by other means such as depletion of Ft (D) or Ds (E), overexpression of Dachs (F), or depletion of Tao-1 (G) has no effect on Kib levels. In contrast, loss of components that association with Kib signaling complex such as Mats (H) and Pez (I) leads to an increase in Kib levels.

J) Ectopic Kib suppresses ex^{e1} lethality. Chi-square analysis shows that ex^{e1} homozygotes survive as expected if ectopic Kib completely suppresses *ex* lethality.

K-L') Wing discs of ex^{e1} heterozygous larvae (K & K') or ex^{e1} homozygous larvae (L & L') carrying *Ubi>Kib-GFP* were stained for Ex to confirm the absence of Ex protein.

M-N) Adult wings of w^{1118}, ex^{e1}/+; *Ubi>Kib-GFP*/+, or ex^{e1}/ex^{e1}; *Ubi>Kib-GFP*/+ flies.

Quantification of wing sizes in (N) is represented as the mean ± SEM; n = number of wings (one wing per fly). Statistical comparison was performed using the One-way ANOVA test followed by Tukey's HSD test.

The WW domains of Kibra are essential for its degradation via the Hippo pathway and Slimb

Our discovery that Kib degradation is tightly compartmentalized suggests that complex formation between Kib and other Hippo pathway components might be an important step both for pathway activation and Kib degradation. Indeed, Kib interacts with Sav, Mer, Hpo (via Sav) and Wts in S2 cells (Baumgartner et al., 2010; Genevet et al., 2010; Yu et al., 2010) and can recruit these components to the apical cell cortex *in vivo* (Su et al., 2017). To test this idea, we first asked if the pathway kinases Hpo and Wts play a structural vs. an enzymatic role in promoting Kib ubiquitination. For these experiments, kinase-dead versions of Hpo or Wts (Hpo^{K71R} and Wts^{K743R}, respectively) (Wu et al., 2003; Huang et al., 2005) were transfected into cells depleted of endogenous Hpo or Wts with dsRNA targeted against their 3'-UTRs (the kinase-dead constructs lacked endogenous UTRs). To our surprise, expression of Hpo^{K71R} or Wts^{K743R} restored Kib ubiquitination when the endogenous kinases were depleted, indicating that these kinases promote Kib ubiquitination via complex formation rather than phosphorylation (Figure 2.4F).

Next, we performed a structure/function analysis to map the region in Kib that could mediate complex formation and promote its degradation by the Hippo pathway components. Kib is a multivalent adaptor protein that contains at least seven potential functional regions: two N-terminal WW domains (WW1 and WW2), a C2-like domain, a putative aPKC-binding domain, and three coiled-coil regions (CC1, CC2, and CC3; Figure 2.9A). We generated transgenic fly lines expressing different truncations of Kib-GFP under control of the ubiquitin promoter. Two transgenes, one expressing Kib lacking the C2-like domain and another encoding the first 483

Figure 2.9: Truncation analysis to identify Kib domains responsible for pathway mediated degradation

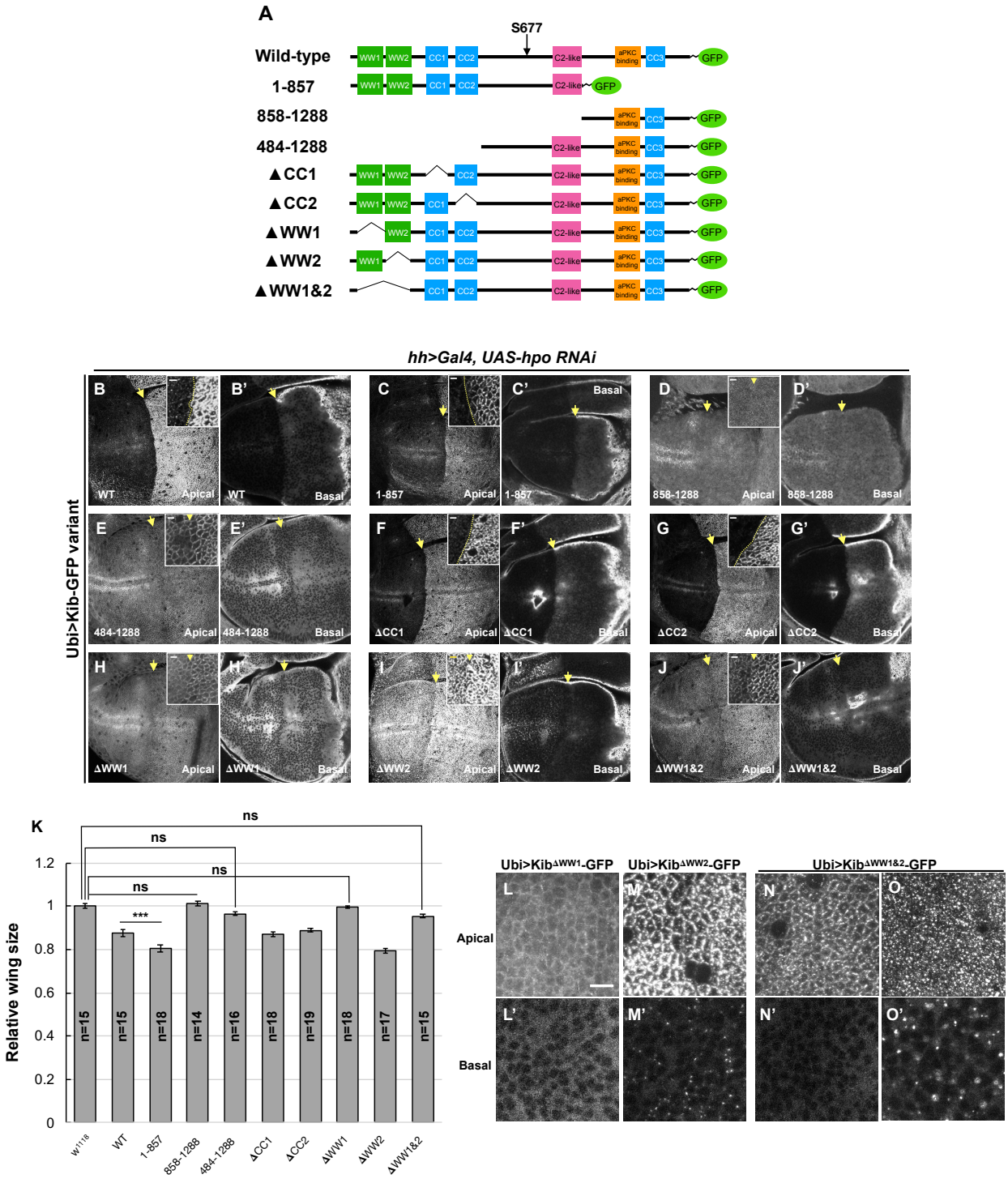

Figure 2.9 continued

A) Diagram of Kib truncations generated for this study.

B-J') Effect of Hpo depletion in the posterior compartment of the wing imaginal disc on different Kib truncations. Deletion of the WW domains, individually (H-I') or together (J & J') stabilizes Kib apically but does not lead to an increase in basal Kib levels. Scale bars in the insets represent 3µm for the insets and 10µm for the corresponding low magnification image.

K) Size comparison (relative to wild-type) of adult wings from flies ectopically expressing different Ubi>Kib-GFP truncations. Quantification is shown as the mean ± SEM; n = number of wings. Statistical comparison was performed using the One-way ANOVA test followed by Tukey's HSD test.

L-O') Localization of Kib lacking WW1 (L & L'), WW2 (M & M') or both WW 1&2 (N-O') in wing imaginal disc cells. Note that Ubi>Kib$^{\Delta WW1\&2}$-GFP localization is variable; sometimes it localizes normally at the junctions (N) and is diffused basally (N'), but usually it accumulates in bright foci both apically and basally (O and O'). Scale bar = 10µm.

amino acids (aa) of Kibra, produced sterile transformants and could not be maintained as stable lines. The rest of the transgenes produced viable and fertile flies.

A Kib truncation lacking the C-terminal third of the coding sequence (Kib^{1-857}-GFP) but retaining the degron motif was strongly upregulated upon Hpo depletion, similar to wild-type Kib (Figure 2.9B-B'). Flies expressing Kib^{1-857}-GFP had smaller wings than those expressing wild-type Kib-GFP (Figure 2.9K), suggesting that deletion of the C-terminal region enhances Kib activity and that amino acids 858-1288 are not necessary for growth suppression. As expected, $Kib^{858-1288}$-GFP was not sensitive to Hpo depletion (due to the lack of the degron motif) did not affect wing growth (Figure 2.9D-D', K). Interestingly, a Kib truncation lacking the first 483 aa ($Kib^{484-1288}$-GFP) was also insensitive to Hpo depletion even though it retained the Slimb degron motif (Figure 2.9E-E'), suggesting that the degron alone is not sufficient for pathway-mediated degradation of Kib. $Kib^{484-1288}$-GFP was also much less potent at suppressing wing growth compared to wild-type Kib-GFP (Figure 2.9K), indicating that the first 483 amino acids of Kib are also essential for Hippo pathway activation.

The first 483 amino acids of Kib contain two WW domains, as well as CC1 and CC2 regions (Figure 2.9A). Deletion of either CC1 or CC2 did not prevent Kib upregulation upon Hpo depletion, indicating that these regions do not mediate pathway-dependent Kib degradation (Figure 2.9F-G'). However, Kib variants lacking the WW domains, either individually ($Kib^{\Delta WW1}$-GFP and $Kib^{\Delta WW2}$-GFP) or together ($Kib^{\Delta WW1\&2}$-GFP) were not sensitive to Hpo depletion (Figure 2.9H-J'). Remarkably, WW-deficient transgenes expressed at markedly higher levels than wild-type Kib (Figure 2.10A). Although these proteins accumulated at the junctional cortex upon Hpo depletion, they appeared to be depleted basally and were not overall upregulated (Figure 2.10B-B'' and Figure2.9I-J'). Thus, the WW domains of Kib are necessary

Figure 2.10: The WW domains of Kib are required for Hippo pathway- and Slimb-mediated degradation

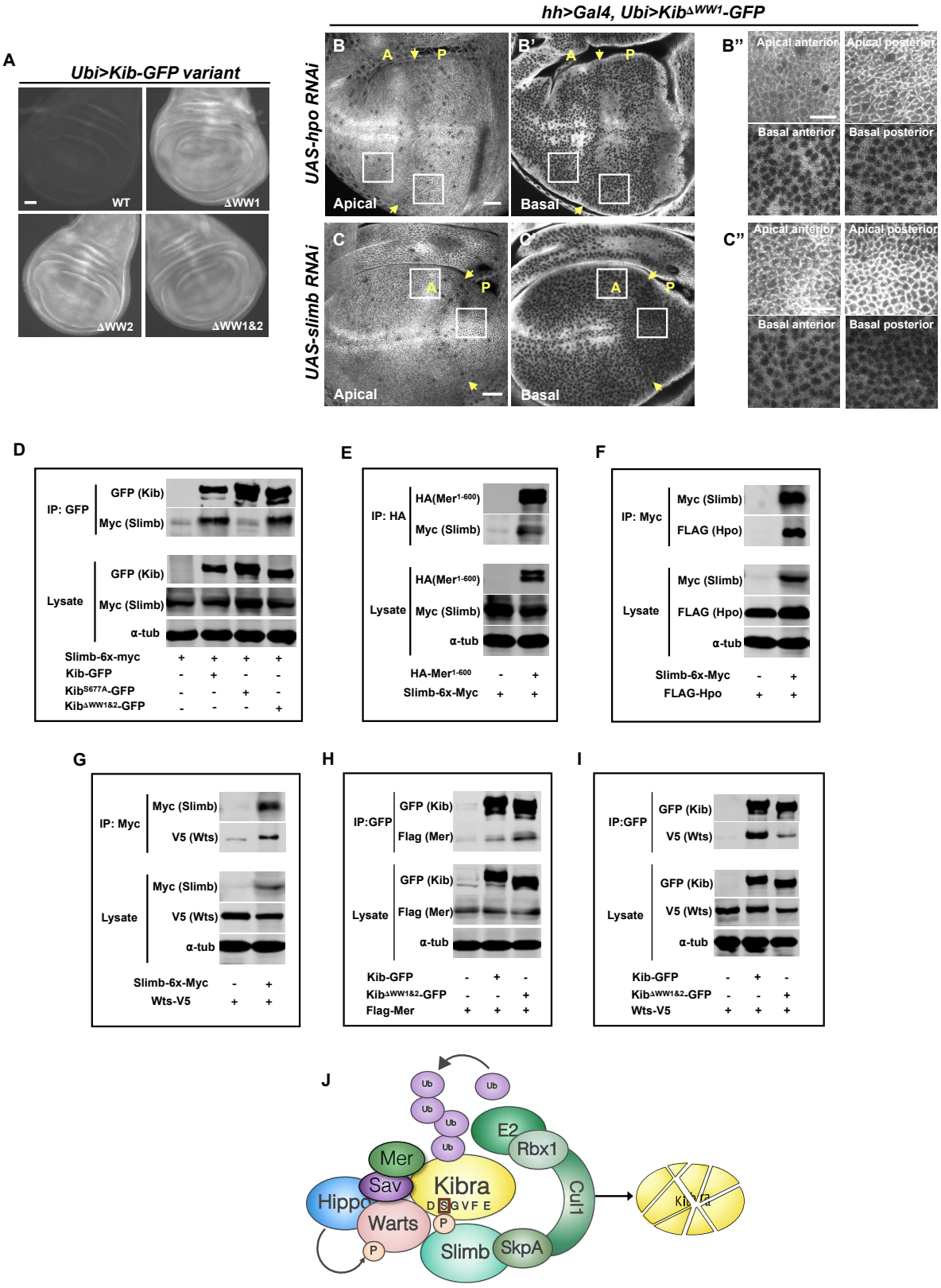

Figure 2.10 continued
A) Widefield fluorescence images of wing imaginal discs expressing wild-type and WW-domain truncations of Kib-GFP expressed under the ubiquitin promoter. All images were taken with identical settings. Scale bar = 40µm.
B-B'') Depletion of Hpo does not affect expression of *Ubi>Kib$^{\Delta WW1}$-GFP*. Note that Hpo depletion leads to apical stabilization and basal depletion of Kib$^{\Delta WW1}$-GFP(C'').
C-C'') Depletion of Slimb does not affect expression of *Ubi>Kib$^{\Delta WW1}$-GFP*. Note that similar to Hpo depletion, loss of Slimb leads to slight apical stabilization and basal depletion of Kib$^{\Delta WW1}$-GFP (D''). Yellow arrows in indicate A-P boundary of the wing discs. Scale bars are 20µm (B and C) and 10µm (B'' and C'').
D-G) Slimb forms a complex with wild-type Kib and Kib$^{\Delta WW1\&2}$ (D), Mer$^{1-600}$ (E), Hpo (F), and Wts (G) in S2 cells.
H-I) Co-IP of wild-type Kib or Kib$^{\Delta WW1\&2}$ with Mer (H) or Wts (I) from S2 cells.
J) A model of Kib degradation by the Hippo pathway and Slimb.

for its degradation via the Hippo pathway. Importantly, while Kib lacking the WW domains were also insensitive to Slimb depletion (Figure 2.10C-C''), even though they still contained an intact degron and interacted with Slimb normally in S2 cells (Figure 2.10D).

Further characterization of the WW domain truncations revealed differences in effects on growth and subcellular localization (Figure 2.9K-O). Kib$^{\Delta WW1\&2}$-GFP often had an extremely punctate appearance in imaginal tissues (Figure 2.9N-O'). Adult flies expressing Kib$^{\Delta WW1\&2}$-GFP were homozygous viable and had wings almost the size of w^{1118} controls (Figure 2.9K) despite the fact that it expressed at higher levels (Figure 2.10A). Kib$^{\Delta WW2}$-GFP also had a punctate appearance (Figure 2.9M-M'), but adults expressing Kib$^{\Delta WW2}$-GFP had significantly smaller wings than flies expressing wild-type Kib-GFP (Figure 2.9K). Deletion of WW1 (Kib$^{\Delta WW1}$-GFP) resulted in a protein that localized at the apical cortex but did not form puncta (Figure 2.9L-L'). Flies expressing Kib$^{\Delta WW1}$-GFP had wings equal in size to w^{1118} control (Figure 2.9K). Taken together, these results indicate that while both WW domains are required for pathway mediated Kib turnover, only the WW1 domain of Kib is necessary for Hippo pathway activation.

We reasoned that if complex formation between Kib and other Hippo pathway components is necessary for Kib degradation, then Slimb might also be a part of this complex. Consistent with this prediction, Slimb co-immunoprecipitated with Mer, Hpo, and Wts in S2 cells (Figure 2.10E-G). We then asked whether the role of the WW domains in Kib degradation was to mediate Kib interaction with other Hippo pathway components. A previous study found that deletion of both WW domains enhanced Kib interaction with Mer in S2 cells (Baumgartner et al., 2010), a result we confirmed (Figure 2.10H). Kib interacts with Wts in flies (Genevet et al., 2010; Yu et al., 2010), and mammalian Kibra interacts with Lats2 (a mammalian homolog of

Wts) via the WW domains (Xiao et al., 2011). We found that the interaction of $Kib^{\Delta WW1\&2}$ with Wts was significantly weakened (Figure 2.10I). Additionally, it was previously reported that Pez interacts with Kib via the WW domains in S2 cells (Poernbacher et al., 2012), consistent with our *in vivo* observation that loss of Pez leads to higher Kib levels. Collectively, these results demonstrate that in addition to the physical association with Slimb, Kib degradation also requires complex formation via the WW domains (Figure 2.10J).

Mechanical tension patterns Kibra degradation across the wing disc epithelium

We next sought to address the potential developmental significance of Kib degradation by the Hippo pathway and Slimb. Observation of wing discs ectopically expressing either *UASp-Kib-GFP* or *UASp-*Kib^{S677A}*-GFP* revealed strikingly different patterns of Kib abundance throughout the tissue. Ectopically expressed wild-type Kib-GFP appeared more abundant at the center of the wing pouch with a marked decrease in fluorescence at the tissue periphery (Figure 2.11A-A'). In contrast, ectopically expressed Kib^{S677A}-GFP fluorescence was distributed more uniformly throughout the wing pouch (Figure 2.11B-B). Because both transgenes were expressed from identical genomic locations and under the same ectopic promoter, we reasoned that the difference between Kib and Kib^{S677A} abundance throughout the tissue was likely a result of differential protein turnover.

If the abundance of Kib^{S677A}-GFP is disproportionately higher at the periphery of the wing blade, which corresponds to the proximal regions of the adult wing, then that region should display more severe growth defects when compared to wild-type Kib-GFP. To ask whether growth was disproportionately inhibited in the proximal region of the wing, we first measured the wing aspect ratios comparing the width of the proximal or distal wing regions to the overall

Figure 2.11: Kib degradation is patterned by mechanical tension in the wing pouch to control proportional growth

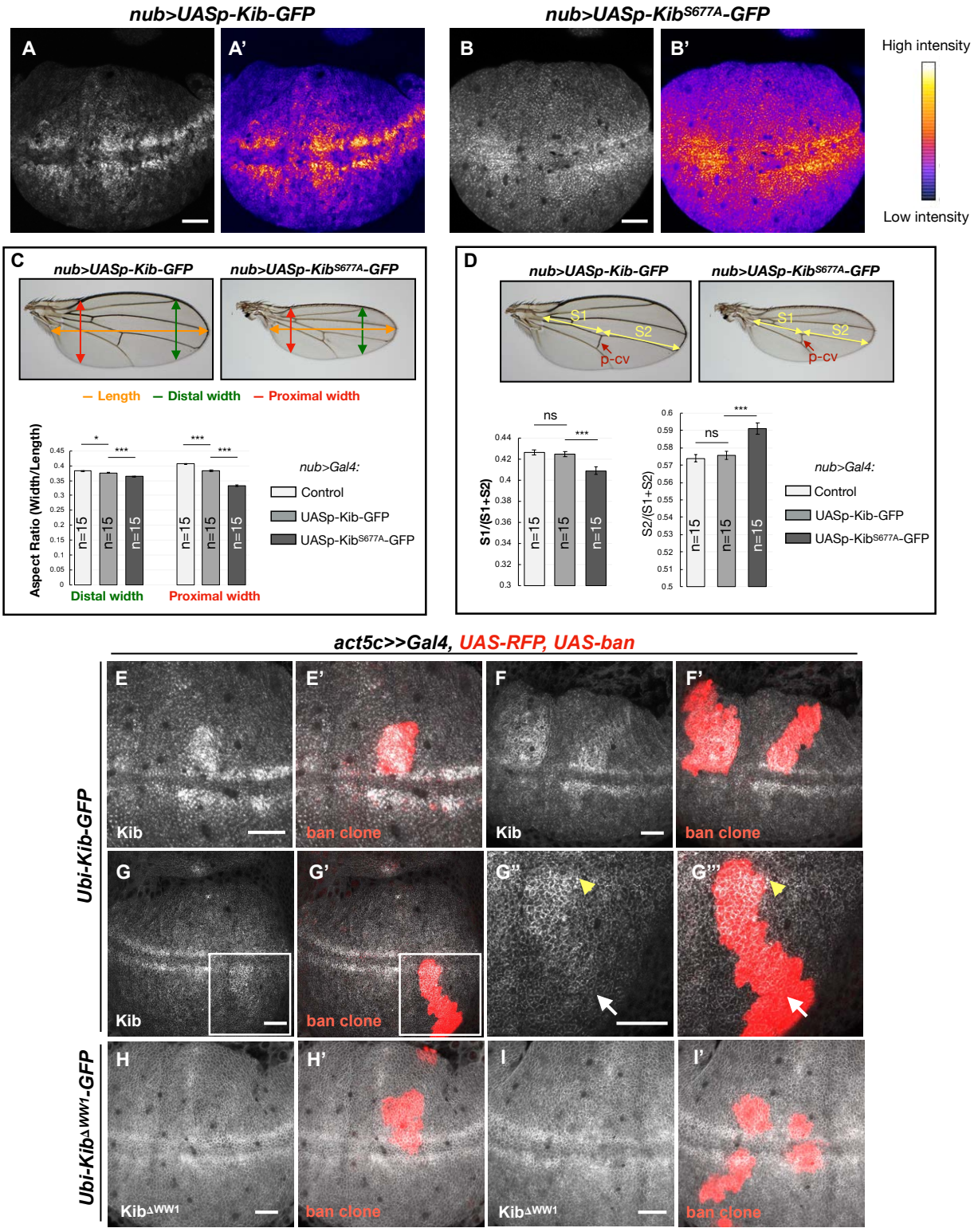

Figure 2.11 continued

A-B') Grayscale images of the wing pouch, which produces the adult wing blade, expressing *UASp-Kib-GFP* (A) or *UASp-Kib^{S677A}-GFP* (B) at identical genomic locations under the *nub>Gal4* driver. Corresponding heatmap intensity images are shown in A' and B'. Note that Kib^{S677A}-GFP displays a more uniform distribution across the pouch than wild-type Kib-GFP.

C) Quantification of aspect ratios of adult wings expressing *nub>Gal4* alone or with *UASp-Kib-GFP* and *UASp-Kib^{S677A}-GFP*. The color-coded segments in the wing image represent the wing length (orange), distal width (green), and proximal width (red).

D) Quantification of the length of proximal (S1) or distal (S2) wing region with respect to total wing length in wings expressing *nub>Gal4* alone or with *UASp-Kib-GFP* and *UASp-Kib^{S677A}-GFP*; p-cv = posterior cross vein. All quantification is represented as the mean ± SEM; n = number of wings (one wing per fly). Statistical comparison was performed using the One-way ANOVA test followed by Tukey's HSD test.

E-F') Kib-GFP levels are elevated in rapidly proliferating *UAS-bantam* clones.

G-G''') Increased Kib abundance is more pronounced at the center of the wing pouch (yellow arrowhead) than at its periphery (white arrow).

H-I') Kib$^{\Delta WW1}$-GFP levels do not change in *bantam* expressing clones. All scale bars = 20μm.

proximal-distal length. Strikingly, while the relative decrease in width distally was mild in *nub>UASp-Kib-GFP* or *nub>UASp-Kib^{S677A}-GFP* wings compared to control wings, the proximal width decreased dramatically in wings expressing Kib^{S677A}, indicating that expression of Kib^{S677A} inhibited growth disproportionately more in the proximal region (Figure 2.11C). Similarly, when the wing length was measured in the proximal-distal (P-D) axis, using L4 vein as an estimate of total length and the posterior crossvein (p-cv) as the approximated midpoint, we found that wing growth was more severely inhibited proximally than distally (Figure 2.11D). Collectively, these results suggest that Kib degradation occurs in a patterned manner in the wing imaginal epithelium and could serve to pattern growth of this tissue.

The pattern of Kib degradation we observe, higher at the periphery and lower in the center, is similar to the pattern of junctional tension in the wing blade reported previously (LeGoff et al., 2013; Mao et al., 2013). This similarity raises the possibility that mechanical tension patterns Kib degradation to regulate pathway activity in parallel to previously described tension-sensing mechanisms that regulate pathway output (Rauskolb et al., 2014; Deng et al., 2015; Alégot et al., 2019). As an initial test of this hypothesis, we used a previously described method of reducing tension in the wing imaginal epithelium that uses somatic mosaic clones expressing the growth promoting miRNA gene *bantam* (Pan et al., 2016). These clones proliferate faster than and therefore are compressed by the surrounding wild-type cells, leading to lower junctional tension within the clones and higher Hippo pathway activity (Pan et al., 2016). Indeed, we observed higher levels of Kib-GFP within *bantam* clones (Figure 2.11E-G'''). Interestingly, the increase in Kib abundance in *bantam*-expressing clones was stronger near the center of the wing pouch than its periphery (Figure 2.11G-G'''), consistent with previous observations that the compression within *bantam*-expressing clones is greater at the center of the

pouch than at the periphery, presumably because cells near the center of the wing pouch are already more compressed (Pan et al., 2016). Importantly, Kib$^{\Delta WW1}$-GFP levels did not change in *bantam* clones (Figure 2.11H-I'), as expected if tension-induced Kib degradation requires Kib-mediated Hippo signaling complex formation. Taken together, these results suggest that Kib degradation is patterned by mechanical tension across the wing pouch resulting in decreased Kib in regions of high tension and greater Yki promoted growth.

2.3 Discussion

In this study, we show that the Hippo pathway negatively regulates Kib levels via a previously unrecognized post-translational feedback loop. Several key results indicate that this feedback is independent of Yki transcriptional activity. First, loss of Mer leads to a dramatic increase in Kib levels without a detectable increase in Yki transcriptional activity. Second, removing Sd, which blocks Yki-mediated transcription, does not suppress the elevated Kib levels upon Hippo pathway inactivation. Third, the abundance of Kib-GFP expressed under a Yki-insensitive promoter (*Ubi>Kib-GFP*) still increases upon Hippo pathway inactivation. Additionally, we show that Kib is phosphorylated and ubiquitinated in a pathway-dependent manner, and that Kib ubiquitination is mediated via SCF^{Slimb}.

Multiple upstream components regulate the core Hippo kinase cassette, but their organization and the degree of crosstalk between them has not been well elucidated. A striking aspect of our findings is the extent to which Kib degradation by the Hippo pathway is insulated from the activity of other upstream pathway regulators. Previous studies have shown that Crb and Ex function together at the junctional cortex (Chen et al., 2010; Ling et al., 2010; Robinson et al., 2010; Sun et al., 2015) and in parallel to Kib at the medial cortex (Su et al., 2017). Ft can influence Ex stability at the junctions (Silva et al., 2006; Wang et al., 2019), suggesting linkage between these Hippo signaling branches, and Tao-1 functions downstream of Ex (Chung et al., 2016). Although Ex can form a complex with Kib in S2 cells (Genevet et al., 2010; Yu et al., 2010) and Kib junctional localization is dependent on Crb (Su et al., 2017), our results show that depletion of Crb, Ex, Ft, or Tao-1 does not affect Kib-GFP levels. Together with our results that Hpo and Wts promote Kib ubiquitination independently of their kinase activity (Figure 2.4F), these data strongly suggest that Kib degradation is triggered by Kib-mediated complex

formation. Given the importance of the putative phospho-degron in Kib turnover, we propose that Kib is phosphorylated at S677 upon formation of the signaling complex by an as yet unidentified kinase, leading to the recruitment of SCF^{Slimb} and Kib ubiquitination. This model potentially explains the striking compartmentalization of Kib degradation that we observe - loss of Ex or Crb has no effect on Kib abundance because they do not participate in Kib-mediated signaling complexes. Compartmentalized, parallel regulation of pathway activity could clearly have functional implications for the control of tissue growth but at the moment is poorly understood.

The precise dynamics that lead to Hippo pathway activation vs. Kib degradation remain to be uncovered. In the simplest scenario, we propose that the same complex can function to repress Yki activity or target Kib for degradation. If so, the impact of Kib-mediated complex formation on overall pathway activity could be altered by the relative dynamics of Slimb-mediated degradation vs. Yki phosphorylation. As a consequence, this mechanism could provide a means for regulation of pathway output by factors outside of the pathway itself.

A remaining question our work defines relates to the functional significance of this mechanism to regulate Kib abundance in developing tissues. Our results suggest that Kib-mediated Hippo signaling is patterned across the wing imaginal epithelium by regulated Kib degradation. Specifically, Kib degradation via the degron-dependent mechanism we have identified is greater at the periphery of the wing pouch than at its center. Previous studies have shown that junctional tension also is greater at the periphery of the wing pouch (LeGoff et al., 2013; Mao et al., 2013). Higher tension at the wing pouch periphery has been proposed to drive tissue growth, possibly by promoting Yki function, as a compensatory mechanism for low levels of diffusible morphogens that are expressed in narrow bands of cells at the center of the pouch

(Shraiman, 2005; Aegerter-Wilmsen et al., 2007; Hariharan, 2015; Pan et al., 2018). Interestingly, junctional tension is known to repress Hippo pathway activity via inhibition of Wts (Lats1/2 in mammals) (Rauskolb et al., 2014; Ibar et al., 2018), though it remains unknown whether junctional tension also affects upstream Hippo pathway regulators such as Kib. Given our results, we propose that tension also promotes Kib degradation and thereby reduces Kib mediated upstream pathway activation.

It might seem paradoxical that Kib degradation, which is dependent on signaling complex assembly, is greater at the periphery of the wing pouch where net Hippo pathway activity is thought to be lower (Hariharan, 2015; Pan et al., 2018). However, our results using kinase-dead forms of Hpo and Wts clearly suggest that Kib ubiquitination and degradation can be uncoupled from activation of pathway kinases. We imagine that tension might regulate access of the degradation components (e.g. the putative kinase or SCF^{Slimb}) to Kib-organized signaling complexes and thereby regulate Kib-mediated pathway activation. We currently know little about how dynamic Hippo pathway output is in developing tissues, largely because there are no available single-cell resolution reporters for pathway activity. Our findings suggest that pathway output mediated by Kib could be tightly and dynamically regulated in response to mechanical tension or other factors that affect the degradation mechanism described here.

Another question our study raises is the functional significance of having both transcriptional and post-translational negative feedback mechanisms that regulate Kib levels. Feedback regulation is a common feature in cell signaling, and transcriptional negative feedback can serve to limit the output of a signaling pathway over time (Perrimon and McMahon, 1999). In the case of the Hippo pathway, transcriptional feedback mediated by Yki is not specific to Kib, as Ex and Mer expression is also promoted by Yki activity. Moreover, loss of any upstream

Hippo pathway regulator, including Ex, Crb, Ft, or Tao-1 would presumably affect Kib levels via the transcriptional feedback. In contrast, the post-translational feedback identified in this study would silence Kib function in a more rapid and specific manner. The role of the post-translational feedback could be to enhance the robustness of Kib-mediated signaling (Stelling et al., 2004), possibly by preventing drastic fluctuations in Kib levels, to ensure optimally scaled and patterned tissue growth. On a broader level, our identification of Kib-specific feedback highlights the importance of understanding why there are multiple upstream inputs regulating the Hippo pathway and how they function during development.

2.4 Methods

Fly genetics

For expression of UAS transgenes, the following drivers were used: *hh>Gal4, en>Gal4,*

ap>Gal4, nub>Gal4.

To generate mutant clones, the following crosses were performed:

Kib::GFP in *ex* or *Mer* mutant clones

y w hsFlp; Ubi-RFP 40A FRT X ex^{e1} 40A FRT/CyO, dfdYFP; Kib::GFP/TM6, Tb
Mer^{4} 19A FRT/FM7, actGFP; MKRS/TM3, Ser, actGFP X hsFLP, w^{1118}, Ubi-RFP-nls 19AFRT; Kib::GFP/TM3, Ser, actGFP

Yki-YFP in *ex* or *Mer* mutant clones

y w hsFlp; Ubi-RFP 40A FRT X ex^{e1} Yki-YFP yki^{B5}/CyO, dfdYFP
Mer^{4} 19A FRT/+; Yki-YFP/CyO, dfdYFP X hsFLP, w^{1118}, Ubi-RFP-nls 19AFRT;MKRS/TM3, Ser, actGFP

ban3-GFP in *ex* or *Mer* mutant clones

y w hsFlp; Ubi-RFP 40A FRT X ex^{e1} 40A FRT/CyO, dfdYFP; ban3-GFP/TM6, Tb
Mer^{4} 19A FRT/FM7, actGFP; MKRS/TM3, Ser, actGFP X hsFLP, w^{1118}, Ubi-RFP-nls 19AFRT; ban3-GFP/TM3, Ser, actGFP

Kib::GFP in *sd Mer* double mutant clones

sd^{47} Mer^{4} 19A FRT/FM7, dfdYFP; Sco/CyO, dfdYFP X hsFLP, w^{1118}, Ubi-RFP-nls 19AFRT; Kib::GFP/TM3, Ser, actGFP

Ubi>Kib-GFP in single *sd* or *hpo* mutant clones or in *sd hpo* double mutant clones

sd^{47} 19A FRT/FM7, dfdYFP; FRT 42D hpo^{BF33}/CyO, dfdYFP X ey>Flp Ubi-GFP 19A FRT; FRT 42D Ubi-RFP/CyO, dfdYFP; Ubi>Kib-GFP/+

UASp-Kib-GFP or UASp-Kib^{S677A}-GFP in *Mer* or *hpo* mutant clones

Mer^{4} 19A FRT/+; nub>Gal4/CyO, dfdYFP X hsFLP, w^{1118}, Ubi-RFP-nls 19AFRT; UASp-Kib-GFP/TM3, Ser, actGFP
Mer^{4} 19A FRT/+; nub>Gal4/CyO, dfdYFP X hsFLP, w^{1118}, Ubi-RFP-nls 19AFRT; UASp-Kib^{S677A}-GFP/TM3, Ser, actGFP

nub>Gal4 FRT 42D hpo^{BF33}/CyO, dfdYFP X y w hsFLP; FRT 42D Ubi-RFP/CyO, dfdYFP; UASp-Kib-GFP/+
nub>Gal4 FRT 42D hpo^{BF33}/CyO, dfdYFP X y w hsFLP; FRT 42D Ubi-RFP/CyO, dfdYFP; UASp-Kib^{S677A} -GFP/+

Table 2.1. Reagents

Reagent type (species) or resource	**Designation**	**Source or reference**	**Identifiers**	**Additional information**
genetic reagent (*D. melanogaster*)	Kib::GFP	DOI: 10.1016/j.devcel.2017.02.004		
genetic reagent (*D. melanogaster*)	*Mer^{4} 19AFRT*	DOI: 10.1083/jcb.141.7.1589		
genetic reagent (*D. melanogaster*)	*ex^{e1} 40AFRT*	PMID: 8269855		
genetic reagent (*D. melanogaster*)	*19AFRT sd^{47M}*	10.1016/j.devcel.2008.01.007		
genetic reagent (*D. melanogaster*)	*hpo^{BF33} 42DFRT*	10.1101/gad.1134003		
genetic reagent (*D. melanogaster*)	*ban3-GFP*	DOI: 10.1242/dev.070367		
genetic reagent (*D. melanogaster*)	*UAS-Mer RNAi*	DOI: 10.1016/j.devcel.2017.02.004		

Table 2.1. Continued

genetic reagent (*D. melanogaster*)	*UAS-sav RNAi*	Bloomington Drosophila Stock Center	BL 28006	
genetic reagent (*D. melanogaster*)	*UAS-hpo RNAi*	Vienna Drosophila Resource Center	VDRC 104169	
genetic reagent (*D. melanogaster*)	*UAS-wts RNAi*	Vienna Drosophila Resource Center	VDRC 106174	
genetic reagent (*D. melanogaster*)	*UAS-ex RNAi*	Vienna Drosophila Resource Center	VDRC 109281	
genetic reagent (*D. melanogaster*)	*UAS-crb RNAi*	Vienna Drosophila Resource Center	VDRC 39177	
genetic reagent (*D. melanogaster*)	*UAS-yki RNAi (III)*	Vienna Drosophila Resource Center	VDRC 40497	
genetic reagent (*D. melanogaster*)	*UAS-slimb RNAi*	Bloomington Drosophila Stock Center	BL 33898	
genetic reagent (*D. melanogaster*)	*UAS-Cul1 RNAi*	Bloomington Drosophila Stock Center	BL 29520	
genetic reagent (*D. melanogaster*)	*UAS-SkpA RNAi*	Bloomington Drosophila Stock Center	BL 32870	

Table 2.1. Continued

genetic reagent (*D. melanogaster*)	*UAS-mahj RNAi*	Bloomington Drosophila Stock Center	BL 34912	
genetic reagent (*D. melanogaster*)	*UAS-Nedd4 RNAi*	Bloomington Drosophila Stock Center	BL 34741	
genetic reagent (*D. melanogaster*)	*UAS-POSH RNAi*	Bloomington Drosophila Stock Center	BL 64569	
genetic reagent (*D. melanogaster*)	*UAS-POSH*	Bloomington Drosophila Stock Center	BL 58990	
genetic reagent (*D. melanogaster*)	*UAS-Su(dx) RNAi*	Bloomington Drosophila Stock Center	BL 67012	
genetic reagent (*D. melanogaster*)	*UAS-Herc4*	DOI: 10.1371/journal.pone.0131113		
genetic reagent (*D. melanogaster*)	*UAS-Smurf RNAi*	Bloomington Drosophila Stock Center	BL 40905	
genetic reagent (*D. melanogaster*)	*UAS-Fbxl7 RNAi*	Vienna Drosophila Resource Center	VDRC 108628	
genetic reagent (*D. melanogaster*)	*UAS-ft RNAi*	Bloomington Drosophila Stock Center	BL 34970	

Table 2.1. Continued

genetic reagent (*D. melanogaster*)	*UAS-ds RNAi*	Vienna Drosophila Resource Center	VDRC 36219	
genetic reagent (*D. melanogaster*)	*UAS-dachs-V5*	DOI: 10.1242/dev.02427		
genetic reagent (*D. melanogaster*)	*UAS-Tao1 RNAi*	Vienna Drosophila Resource Center	VDRC 17432	Previously used in DOI: 10.1016/j.devcel.2011.08.028
genetic reagent (*D. melanogaster*)	*UAS-mats RNAi*	Bloomington Drosophila Stock Center	BL 34959	
genetic reagent (*D. melanogaster*)	*UAS-Pez RNAi*	Bloomington Drosophila Stock Center	BL 33918	
genetic reagent (*D. melanogaster*)	*Ey>Flp 19AFRT Ubi-GFP; Ubi-RFP 42DFRT*	DOI: 10.1016/j.devcel.2013.04.021		
genetic reagent (*D. melanogaster*)	*Ft-GFP*	VDRC 318477		
genetic reagent (*D. melanogaster*)	*Ds:GFP*	DOI: 10.1016/j.cub.2012.03.053		
genetic reagent (*D. melanogaster*)	*Ubi-Kib-GFP-FLAG 86Fb*	This paper		See Materials & Methods

Table 2.1. Continued

genetic reagent (*D. melanogaster*)	*UASp-Kib-GFP-FLAG 86Fb*	This paper		See Materials & Methods
genetic reagent (*D. melanogaster*)	*UASp-Kib^{S677A}-GFP-FLAG 86Fb (this study)*	This paper		See Materials & Methods
genetic reagent (*D. melanogaster*)	*Ubi-Kib-GFP-FLAG VK37*	This paper		See Materials & Methods
genetic reagent (*D. melanogaster*)	*Ubi-Kib$^{\Delta WW1}$-GFP-FLAG VK37*	This paper		See Materials & Methods
genetic reagent (*D. melanogaster*)	*Ubi-Kib$^{\Delta WW2}$-GFP-FLAG VK37*	This paper		See Materials & Methods
genetic reagent (*D. melanogaster*)	*Ubi-Kib$^{\Delta WW1\&2}$-GFP-FLAG VK37*	This paper		See Materials & Methods
genetic reagent (*D. melanogaster*)	*Ubi-Kib$^{1-857}$-GFP-FLAG VK37*	This paper		See Materials & Methods
genetic reagent (*D. melanogaster*)	*Ubi-Kib$^{484-1288}$-GFP-FLAG VK37*	This paper		See Materials & Methods
genetic reagent (*D. melanogaster*)	*Ubi-Kib$^{858-1288}$-GFP-FLAG VK37*	This paper		See Materials & Methods

Table 2.1. Continued

genetic reagent (*D. melanogaster*)	*Ubi-Kib$^{\Delta CC1}$-GFP-FLAG VK37*	This paper		See Materials & Methods
genetic reagent (*D. melanogaster*)	*Ubi-Kib$^{\Delta CC2}$-GFP-FLAG VK37*	This paper		See Materials & Methods
antibody	anti-Ex (Guinea pig polyclonal)	DOI: 10.1016/j.cub.2006.02.063	RRID:AB_2568722	Tissue staining (1:5000)
antibody	anti-FLAG (Mouse monoclonal)	Sigma Aldrich	Cat#F1804; RRID:AB_262044	IB (1:20,000)
antibody	anti-Sd (Guinea pig polyclonal)	10.1002/dvdy.23942	RRID:AB2567874	Tissue staining (1:1000)
antibody	anti-GFP (Guinea pig polyclonal)	DOI: 10.1091/mbc.E19-07-0387	NA	IP (1:1250)
antibody	anti-GFP (Rabbit polyclonal)	Michael Glotzer (University of Chicago)	NA	IB (1:5000)
antibody	anti-Hpo (mouse polyclonal)	DOI: 10.1016/j.devcel.2017.02.004	NA	IB (1:5000)
antibody	anti-HA (Rabbit polyclonal)	Santa Cruz	Cat#sc-805; RRID:AB_631618	IB (1:5000)

Table 2.1. Continued

antibody	anti-Myc 9B11 (Mouse monoclonal)	Cell Signaling	Product #2276	IP (1:1000) IB (1:40,000)
antibody	anti-V5 (Mouse monoclonal)	GenScript	Cat# A01724-100	IB (1:2500)
antibody	anti-alpha tubulin (Mouse monoclonal)	Sigma Aldrich	Cat# T 9026	IB (1:2500)
Cell line (*D. melanogaster)*	S2-DGRC	Cherbas Lab, Indiana University	RRID:CVCL_TZ72	https://dgrc.bio.indiana.edu/product/View?product=6

Expression constructs and generation of *Drosophila* transgenic lines

To generate Ubi>Kib-GFP, Kib was fused to GFP-FLAG with a linker sequence 5'-TCCGGTACCGGCTCCGGC-3', and the entire Kib-GFP-FLAG cassette was first cloned into UAStattB backbone to generate UASt-Kib-GFP-FLAG, with unique NotI (immediately 5' of the Kozak sequence) and KpnI (in the linker region) restriction sites flanking Kib sequence. To make Kib^{1-857}, $Kib^{858-1288}$, $Kib^{484-1288}$, the corresponding regions were amplified (Table 2.2); UAStattB was linearized with NotI and KpnI and the amplified fragments were cloned into linearized backbone via Gibson assembly (Gibson et al., 2009). Fragments lacking CC or WW domains were made using an inverse PCR approach with flanking primers (Table 2.2) and the amplified linear pieces including the plasmid backbone were circularized via Gibson assembly. Kib-GFP-FLAG cassettes (full-length or truncations) were amplified using flanking primers (Table 2.2) and cloned via Gibson assembly into *p63E-ubiquitin* backbone (Munjal et al., 2015) linearized with NotI and XbaI. The transgenes were inserted at the 86Fb (full-length Kib) or VK37 (full-length and truncated Kib) docking site via phiC31-mediated site-specific integration.

pMT-Kib-GFP-FLAG was generated by cloning Kib-GFP-FLAG cassette via Gibson assembly (Gibson to pMT primers, Table 2.2) into the pMT backbone (Klueg et al., 2002) linearized by KpnI and EcoRV.

UASp-Kib^{S677A}-GFP-FLAG was generated using Q5® Site-Directed Mutagenesis Kit (New England Biolabs, Catalog #E0554S) using primers KibS677A (Table 2.2). pMT-Kib-GFP-FLAG was used as a template due to smaller size of the plasmid. The mutant Kib^{S677A}-GFP-FLAG cassette was excised with NotI and XbaI and ligated into pUASp (Rørth, 1998) to generate UASp-Kib^{S677A}-GFP. Both UASp-Kib^{S677A}-GFP and UASp-Kib-GFP were inserted at the 86Fb docking site via phiC31-mediated site-specific integration.

Immunostaining of imaginal tissues

In Figures 2.4A-C'''' wing or eye imaginal discs from wandering late third instar larvae were fixed and stained as previously described (McCartney and Fehon, 1996). Primary antibodies, listed in Key Resources table, were diluted as follows: anti-Ex (1:5000), anti-FLAG (1:20,000), anti-Sd (1:1000). Secondary antibodies (diluted 1:1000) were from Jackson ImmunoResearch Laboratories. Immunostaining samples were imaged using either a Zeiss LSM 800 or LSM 880 confocal microscope and the images were analyzed with *Image J.*

Live imaging of imaginal tissues

Throughout the paper (except in Figures 2A-C'''') live tissues were used for imaging. Live imaging of the *Drosophila* imaginal tissues was performed as previously described (Xu et al., 2019). Briefly, freshly dissected wing or eye imaginal discs from third instar larvae were pipetted into a ~40µl droplet of Schneider's *Drosophila* Medium supplemented with 10% Fetal Bovine Serum and mounted on a glass slide. To support the tissue, spherical glass beads (Cospheric, Product ID: SLGMS-2.5) of ~50µm in diameter were place under the cover slip. The mounted samples were immediately imaged on Zeiss LSM 880 or LSM 800 confocal microscopes. Throughout the paper, apical tissue views were shown as maximum projections of the most apical optical sections (0.75µm/section, 4-5 sections) generated using *Image J*; for basal views, single sections ~10.5µm below the apical surface were shown. Widefield fluorescence imaging of live wing imaginal discs was done using a Zeiss Axioplan 2ie microscope with an Orca ER camera and Zeiss AxioVision software.

Co-immunoprecipitation from S2 cells

The following constructs were used in co-IP experiments: *pMT-Kib-GFP-FLAG* (this study), *pMT-Kib$^{\Delta WW1\&2}$-GFP-FLAG* (this study), *pAc5.1-Slimb-6x-myc* (from J. Chiu, UC Davis), *pAFW-Mer, pAHW-Mer$^{1-600}$, pMT-FLAG-Hpo,* and *pAC5.1-V5-Wts* (Huang et al., 2005).

Briefly, 3.5 x 10^6 S2 cells (S2-DGRC) were transfected with total of 500ng of the indicated DNA constructs using DDAB (dimethyldioctadecylammonium bromide, Sigma) (Han, 1996) at 250 μg/ml in six-well plates. Immunoprecipitation (IP) was performed 3 days after transfection. For expression of pMT constructs, 700 μM $CuSO_4$ was added to the wells 24h prior to cell lysis (2 days after transfection). For GFP or Myc IPs, guinea pig anti-GFP (1:1,250) or mouse anti-Myc (1:1,000) antibodies were used. Pierce™ Protein A (Thermo Scientific™) magnetic beads were used to precipitate antibody-bound target proteins. For immunoblotting the following antibody concentrations were used: rabbit anti-GFP (1:5,000), mouse anti-Hpo (1:5,000), mouse anti-α-tubulin (1:2,500), mouse anti-Myc (1:40,000), mouse M2 anti-Flag (1:20,000), mouse anti-V5 (1:2,500), and rabbit anti-HA (1:5,000). Immunoblots were scanned using an Odyssey CLx scanner (LI-COR Biosciences).

Cells were harvested and lysed on ice in buffer containing 25 mM Hepes, 150 mM NaCl, 1 mM EDTA, 0.5 mM EGTA, 0.9 M glycerol, 0.1% Triton X-100, 0.5 mM DTT, and Complete protease inhibitor cocktail (Roche) at 1 tablet/10ml concentration.

For detection of phosphorylated Kib *in vivo*, dissected wing discs from wandering third-instar larvae (200 discs per condition) expressing *nub>Gal4* with Ubi>Kib-GFP alone or together with an indicated RNAi transgene were immediately flash-frozen in a bath of dry ice and 95% ethanol and stored at -80°C. On the day of IP, the discs were briefly thawed on ice and lysed in buffer described above. PhosSTOP™ (Sigma Aldrich) phosphatase inhibitor cocktail

was added to the lysis buffer to inhibit phosphorylation (1 tablet/10ml of buffer). Kib-GFP was immunoprecipitated with guinea-pig anti-GFP antibody (1:1,250). A control sample was treated with lambda phosphatase. Samples were run on 8% polyacrylamide gel, with 118:1 acrylamide/bisacrylamide (Scheid et al., 1999), to better resolve phosphorylated Kib species.

Ubiquitination assay and generation of dsRNA

For ubiquitination assays, pMT-HA-Ub (Zhang et al., 2006) was co-transfected where indicated to provide labeled ubiquitin. To inhibit proteasomal degradation, 50μM MG132 (Cayman Chemical) and 50μM calpain inhibitor I (Sigma Aldrich) was added 4h prior to cell lysis. Cells were lysed in RIPA buffer (150mM NaCl, 1%NP-40, 0.5% Na deoxycholate, 0.1%SDS, 25mM Tris (50mM, pH 7.4), supplemented with 5 mM N-Ethylmaleimide (*NEM*) and Complete protease inhibitor cocktail (Roche, 1 tablet/10ml of buffer). HA-tagged ubiquitin was purified using Pierce anti-HA Magnetic beads (clone 2-2.2.14).

For dsRNA-mediated knockdown experiments, T7 primers (Table 2.2), annealing at the 3'-UTR (for Hpo and Wts) or the coding region (for Slimb), were used to first generate PCR products. The PCR products were then used as templates to transcribe dsRNA using the MEGAscript T7 Transcription Kit (ThermoFisher, Catalog #13345).

Quantification and statistical analysis

Image J was used to quantify mean fluorescence intensity in clones vs. control region in Figures 2.1C & H and Figures 2.7 G, H, O, & P. In all cases, no more than two clones per imaginal disc were used for quantification. To quantify adult wing sizes, wings were mounted in methyl salicylate and photographed with the same settings on a Zeiss Axioplan 2ie microscope using a

Canon camera (EOS rebel T2i). Subsequent measurements of wing size were taken using Image J. Graphical and statistical analyses were performed using MS Excel and R respectively.

Table 2.2. List of primers

Primers	Sequence
Gibson to pUbi_For	TTCTTCCCGCAGATAATCCAAATCGTTAACAGATCTGCGG
Gibson to pUbi_Rev	AAGTAAGGTTCCTTCACAAAGATCC
Gibson to pMT_For	TCAGTGCAACTAAAGGGAATTCGATATCTCGTTAACAGATCTGCGG
Gibson to pMT_Rev	AGGTCGACTCTAGAGGATCCCCGGGAAAGATCCTCTAGAGGTTACTTG
ΔWW1 For	AGCAACAACACCACAGCGACTGCTACACAAAGCCGCAGACTTT
ΔWW Rev	CTTTGTGTAGCAGTCGCTGTGGTGTTGTTGCT
ΔWW2 For	GACTTTCGAGGATTGTGTGGGCGAGTGGAAGACTGTCCAGGAGCA
ΔWW2 Rev	TCTTCCACTCGCCCACACAATCCTCGAAAGTCT
ΔWW 1&2 For	AGCAACAACACCACAGCGACGAGTGGAAGACTGTCCAGGAGCA
ΔWW 1&2 Rev	TCTTCCACTCGTCGCTGTGGTGTTGTTGCT
ΔCC1 For	TCGATGAGTCGCCACGATCCGTACACGGAACGGGGCATGAACA
ΔCC1 Rev	GTTCCGTGTACGGATCGTGGCGACTCATCGAA
ΔCC2 For	ACCTGAACGGAGGAGCCCGTTTCTCGGAGAGCACCTTCTCCATTAGCAGT
ΔCC2 Rev	TGCTCTCCGAGAAACGGGCTCCTCCGTTCAGGT
484-1288 For	TTCGTTAACAGATCTGCGGCCGCGCCACCATGAGTAAGAGCGCCTTGAGCTTCAC
484-1288 Rev	TCGCCCTTGCTCACGCCGGAGCCGGTACCGGACACCTCCACGCCGTAGTTGCGA
1-857 For	TTCGTTAACAGATCTGCGGCCGCGCCACCATGCCGAATCTGCAACAAACCGC
1-857 Rev	TCGCCCTTGCTCACGCCGGAGCCGGTACCGGACTCATCCGACGACTCCTCCCGGTTG
858-1288 For	TTCGTTAACAGATCTGCGGCCGCGCCACCATGTCCACCATTACATCCTCCCAGAC
858-1288 Rev	TCGCCCTTGCTCACGCCGGAGCCGGTACCGGACACCTCCACGCCGTAGTTGCGA
KibS677A For	CCGGCGATGCTGGCGTCTTCGAG
KibS677A Rev	CCACGGATTCATTGCTGACCGC
dsRNA hpo 3'-UTR For	TAATACGACTCACTATAGGGAGAGCAACTCACAATTTCGCAAG
dsRNA hpo 3'-UTR Rev	TAATACGACTCACTATAGGGAGAATGCTTTCGTGCTGGAAGAT
dsRNA wts 3'-UTR For	TAATACGACTCACTATAGGGAGATGGAAATCGAACCTTTCTGG
dsRNA wts 3'-UTR Rev	TAATACGACTCACTATAGGGAGATCGTGGGGCTAAACAATTTC
dsRNA slimb For	TAATACGACTCACTATAGGGAGAGCACAGGCCTTCACAACCACTATG
dsRNA slimb Rev	TAATACGACTCACTATAGGGAGATTGCAGACCAGCTCGGATGATTT

CHAPTER 3

Tension regulates Kibra abundance via Par-1

3.1 Introduction

Organs grow proportionally to the overall animal body size irrespective of the species. How organs stop growing after achieving their optimal size is a fundamental question in developmental biology. Studies over the last century have established that in many organs, including limbs, growth is regulated autonomously (Twitty and Schwind, 1931; Swanson and Lewis, 1982; Bryant and Levinson, 1985). The discovery of morphogens and their function in both tissue patterning and cell proliferation provided a possible explanation for self-regulatory nature of tissue growth (Schwank and Basler, 2010). However, by definition morphogens are distributed unevenly while growth occurs uniformly in many developing tissues, raising the question of what drives cell proliferations in tissue regions that receive less morphogen.

Work in the Drosophila wing imaginal epithelium has served as a useful system for studying tissue growth regulation and elucidating models of growth control beyond morphogen gradients (Hariharan, 2015; Vollmer et al., 2017). One model that has gained attention is the mechanical feedback model, which combines the role of morphogens and mechanical forces in ensuring uniform growth across a tissue with non-uniform morphogen distribution (Shraiman, 2005; Aegerter-Wilmsen et al., 2007, 2012). According to this model, tissue growth initially is driven mainly by morphogens concentrated at the center of the tissue; but as the tissue grows larger, cells at the periphery will receive lower morphogen dose and proliferate slower. As a result, faster growing central cells will begin to push against the peripheral cells, thereby generating tension at tissue periphery (Fig. 1.3). Tension could promote growth and compensate

for the lack of morphogens at the periphery, while compression in the center would inhibit growth, thereby leading to uniform cell proliferation across tissue.

Since the mechanical feedback model was proposed, multiple studies have found data in its support. For example, observations that the growth rate of mammary epithelial cell acini was proportional to the stiffness of the ECM matrix in which they were cultured provided evidence that mechanical forces can influence growth (Paszek et al., 2005). With the discovery of the Hippo pathway and the realization that its growth-promoting transcriptional effector Yki/YAP/TAZ is stimulated by tension (Dupont et al., 2011; Wada et al., 2011; Aragona et al., 2013), growing attention has been directed to understanding how mechanical stimuli could regulate tissue growth via Hippo signaling. Studies in Drosophila and mammalian cells have shown that tension promotes Yki/YAP activity via LIM domain Ajuba family proteins, such as Jub, which accumulate at cell-cell junctions in response to tension and sequester Wts/LATS (Rauskolb et al., 2014; Pan et al., 2016; Ibar et al., 2018). However, this mechanism acts directly on the core kinase cascade, and it remains unclear whether or how tension could also regulate the upstream Hippo signaling components, such as Kib.

Par-1 is a serine/threonine kinase known for its role in polarity establishment and regulation of microtubule stability (Kemphues et al., 1988; Benton and St Johnston, 2003; Doerflinger et al., 2003; Bayraktar et al., 2006). However, several key studies of Par-1 have elucidated its association with actomyosin network and function in tissue growth regulation. For example, Par-1 can directly interact with the myosin heavy chain and can regulate myosin activity and F-actin dynamics in various contexts (Guo and Kemphues, 1996; Majumder et al., 2012; Jiang and Harris, 2019). Conversely, a recent study suggested that myosin activity promotes cortical Par-1 localization in the Drosophila oocyte (Doerflinger et al., 2021). Finally,

Par-1 regulates tissue growth via Hippo pathway inhibition by phosphorylating Hpo and preventing Hpo-Sav association (Huang et al., 2013). These findings raise an intriguing question of whether Par-1 could regulate Hippo signaling in a mechanosensitive manner.

In the previous chapter, we described a mechanism whereby Kib targets itself for ubiquitin-mediated degradation upon assembly of the Hippo signaling complex. Notably, our work suggested that this degradation mechanism could be modulated by cytoskeleton tension. Here, using genetic and acute manipulations of myosin activity, we report that actomyosin-generated cortical tension modulates Kib abundance. We find that increasing myosin activity and tension lowers Kib abundance, while acutely inhibiting myosin activity elevates Kib levels. Importantly, we find that tension-mediated Kib degradation occurs independently of the previously identified Jub-Wts mechanism. Instead, we find that Par-1 promotes Kib degradation in a tension dependent manner. Together, our findings provide strong evidence that tension regulates upstream Hippo signaling and provide additional mechanistic understanding of how mechanical forces can influence the activity of a signaling pathway.

3.2 Results

Cortical tension promotes Kibra degradation

In Chapter 2, we showed that upon assembling the Hippo signaling complex, Kib destines itself for degradation (Tokamov et al., 2021). Additionally, our results suggested that this mechanism could be modulated by cortical tension because cell clones under compression display higher levels of Kib than their wild type neighbors (Tokamov et al., 2021). To better understand how Kib abundance is regulated, we sought to genetically manipulate myosin activity as a means to alter cortical tension. To visualize Kib, we used Kib tagged with the green fluorescent protein (GFP) and expressed under the ubiquitin promoter (Ubi>Kib-GFP), a transgene that we previously showed to be an effective reporter of post-translational changes in Kib abundance (Tokamov et al., 2021).

We first transiently ectopically expressed RhoGEF2 to activate Rho1 upstream of myosin in the posterior compartment of the wing imaginal disc using the *hh>Gal4* driver combined with ubiquitously expressed $Gal80^{ts}$ (*tub>*$Gal80^{ts}$). Strikingly, expression of RhoGEF2 for 24h resulted in a significant decrease in Kib levels (Figs. 3.1A-B). In contrast, the abundance of Ubi>$Kib^{\Delta WW1}$-GFP, a variant of Kib that is insensitive to Hippo complex-mediated degradation (Tokamov et al., 2021), was not affected by RhoGEF2 expression (Figs. 3.1C-D). Using phospho-specific antibody against the phosphorylated myosin regulatory light chain (pMRLC, Zhang and Ward, 2011), we confirmed that myosin activity was upregulated after 24h of RhoGEF2 overexpression (Fig. 3.1E-E''). Additionally, consistent with the function of Kib in repressing Yki and the role of tension in promoting Yki transcriptional activity (Genevet et al., 2010; Yu et al., 2010; Baumgartner et al., 2010; Rauskolb et al., 2014), we saw increased nuclear Yki accumulation upon RhoGEF2 overexpression (Fig. 3.1F-F''). These results are consistent

Figure 3.1: RhoGEF2 overexpression promotes Kib degradation

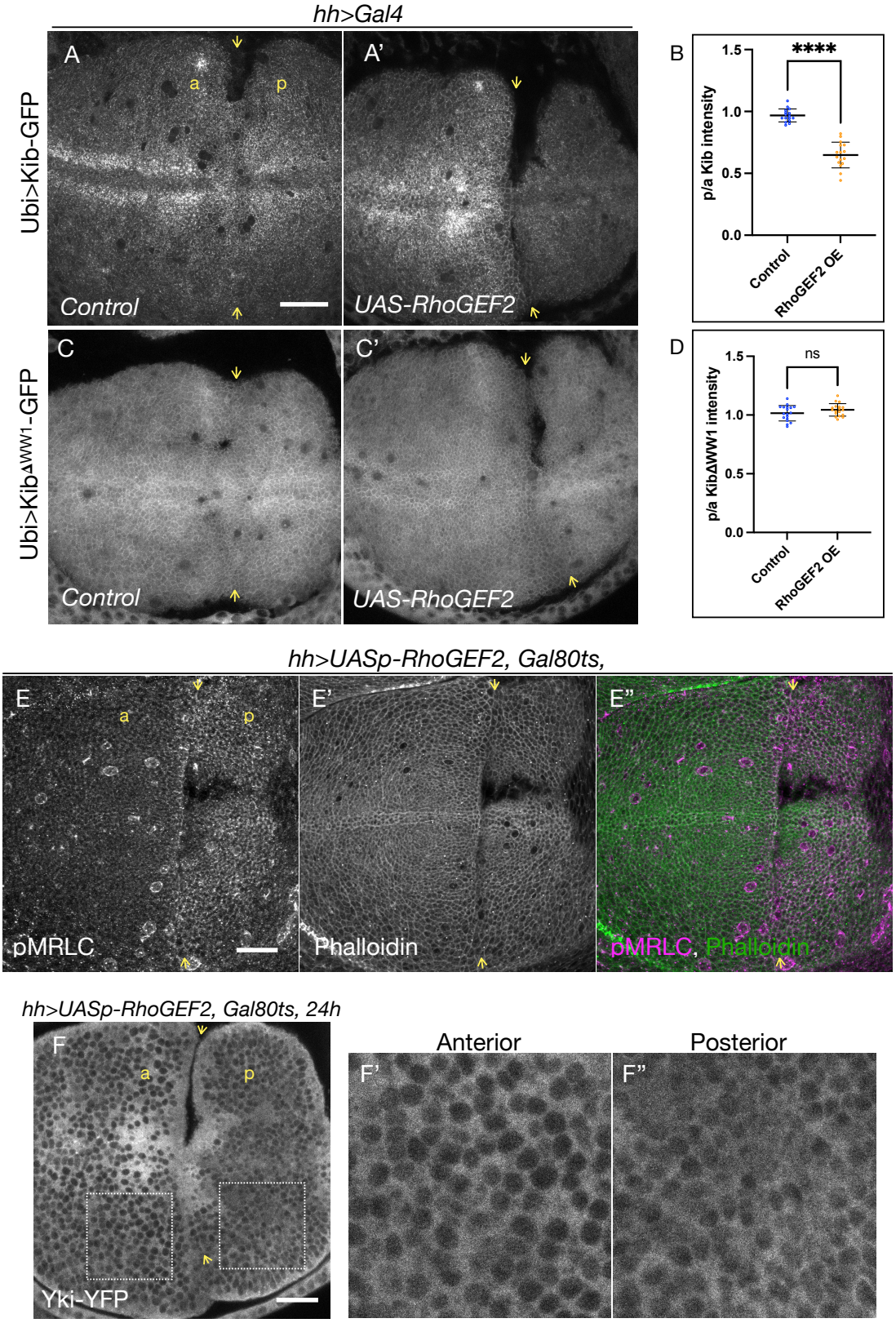

Figure 3.1 continued
A & B) Compared to control tissues (A), ectopic RhoGEF2 expression results in a significant decrease in Kib levels (A' & B). Yellow arrows indicate anterior (a)-posterior (p) boundary.
C-D) In contrast to wild-type Kib, $Kib^{\Delta WW1}$ is not affected by RhoGEF2 expression.
Plots in B and D show the ratio of posterior to anterior Kib-GFP mean intensity. Statistical significance was calculated using Mann-Whitney test. Throughout the study, data is represented as the mean ± SD. Significance values are represented as follows: ****$p \leq 0.0001$, ***$p \leq 0.0001$, **$p \leq 0.001$, *$p \leq 0.05$, ns = not significant.
E-E'') pMRLC staining shows that ectopic RhoGEF2 expression for 24h increases myosin activity.
F-F'') Yki-YFP becomes more nuclear under transient overexpression of RhoGEF2 in live wing imaginal tissues. Scale bars = 20μm.

with our previous observation that the abundance of wild-type Kib, but not $Kib^{\Delta WW1}$, was upregulated in mosaic clones with decreased cortical tension (Tokamov et al., 2021), and suggest that cortical tension regulates Kib abundance via complex mediated degradation.

We previously showed that cortically localized Yki promotes myosin activation via a myosin light chain kinase called Stretchin (Strn-MLCK, Xu et al., 2018). Specifically, ectopic expression of myristoylated Yki (myr-Yki) leads to a significant increase in myosin activation. Therefore, we asked if myr-Yki expression also affected Kib levels. As with RhoGEF2 expression, ectopic myr-Yki expression substantially diminished Kib levels (Figs. 3.2A & D). Strikingly, depletion of Strn-MLCK strongly suppressed the effect of myr-Yki, suggesting that this effect was mediated via myosin activity (Figs. 3.2B & D). However, Strn-MLCK depletion alone did not increase Kib levels (Figs. 3.2C' & D), indicating that Strn-MLCK does not regulate Kib levels under physiological conditions.

Changes in osmotic pressure alter myosin activity and junctional tension

Our genetic manipulations of cortical tension support the model that tension promotes Kib turnover. We next sought to further test this model by acutely manipulating myosin activity and cortical tension. Changes in osmotic pressure have been used extensively to alter membrane tension and F-actin organization. In cultured cells, hypotonic conditions increase membrane tension, while hypertonic conditions lead to lower membrane tension (Di Ciano et al., 2002; Guilak et al., 2002; Sinha et al., 2011; Boulant et al., 2011; Pietuch et al., 2013; Diz-Muñoz et al., 2016; Roffay et al., 2021). However, to our knowledge, the effects of osmotic changes on myosin activity and cortical tension in epithelial tissues such as the wing imaginal disc have not been characterized. Therefore, we decided to subject wing imaginal discs to different osmotic

Figure 3.2: myr-Yki overexpression promotes Kib degradation

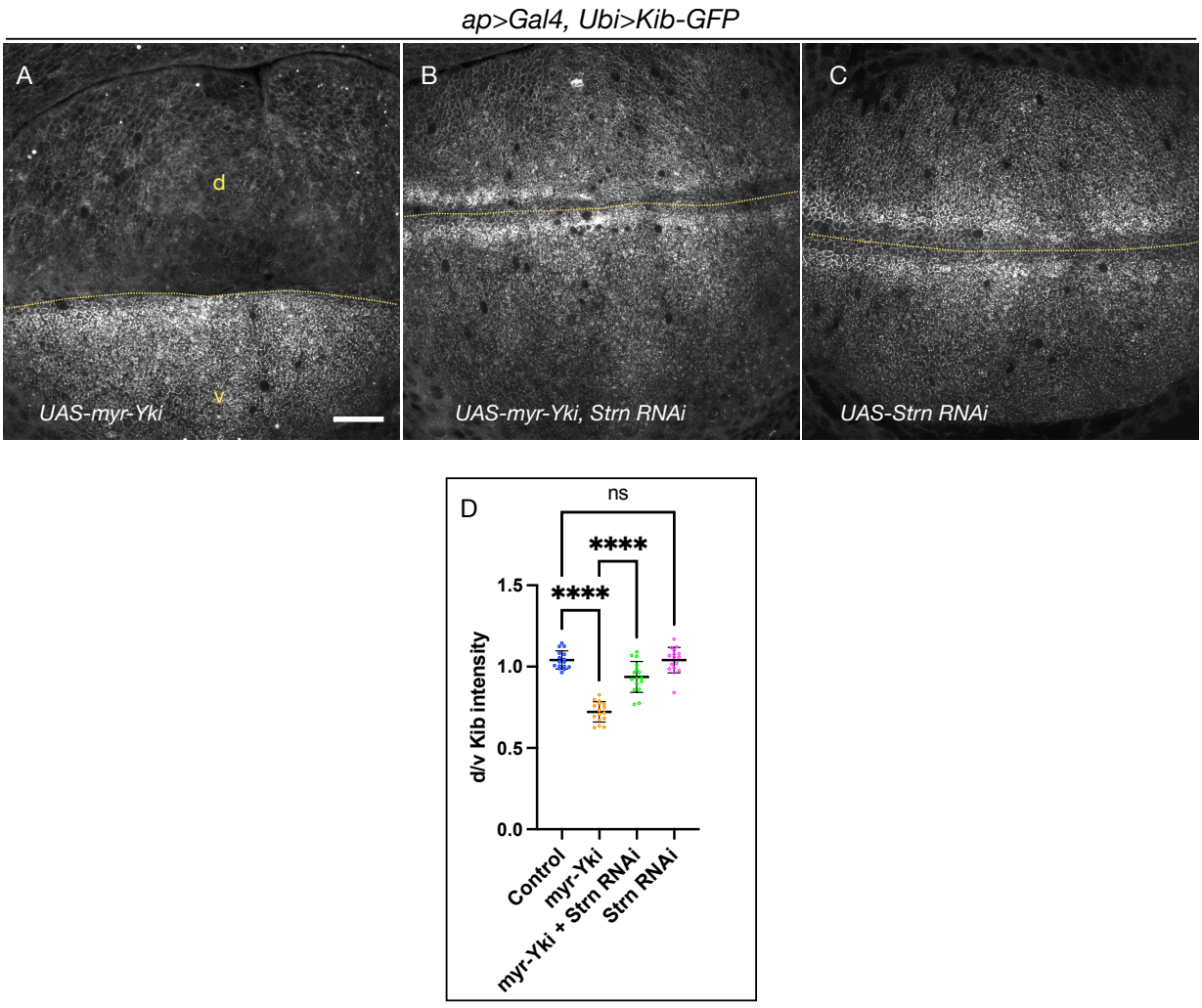

A-D) myr-Yki overexpression leads to a significant decrease in Kib levels (A), and depletion of Strn-MLCK suppresses the effect of myr-Yki overexpression (B). Depletion of Strn-MLCK alone has no effect on Kib levels (C). Dashed lines indicate the dorsal-ventral (d-v) boundary. Scale bars = 20μm.
Plot in D shows dorsal to ventral ratios of Kib-GFP mean intensity. Statistical significance was calculated using One-way ANOVA followed by Tukey's HSD test.

conditions and examine the effect on myosin activity and junctional tension.To this end, we adapted a previously described transwell filter system, which allows for easy exchange of culture media and imaging of live tissues for longer periods (Restrepo et al., 2016). We aimed to alter medium osmolarity gently enough to avoid cell death or tissue rupture and ensure reversibility of the effected changes. We used Schneider's 2 (S2) cell medium (360mOsm) as our isotonic control and either reduced osmolarity (216mOsm) by adding de-ionized water or increased osmolarity (460mOsm) by adding NaCl to the isotonic medium (see Methods for more details).

We first examined the effect of different osmotic conditions on myosin activity using the anti-pMRLC antibody. Compared to isotonic controls, we saw a slight decrease in pMRLC staining under hypertonic conditions and a substantial increase in pMRLC under hypotonic conditions (Figs. 3.3A-C'), indicating that these osmotic manipulations can rapidly alter myosin activation. To ask if the observed changes in myosin activity affected cortical tension, we performed laser-cutting experiments on individual cell-cell junctions and measured their initial recoil velocity. Because of the inherent heterogeneity of cell junctional lengths and apical areas across the wing imaginal epithelium, we restricted all laser cuts to the ventral-anterior region of the presumptive wing blade (which normally contains cells with larger apical areas and longer junctions) and were careful to avoid proximity to mitotic cells (Fig. 3.3D). Consistent with the observed differences in pMRLC staining, we saw a milder, but significant, decrease in recoil velocities under hypertonic conditions and a more profound increase in recoil upon hypotonic shift (Fig. 3.3E). Importantly, there was no correlation between junctional recoil and the initial junction length (Fig. 3.3F).

To further validate that osmotic shifts can be used to induce biological functional changes in tension, we examined the localization of Yki-YFP. Because tension is known to promote

Figure 3.3: Changes in osmotic conditions affect myosin activity and junctional tension

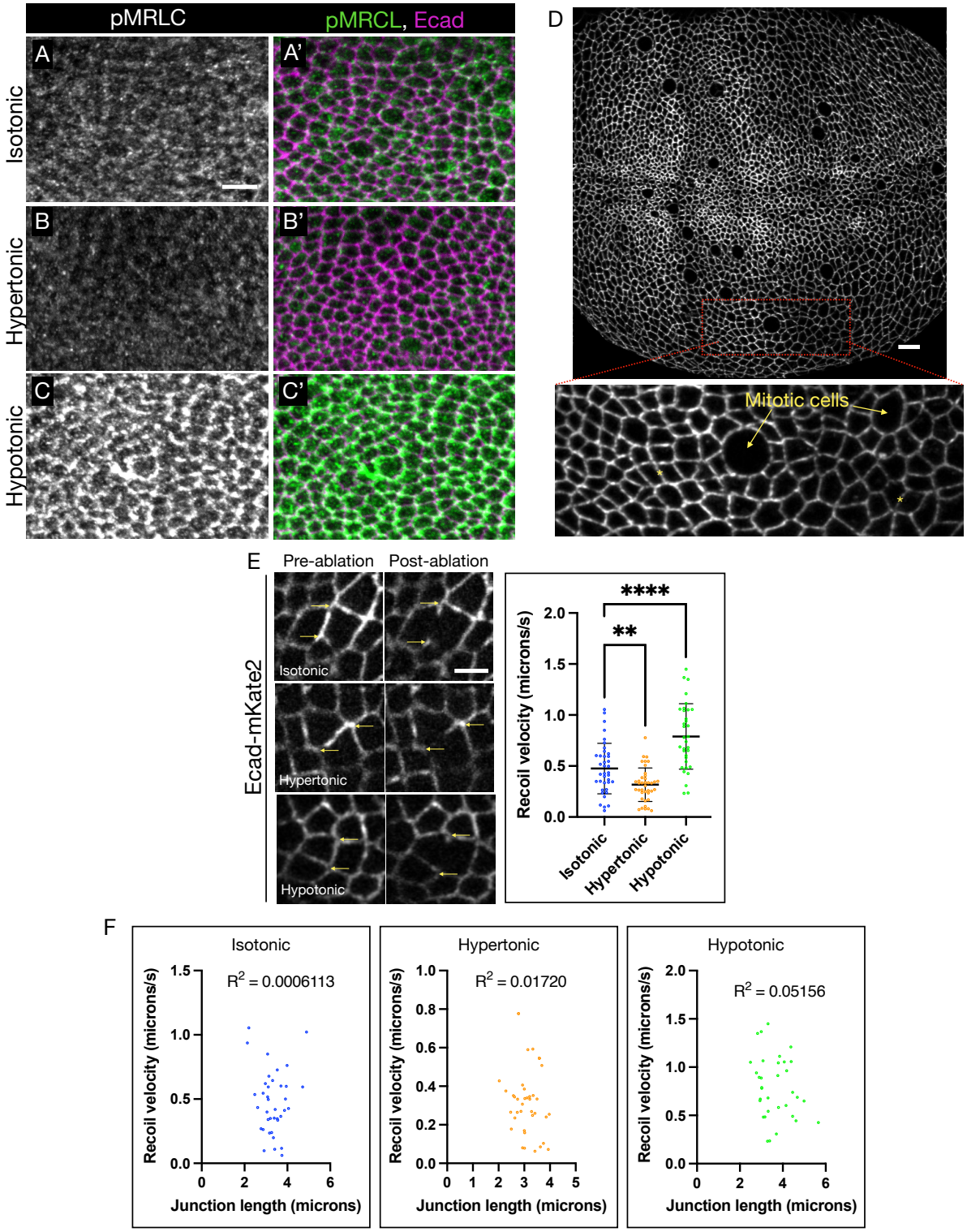

Figure 3.3 continued
A-C) Compared to isotonic conditions (A), hypertonic conditions lead to a slight decrease in pMRLC (B), whereas hypotonic conditions significantly increase pMRLC signal (C). Scale bar = 5μm.
D) An example of a wing imaginal tissue expressing Ecad-mKate2 as a junctional marker used for laser cutting experiments. The enlarged region indicates an approximate area (anterior ventral region) from which all data was collected. No more than two junctions (yellow asterisks) were cut per tissue. Junctions were always many cells apart and never in direct contact with mitotic cells. Scale bars = 10μm.
E) Relative to isotonic controls, initial recoil velocity decreases under hypertonic conditions and increases under hypotonic conditions. Yellow arrows indicate the vertices used to measure recoil velocities. Scale bar = 3μm. Statistical significance was calculated using One-way ANOVA followed by Tukey's HSD test.
F) There was no relationship between initial junction lengths and recoil velocities. The R^2 values represent Pearson correlation coefficients.

nuclear Yki accumulation, we hypothesized that hypertonic conditions (lower tension) should lead to less nuclear Yki, while hypotonic conditions should result in more nuclear Yki. For these experiments, in order to see a definitive effect on Yki localization, we increased the incubation time to 30 min. Consistent with our hypothesis, shifting tissues from an isotonic to a hypertonic solution resulted in a decrease in nuclear Yki-YFP (Figs. 3.4A-B'', D). Conversely, shifting to a hypotonic solution led to a dramatic increase in nuclear Yki-YFP (Figs. 3.4C-D). To further demonstrate the significance of this effect, we decided to first concentrate Yki in the nuclei under hypotonic conditions and then shift to a hypertonic environment. Strikingly, while Yki-YFP accumulated in the nuclei under hypotonic conditions, this effect was completely reversed after incubation in a hypertonic solution (Fig. 3.4E-G''). Together, these results show that osmotic manipulations can be used to acutely modulate myosin activity and junctional tension in an epithelial monolayer with biologically relevant consequences.

Osmotic shifts affect Kibra abundance and localization

Given our result that changes in the medium osmolarity can influence cortical tension, we asked if the osmotic manipulations also affected Kib abundance. Compared to isosmotic conditions, incubating tissues in a hypertonic solution resulted in an increase in Kib abundance (Figs. 3.5A, B, & D). Moreover, Kib fluorescence also increased in more basal tissue sections, suggesting that the apical increase in Kib was not due to apical recruitment from the cytoplasmic pool (Fig. 3.5E). Conversely, in tissues incubated in a hypotonic solution, Kib abundance decreased dramatically both at the apical cortex and in more basal tissue sections compared to isotonic controls (Figs. 3.5C-E). In contrast, fluorescence intensity of Ecad-mKate2 (not shown) did not

Figure 3.4: Effect of osmotic shifts on nuclear Yki localization

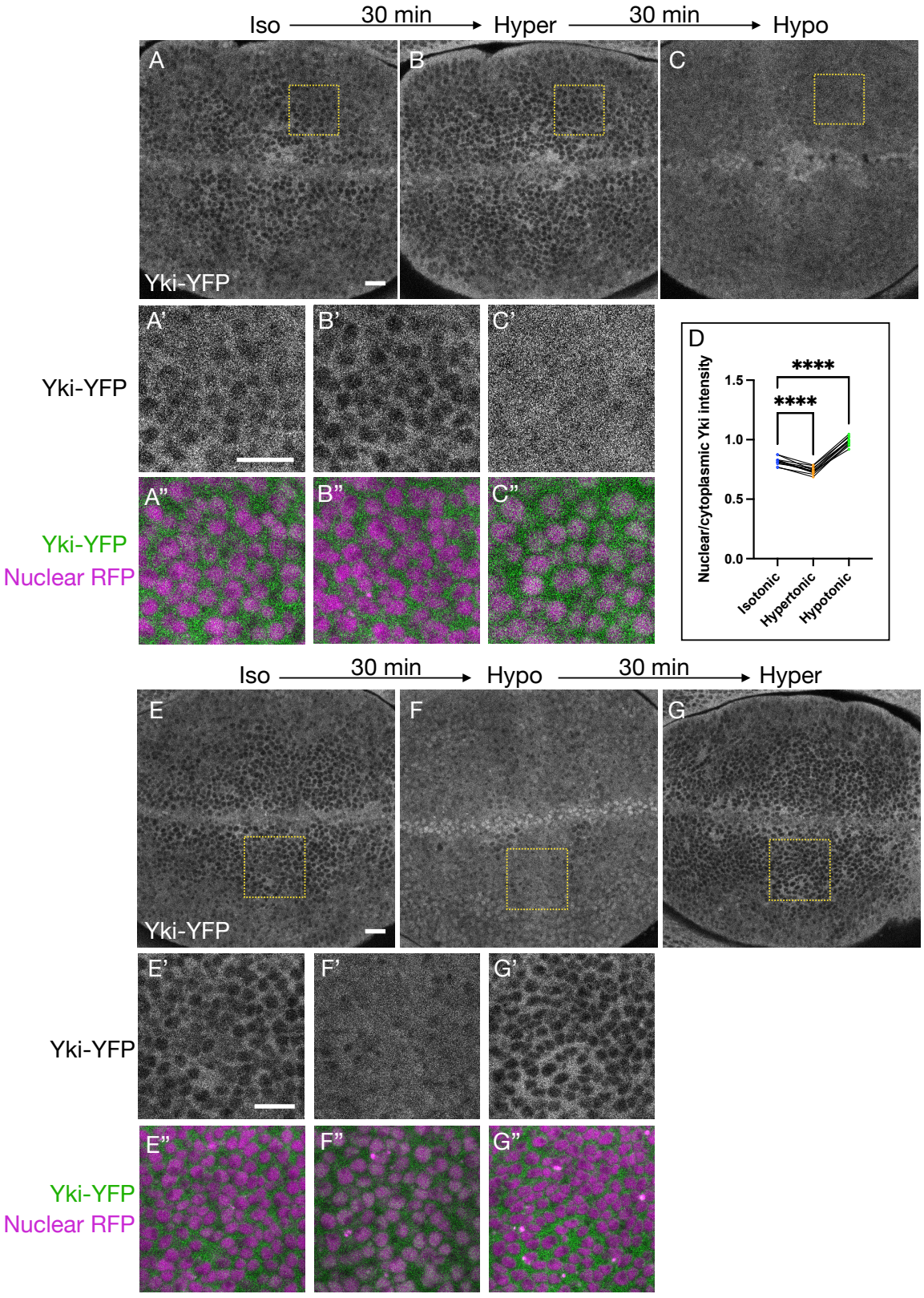

Figure 3.4 continued
A-C'') Compared to isotonic conditions (A-A''), Yki becomes less nuclear under hypertonic shift (B-B'') and more nuclear under hypotonic shift (C-C'').
D) Quantification of nuclear/cytoplasmic mean Yki-YFP fluorescence. Significance was calculated using RM one-way ANOVA test followed by Tukey's HSD test.
E-G'') Similar experiment as shown in A-C'', except tissues were first shifted from isotonic (E-E'') to hypotonic (F-F'') environment to concentrate Yki in the nuclei. Shifting from hypotonic to hypertonic conditions resulted in a dramatic export of nuclear Yki into the cytoplasm (G-G''). Scale bars = 10μm.

change significantly under osmotic shifts (Fig. 3.5F). These results demonstrate that cortical tension dynamically regulates Kib abundance.

We also considered that changes in apical area could alter Kib distribution and fluorescence intensity by concentrating or diluting the protein at the cortex. To address this possibility, we imaged tissues expressing fluorescently labeled Ecad over time under osmotic shifts. We then segmented individual cells and tracked area changes. Immediately after the addition of a hypotonic solution, apical areas began to rise rapidly during the first ~3 min of incubation (Fig. 3.5G). However, this initial increase was followed by a steady decrease of areas in the next 12 min, until on average the areas returned to their initial values (Fig. 3.5G). This effect was presumably due to the ability of cells to ionically compensate for the osmotic changes. Similarly, addition of the hypertonic solution resulted in a transient reduction in apical areas during the first ~3 min, followed by a return to their starting values by 15 min of incubation (Fig. 3.5H). Because we measured Kib fluorescence after 15 min of incubation, changes in apical area do not explain the observed changes in cortical Kib abundance under osmotic shifts. These results suggest that changes in myosin activity are responsible for changes in Kib abundance under osmotic shifts.

Inhibition of myosin activity blocks Kib degradation under hypotonic shift

If the changes in Kib levels under osmotic shifts are caused by myosin activity, then blocking myosin activation under hypotonic conditions should block Kib degradation. To test this idea, we used Y-27632, a commonly used pharmacological inhibitor of Rho kinase (Rok) activity. We first asked if Y-27632 can inhibit myosin hyperactivation induced by a hypotonic solution. Under isotonic conditions, we observed a slight reduction in pMRLC staining when

Figure 3.5: Osmotic changes alter Kib abundance

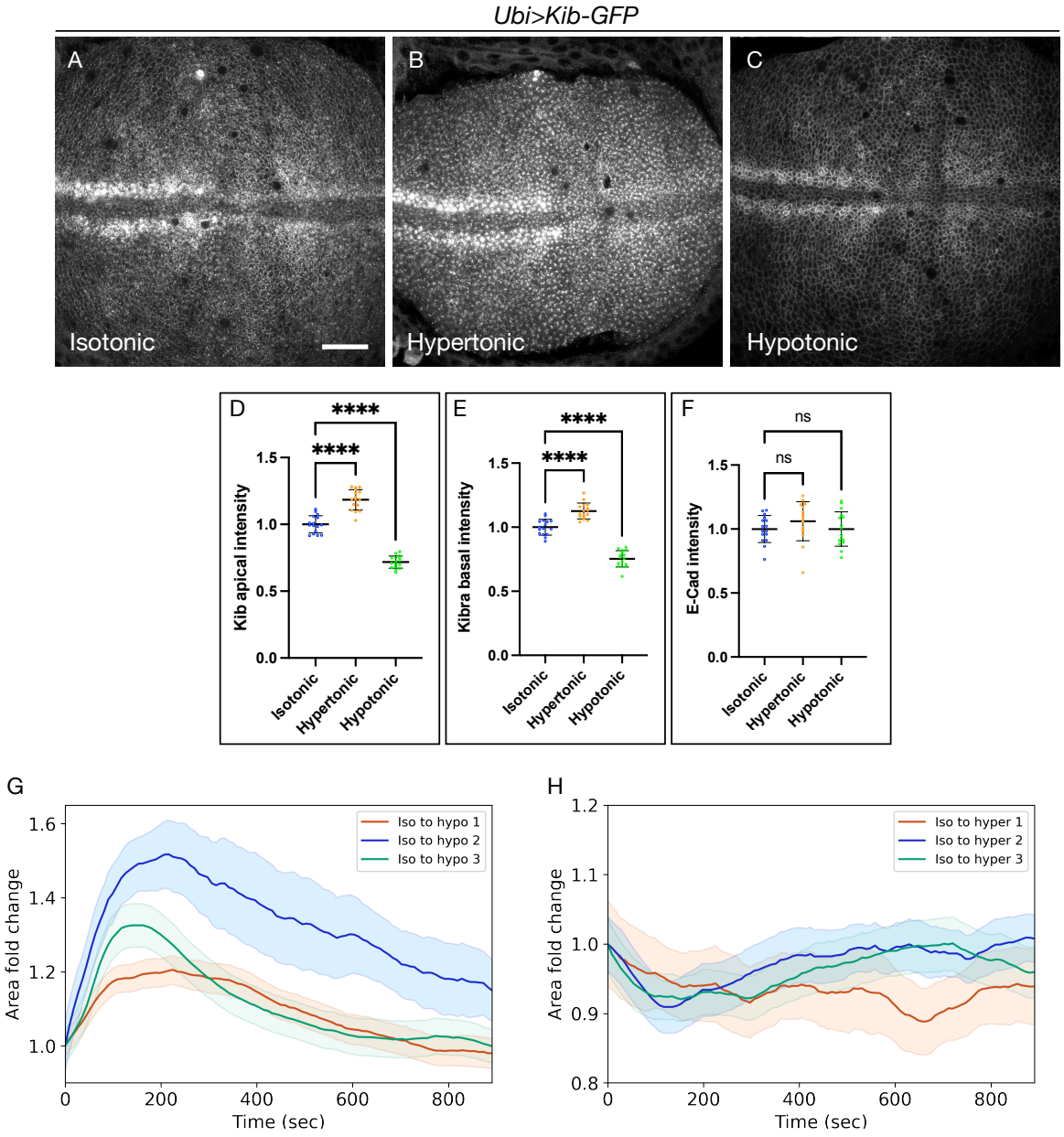

A-C) Compared to isotonic conditions (A), hypertonic shift results in higher Kib abundance (B), while hypotonic shift leads to lower Kib abundance (C). Scale bar = 20µm.
D-F') Quantification of mean apical Kib-GFP (D), basal Kib-GFP (E), and apical Ecad-mKate2 fluorescence (F). Ecad-mKate2 intensities were measured in the same regions as mean apical Kib-GFP. Statistical significance was calculated using One-way ANOVA followed by Tukey's HSD test.
G & H) Plots of area changes (mean ± SEM) of segmented tissues subjected to hypotonic (G) or hypertonic (H) shifts.

Figure 3.6: Treatment with Y-27632 raises Kib abundance and reverses the effect of hypotonic shift

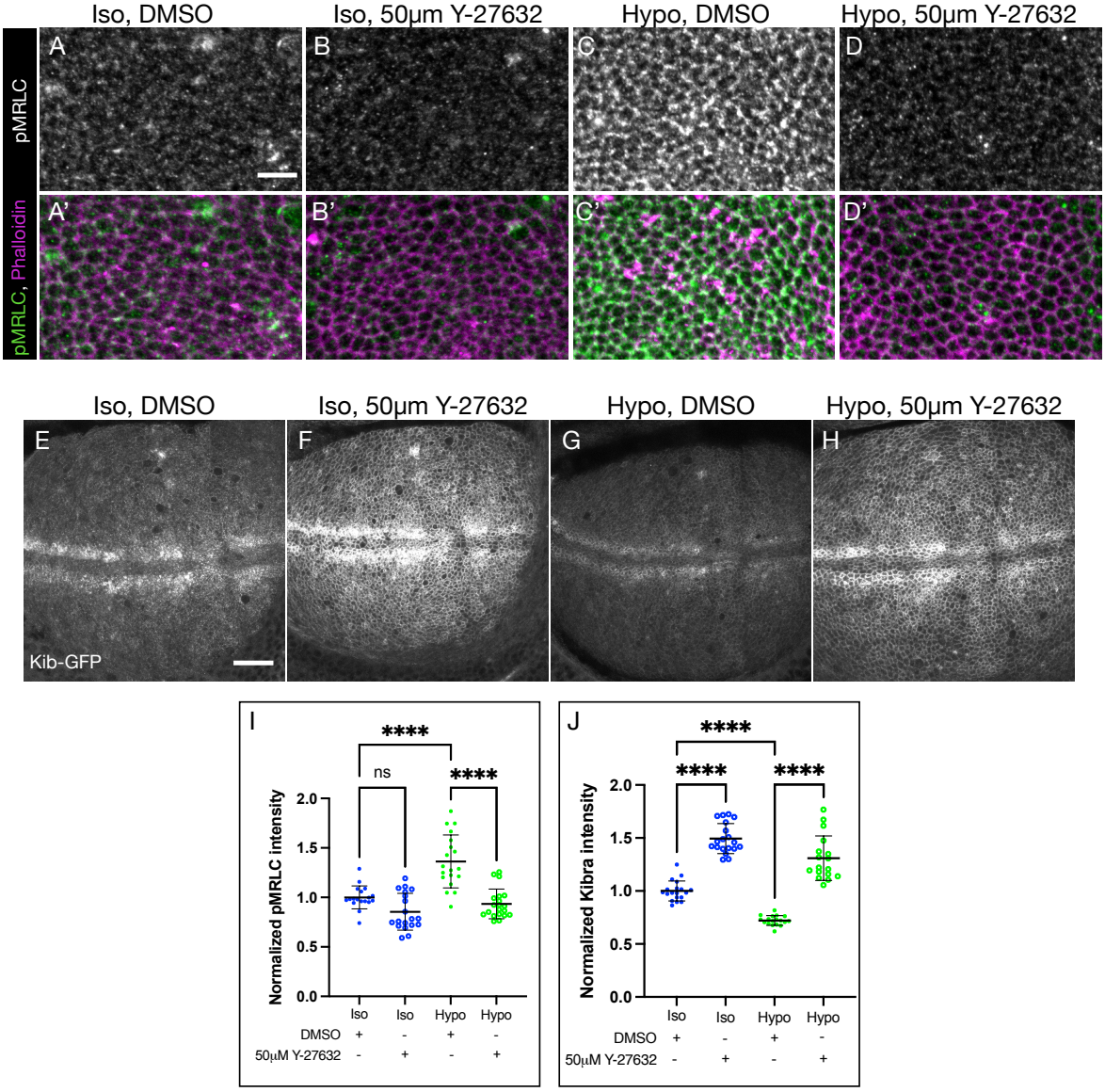

A-D') Staining with the antibody against pMRLC shows a slight decrease in pMRLC staining with Y27632 treatment under isotonic conditions (A-B') and a significant reversal of pMRLC upregulation under hypotonic shift (C-D'). Scale bar = 5µm.
E-H) Compared to control (E), treatment with Y-27632 significantly increases Kib abundance under isotonic conditions (F). Treatment with Y-27632 also reverses the decrease in Kib abundance induced by hypotonic shift (G & H). Scale bar = 20µm.
I) Quantification of normalized mean pMRLC intensities obtained from experiments represented in A-D'.
J) Quantification of normalized mean Kib-GFP intensities obtained from experiments represented in E-H. Statistical significance was calculated using One-way ANOVA followed by Tukey's HSD test.

tissues were treated with Y-27632 (Figs. 3.6A-B'), though this effect was not statistically significant (Fig. 3.6I). However, Y-27632 potently inhibited myosin hyperactivation induced by hypotonic conditions (Figs. 3.6C-D', I). Next, we asked if Y-27632 treatment would affect Kib abundance. Strikingly, we observed a substantial increase in Kib abundance after 15 min of Y-27632 treatment under isotonic conditions (Figs. 3.6E, F, & J), supporting the idea that myosin activity promotes Kib degradation. To test if Rok inhibition could block the effect of hypotonic shift, we first incubated our tissues in a hypotonic solution containing DMSO and then treated them with Y-27632, still in a hypotonic medium. Treatment with Y-27632 strongly reversed the effect of the hypotonic solution on Kib abundance (Figs. 3.6G, H, & J), suggesting that the effect of osmotic shifts on Kib abundance is caused by myosin activity.

We also considered the possibility that the effect of Y-27632 could be mediated via inhibition of another known target of this inhibitor, the atypical protein kinase C (aPKC). To test this possibility, we took advantage of a conditional allele of aPKC, *aPKC^{as4}*, which can be potently and acutely inhibited using 1NA-PP1, an allele-specific analog of a potent kinase inhibitor (Hannaford et al., 2019). As expected, under normal conditions, aPKC^{as4} was enriched at the apical cortex in wing imaginal tissues. However, treatment with 1NA-PP1 severely inhibited aPKC cortical localization (Figs.3.7A-B'). In contrast, treatment with Y27632 did not significantly affect aPKC cortical localization in wild type imaginal discs (Figs. 3.7C-D'). Additionally, we treated wing imaginal discs homozygous for *aPKC^{as4}* allele with 1NA-PP1and did not observe any changes in Kib abundance upon aPKC inhibition (Figs. 3.7E-G). Collectively, these results show that decreased Kib abundance we observed under hypotonic conditions is mediated via myosin activity.

Figure 3.7: aPKC inhibition does not affect Kib levels

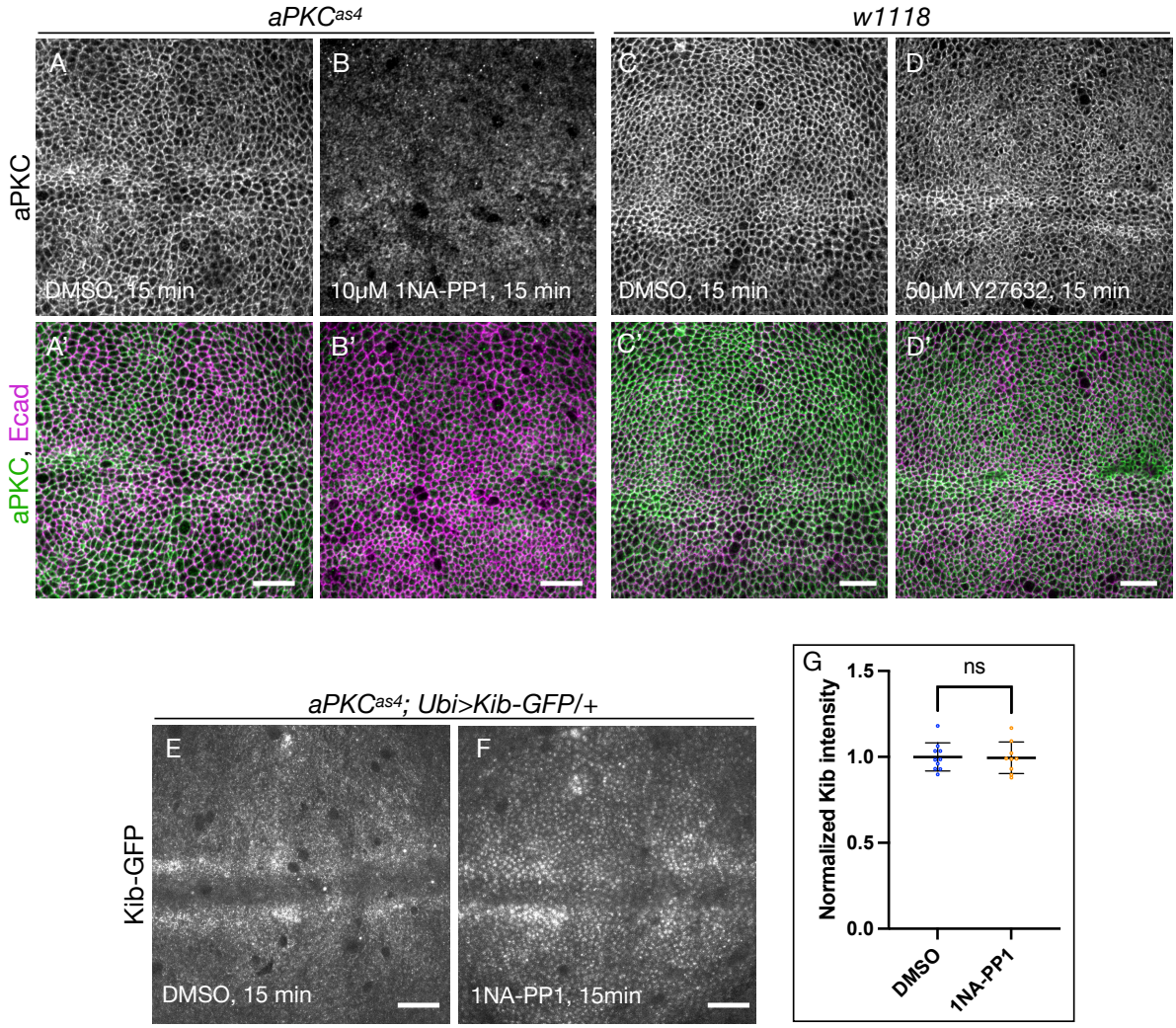

A-B') aPKC and Ecad immunostaining shows that while aPKC^{as4} is normally cortical in DMSO-treated wing discs (A & A'), cortical localization of aPKC was significantly inhibited upon treatment with 1NA-PP1 (B & B'). Scale bars = 10μm.
C-D') In wild type tissues aPKC localizes cortically under DMSO treatment (C & C'). Treatment with Y27632 does not significantly affect cortical aPKC localization (D & D'). Scale bars = 10μm.
E-G) In the background of homozygous *aPKC^{as4}* allele, Kib abundance was similar in DMSO-treated (E) and 1NA-PP1-treated tissues (F). Scale bars = 10μm. Statistical significance was calculated using Mann-Whitney test.

Par-1 regulates Kib abundance

How can tension influence abundance of a signaling protein such as Kib? Previous work identified a mechanism whereby tension inhibits Hippo signaling via Jub-mediated sequestration and inactivation of Wts/LATS at the cell-cell junctions (Rauskolb et al., 2014; Ibar et al., 2018). However, three lines of evidence suggest that tension-mediated regulation of Kib levels does not occur through the Jub-Wts mechanism. First, because we showed previously that Wts promotes Kib degradation (Tokamov et al., 2021), the decrease in Kib levels under higher cortical tension is unlikely to be explained by Jub-mediated Wts sequestration. Second, although we see a significant increase in myosin activity under hypotonic conditions (Fig. 3.3C), we do not detect significant changes in cortical Jub levels under osmotic shifts (Figs. 3.8A-D). Third, loss of Jub does not affect Kib levels (Fig. 3.8E).

Recently, myosin activity was shown to promote cortical localization of the serine/threonine kinase Par-1 in the Drosophila oocyte (Doerflinger et al., 2021). Interestingly, Par-1 mediates proteolytic degradation of an SCF^{Slimb} substrate Oskar (Morais-de-Sá et al., 2013) and is known to promote tissue growth via Hippo pathway inhibition (Huang et al., 2013). We therefore hypothesized that tension could promote Kib degradation via Par-1. To begin to test this idea, first we asked if Par-1 regulates the abundance of Ubi>Kib-GFP. Strikingly, Kib levels increased significantly upon Par-1 depletion (Figs. 3.9A & C). Conversely, ectopic Par-1 expression resulted in a significant reduction in Kib levels (Figs. 3.9B & C). In contrast, loss of Par-1 did not affect the abundance of $Kib^{\Delta WW1}$ (Figs. 3.9D & E), suggesting that Kib-mediated Hippo complex assembly is necessary for Par-1 regulation of Kib abundance.

Par-1 was previously shown to inhibit Hpo activity by direct phosphorylation on Ser30, which prevents Hpo association with Sav (Huang et al., 2013). Therefore, we considered the

Figure 3.8: Tension-mediated Kib degradation is independent of Jub-Wts mechanism

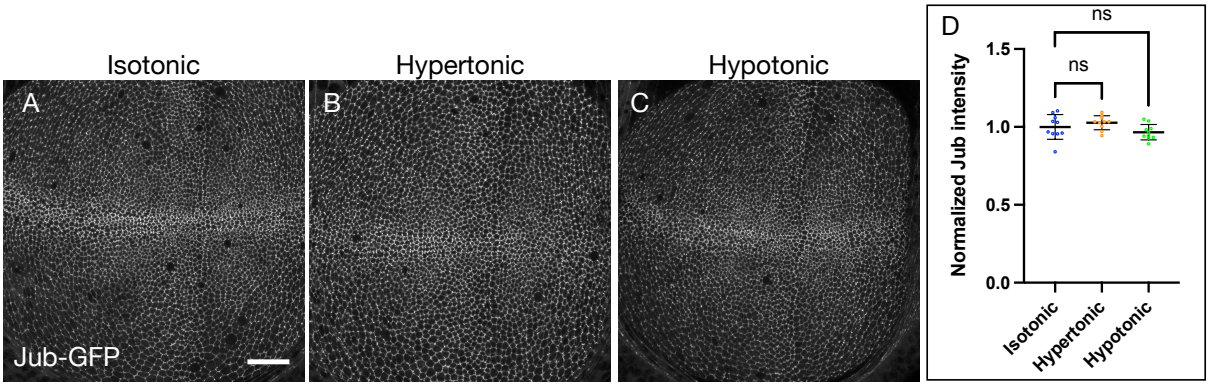

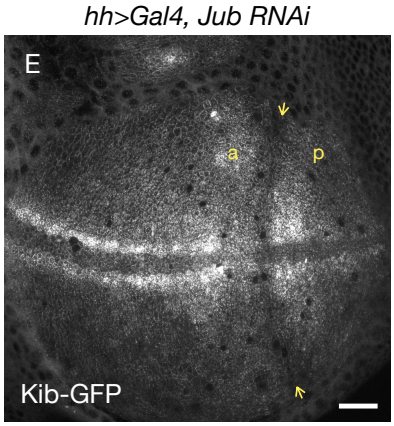

A-D) Jub cortical accumulation is not affected by osmotic shifts. Statistical significance was calculated using One-way ANOVA followed by Tukey's HSD test.
E) Depletion of Jub in the posterior compartment of the wing disc does not affect Kib levels. Yellow arrows indicate the anterior-posterior (a-p) boundary. Scale bars = 20μm.

possibility that the increase in Kib abundance under loss of Par-1 was indirectly caused by the lack of Hpo phosphorylation on Ser30. If this were the case, we reasoned that ectopic expression of Hpo construct that is refractory to Par-1 phosphorylation (Hpo^{S30A}), would also lead to increased Kib abundance. To this end, we first transiently overexpressed wild-type Hpo in the posterior compartment of the wing imaginal disc and examined the effect on Kib levels. Consistent with our previous finding that Hpo promotes Kib ubiquitination and degradation (Tokamov et al., 2021), Kib levels decreased significantly under ectopic Hpo expression (Fig. 3.9F). Similarly, erexpression of Hpo^{S30A} resulted in decreased Kib abundance (Fig. 3.9G), suggesting that the effect of Par-1 on Kib is not mediated through Hpo phosphorylation. Together, these results indicate that Par-1 regulates Kib abundance and suggest that tension could mediate Kib degradation via Par-1.

Tension controls cortical Par-1 localization in the wing epithelium

Given our results that Par-1 regulates Kib abundance, we next wondered if cortical tension affects cortical Par-1 localization, as was previously shown in the *Drosophila* oocyte (Doerflinger et al., 2021). To this end, we first examined Par-1 localization in control cells or in cells ectopically expressing RhoGEF2. Although known as a basolateral component, in the Drosophila blastoderm Par-1 also localizes at the apicolateral cortex (Bayraktar et al., 2006). In the wing imaginal disc, Par-1 displayed apical and basolateral localization, though its localization appeared diffused in both places (Fig. 3.10A & A'). Strikingly, transient expression of RhoGEF2 resulted in sharper Par-1 localization at the cell cortex both apically and basolaterally (Fig. 3.10B & B'). As an alternative approach, we also examined Par-1 localization under hypotonic conditions. Similar to RhoGEF2 expression, Par-1 was more tightly associated

Figure 3.9. Par-1 regulates Kib abundance independently of Hpo phosphorylation

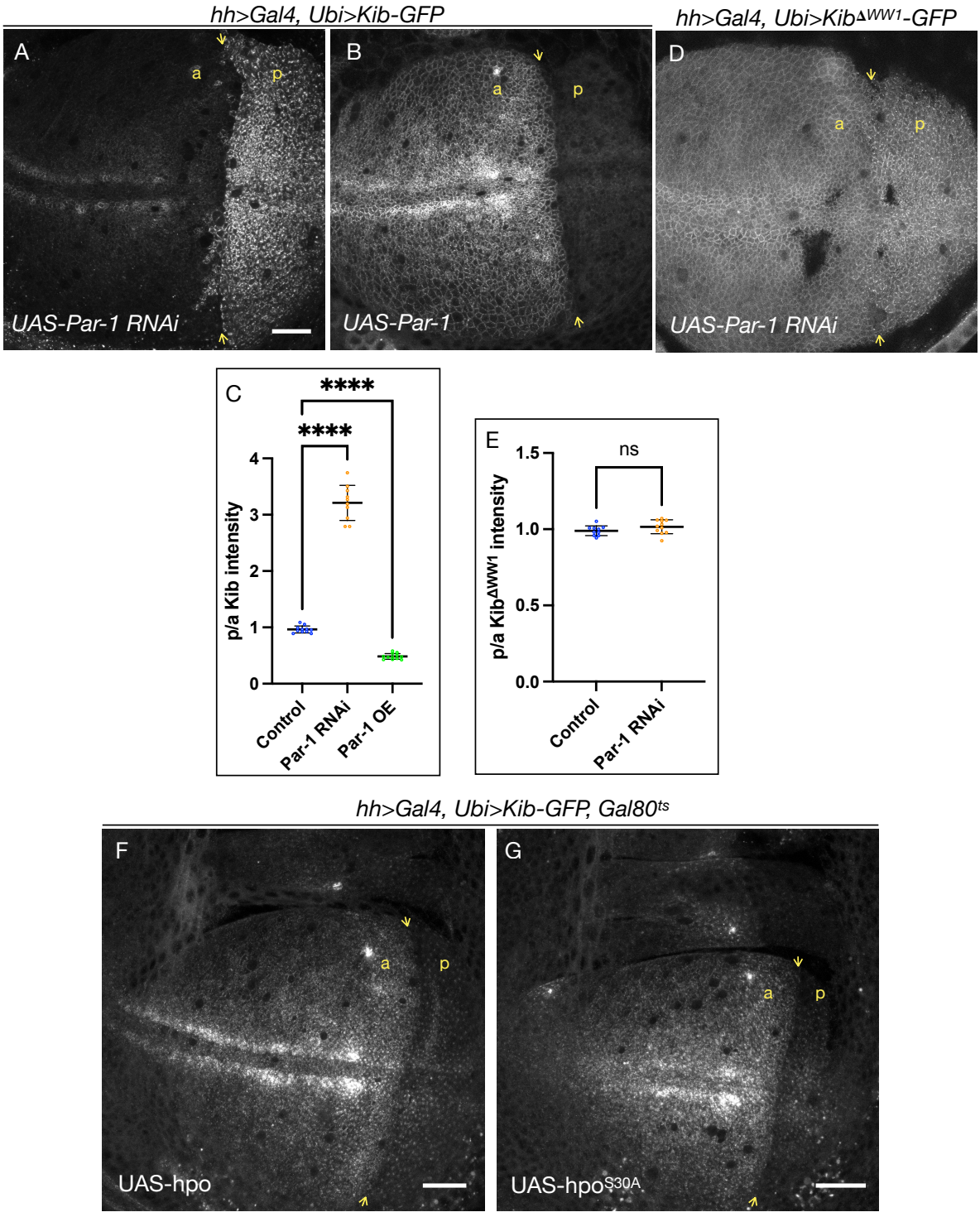

Figure 3.9 continued
A) Loss of Par-1 in the posterior wing disc compartment leads to a dramatic increase in Kib abundance. Yellow arrows indicate the anterior-posterior (a-p) boundary. Scale bar = 20μm.
B) Ectopic Par-1 expression results in Kib degradation.
C) Quantification of loss or gain of Par-1 function on Kib abundance as a p/a ratio of mean fluorescence intensity. Statistical significance was calculated using One-way ANOVA followed by Tukey's HSD test.
D) Loss of Par-1 does not affect $Kib^{\Delta WW1}$ abundance.
E) Quantification of loss of Par-1 function on $Kib^{\Delta WW1}$ abundance as a p/a ratio of mean fluorescence intensity. Statistical significance was calculated using Mann-Whitney test.
F-G) Transient overexpression of wild-type Hpo and Hpo^{S30A} in the posterior compartment of the wing imaginal disc leads to similar decrease in Kib abundance. Yellow arrows indicate the anterior-posterior (a-p) boundary. Scale bars = 20μm.

Figure 3.10: Tension promotes Par-1 association with the cell cortex

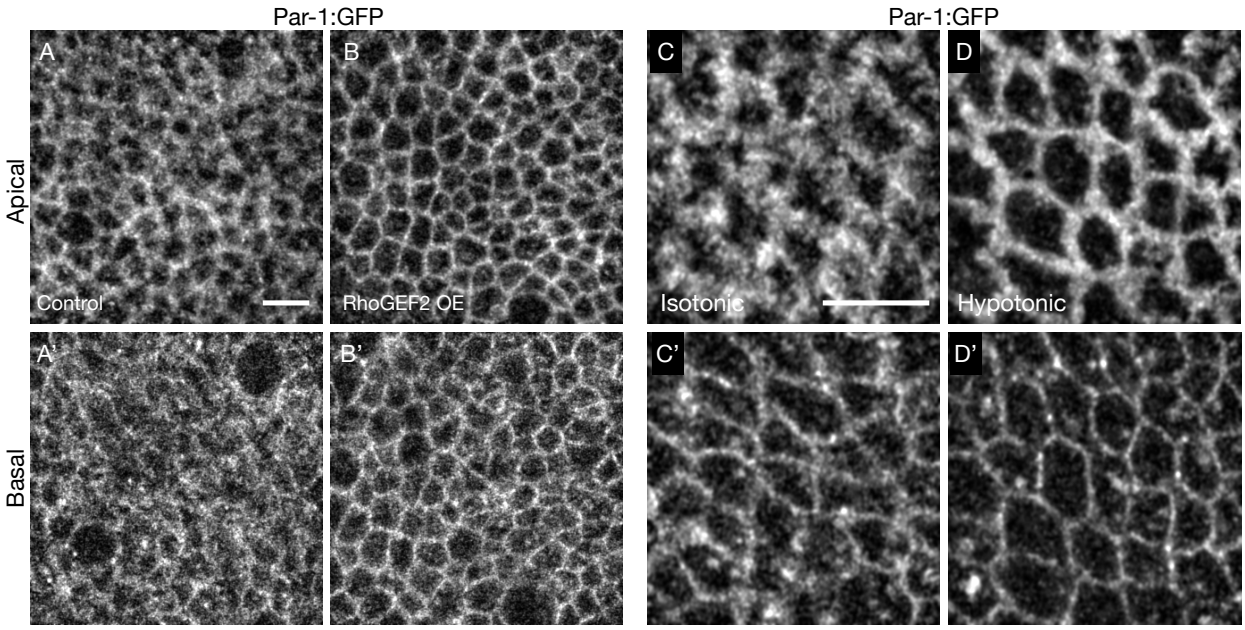

A & B') Compared to control cells (A & A'), ectopic RhoGEF2 expression leads to tighter Par-1 localization at the apical and basolateral cortex (B & B'). Scale bar = 5μm.
C & D') Airyscan confocal images showing that compared to isotonic conditions (C & C'), Par-1 becomes more cortical under hypotonic shift (D & D'). Scale bar = 5μm.

with the apical and basolateral cortex under hypotonic compared to isotonic conditions (Figs. 3.10C-D'). These results suggest that myosin activity can promote Par-1 cortical association in the wing imaginal epithelium as was previously shown in the oocyte.

In Chapter 2, we showed that Kib abundance was upregulated in rapidly proliferating mosaic clones (bantam clones) that display lower cortical tension (Pan et al., 2016; Tokamov et al., 2021). Therefore, we examined Par-1 in these clones. Unexpectedly, we found that while Par-1 remained cortical, its levels were downregulated in bantam clones (Figs. 3.11A-D). The decrease in Par-1 was more pronounced in the apical sections of the tissue and relatively mild in the basal sections (Figs. 3.11C & D). Interestingly, this effect was observed only in larger, more coherent clones, whereas Par-1 levels were not changed in smaller and irregularly shaped clones (Figs. 3.11B-B'), suggesting that it is not the expression of bantam per se, but likely the change in clone mechanical properties that affected Par-1 cortical levels. We suspect that on the timescale of a genetic experiment, lower cortical tension may destabilize Par-1 and lead to its degradation, but we have not formally tested this possibility. Because it was previously shown that Yki activity decreases in bantam clones, we also tested the possibility that Par-1 could be transcriptionally regulated by Yki. However, we saw no effect on Par-1 levels upon ectopic Yki expression (Fig. 3.11E), suggesting that the decrease in Par-1 in bantam clones was not due to diminished Yki activity.

Tension-mediated Kib degradation requires Par-1

We reasoned that if tension regulates in Kib abundance via Par-1, then in the absence of Par-1 tension should have no effect on Kib levels. To test this idea, we depleted Par-1 in the posterior compartment of the wing imaginal disc using the *hh>Gal4* driver and quantified

Figure 3.11: Par-1 levels are downregulated in *bantam* colones

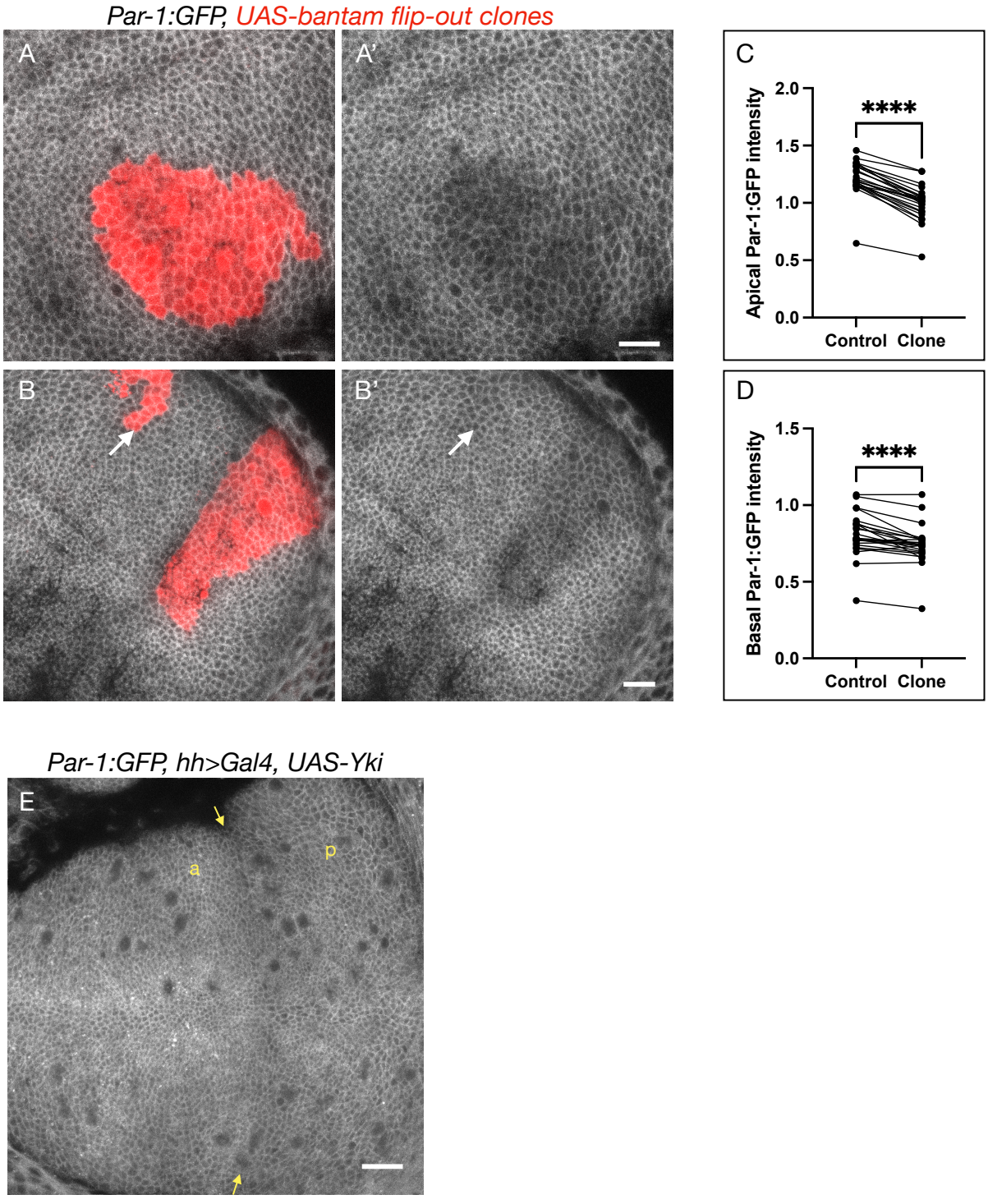

Figure 3.11 continued
A-B') Examples of *UAS-bantam* clones (RFP positive) induced in wing imaginal discs expressing Par-1:GFP. While arrows in B & B' point to a smaller, irregularly shaped clone in which Par-1 levels are unaffected. Scale bars = 10μm.
C-D) Pair-wise comparison of apical (C) or basal (D) Par-1:GFP intensity in clone vs. control cells. Each line represents a clone-control pair from the same tissue. Statistical significance was calculated using Wilcoxon matched-pairs signed rank test.
E) Overexpression of Yki in the posterior compartment of the wing imaginal disc has no effect on Par-1 levels. Yellow arrows indicate the anterior-posterior (a-p) boundary. Scale bar = 20μm.

Figure 3.12: Par-1 regulates Kib abundance in tension dependent manner

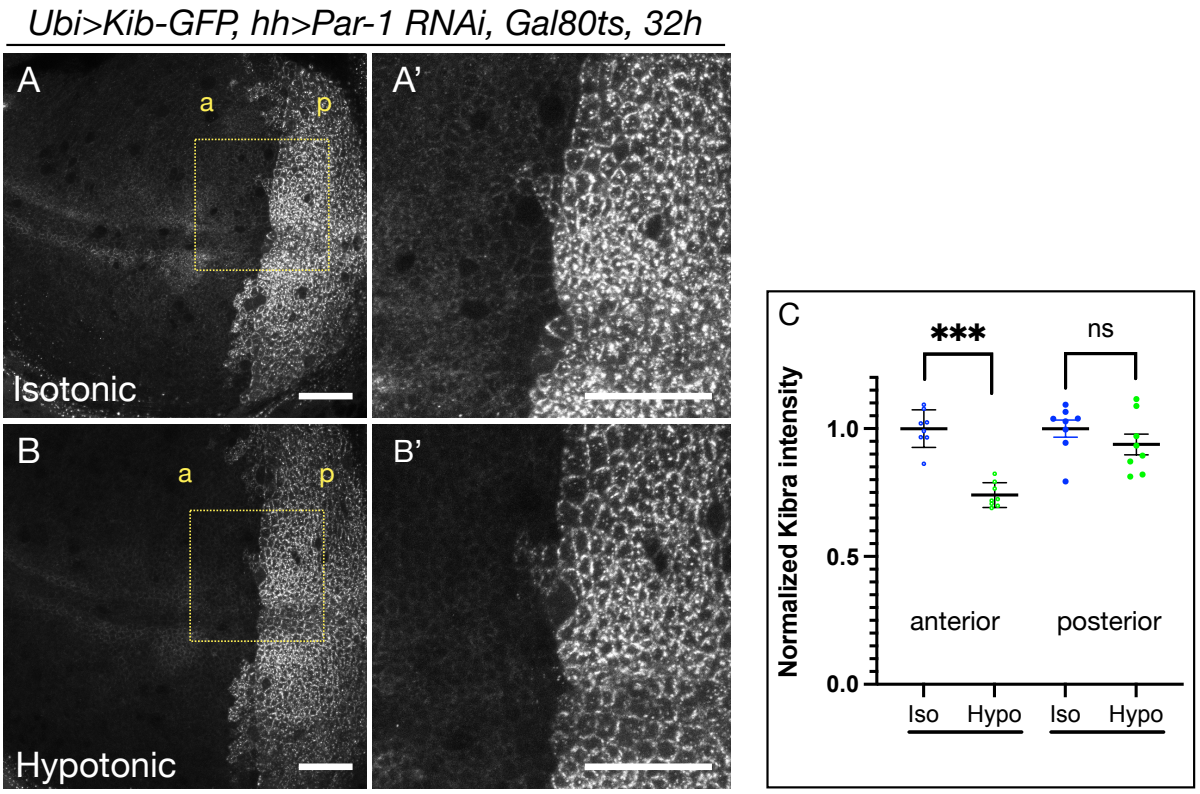

A-B') Under isotonic conditions, depletion of Par-1 in the posterior compartment (p) leads to a significant increase in Kibra levels (A & A', C). Shift to hypotonic conditions leads to a significant decrease in Kibra abundance in the anterior region, but only a mild (not statistically significant) decrease in the posterior region where Par-1 was depleted (B & B', C). Scale bars = 20μm. Statistical significance was calculated using Mann-Whitney test.

changes in Kib levels when tissues were shifted from isotonic to hypotonic conditions. While we observed a significant decrease in Kib intensity in the anterior (control) compartment, there was no significant change in the posterior (Par-1 depleted) compartment (Figs. 3.12A-C). Collectively, these results suggest that tension modulates Kib abundance by controlling Par-1 cortical association.

3.3 Discussion

In this study, we show that mechanical forces can dynamically modulate Kib abundance. We demonstrate that increasing myosin activity genetically or acutely results in Kib degradation. Conversely, inhibiting myosin activity leads to increased Kib levels. We find that tension-mediated Kib degradation occurs independently of the previously described Jub-Wts mechanism. Instead, increased tension leads to more cortically localized Par-1, and Par-1 promotes Kib degradation. This work sheds light on the regulation of an upstream Hippo signaling component by mechanical forces and provides further support for the mechanical feedback model in tissue growth control.

Our observations that Jub cortical accumulation was not affected by the increased myosin activity and junctional tension induced by hypotonic conditions raises a question of how the previously described Jub-Wts mechano-sensing mechanism is different from the one we describe here. Previous reports have shown that Jub physically associates with the N-terminal region of α-catenin, which becomes accessible to Jub by tension-mediated opening of α-catenin (Alégot et al., 2019; Sarpal et al., 2019). Under this model, α-catenin opening is thought to be induced by forces applied perpendicularly to cell-cell junctions (Rauskolb et al., 2019). Indeed, in the developing Drosophila notum, where apical stress fibers are generated in response to axial tension and connect two opposing junctions, Jub accumulates at the points of attachment of the stress fibers to the junctions (López-Gay et al., 2020). It is possible that in contrast to Jub, Kib abundance is regulated by the forces applied parallel to cell-cell junctions, such as when junctions are physically stretched. Observing changes in Kib abundance via direct mechanical tissue stretching, as was recently described (Duda et al., 2019), could further reveal the dynamics of how forces regulate Kib and other Hippo pathway components.

Our work also raises the question about the role of Par-1 in the regulation of Hippo signaling. Previous work suggested that Par-1 phosphorylates Hpo, which prevents Hpo association with Sav (Huang et al., 2013). Here, we find that Par-1 regulates Kib abundance independently of Hpo phosphorylation (Fig. 3.9). Our observation that Par-1 affects wild-type Kib but not $Kib^{\Delta WW1}$ suggests that Par-1 regulates Kib via the Hippo complex-mediated degradation mechanism involving Slimb described in Chapter 2 (Tokamov et al., 2021). This idea is supported by a previous finding that Par-1 functions with Slimb in promoting degradation of Oscar during Drosophila oocyte development (Morais-de-Sá et al., 2013). Notably, active Par-1 was also found to be a target of Slimb-mediated degradation (Lee et al., 2012), further highlighting the tight association between Par-1, Slimb, and Kib. Based on these findings, we propose that when Kib assembles a signaling complex, Par-1 can be recruited to this complex in a tension-dependent manner and phosphorylate Kib, leading to Slimb recruitment and subsequent Kib turnover. It is still unclear what happens to the rest of the signaling complex after Kib is degraded. The dual role of Par-1 in inhibiting Hpo-Sav interaction and promoting Kib degradation, and the fact that active Par-1 is also degraded by Slimb, could provide a means of disassembling the entire signaling complex upon Kib turnover.

An intriguing question this study raises is whether Kib degradation and Kib signaling occur in distinct subcellular compartments. Previous work has shown that Kib and Mer localize at two distinct subcellular regions – the junctional and apicomedial cortex – and that apicomedial Kib is more active in promoting pathway activation (Su et al., 2017). This organization of cortical Kib is similar to the actomyosin distribution in epithelia (Martin et al., 2009; Booth et al., 2014; Garcia De Las Bayonas et al., 2019). Furthermore, our preliminary studies (Chapter4) suggest that Kib is tightly linked to this network.

Although the relationship between Kib and the actomyosin cytoskeleton at the subcellular level has not yet been shown, our findings raise the possibility that distinct pools of actomyosin network could differently regulate Kib degradation and signaling. We find that under hypotonic conditions, increased myosin accumulation and junctional tension leads to more junctional Par-1 and decreased Kib levels (Figs.3.5A-D & 3.10C-D'). These observations suggest that tension-mediated Kib degradation could occur at the junctional cortex. This would be consistent with the known role of junctional tension in inhibiting Hippo signaling and promoting Yki/YAP activity (Rauskolb et al., 2014; Ibar et al., 2018; Alégot et al., 2019; Sarpal et al., 2019).

To date, the role of apicomedial actomyosin pool in the regulation of Hippo signaling and tissue growth has not been elucidated. However, the spectrin cytoskeleton is known to promote Hippo signaling by modulating myosin contractility (Deng et al., 2015; Fletcher et al., 2015; Deng et al., 2020), and a recent study found that βH-spectrin is required for the ratcheting behavior of apicomedial myosin during Drosophila mesoderm invagination (Krueger et al., 2020). Combined with a previously reported physical interaction of βH-spectrin with Kib and Mer (Fletcher et al., 2015), these studies collectively point to a possibility that the spectrin cytoskeleton and apicomedial actomyosin could promote the activity of Kib and Mer at the apicomedial cortex. Closer examination of the dynamics of Kib and Mer together with the spectrin and actomyosin networks is needed to understand how cortical cytoskeleton can organize upstream Hippo signaling components and affect tissue growth.

3.4 Methods

Table 3.1. Reagents

Reagent type (species) or resource	Designation	Source or reference	Identifiers	Additional information
genetic reagent (*D. melanogaster*)	*Ubi>Kib-GFP-FLAG*	10.7554/eLife.62326		
genetic reagent (*D. melanogaster*)	*Ubi-Kib$^{\Delta WW1}$-GFP-FLAG*	10.7554/eLife.62326		
genetic reagent (*D. melanogaster*)	*UASp-T7-RhoGEF2*	Bloomington Drosophila Stock Center	BL9387	
genetic reagent (*D. melanogaster*)	*UASt-myr-Yki*	10.1016/j.devcel.2018.06.017		
genetic reagent (*D. melanogaster*)	*UAS-Strn RNAi*	Bloomington Drosophila Stock Center	BL26736	Validated in 10.1016/j.devcel.2018.06.017
genetic reagent (*D. melanogaster*)	*UAS-Par-1 RNAi*	Bloomington Drosophila Stock Center	BL32410	
genetic reagent (*D. melanogaster*)	*UAS-jub RNAi*	Bloomington Drosophila Stock Center	BL30806	Validated in 10.1016/j.cub.2010.02.035

Table 3.1. Continued

genetic reagent (*D. melanogaster*)	*Ecad-3XmKate2*	10.1038/nature22041		
genetic reagent (*D. melanogaster*)	*Par-1:GFP (protein trap)*	Bloomington Drosophila Stock Center	BL64452	
genetic reagent (*D. melanogaster*)	*Jub:GFP*	Bloomington Drosophila Stock Center	BL56806	
genetic reagent (*D. melanogaster*)	w^{1118};yki^{B5} {yki-YFP} VK37	10.1016/j.devcel.2018.06.017		
genetic reagent (*D. melanogaster*)	$aPKC^{as4}$	10.1242/dev.170589		
Antibody	anti-pSqh (Guinea pig, polyclonal)	10.1016/j.gep.2010.09.008		Tissue staining (1:300)
Antibody	anti-DEcad (Rat, polyclonal)	Developmental Studies Hybridoma Bank	Cat#AB_528120; RRID:AB_528120	Tissue staining (1:1000)
Chemical	Y-27632	Fisher Scientific	Cat. # 12541	Rho kinase inhibitor
Chemical	1-NA-PP1	Cayman	Cat. # CAYM-10954-1	Inhibitor

Drosophila husbandry

Drosophila melanogaster was cultured using standard techniques at 25°C (unless otherwise noted). For Gal80^{ts} experiments, crosses were maintained at 18°C and moved to 29°C for the duration specified in each experiment. To generate *UAS-ban* flip-out clones, larvae were grown at 25°C and heat shocked at 48h after egg laying in an EchoTherm IN35 incubator using the following program: 38°C for 1h, 25°C for 1h, 38°C for 1h.

Live imaging

Live imaging method of the wing imaginal discs was adapted from Restrepo et al. (2016). Briefly, wing imaginal tissues were first dissected in Schneider's Drosophila Medium (Sigma) supplemented with 10% Fetal Bovine Serum (Thermo Fisher Scientific) on a siliconized glass slide. The tissues were then transferred with a pipette in 5-10µl of medium to a glass bottom microwell dish (MatTek, 35mm petri dish, 14mm microwell) with No. 1.5 coverglass. The discs were oriented so that the apical side of the disc proper faced the coverglass. A Millicell culture insert (Sigma, 12mm diameter, 8µm membrane pore size) was prepared in advance by cutting off the bottom legs with a razor blade and removing any excess membrane material around the rim of the insert. The insert was carefully placed into the 14mm microwell space, directly on top of the drop containing properly oriented tissues. To prevent the tissue from moving, the space between the insert and the microwell was sealed with ~15µl of mineral oil. Media with indicated osmolarity and/or chemical inhibitor was then added into the chamber of the insert (200µl in all experiments). An inverted Zeiss LSM880 laser scanning confocal microscope equipped with a GaAsP spectral detector and the Airyscan module was used for all imaging (except for laser ablation experiments, see below).

Osmotic shift experiments

Schneider's Drosophila Medium (Sigma) supplemented with 10% Fetal Bovine Serum (Thermo Fisher Scientific) was used as isotonic medium (~360mOsm). To make a hypertonic solution, the osmolarity of the isotonic solution was increased to 460mOsm using 1M NaCl (5µl of 1M NaCl per 100 µl of solution). To make a hypotonic solution, the isotonic medium was diluted with deionized water to 216mOsm (40µl dH_2O per 100µl of solution). All osmotic solutions were prepared fresh immediately before the experiments. In most experiments, tissues were incubated for 15 min. For practical reasons, in laser ablation experiments, tissues were incubated for 8 min to allow for measurements to be taken at an average of 15 min under osmotic incubations. To observe changes in Yki-YFP localization, tissues were incubated for 30min.

pSqh staining experiments

During experiments, wandering third instar larvae were dissected in an isotonic solution and the wing imaginal discs were transferred into a 150µl drop of prepared osmotic medium. For experiments with Y-27632, osmotic media with 50µM of Y-27632 were prepared. The tissues were incubated for 15 min. After incubation, the discs were washed with 1X Ringer's buffer with correspondingly adjusted osmolarity (i.e. for hypertonic experiments, a hypertonic wash was prepared the same way as described above, except 1X Ringer's was used instead of the Schneider's medium) and fixed for 20 min in 2% paraformaldehyde/1X Ringer's solution also with properly adjusted osmolarity (for Y-27632 experiments, 50µM of Y-27632 was also added in the wash and the fix solutions). Tissues were then stained as previously described (McCartney and Fehon, 1996).

Laser ablation experiments

Laser cuts were conducted using a pulsed Micropoint nitrogen laser (Andor Technology) tuned to 365 nm and mounted on an Andor Revolution XD spinning disk confocal microscope. Individual junctions were ablated by delivering 3 pulses at a single point with a duration of 67 ms/pulse. The tissue was imaged 2x before and 20x immediately after ablation, with a time interval of 4 s. Images were acquired using a 100X oil-immersion lens (Olympus, NA 1.40), an iXon Ultra 897 camera (Andor), and Metamorph (Molecular Devices) as the image acquisition software. Sixteen-bit Z-stacks were collected at each time point consisting of 7 slices with 0.5 μm interval.

To measure initial recoil velocity, the positions of the two tricellular vertices connected by the ablated junction were manually tracked using the SIESTA image analysis platform (Fernandez-Gonzalez and Zallen, 2011), and the initial retraction velocities were calculated using custom MATLAB scripts.

Image analysis and quantification of fluorescence intensity

All images were processed in ImageJ. Mean fluorescence intensity measurements were taken from maximum apical projections (~0.75 μm/section, four to five sections) or from single basal optical sections (~7.5-10μm below the apical surface). Plots and statistical analyses of mean fluorescence intensities were generated using GraphPad Prism software.

To measure changes in apical areas under osmotic shifts, cells were segmented using Cellpose (Stringer et al., 2021) and tracked via a custom written algorithm. Areas and the corresponding standard error values were plotted using Python.

CHAPTER 4

Kibra organization at the apical cortex is regulated via actomyosin dynamics

4.1. Introduction

The Hippo signaling pathway is a key regulator of tissue growth. At the core of the Hippo pathway, a kinase cascade consisting of serine/threonine kinases Tao-1, Hippo (Hpo), and Warts (Wts) culminates in the phosphorylation of a pro-growth transcriptional co-activator Yorkie (Yki). Phosphorylation inhibits Yki transcriptional activity by blocking its nuclear translocation (Zheng and Pan, 2019). The core kinase cascade is regulated by upstream components Kibra (Kib), Merlin (Mer), and Expanded (Ex). Since the discovery of the Hippo pathway, much progress has been made in understanding the biochemical mechanisms by which the core kinase cassette regulates Yki (Manning et al., 2020). However, less is known about the regulation of the upstream components and whether their activity is modulated by any external or internal cues.

All of the upstream Hippo pathway components are enriched at the apical cortex of epithelial cells, where they are thought to activate the kinase cascade. Kib is a multivalent protein that recruits the associated Hippo pathway components Merlin (Mer), Salvador (Sav), Hippo (Hpo), and Warts (Wts) into a signaling complex (Genevet et al., 2010; Yu et al., 2010; Su et al., 2017). Ex is recruited to the cell cortex by an apical polarity protein Crumbs (Crb) and assembles a similar signaling complex that functions in parallel to Kib (Boedigheimer et al., 1997; Robinson et al., 2010; Su et al., 2017; Sun et al., 2015; Tokamov et al., 2021; Yu et al., 2010). At the subcellular level, both Kib and Ex localize at the junctional cortex independently of one another (Genevet et al., 2010; Su et al., 2017; Tokamov et al., 2021). However, unlike Ex, Kib also localizes at a non-junctional region at the apical surface, known as the apicomedial (or medial) cortex (Su et al., 2017). Kib recruits Mer to the medial cortex, and Mer is required to

recruit Sav and the core kinases Hpo and Wts. Thus, Kib is a key scaffold that assembles a functional Hippo signaling complex at the medial cortex. Indeed, when untethered from the junctional region and localized exclusively at the apicomedial cortex, Kib was shown to more potently suppress growth, suggesting Kib-mediated signaling is enhanced at the medial region (Su et al., 2017). Despite the apparent importance of Kib localization, it remains unknown how Kib is organized at the cell cortex and whether there is a biological significance of its partitioning into distinct subcellular pools.

The localization of Kib at the junctional and apicomedial cortex strikingly resembles actomyosin organization in epithelial cells (Lecuit et al., 2011; Heer and Martin, 2017). It has long been recognized that actomyosin-generated forces regulate the activity of Yki and its mammalian homolog YAP/TAZ (Misra and Irvine, 2018; Zheng and Pan, 2019). Junctional tension promotes accumulation of a LIM domain protein Ajuba (Jub) at the adherens junctions, and Jub sequesters and inhibits Wts, thereby stimulating Yki/YAP activity (Rauskolb et al., 2014; Ibar et al., 2018). Similarly, as our data in Chapter 3 suggest, junctional tension promotes Yki activity via Kib degradation. However, the possibility that the apicomedial actomyosin network regulates Hippo signaling has not been explored.

Myosin dynamics are known to organize signaling molecules at the cell cortex of epithelial and non-epithelial cells (Munro et al., 2004; Goehring et al., 2011; Munjal et al., 2015; Oon and Prehoda, 2021). In this chapter, we set out to explore the potential association of Kib with the actomyosin network in the wing imaginal epithelium. Our results show that Kib decorates apical F-actin structures and displays dynamics similar to F-actin and myosin. Furthermore, acute manipulation of actomyosin organization leads to concomitant changes in Kib localization and blocking actomyosin dynamics blocks medial Kib localization. Finally,

actomyosin-driven medial Kib recruits Mer and Hpo to the medial cortex, suggesting that in contrast to junctional forces, medial myosin dynamics positively regulate Hippo signaling by promoting Kib-mediated complex formation. Together, our results uncover a novel role of medial actomyosin pool in the regulation of Hippo signaling via Kib.

4.2 Results

Kibra decorates apicomedial F-actin and is associated with actomyosin dynamics

The link between actomyosin-generated tension and Kib degradation described in Chapter 3, as well as the similarity between Kib and actomyosin subcellular distribution, prompted us to look more closely at the possible subcellular association of Kib with the apical actomyosin network. Using the Airyscan confocal microscope for better spatial resolution, we first examined the localization of endogenous Kib tagged with GFP (Kib::GFP) or Kib tagged with the Halo tag and expressed under the ubiquitin promoter (Ubi>Kib-Halo) with respect to F-actin. To visualize F-actin, we used either UAS-driven LifeAct-Halo or a GFP-tagged Moesin actin-binding domain expressed under the *spaghetti squash* promoter (sGMCA). In the wing imaginal epithelial cells, both Kib::GFP and Ubi>Kib-Halo localized at the junctional and apicomedial cortex, as observed previously (Su et al., 2017; Tokamov et al., 2021). Although both Kib and F-actin localize junctionally, Kib's punctate pattern is quite distinct from the more uniformly distributed F-actin. In contrast, apicomedial Kib distribution seemed superficially similar to that of F-actin. Indeed, close examination revealed that both Kib::GFP and Ubi-Kib-Halo localized adjacently to or decorated apicomedial F-actin structures (Figs. 4.1A-B''), suggesting that Kib might be associated with the apical actomyosin network.

We next examined Kib subcellular dynamics with F-actin or myosin via time lapse imaging. Because endogenous Kib is normally expressed at low levels in the wing imaginal discs, we used UASp-Kib-GFP, which produces functional Kib protein with normal subcellular localization (Tokamov et al., 2021), or Ubi>Kib-Halo. Intriguingly, we observed co-movement of Kib with F-actin and in some cases Kib punctae that appeared to be carried by F-actin from the junctional to medial cortex, where these punctae then fused with the pool of Kib that was

Figure 4.1: Kib decorates apical F-actin network

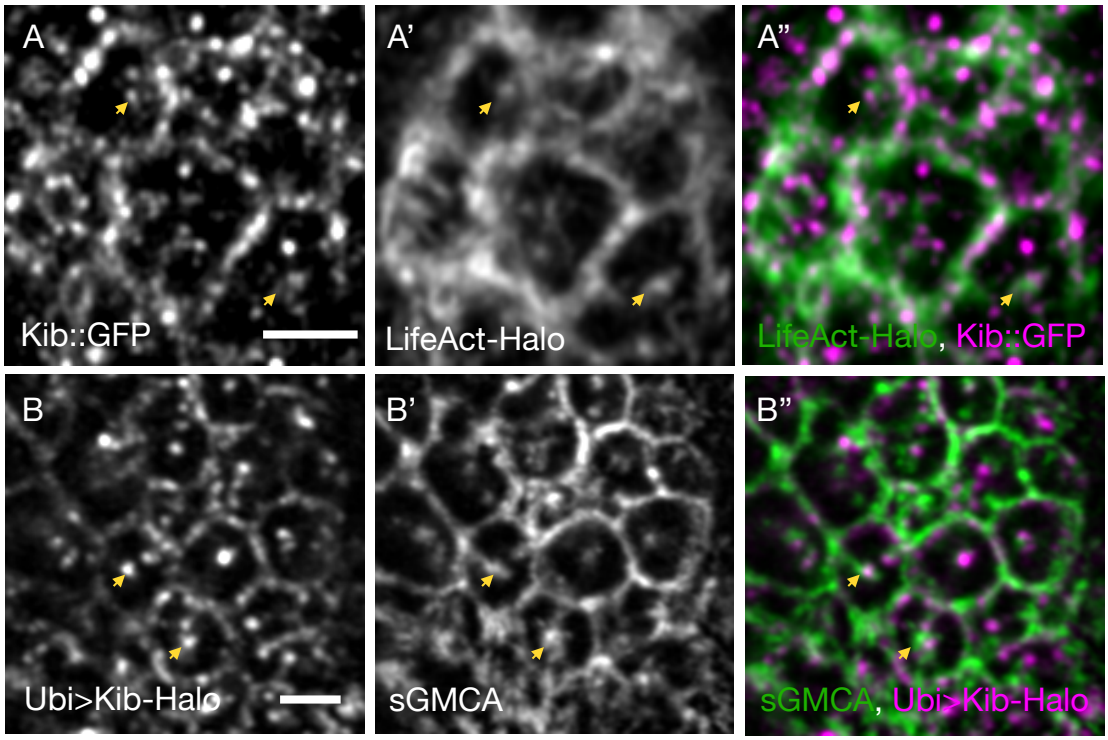

A-B'') Apical projections of wing imaginal tissues expressing either endogenous Kib::GFP and LifeAct-Halo (A-A'') or Ubi>Kib-Halo and sGMCA (B-B''). Yellow arrowheads point at apicomedial Kib punctae decorating apical F-actin structures. Scale bars = 2µm.

Figure 4.2: Kib is associated with actomyosin dynamics

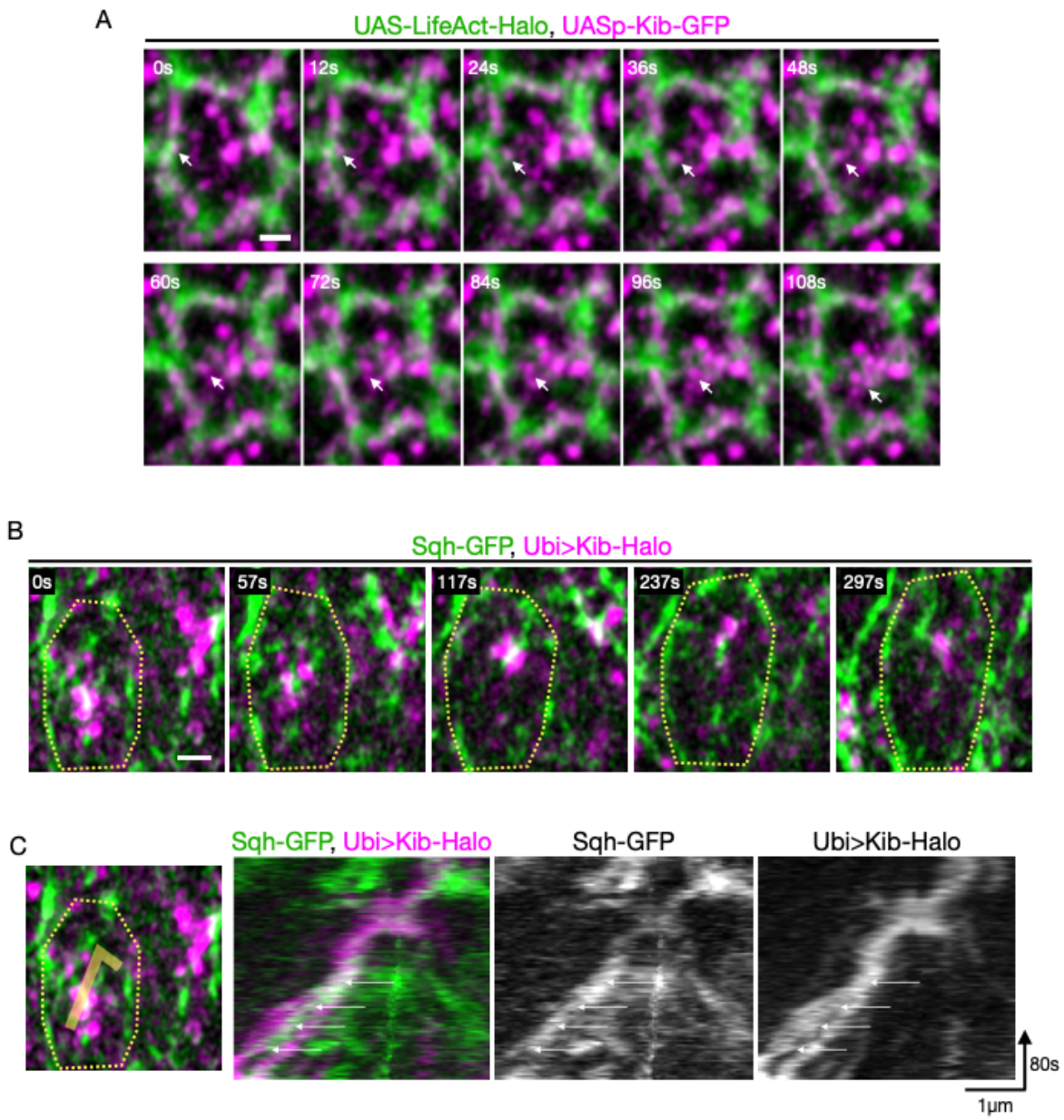

A) Single frames from a timelapse movie of a single cell showing co-migration of a Kib punctum (magenta) with F-actin (green) from the junctional to the apicomedial region (white arrow), where it fuses with the rest of the apicomedial Kib pool. Scale bar = 1µm.
B) Single frames from a timelapse movie of a single cell co-migration of medial Kib (magenta) with myosin (green). The contours roughly outline the cell. Scale bar = 1µm.
C) A kymograph tracking co-migration of medial Kib and myosin shown in B. The white arrows point to a myosin pulse that increases in intensity over time that is associated with the merger of two initially separate Kib punctae.

already present at the medial cortex (Fig.4.2A). Similarly, timelapse imaging of Kib with myosin revealed comigration of both proteins at the apicomedial cortex (Fig. 4.2B). Specifically, we observed coalescence of medial myosin associated with the merging of Kib punctae, suggesting that myosin contractility promotes apicomedial clustering of Kib (Fig. 4.2C). Together, these results suggest that Kib is associated with the apical actomyosin network and that actomyosin dynamics might regulate Kibra localization at the apical cortex.

Osmotic shifts can be used to acutely alter actomyosin organization

To further test the relationship between actomyosin dynamics and Kib localization, we next sought to acutely alter actomyosin organization and examine any potential changes in Kib localization. To this end, we turned to osmotic manipulations (see Chapter 3). As shown in the previous chapter, changes in medium osmolarity can dramatically affect myosin activity and junctional tension. Therefore, we wondered if osmotic shifts also affect subcellular actomyosin organization.

In wing imaginal discs incubated under isotonic conditions, both F-actin and myosin are apically enriched and display junctional and apicomedial subcellular localization (Figs. 4.3A-A', E-E'). Strikingly, incubating wing imaginal tissues in a hypertonic solution led to apicomedial enrichment of F-actin (Figs. 4.3B-B'). Conversely, under hypotonic conditions F-actin accumulated predominantly at the junctional cortex (Figs. 4.3C-C'). To quantify these changes, we used Ecad-mKate2 fluorescence to segment the junctional cell outlines, applied the mask to separate junctional and apicomedial F-actin signal, and calculated the ratio of junctional to apicomedial F-actin intensity. Consistent with the observed changes in F-actin distribution, we

Figure 4.3: Osmotic shifts modulate junctional-apicomedial actomyosin organization

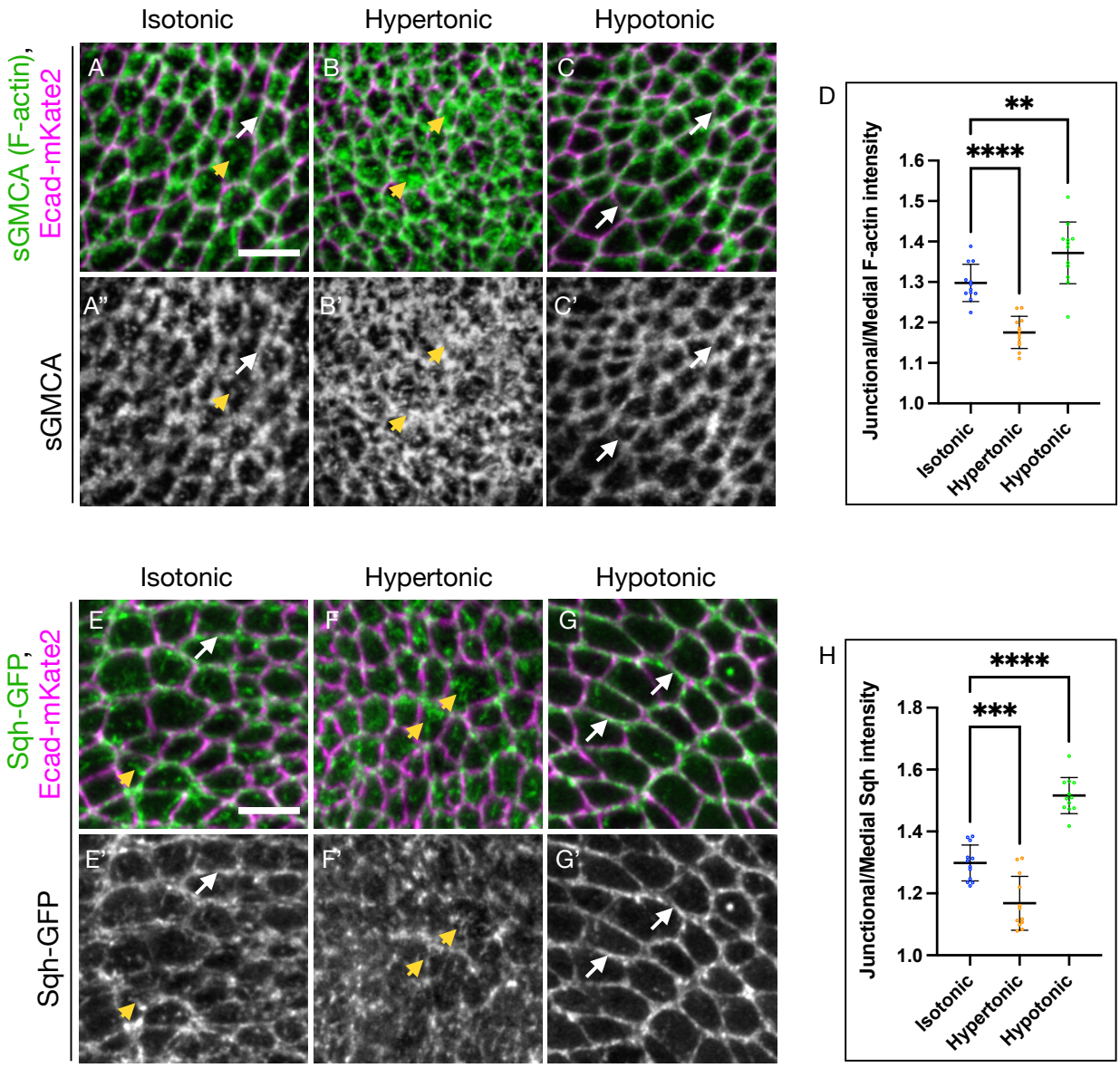

Figure 4.3 continued
A-C') Apical projections of wing imaginal tissues expressing Ecad-mKate2 and an F-actin marker, sGMCA. F-actin is both junctional (white arrows) and apicomedial (yellow arrowheads) under isotonic conditions (A & A'); under hypertonic conditions (B & B'), F-actin accumulates more medially; in contrast, under hypotonic conditions (C-C'), F-actin is more junctional.
D) Quantification of F-actin distribution under different osmotic conditions as a ratio of junctional to medial sGMCA mean intensity.
E-G') Apical projections of wing imaginal tissues expressing Ecad-mKate2 and an Sqh-GFP. Sqh is both junctional (white arrows) and apicomedial (yellow arrowheads) under isotonic conditions (A & A'); under hypertonic conditions (B & B'), Sqh becomes mostly apicomedial and is decreased at the junctions; in contrast, under hypotonic conditions (C-C'), Sqh is more junctional. Scale bars = 5μm.
H) Quantification of Sqh distribution under different osmotic conditions as a ratio of junctional to medial Sqh mean intensity.
Statistical significance in D and H was calculated using One-way ANOVA followed by Tukey's HSD test. Throughout the study, data is represented as the mean ± SD. Significance values are represented as follows: ****$p \leq 0.0001$, ***$p \leq 0.0001$, **$p \leq 0.001$, *$p \leq 0.05$, ns = not significant.

saw a decrease and increase in junctional/medial F-actin intensity under hypertonic and hypotonic conditions, respectively (Fig. 4.3D). Similar to F-actin distribution, myosin also became slightly more apicomedially enriched under hypertonic conditions, though it was more prominently lost from the junctions (Figs. 4.3F-F'). However, as with F-actin localization, hypotonic shift led to a significant junctional accumulation of myosin (Figs. 4.3G-G', H). These results are consistent with the changes in junctional tension induced by osmotic manipulations (see Chapter 3) and suggest that osmotic shifts can be used to acutely manipulate actomyosin organization.

Osmotic shifts affect Kibra abundance and localization

We next examined how osmotic shifts affected Kib localization. Under isotonic conditions Kib localized at the junctional and apicomedial cortex (Figs. 4.4A-A'). Strikingly, Kib accumulated in apicomedial clusters and became almost undetectable at the junctional cortex under hypertonic conditions (Figs. 4.4B-B'). Ecad localization was unaffected, indicating that the effect on Kib was not due to a general collapse of cell junctions. In sharp contrast, Kib localized mostly at the junctional cortex under hypotonic conditions (Figs. 4.4C-C'). As with changes in F-actin and myosin organization, we quantified the changes in Kib localization by measuring the ratio of junctional to medial Kib fluorescence. Consistent with our observations and similar to changes in F-actin and myosin localization, junctional/medial Kib fluorescence decreased under hypertonic and increased under hypotonic conditions relative to isotonic controls (Fig. 4.4D).

The drastic effect of osmotic shifts on Kib localization made us wonder if this effect was specific to Kib. To address this, we examined the localization of another cortical protein called Short stop (Shot), a spektraplakin that links minus-ends of apico-basal microtubule arrays of

Figure 4.4: Osmotic changes modulate Kib localization

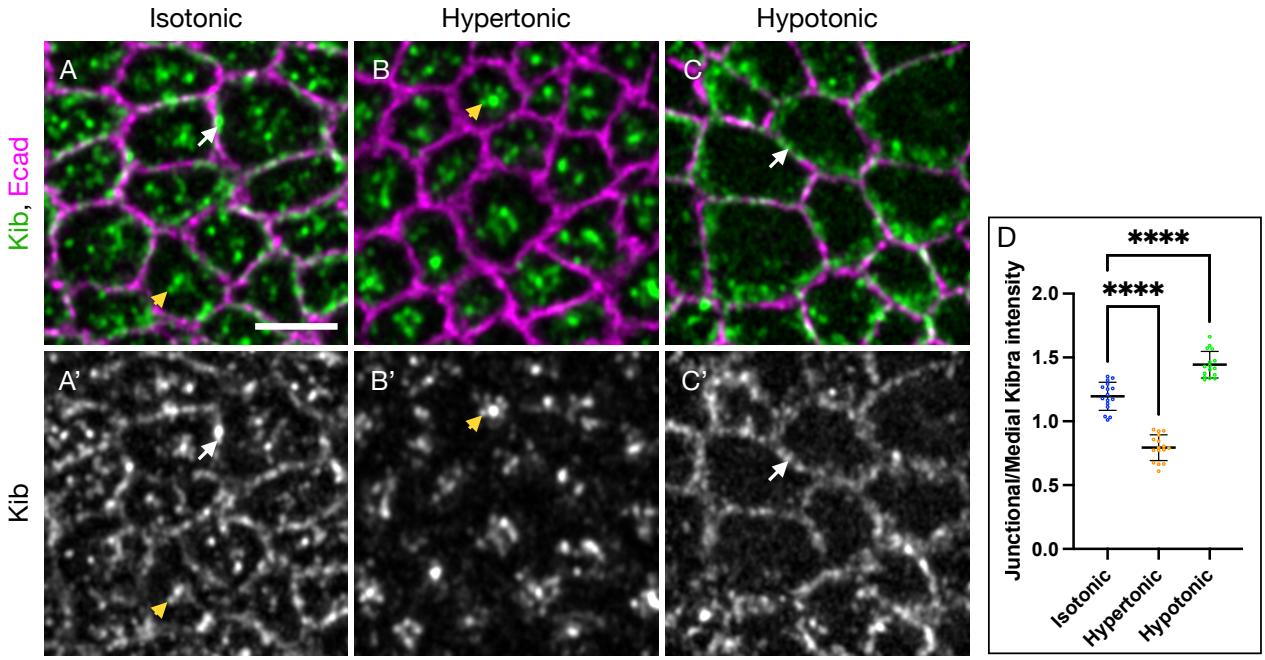

A-C') In isotonic conditions (D and D'), Kib is both junctional (white arrow) and apicomedial (yellow arrowhead). Under hypertonic conditions (E and E'), Kib becomes predominantly apicomedial. In contrast, under hypotonic conditions (F and F') Kib is mostly junctional. Scale bar = 3µm.
D) Quantification of junctional/medial Kib mean intensity under different osmotic conditions. Statistical significance was calculated using One-way ANOVA followed by Tukey's HSD test.

polarized epithelia to the apical actin cortex and was shown to re-localize from the junctional to the apicomedial cortex during early salivary gland invagination (Booth et al., 2014). Similar to Kib under isotonic conditions, Shot localizes at the apical junctional and medial cortex in the wing imaginal epithelial cells (Figs. 4.5A-A'). However, in marked contrast to Kib, Shot seemed to enrich more junctionally under hypertonic conditions and accumulated mostly in apicomedial clusters under hypotonic conditions (Figs. 4.5B-C'). We also examined the localization of Ex, another Hippo pathway component that localizes exclusively at the junctional cortex via direct association with Crb and activates Hippo signaling in parallel to Kib (Ling et al., 2010; Robinson et al., 2010; Su et al., 2017; Tokamov et al., 2021). Unlike Kib, Ex remained junctional under osmotic shifts (Figs. 4.5D-D''). Collectively, our data suggest that actomyosin dynamics may specifically modulate Kib localization at the apical cell cortex.

Apicomedial Kibra relocalization is controlled by actomyosin dynamics

Given the correlation between Kib and actomyosin dynamics and the similar changes in actomyosin and Kib organization under osmotic shifts, we next asked if changes in Kib localization were mediated by actomyosin dynamics. We first decided to block F-actin dynamics using Jasplakinolide (Jasp), which blocks F-actin polymerization, and ask if this affects Kib localization. Using sGMCA, we first confirmed that Jasp stabilized F-actin. Indeed, relative to control tissues, sGMCA fluorescence intensity increased dramatically in the wing discs incubated for only 15 min in the presence of Jasp (Figs. 4.6A-C). We also noticed that not only did F-actin intensity increase significantly with Jasp treatment, but also subcellular F-actin was stabilized in a "donut" pattern below the apical cortex, with some junctional F-actin stabilized

Figure 4.5: The effect of osmotic shifts on Kib localization is specific

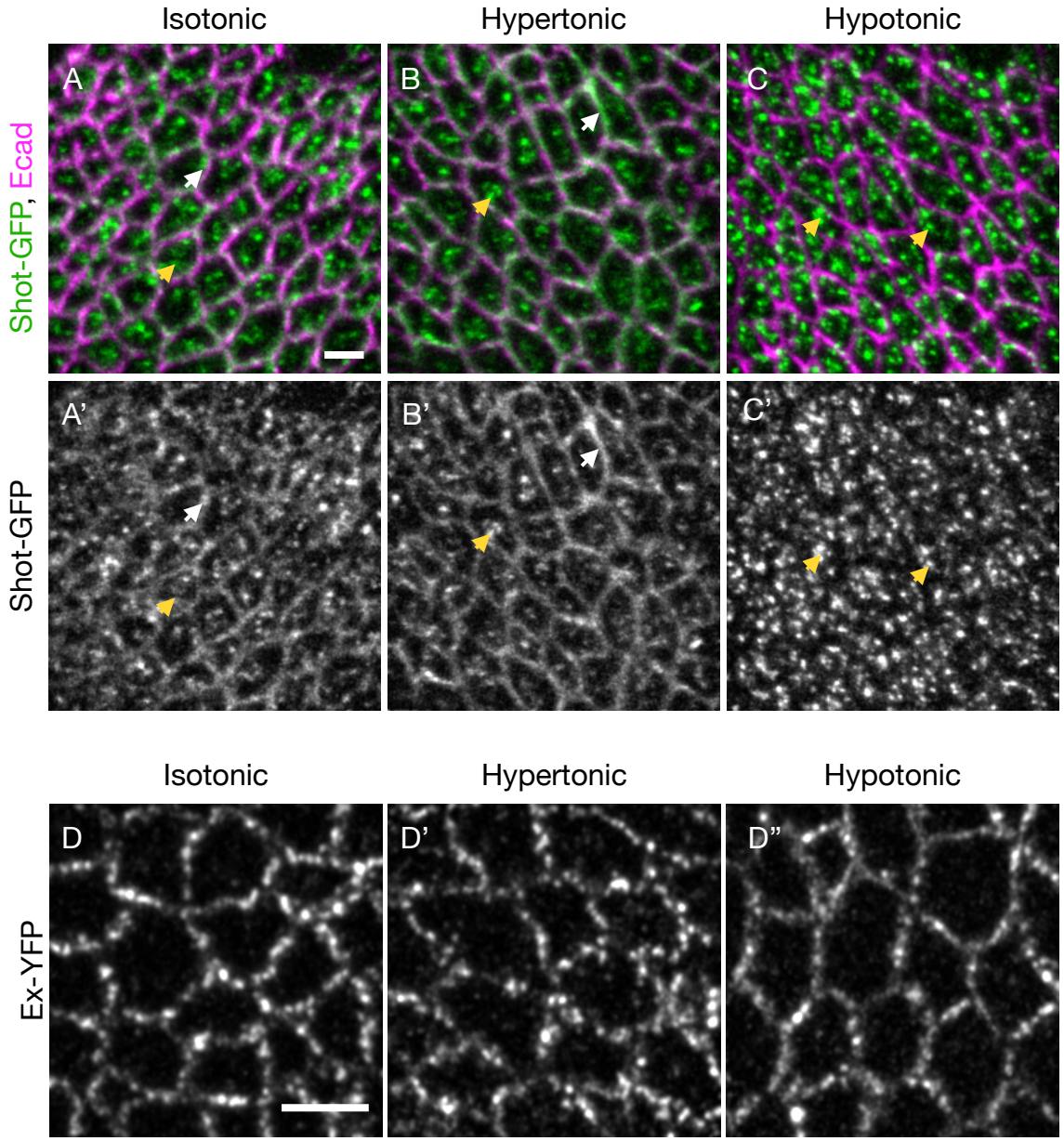

A-C') Similar to Kib, Shot localizes at the junctional (white arrow) and apicomedial cortex (yellow arrowhead) under isotonic conditions (A-A'). However, Shot remains both junctional and medial, with more enhanced junctional pool, under hypertonic conditions (B-B') and becomes more medial under hypotonic conditions (C-C').
D-D'') Unlike Kib, Ex remains junctional under osmotic shifts. Scale bars = 3µm.

Figure 4.6: Treatment with Jasp acutely stabilizes F-actin

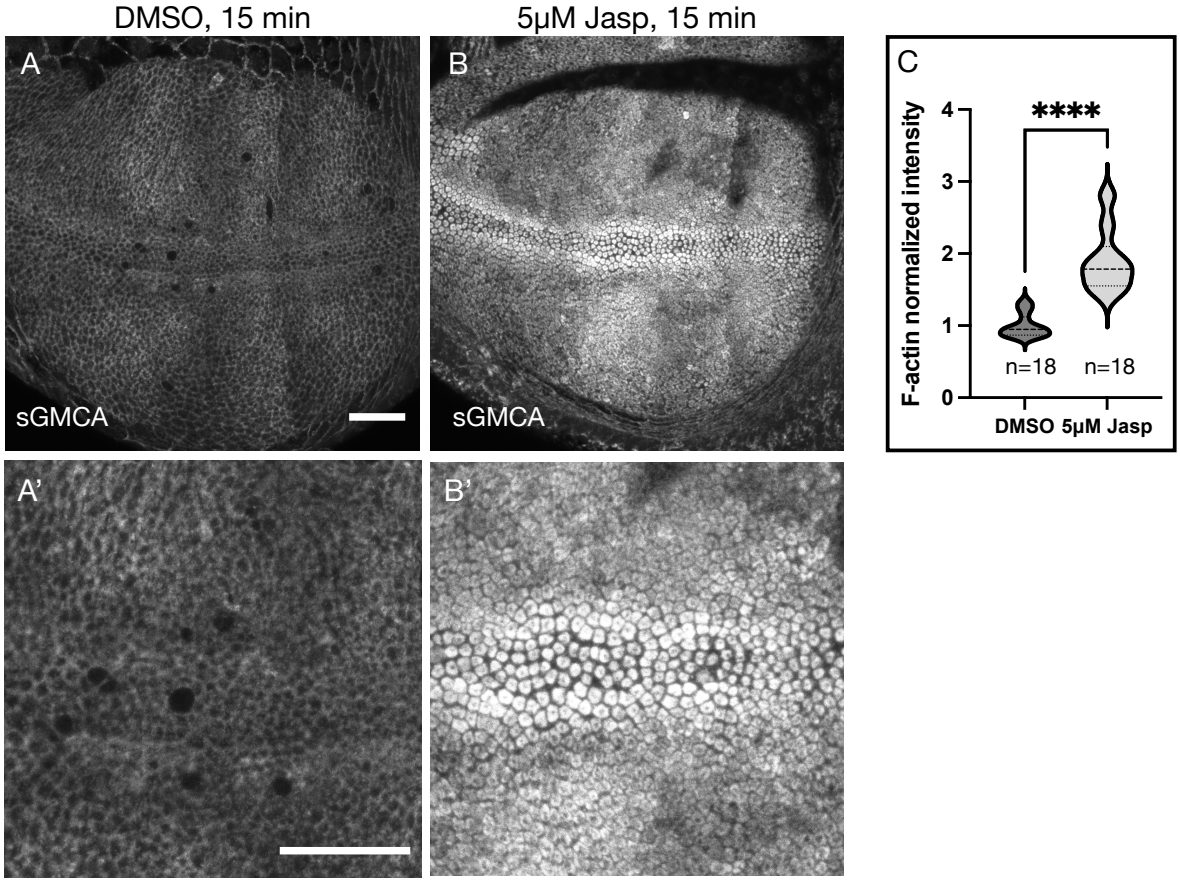

A-A') Compared to control tissues (A-A'), F-actin was stabilized in tissues treated with 5μM Jasp (B-B'). Note the accumulation of F-actin in apical donut-shaped structures in B'. Scale bars = 20μm.
C) Quantification of mean sGMCA intensity in tissues treated with DMSO or 5μM Jasp. Statistical significance was calculated using Mann-Whitney test.

more apically (Figs.4.6A' & B'). Consistent with the hypothesis that F-actin dynamics mediate apicomedial Kib localization, treating tissues with Jasp for only 15 min under isotonic conditions was sufficient to increase junctional Kib (Fig. 4.7A-B', E). Strikingly, while Kib accumulated apicomedially in a hypertonic solution with DMSO, this relocalization was blocked when tissues were incubated in a hypertonic solution with Jasp (Figs. 4.7C-E), indicating that medial Kib accumulation requires F-actin dynamics. We also asked if F-actin dynamics were required to maintain the medial Kib pool. To test this, we first concentrated Kib medially by incubating tissues for 15 min in a hypertonic solution and then transferred them into a hypertonic solution with or without Jasp. Treatment with Jasp reversed hypertonically induced apicomedial Kib accumulation (Figs. 4.7F-G'), indicating that F-actin dynamics are necessary to not only promote but also maintain Kib at the apicomedial cortex.

We next sought to inhibit myosin dynamics and examine the effect on Kib localization. Dynamic phosphorylation-dephosphorylation cycling of the myosin light chain is required for proper pulsatile myosin activity during morphogenesis (Vasquez et al., 2014). To test if myosin phosphorylation dynamics are also important for apicomedial Kib localization, we overexpressed a phosphomimmetic version of the myosin regulatory light chain (Sqh^{DD}, Mitonaka et al., 2007). We first tested the effect of Sqh^{DD} expression on myosin organization by examining a GFP-tagged myosin heavy chain (Zip-GFP). Interestingly, similar to F-actin under Jasp treatment, Sqh^{DD} ectopic expression led to a significant increase in Zip-GFP intensity, and subcellular Zip-GFP was stabilized in "donut"-shaped structures below the apical cortex (Figs. 4.8A-C). Overexpression of Sqh^{DD} under isotonic conditions resulted in a more junctional appearance of Kib (Fig. 4.8D-E'), though the effect was not quantitatively significant (Fig. 4.8H), likely

Figure 4.7: Kib apicomedial localization is dependent of F-actin dynamics

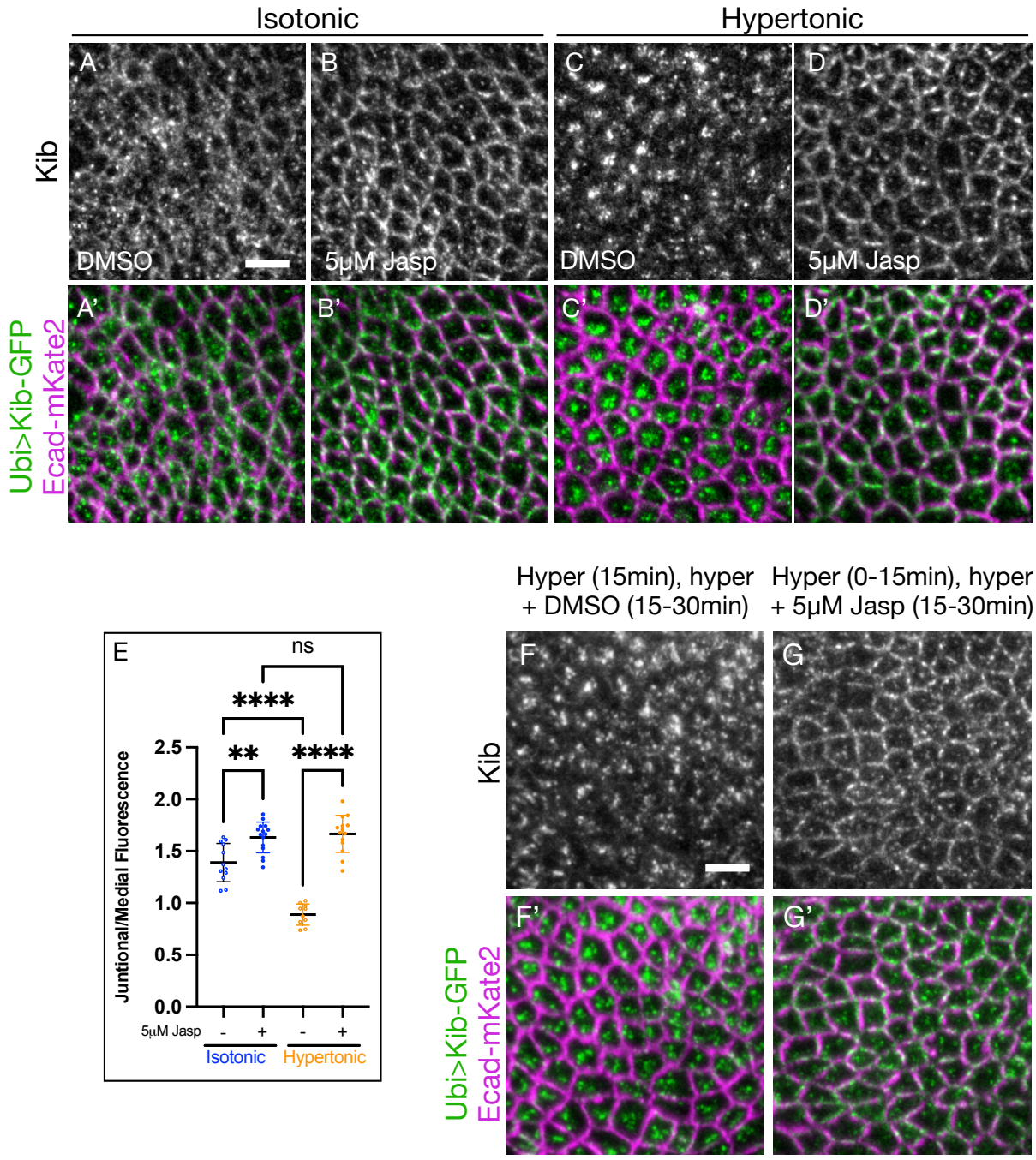

Figure 4.7 continued
A-E) Blocking F-actin dynamics prevents apicomedial Kib localization. Compared to isotonic controls (A and A'), treating wing imaginal tissues with 5µM Jasp results in more junctional Kib (B, B', E). Significantly, while Kib is mostly apicomedial under hypertonic conditions (C and C'), treatment with 5µM Jasp blocks the effect of the hypertonic shift on Kib localization (D-E). Statistical significance was calculated using One-way ANOVA followed by Tukey's HSD test. F-G') F-actin dynamics are required to maintain Kib at the apicomedial cortex. Tissues were first incubated under plain hypertonic conditions for 15 min to concentrate Kib medially, and then transferred to a hypertonic medium with DMSO (F-F') or 5µM Jasp (G-G'). Treatment with 5µM Jasp prevents Kib clusters from staying at the apicomedial cortex. Scale bars = 5µm.

Figure 4.8: Kib apicomedial localization is dependent of myosin dynamics

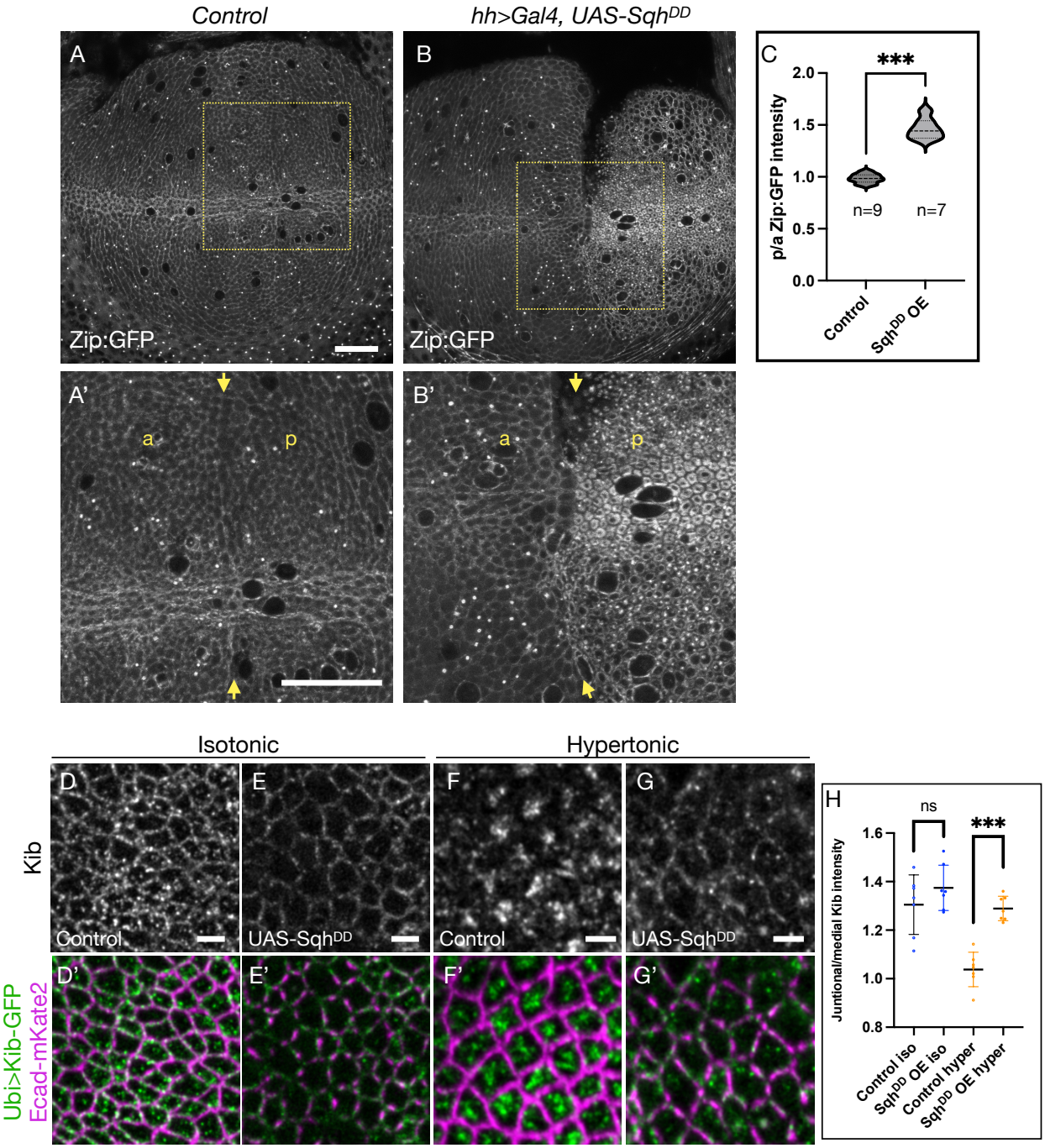

Figure 4.8 continued
A-B') Compared to control tissues (A-A'), overexpression of Sqh^{DD} in the posterior compartment of the wing disc results in significant stabilization of myosin (B-B'). Yellow arrows indicate the anterior-posterior (a-p) boundary. Scale bars = 20μm.
C) Quantification of the posterior/anterior (p/a) mean Zip:GFP intensity in control tissues and tissues transiently overexpressing Sqh^{DD} in the posterior compartment. Statistical significance was calculated using Mann-Whitney test.
D-H) Dynamic myosin phosphorylation is required for apicomedial Kib accumulation. While overexpression of Sqh^{DD} leads to mildly, but not significantly, more junctional Kib under isotonic conditions (D-E', H), Sqh^{DD} overexpression strongly inhibits apicomedial Kib relocalization under hypertonic conditions (F-G', H). Scale bars = 3μm. Statistical significance was calculated using One-way ANOVA followed by Tukey's HSD test.

because the transgene was expressed transiently in the background of endogenous, wild type Sqh. However, Sqh^{DD} overexpression significantly blocked apicomedial Kib relocalization under hypertonic conditions (Fig. 4.8F-G', H). Collectively, our data show that Kib cortical organization is regulated by actomyosin dynamics and that apicomedial actomyosin contractility is required to cluster Kib at the medial cortex.

Osmotic shifts influence Kibra-mediated complex formation

Previous work has shown that Kib is a key protein that recruits other associated Hippo pathway components into a signaling complex at the apicomedial cortex, and that medially-localized Kib is more efficient at promoting Hippo signaling and suppressing growth (Su et al., 2017). Activation of Hippo signaling requires the recruitment of Sav, which activates the kinase cascade by linking Hpo and Wts, and Kib recruits Sav to the apicomedial cortex via Mer (Tapon et al., 2002; Callus et al., 2006; Su et al., 2017). Therefore, to test if actomyosin-mediated apicomedial Kib promotes Hippo signaling, we examined the localization of Mer under osmotic shifts. Under isotonic conditions, Kib colocalized with Mer medially and junctionally (Figs. 4.9A-A''). Strikingly, under hypertonic conditions, both Kib and Mer co-clustered strongly at the medial cortex (Figs. 4.9B-B''), suggesting that Kib recruits Mer into a signaling complex under hyperosmotic shift. In contrast, Kib and Mer were both mainly at the junctional cortex under hypotonic conditions (Figs.4.9C-C'').

We also examined the effect of Kib relocalization under osmotic shifts on Hpo recruitment using endogenously expressed Hpo-YFP. Under isotonic conditions, Hpo-YFP appeared mostly diffuse, with no discernable localization pattern (Figs. 4.9D-D'). However, as was observed with Mer, distinct Hpo clusters formed and colocalized with medial Kib under

hypertonic shift (Figs. 4.9E-E'). Conversely, shift to hypotonic conditions led to predominantly diffuse Hpo-YFP, with no detectible junctional localization (Figs. F-F'). Collectively, these data suggest that actomyosin-driven medial Kib recruits downstream Hippo pathway components into a signaling complex.

Figure 4.9: Mer and Hpo are recruited to Kib punctae via actomyosin dynamics

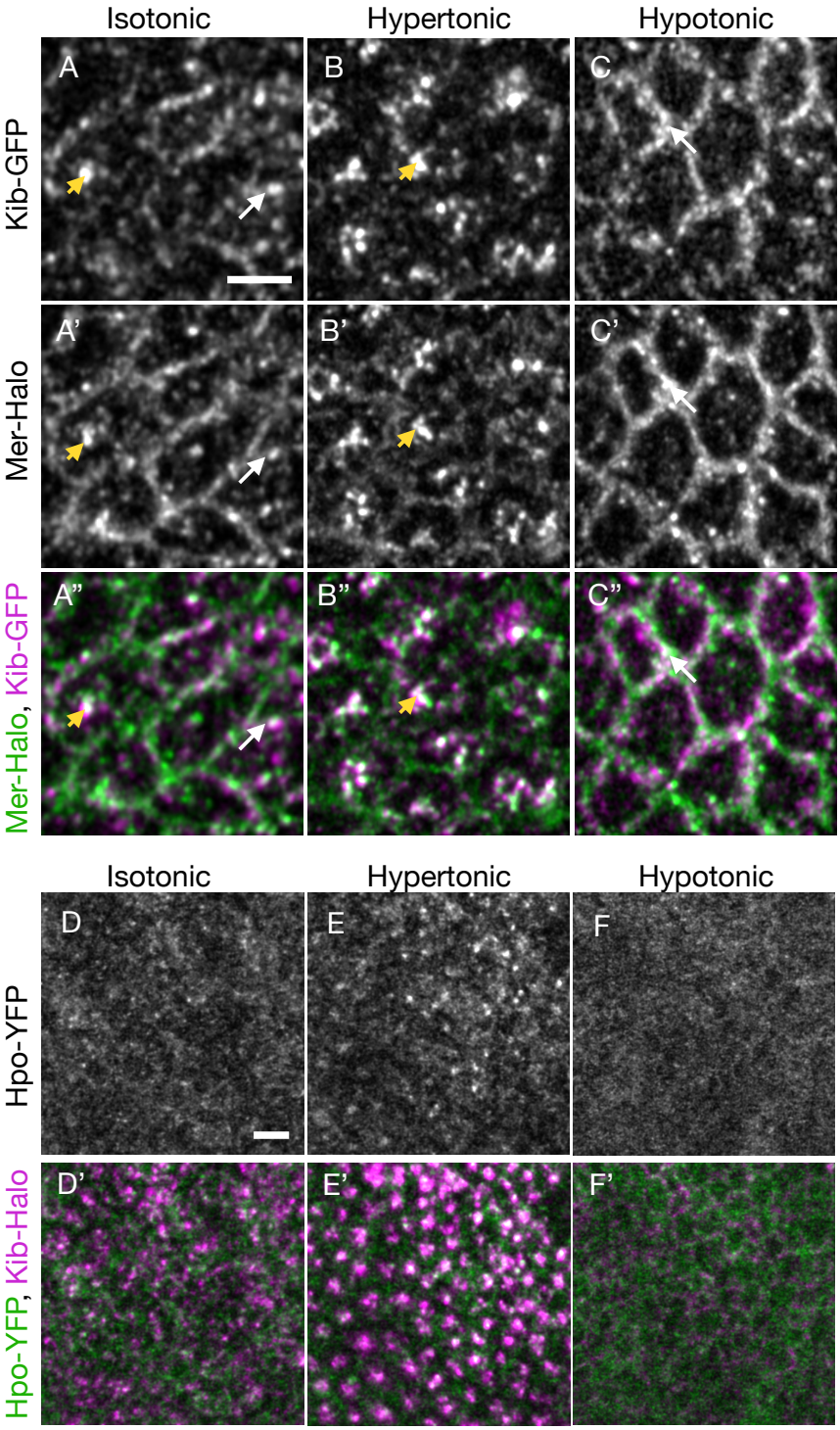

Figure 4.9 continued
A-C'') Ubi>Mer-Halo co-localizes with Ubi>Kib-GFP under isotonic conditions at the junctional (white arrows) and apicomedial (yellow arrowheads) cortex (A-A''). Under hypertonic conditions, Mer is strongly recruited into apicomedial Kib clusters (B-B''). Conversely, under hypotonic conditions, both Mer and Kib localize mainly at the junctional cortex (C-C'').
D-F') Hpo is normally diffuse under isotonic conditions (D-D'). However, under the hypertonic shift, Hpo is recruited to apicomedial Kib clusters (E-E'). In contrast, Hpo remains diffuse under hypotonic conditions (F-F'). Scale bars = 3μm.

4.3 Discussion

While the role of the actomyosin cytoskeleton in Hippo pathway regulation has been explored in multiple studies in the past, the association of Hippo pathway components with the actomyosin cortex and their collective dynamics have not been carefully observed. In this study, we examined Kib association with the actomyosin cytoskeleton and observed that Kib decorates cortical F-actin and co-migrates with F-actin and myosin flows. We find that inducing acute changes in actomyosin organization leads to concomitant changes in Kib localization, and that acute or genetic stabilization of actomyosin network prevents apicomedial Kib localization. Importantly, actomyosin-mediated apicomedial Kib accumulation also promotes Mer and Hpo recruitment to medial Kib clusters. Together, our results reveal how actomyosin dynamics can modulate Hippo signaling by controlling Kib localization at the apical cortex.

To date, multiple studies have shown that Yki/YAP activity correlates with actomyosin activity, suggesting that actomyosin acitivty inhibits the Hippo pathway (Misra and Irvine, 2018; Zheng and Pan, 2019). However, these studies relied heavily on genetic manipulations of actomyosin contractility (e.g. overexpression of constitutively active Rho kinase), and it remains unclear how actomyosin cytoskeleton modulates Hippo signaling at the subcellular level. Additionally, there are two distinct pools of actomyosin that exist in epithelial cells, junctional and apicomedial pool, which are different in their organization and function (Heer and Martin, 2017; Garcia De Las Bayonas et al., 2019; Silver et al., 2019). Junctional tension caused by actomyosin activity is known to inhibit Hippo signaling via Jub-mediated inhibition of Wts (Rauskolb et al., 2014; Ibar et al., 2018), and our data in Chapter 3 indicate that junctional tension also leads to Kib degradation. However, the role of the apicomedial actomyosin pool in Hippo pathway regulation has not been explored. Given our previous observation that Kib

signals more potently when localized at the apicomedial cortex (Su et al., 2017), this study suggests that apicomedial actomyosin dynamics may activate Hippo signaling by promoting medial accumulation of Kib and other associated Hippo pathway components. Thus, junctional and apocomedial actomyosin networks may, in essence, regulate Hippo signaling in completely opposite directions.

Our work also raises the question of how Kib interacts with the actomyosin network. Kib is a multivalent protein but does not contain a canonical F-actin binding domain, so it is unlikely that Kib directly interacts with F-actin. We also do not observe strong co-localization of Kib with F-actin or myosin. Instead, Kib punctae appear to move adjacently to F-actin and merge as medial myosin coalesces. A more plausible alternative is that Kib indirectly associates with the actomyosin network by interacting with another cytoskeletal component. For example, the spectrin cytoskeleton is associated with the actomyosin network and mediates the ratcheting pulsatile myosin activity during Drosophila mesoderm invagination (Krueger et al., 2020). The spectrin cytoskeleton is also known to promote Hippo pathway activity, and both Kib and Mer were shown to physically interact with the spectrin cytoskeleton component Karst, the Drosophila version of β-heavy spectrin (Deng et al., 2015; Fletcher et al., 2015). Although the mechanism by which the spectrin cytoskeleton promotes Hippo signaling is still not well understood, our findings suggest the possibility that Karst could activate Hippo signaling by promoting apicomedial Kib localization. Further observations of Kib, Mer, and Karst dynamics and manipulations of the spectrin cytoskeleton could lead to a better understanding of the relationship between upstream Hippo signaling components and the cortical cytoskeletal networks.

4.4 Methods

Table 4.1. Reagents

Reagent type (species) or resource	Designation	Source or reference	Identifiers	Additional information
genetic reagent (*D. melanogaster*)	*Kib::GFP*	10.1016/j.devcel.2017.02.004		
genetic reagent (*D. melanogaster*)	*UAS-LifeAct-Halo2*	Bloomington Drosophila Stock Center	BL67625	
genetic reagent (*D. melanogaster*)	*Ubi>Kib-Halo*	This study		
genetic reagent (*D. melanogaster*)	*sGMCA*	10.1016/j.devcel.2018.06.017		
genetic reagent (*D. melanogaster*)	*Sqh-GFP*	Bloomington Drosophila Stock Center	BL57145	
genetic reagent (*D. melanogaster*)	*Zip-GFP*	10.1016/j.cell.2014.05.035		
genetic reagent (*D. melanogaster*)	*UAS-Sqh^{DD}*	10.1016/j.ydbio.2007.06.021		

Table 4.1. Continued

genetic reagent (*D. melanogaster*)	*Ecad-3XmKate2*	10.1038/nature22041		
genetic reagent (*D. melanogaster*)	*Ex-YFP*	10.1016/j.devcel.2017.02.004		
genetic reagent (*D. melanogaster*)	*Ubi-Mer-Halo*	This study		
genetic reagent (*D. melanogaster*)	*Hpo-YFP*	10.1016/j.devcel.2017.02.004		
Chemical	Jasplakinolide	Cayman		

Drosophila husbandry

Drosophila melanogaster was cultured using standard techniques at 25°C (unless otherwise noted). For Gal80^{ts} experiments, crosses were maintained at 18°C and moved to 29°C for the duration specified in each experiment.

Live imaging

Live imaging of Drosophila wing imaginal discs was performed as described in Chapter 3. All images were taken on an inverted Zeiss LSM880 laser scanning confocal microscope equipped with a GaAsP spectral detector and the Airyscan module. All timelapse images and still images

in Fig. 4.1, 4.4, 4.5D-D'', and 4.9A-C'' were taken using the Airyscan in superresolution mode. Timelapse acquisition was performed using the Zeiss Z-Piezo, Images were processed in ImageJ.

Image analysis and quantification

To quantify junctional/medial intensity, tissue crops were segmented via Cellpose and a standard scikit watershed algorithm using Ecad-mKate2 as a junctional marker to generate a mask (van der Walt et al., 2014; Stringer et al., 2021). The junctional mask was then applied to quantify mean junctional Kib intensity, while remaining non-junctional signal was classified as medial. The ratio of mean junctional to medial intensity was then calculated. Plots and statistical analyses of mean fluorescence intensities were generated using GraphPad Prism software.

The kymograph in Fig. 4.2C was generated using ImageJ. For individual channel, a segmented line (8 pixels wide) was applied to the maximum projection of the movie to trace the direction of myosin/Kibra cluster movement. The line was then straightened and resliced avoiding interpolation to generate an 8-pixel kymograph. A maximum projection across 8 pixels was then taken to generate the final kymograph.

Osmotic shift and Jasplakinolide treatment experiments

Osmotic shift experiments were performed as described in Chapter 3. To inhibit F-actin dynamics, tissues were incubated in an isotonic or hypertonic solution with 5μM Jasplakinolide. Unless otherwise indicated, all incubations were done for 15 min.

CHAPTER 5

Discussion: conclusions and future questions

Since the discovery of the Hippo pathway, much progress has been made in understanding its composition, the biochemical interactions of its components, and its role in tissue growth regulation. However, while much attention has been focused on the core Hippo kinase cassette and the regulation of the pathway's transcriptional effector Yki/YAP/TAZ, how the upstream regulatory network of the Hippo pathway is organized and regulated has been poorly understood.

In this dissertation, I explored the regulation and subcellular organization of a key upstream Hippo signaling component, Kibra (Kib). In Chapter 2, I demonstrated that when Kib assembles a Hippo signaling complex, it destines itself for degradation. My work in Chapter 3 shows that this degradation mechanism is modulated by actomyosin-generated tension. In Chapter 4, I investigated how actomyosin organization regulates Kib at the subcellular level and showed that apicomedial Kib localization and Hippo complex assembly depends on actomyosin dynamics. In this chapter, I will briefly discuss additional questions and potential future research avenues based on my thesis work.

Is Kib degradation spatially organized?

The work in this dissertation, combined with the previous work from our lab, highlight the importance of Kib abundance and subcellular localization in the regulation of Hippo signaling and raises an intriguing possibility that Kib degradation may depend on its localization. The results in Chapter 2 indicate that Kib degradation via Slimb requires both a functional degron and complex formation. Where does the degradation complex form? Does it form at the junctional or apicomedial cortex, or both? Our observations in Chapter 3 and Chapter 4 that

hypertonic treatment leads to higher abundance and apicomedial localization of Kib, while hypotonic treatment leads to Kib degradation and more junctional localization suggest that Kib degradation could occur mainly at the junctional cortex. An ideal experiment would be to perturb Kib-mediated complex formation specifically at the junctional or apicomedial cortex, which we currently do not know how to do. However, we could also pose this question in a different way – can Kib form a functional complex at either the junctional or apicomedial cortex without being degraded?

A result that may provide a clue to the question above is our observation that unlike ectopic Hpo expression, which leads to lower Kib abundance (Fig. 3.9F), ectopic expression of a wild-type Wts or kinase-dead version of Wts (Wts^{KD}) leads to Kib stabilization at the apicomedial cortex (Fig. 5.1A-B). The difference in Kib abundance under Hpo and Wts expression can be explained if Kib can interact with Wts but not Hpo, resulting in Wts-mediated stabilization of Kib at the apicomedial cortex. The fact that the catalytic activity of Wts does not play a role in this stabilization supports the scaffolding function of Wts, though it is possible that this stabilization involves posttranslational modifications of Kib that are not mediated directly by Wts.

What is interesting about this experiment is that apicomedial stabilization of Kib under ectopic Wts expression leads to the recruitment of Mer and Hpo into the medial complex (Fig. 5.1C-E'') and significant tissue undergrowth, even when Wts^{KD} was expressed (not shown). Though it is possible that tissue undergrowth under Wts^{KD} expression is caused by increased medial Kib abundance, this has not been shown formally. It should also be noted these experiments were done with ectopically expressed Ubi>Kib-GFP. Nevertheless, these results

Figure 5.1: Ectopic Wts expression promotes medial Kib recruitment and Hippo complex formation without promoting Kib degradation

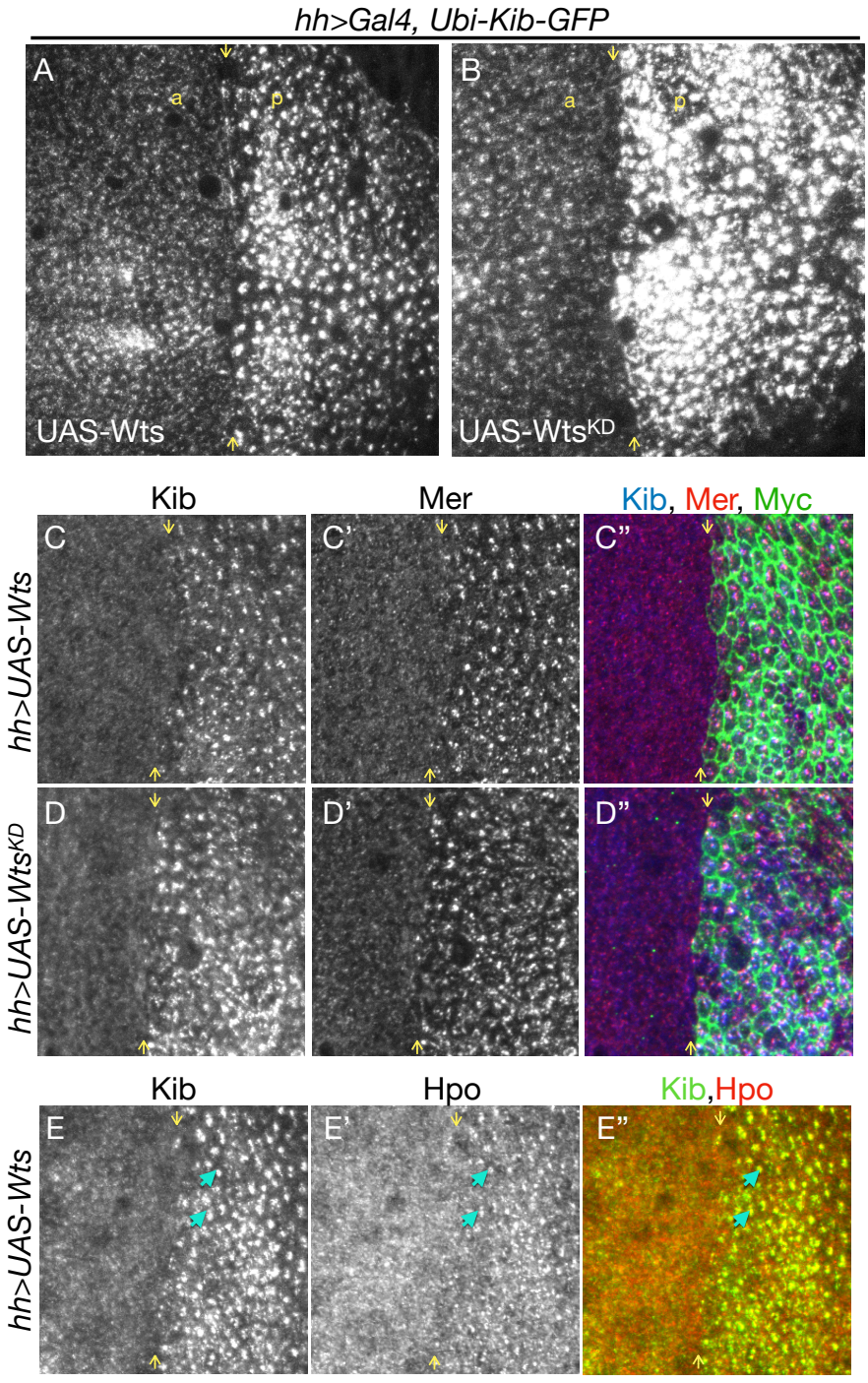

Figure 5.1 continued
A-B) Ectopic expression of wild type (A) or kinase dead forms of Wts (B) leads to medial stabilization of Kib. Yellow arrows mark the anterior-posterior (a-p) boundary.
C-D'') Ectopic expression of wild type (C-C'') or kinase dead forms of Wts (D-D'') results in Mer recruitment to the medially stabilized punctae.
E-E'') Ectopic Wts expression results in Hpo recruitment to the medially stabilized Kib punctae (blue arrows).

Experiments in A-E'' were performed in the background of ectopically expressed Ubi>Kib-GFP.

suggest that Kib can form a functional complex at the apicomedial cortex without being degraded there. One way to test the possibility that ectopic Wts and Hpo promote Kib degradation specifically at the junctions is by combining these manipulations with Slimb RNAi or heterozygous *slimb*-null alleles. Finally, the robust medial Kib stabilization under Wts^{KD} expression could be used to perform a candidate RNAi screen of potential components that are necessary for medial Kib localization.

Is Kib activity at the cell cortex potentiated via clustering?

Previous work in our lab (Su et al., 2017) and work in this dissertation shows that Kib localizes in distinct punctae at the junctional and medial cortex. Furthermore, increasing medial Kib localization either via Crb removal or hypertonic manipulation (or ectopic Wts expression, as discussed above) leads to an apparent coalescence of Kib punctae into larger subcellular assemblies. Our work raises several interesting questions that could be investigated in the future. First, does Kib form molecular clusters at the apical cortex via oligomerization or multivalent interactions? Second, if Kib forms clusters, how is the formation of clusters regulated? And third, if Kib forms clusters, what is the significance of clustering in Kib-mediated Hippo pathway activation and growth regulation?

One of the paradigms of protein clustering is an apical polarity protein Par3, which forms cortical oligomers via a conserved CR1 self-association domain (Benton and Johnston, 2003). In the *C. elegans* zygote, Par3 is segregated to the anterior cell cortex via actomyosin flows (Munro et al., 2004). The formation of oligomeric Par3 clusters is critical for its ability to signal via other apical polarity proteins, including aPKC and Par6, to antagonize the posterior polarity determinants, thereby establishing the anterior-posterior axis of the animal (Benton and

Johnston, 2003; Lang and Munro, 2017; Chang and Dickinson, 2022). Cortical actomyosin flows are known to promote Par3 clustering, and work over the years has shown that clustering enables a more efficient advective transport of Par3 by cortical flows (Benton and Johnston, 2003; Munro et al., 2004; Dawes and Munro, 2011; Dickinson et al., 2017; Wang et al., 2017; Chang and Dickinson, 2022).

Could Kib form clusters and be regulated by actomyosin dynamics in an analogous manner to Par3? Unlike Par3, Kib does not seem to contain a known oligomerization domain. However, Kib is a multivalent protein that contains at least several domains/motifs, including two N-terminal WW domains, that individually or collectively could facilitate protein-protein interactions and cluster formation (Fig. 2.9A). Another Hippo signaling component, Sav, also contains two WW domains that are known to mediate Sav dimerization (Lin et al., 2020). Thus, it is possible that Kib also dimerizes via its WW domains. However, while deletion of WW1 domain in Kib results in more diffuse cortical Kib, deletion of WW2 or both WW domains leads to more punctate Kib (Fig. 2.9L-O), suggesting that a more complex interaction mechanism may govern subcellular Kib distribution. Kib also contains three coiled-coil (CC) motifs, two of which are in the N-terminal portion of the protein following the two WW domains. Interestingly, deleting the region containing the two WW domains and two CC motifs ($Kib^{484\text{-}1288}$) significantly decreases the ability of Kib to form cortical punctae and abolishes Kib medial localization (Fig. 5.2A-B). Thus, Kib could form clusters via multivalent interactions with other Hippo pathway components, including Sav, and cluster formation may be necessary to promote apicomedial Kib transport via actomyosin flows. Future biochemical work is needed to test if Kib can form higher order oligomers.

Figure 5.2: Deletion of the first 483 amino acids of Kib prevents the formation of Kib assemblies at the apicomedial cortex

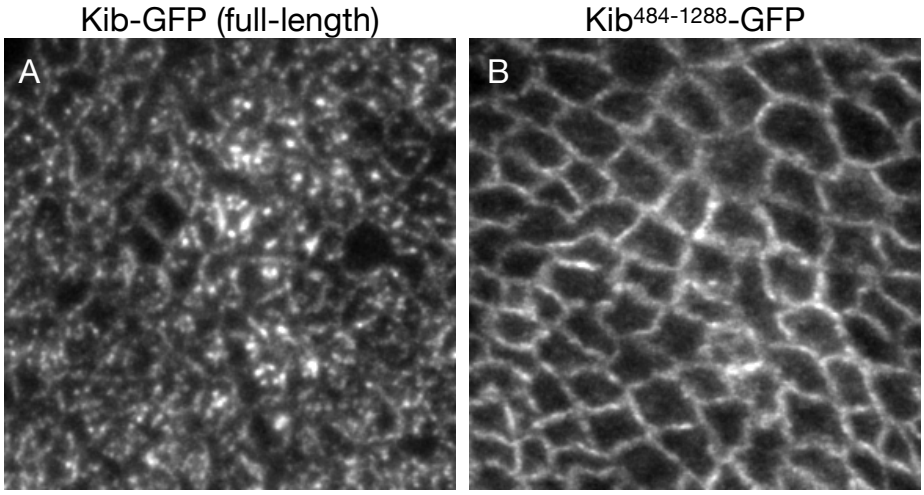

A) Full-length GFP-fused Kib expressed under the ubiquitin promoter (Ubi>Kib-GFP) B) A truncated version of GFP-fused Kib lacking the first 483 amino acids fused also expressed under the ubiquitin promoter (Ubi>Kib$^{484-1288}$-GFP). Both transgenes were expressed from an identical genomic location (VK37, chromosome 2).

What is the significance Kib-mediated assemblies at the cell cortex? Studies of T-cell receptors have shown that receptor clustering facilitates local enrichment of signaling components that can amplify signaling (Hartman and Groves, 2011; Dustin and Groves, 2012). Thus, if Kib indeed forms microclusters at the apicomedial cortex, then clustering could potentiate Kib-mediated Hippo pathway activation and growth suppression. Consistent with this, we previously showed that loss of Crb leads to more medially "clustered" and more active Kib (Su et al., 2017). Directly inducing Kib clustering could help test the hypothesis that clustering promotes Kib signaling. An optogenetic approach involving the plant-derived Cry2-CIB1 system has been used to activate Wnt and Hippo signaling (Bugaj et al., 2013; López-Gay et al., 2020). Employing this approach to induce Kib clustering and monitoring the effect of clustering on Yki localization and/or growth could provide the means to directly test the biological significance of cortical Kib assemblies.

Does Kib regulate the actomyosin network?

In Chapter 4, we show that actomyosin dynamics promote apicomedial Kib localization and Hippo complex assembly. Our observations that subcellular Kib dynamics correlate with F-actin and myosin movement raise a question of whether Kib could regulate the actomyosin network. Indeed, studies in *Drosophila* have implicated Hippo pathway components in the regulation of F-actin polymerization. For example, in the wing imaginal tissue, loss of Ex, Hpo, Sav, Mats, or Wts leads to apical accumulation of F-actin independently of Yki activity (Fernandez et al., 2011). This effect on F-actin levels could be mediated through Wts, which is thought to phosphorylate and inhibit an F-actin polymerizing protein Ena in border cells (Lucas et al., 2013). Thus, one possibility is that Kib could regulate F-actin through Wts. However, while F-

actin levels are elevated in *ex*-mutant somatic mosaic clones (Fernandez et al., 2011), loss of Kib does not affect F-actin levels (not shown). These results might suggest that junctional Hippo signaling organized by Ex regulates F-actin polymerization and further support the idea that Ex and Kib function through parallel Hippo signaling complexes (see Chapter 2).

While loss of Kib clearly has no effect on F-actin levels in the wing, the potential regulation of other aspects of actomyosin organization and/or activity by Kib remains to be tested. For example, as mentioned in Chapter 1, previous work from our lab showed that Yki itself has a non-transcriptional function at the apical cell cortex, where it promotes myosin activation via a myosin light chain kinase called Stretchin (Strn-MLCK, Xu et al., 2018). It is unclear whether this function of Yki requires other Hippo pathway components such as Kib. Our results in Chapter 3 and 4 suggest that lower junctional tension and apicomedial actomyosin organization under hypertonic conditions lead to increased Kib abundance at the medial cortex. However, the converse relationship is also possible, whereby loss of Kib from the junctions under hypertonic conditions could affect junctional tension by limiting Yki's ability to activate myosin. Thus, future experiments testing whether gain or loss of Kib function affects myosin activity could be informative. Our work highlights the importance of understanding not only how the actomyosin network modulates Hippo signaling, but also how Hippo signaling components could potentially feedback to regulate actomyosin contractility and physical forces across tissue.

Does Kib contribute to the non-transcriptional functions of the Hippo pathway?

Despite its identification as a key Hippo pathway regulator over a decade ago, we still know very little about how Kib functions, especially in the contexts beyond Yki/YAP/TAZ regulation. In mammalian cells, Kib is regulated during mitosis via Cdk1-Cdc14 and Aurora-PP1

phosphorylation-dephosphorylation cycles, suggesting that Kib may have a role in cell cycle regulation (Xiao et al., 2011; Ji et al., 2012). However, the significance of this regulation has not been thoroughly explored.

A potentially intriguing function of Kib that could be explored in the future is its role in *Drosophila* NBs. As mentioned above, Hippo signaling components are necessary for proper ACD of NBs, though the role of Kib in this process is not known (Keder et al., 2015). However, genetic interaction experiments indicated that loss of Sav and Mer resulted in more severe ACD defects than loss of Wts, suggesting that Hippo complex formation may play a critical role in ACD regulation (Keder et al., 2015). Intriguingly, our observations of Kib in the *Drosophila* larval NBs revealed that Kib forms an apical crescent during mitosis, similar to apical polarity proteins such as aPKC (see Appendix A). Given the role of Wts in spindle alignment in NBs, one possibility is that Kib-mediated Hippo complex assembly could activate Wts and mediate its function in spindle positioning. Additionally, because Kib contains an aPKC-binding domain and is known to physically interact with aPKC, Kib could provide a physical link between Wts-mediated spindle positioning and apical polarity. Further investigation of Kib in NBs and its link to polarity, spindle alignment, and cell cycle regulation could be a promising avenue for future research.

Concluding statement

In this dissertation, I explored how one of the key upstream Hippo pathway components, Kib, is regulated and organized at the cell cortex of epithelial cells. My work identified a novel mechanism by which Kib is degraded and showed that mechanical forces can modulate Kib abundance via this mechanism to pattern tissue growth. I also showed that Kib localization at the

apical cell cortex is regulated by the opposing action of actomyosin dynamics and apical polarity network, whereby medial actomyosin flows promote medial Kib localization and apical polarity components tether Kib at the junctional cortex. Collectively, this work provides new mechanistic insights into the control of Hippo signaling and tissue growth by the combined action of proteolytic degradation, mechanical inputs, actomyosin dynamics, and cell polarity. At a broader level, this dissertation expands our understanding of how growth regulation is intimately linked to other aspects of epithelial biology and provides a future framework for exploring the potential role of the Hippo pathway in coordinating tissue growth and morphogenesis.

Appendix A

Apical polarity network tethers Kibra at the junctional cortex

One of the driving questions of my research is how Kibra (Kib) localization at the apical cortex is regulated. Previous work from our lab demonstrated that Kib localizes at distinct subcellular regions at the apical cortex of epithelial cells: the junctional cortex and apicomedial (medial) cortex (Su et al., 2017). Importantly, this work also showed that loss of an apical polarity component, a transmembrane protein Crumbs (Crb), untethers Kib from the junctional cortex and makes Kib more active, suggesting that Kib may be silenced at the junctional cortex and that localization of Kib has functionally important (Su et al., 2017). Here, I further investigate how Crb may regulate Kib localization. Specifically, I attempt to distinguish between two possibilities, that are not mutually exclusive: 1) Crb could regulate actomyosin dynamics, which could influence Kib localization as shown in Chapter 4, and 2) Crb could act by stabilizing the apical polarity network to tether Kib at the junctional cortex.

Loss of Crb affects Kib localization at the junctional cortex without significantly affecting Kib abundance

To corroborate our previous findings that loss of Crb alters Kib localization, I first depleted Crb in the posterior compartment of the wing imaginal disc and examined the effect on Ubi>Kib-GPF. As we reported previously, unlike Hippo signaling components that form a complex with Kib, loss of Crb does not lead to an increase Kib abundance (Tokamov et al., 2021), though there appears to be a slight decrease in Kib fluorescence apically, which we interpret to be due to change in Kib localization (Fig. A.1A-A'). As expected, Crb depletion resulted in the loss of Kib at the junctional cortex (Fig. A.1B-C''). Interestingly, loss of Crb also resulted in the appearance

Figure A.1: Loss of Crb leads to the loss of Kib at the junctional cortex without significantly affecting Kib abundance

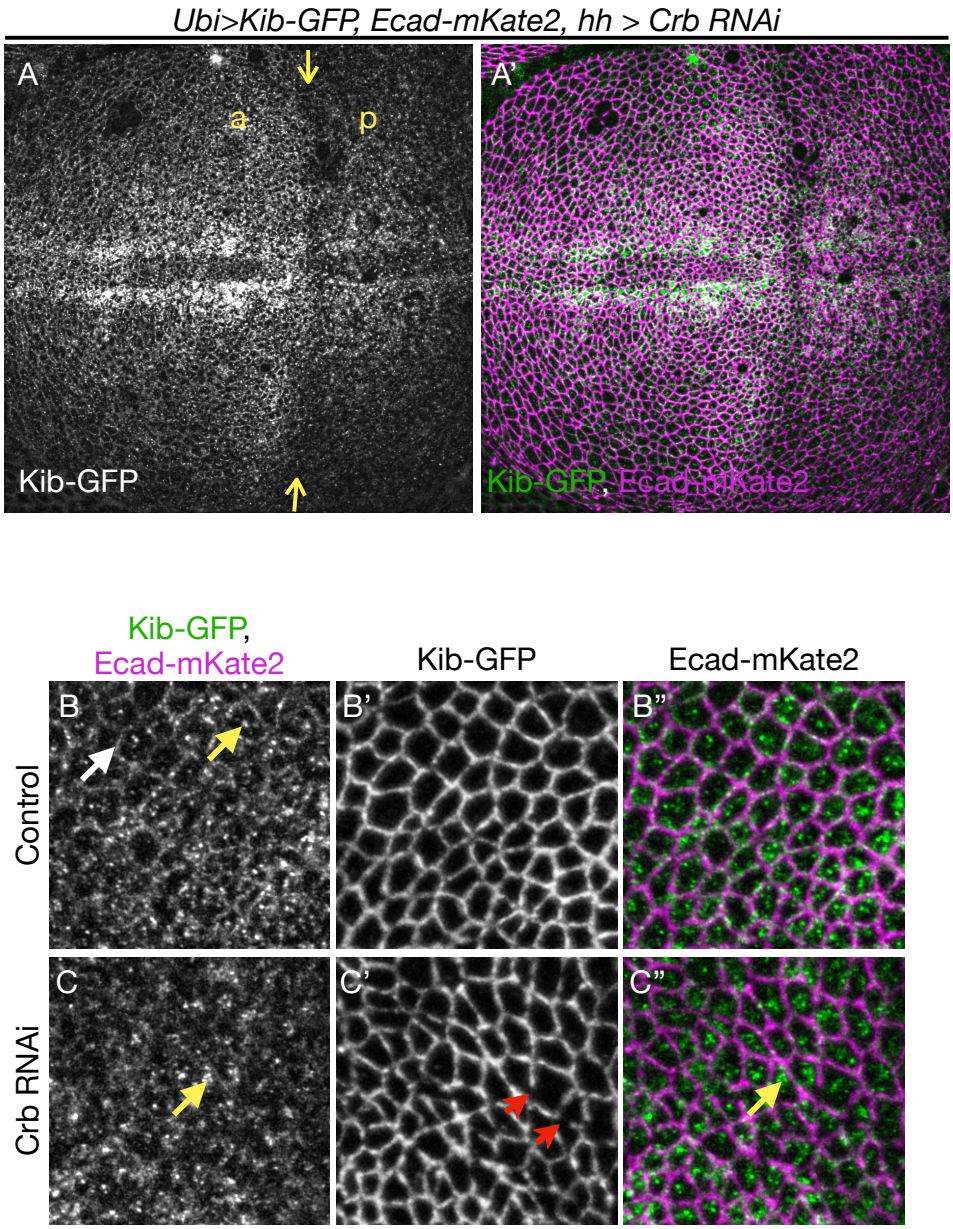

A-A') Loss of Crb does not severely affect Kib abundance. Yellow arrows mark the anterior-posterior (a-p) boundary.
B-C'') While Kib localizes both at the junctional (white arrow) and medial cortex (yellow arrow) in control cells (B-B''), it is mostly medial in cells depleted of Crb (C-C''). Note that loss of Crb also leads to Ecad gaps (red arrowheads), suggesting that Crb is needed for junctional stability.

of gaps at the adherence junctions (Fig. A.1B' & C'), suggesting that Crb may contribute to junctional stability and the organization of the junctional cytoskeleton.

Crb is required for junctional actomyosin organization

Previous work has linked Crb to the regulation of junctional stability and actomyosin organization and dynamics in various contexts. For example, loss of Crb in the amnioserosa of the Drosophila embryo leads to less stable junctions and increased apicomedial actomyosin dynamics (Flores-Benitez and Knust, 2015). In the Drosophila pupal wing, loss of Crb also leads to gaps in adherens junctions, disruption of junctional F-actin, and increased apicomedial F-actin (Salis et al., 2017). Therefore, given our observations in Chapter 4 that increased medial actomyosin organization leads to medial Kib localization, I asked if loss of Crb also affects actomyosin organization in the wing imaginal disc. To this end, I generated somatic mosaic *crb*^{1} mutant clones and examined the effect on F-actin (using Utr-GFP reporter) and myosin (Sqh-GFP) in living tissues. Strikingly, loss of Crb lead to the disruption of junctional F-actin (Fig. A.2A-A'). Similarly, whereas myosin organization in control cells has a clear junctional pattern, this pattern was severely disrupted in *crb*^{1} mutant clones (Fig. A.2B-B'). These results are consistent with previous studies and indicate that Crb is important for junctional stability of the actomyosin network.

The regulation of Kib localization by Crb cannot be explained by changes in actomyosin organization alone

If Crb regulates Kib localization via actomyosin organization and/or dynamics alone, then restoring actomyosin organization or stabilizing its dynamics should block the effect of Crb on

Figure A.2: Loss of Crb disrupts junctional actomyosin organization

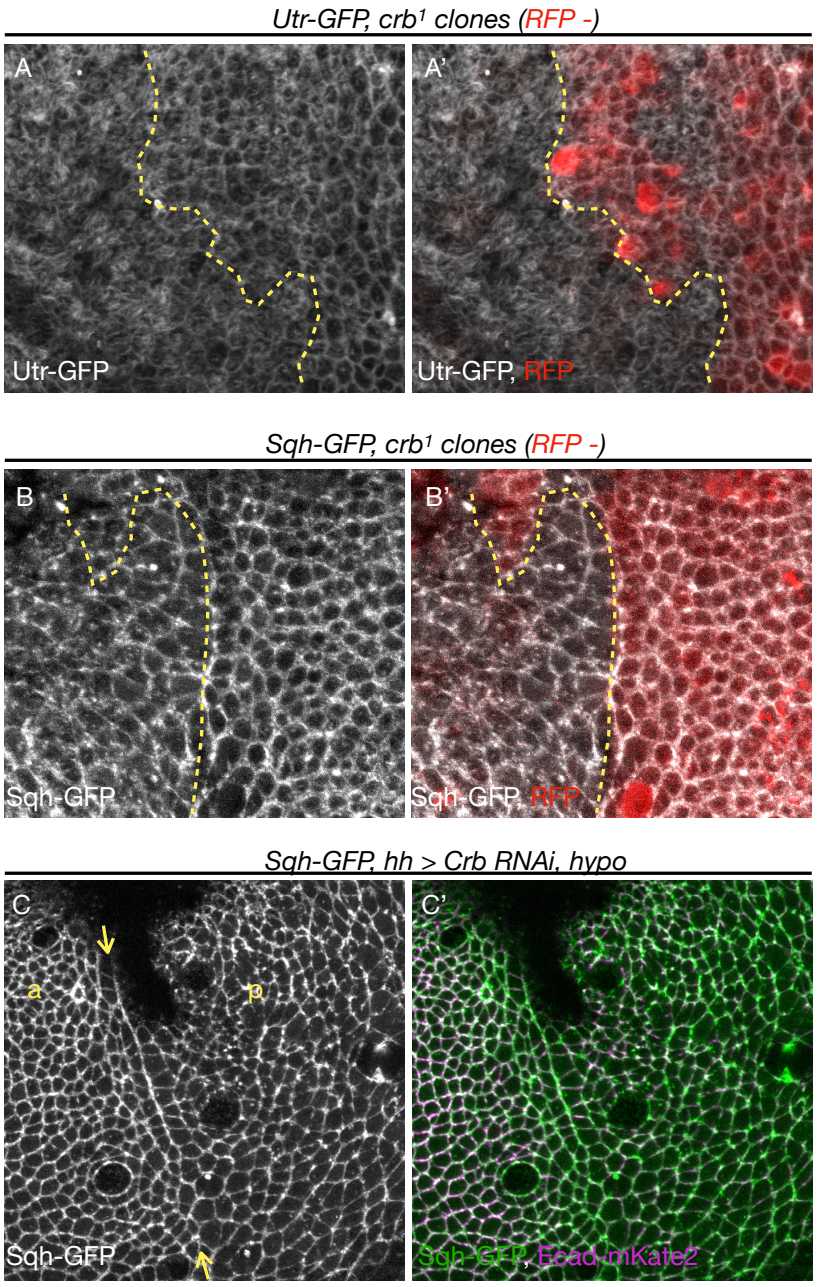

A-A') F-actin marker Utr-GFP becomes less junctional in *crb-null* somatic mosaic clones (clones are negative for RFP). Dashed line demarcates the clone-control boundary.
B-B') Cortical myosin organization is also disrupted in *crb-null* clones.
C-C') An Airyscan confocal image showing that treatment of discs in which Crb is depleted in the posterior compartment with a hypotonic solution restores junctional myosin organization. Yellow arrows mark the anterior-posterior (a-p) boundary.

Figure A.3: Crb is necessary to tether Kib at the junctional cortex

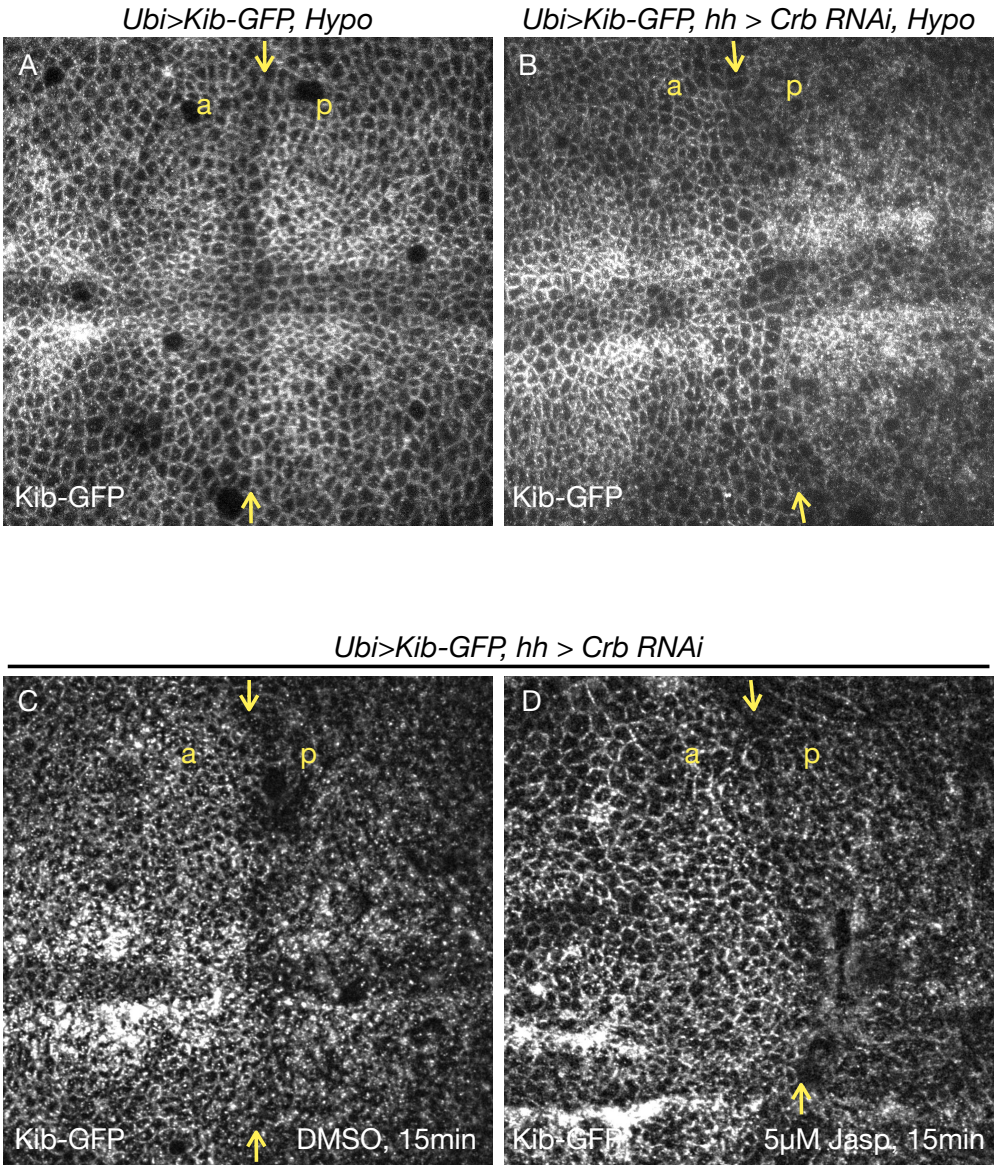

A-B) Normally, hypotonic shift leads to more junctional Kib across the entire tissue (A). However, hypotonic shift fails to relocalize Kib to the junctional cortex when Crb is depleted in the posterior compartment. Yellow arrows mark the anterior-posterior (a-p) boundary. C-D) Loss of Crb in the posterior compartment disrupts junctional Kib localization (C). Freezing F-actin dynamics with Jasp treatment leads to more junctional Kib in the anterior compartment (control) but not in the posterior, where Crb is depleted (D). Yellow arrows mark the anterior-posterior (a-p) boundary.

Kib localization. In Chapter 4, I demonstrated that under hypotonic conditions, F-actin and myosin becomes enriched at the junctions (Fig. 4.3). Therefore, I wondered of hypotonicity could also restore junctional myosin organization under the loss of Crb. Indeed, under hypotonic conditions, myosin regained its junctional organization even in Crb-depleted cells (Fig. A.2C-C'). Interestingly, hypotonic shift failed to restore junctional Kib localization; instead, while Kib became more junctional in the control cells, in cells depleted of Crb Kib became mostly diffuse (Fig. A.3A-B). Alternatively, I sought to freeze F-actin dynamics using Jasplakinolide (Jasp), a pharmacological stabilizer of F-actin which, as I have shown in Chapter 4, leads to more junctional Kib (Fig. 4.7). However, while treatment with Jasp led to more junctional Kib in the control cells, it failed to restore junctional Kib localization in Crb-depleted cells. Collectively, these results suggest that while actomyosin organization and dynamics can control Kib localization, there must a separate mechanism by which Crb mediates the tethering of Kib at the junctional cortex.

Crb tethers Kib at the junctional cortex via aPKC

Crb contains a small intracellular region that contains a PDZ-binding and a FERM-binding domain. With its PDZ-binding domain, Crb recruits downstream polarity components Patj and Stardust (Sdt) and can also stabilize Par6/aPKC complex (Tepass, 2012). The FERM-binding domain of Crb can also recruit the FERM domain proteins Yurt (Yrt), Moesin (Moe), and Expanded (Ex). Depletion of Patj, Sdt, Ex, Yurt, or Moe in the posterior compartment of the wing imaginal discs did not disrupt junctional Kib localization (Fig. A.4A-E). I next asked if Crb could control Kib localization via aPKC. Indeed, Crb depletion in the wing disc leads to a severe reduction of cortical aPKC (Fig. A.5A-A''). Additionally, Kib contains an aPKC binding domain

Figure A.4: Crb does not regulate Kib localization via Patj, Sdt, Ex, Yurt, or Moe

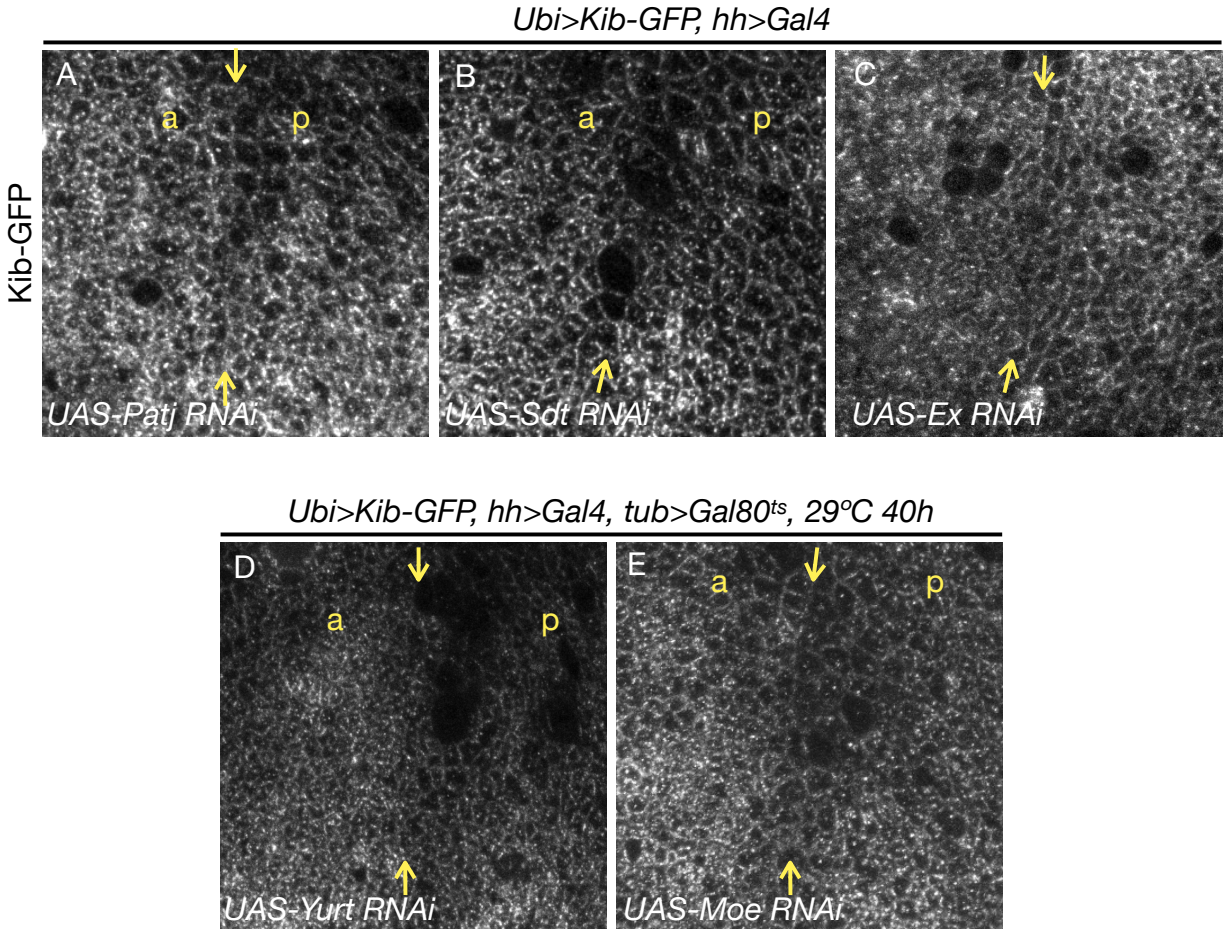

A-D) Depletion of Patj (A), Sdt (B), Ex (C) Yurt (D), or Moe (E) with previously validated RNAi lines does not disrupt junctional Kib localization.

Figure A.5: aPKC tethers Kib at the junctional cortex

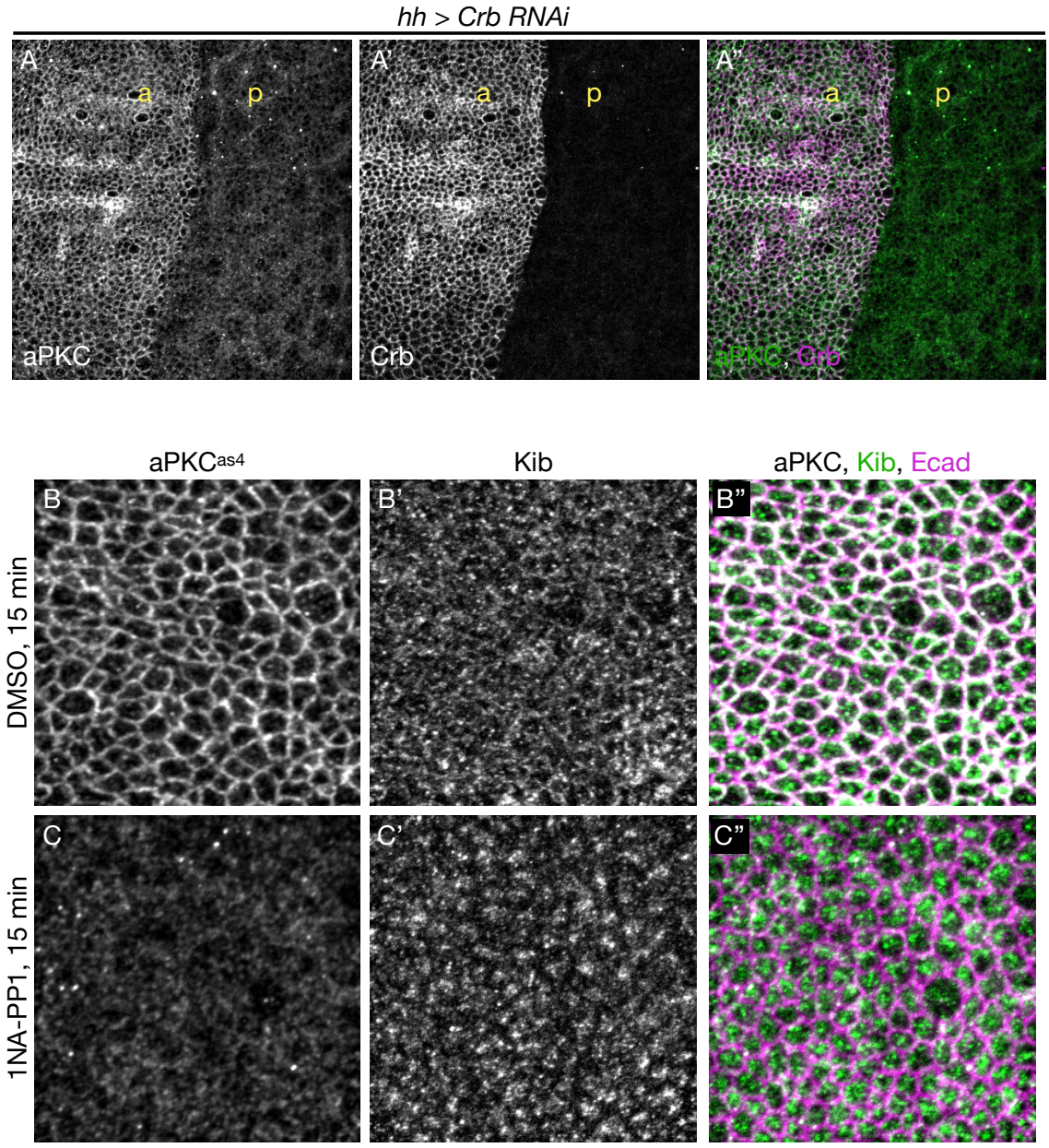

A-A'') Loss of Crb in the posterior compartment (p) leads to a severe loss of aPKC. B-C'') In control tissues homozygous for *aPKC*^{as4} allele, Kib localizes at the junctional and medial cortex and aPKC^{as4} is cortical (B-B''). However, treatment with the analog 1NA-PP1 for 15 min leads to severe displacement of aPKC^{as4} from the cell cortex and loss of Kib from the junctional cortex (C-C''). Note that Ecad-staining indicates that the adherens junctions remain intact.

and was found to interact with aPKC in Drosophila and mammalian cells (Yoshihama et al., 2011; Jin et al., 2015). However, the wing imaginal discs are extremely sensitive to direct manipulations of aPKC, making genetic manipulations of aPKC difficult to perform. Therefore, I turned to a recently engineered analog sensitive aPKC allele, $aPKC^{as4}$, which can be specifically inhibited using a small molecule analog 1NA-PP1 (see also Chapter 3, Fig. 3.7). Strikingly, while Kib localized normally under 15 min DMSO treatment (Fig. A.5B-B''), inhibition of the analog sensitive aPKC for 15 min resulted in a dramatic relocalization of Kib from the junctional to the medial cortex (Fig. A.5C-C''). Together, these results indicate that junctional Kib localization is mediated by aPKC.

What could be the role of apical polarity-mediated tethering of Kib at the junctional cortex? As mentioned earlier, loss of Crb enhances Kib activity, suggesting that apical polarity could inactivate Kib. Mechanistically, it is possible that apical polarity physically antagonize Kib-mediated Hippo complex formation. Indeed, in human cancer cell lines, apical polarity components were reported to sequester Kib from Hippo complexes, thereby preventing Hippo pathway activity (Zhou et al., 2017). Additionally, in *Drosophila* aPKC was reported to antagonize Kib function in autophagy (Jin et al., 2015), further supporting the idea that apical polarity could negatively regulate Kib.

Kib might be associated with the apical polarity network in the Drosophila neuroblasts

Given the results so far, I also wondered if Kib could be associated with the apical polarity network in a non-epithelial context. The neuroblasts of the Drosophila central nervous system (CNS) have been studied extensively to understand the function of apical polarity components in asymmetric cell division (ACD, Prehoda, 2009), and the Hippo pathway was shown to be

required for proper neuroblast ACD (Keder et al., 2015). However, the mechanisms by which the Hippo pathway regulates ACD and the potential role of Kib in this process remains unknown. Apical polarity components, including aPKC, accumulate on the apical side of the embryonic and larval neuroblasts at the onset mitosis, which leads to the segregation of basal components, such as Miranda (Mira) to the basal side of the neuroblast. After cell division, the mother cell inherits the apical polarity protein and remains a neuroblast, while the daughter cell inherits the basal polarity proteins to become the ganglion mother cell (GMC), a precursor cell that later differentiates into neurons and glia. Therefore, the last divided GMC will always be positioned in the axis of polarity.

I first examined endogenous Kib expression and localization in the Drosophila third instar larval brain. Although Kib is expressed at very low levels in the larval CNS, I observed bright punctae of Kib on the apical side of mitotic neuroblasts, opposite of the latest GMC (Fig. A.6A). To better visualize Kib, I turned to Ubi>Kib-GFP and found similar localization pattern in mitotic neuroblast (Fig. A.6B). These results suggest that Kib may be associated with the apical polarity network in other contexts.

To test if loss of Kib has any effect on polarity, I generated somatic mosaic *kib* mutant clones and examined the localization of aPKC in neroblasts. However, I saw no effect of Kib loss on polarity, as aPKC polarized normally across mitotic stages (Fig. A.6C-D'). Asymmetrically dividing cells, such the neuroblasts or *C. elegans* zygote, are known to employ redundant mechanism for ACD (Lang and Munro, 2017). Indeed, the role of Hippo pathway components in ACD was discovered in trans-heterozygous combinations of Hippo component alleles with mutations in other known regulators of ACD (Keder et al., 2015). Therefore, it is

possible that performing loss of Kib function experiments in the background of heterozygous mutations in other ACD regulators will result in detectible phenotypes in polarity and ACD.

Figure A.6: Kib forms an apical crescent in mitotic Drosophila larval neuroblasts

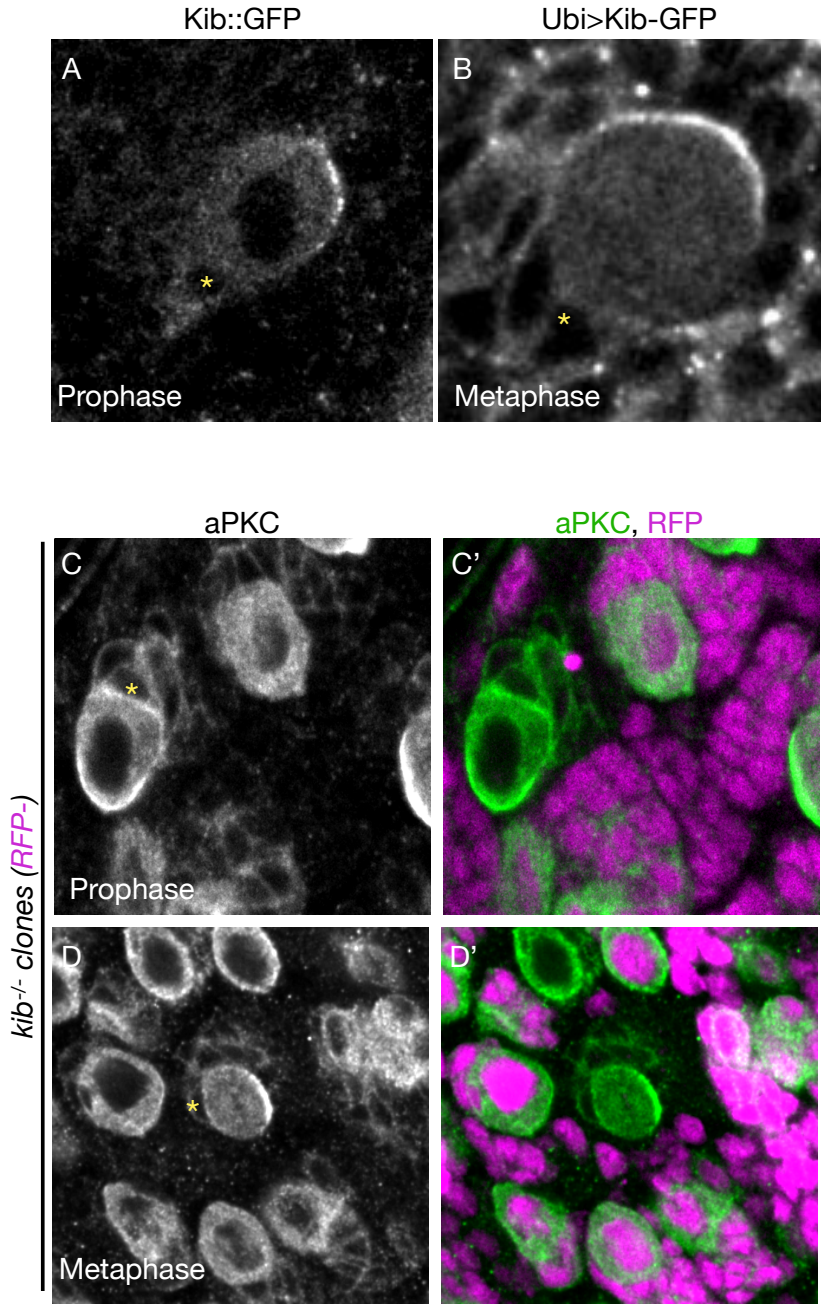

A-B) Localization of endogenous Kib::GFP (A, in prophase) or Ubi>Kib-GFP (B, in metaphase) on the apical side of the Drosophila 3d instar larval neuroblasts, where other apical polarity proteins are known to localize. The yellow asterisks indicate the last progeny of the neuroblast as a proxy of normal polarization axis.
C-D') aPKC polarizes normally, both in prophase (C-C') and metaphase (D-D') in somatic mosaic *kib-null* clones (clones are negative for RFP).

Methods

Table A.1. Reagents

Reagent type (species) or resource	Designation	Source or reference	Identifiers	Additional information
genetic reagent (*D. melanogaster*)	*Ubi>Kib-GFP*	10.7554/eLife.62326		
genetic reagent (*D. melanogaster*)	*Ecad-3XmKate2*	10.1016/j.devcel.2017.02.004		
genetic reagent (*D. melanogaster*)	*UAS-Crb RNAi*	Bloomington Drosophila Stock Center	BL35520	
genetic reagent (*D. melanogaster*)	*UAS-Utr-GFP*	Bloomington Drosophila Stock Center	BL34874	
genetic reagent (*D. melanogaster*)	*Sqh-GFP*	Bloomington Drosophila Stock Center	BL41685	
genetic reagent (*D. melanogaster*)	*UAS-Patj RNAi*	Bloomington Drosophila Stock Center	BL35747	Validated in 10.1083/jcb.201611196
genetic reagent (*D. melanogaster*)	*UAS-Sdt RNAi*	Bloomington Drosophila Stock Center	BL33909	Validated in 10.1083/jcb.201611196

Table A.1. Continued

genetic reagent (*D. melanogaster*)	*UAS-Ex RNAi*	Vienna Drosophila Resource Center	VDRC 109281	Validated in 10.1016/j.devcel.2017.02.004
genetic reagent (*D. melanogaster*)	*UAS-Yurt RNAi*	Bloomington Drosophila Stock Center	BL36118	Validated in 10.1371/journal.pgen.1009146
genetic reagent (*D. melanogaster*)	*UAS-Moe RNAi*	(Karagiosis and Ready, 2004)		
genetic reagent (*D. melanogaster*)	*aPKC^{as4}*	(Hannaford et al., 2019)		
Chemical	1-NA-PP1	Cayman	Cat.# CAYM-10954-1	
Chemical	Jasplakinolide	Cayman		
antibody	anti-PKC	Santa Cruz Biotechnology	Lot#: G2304	tissue staining (1:1000)
antibody	anti-GFP (Guinea pig polyclonal)	DOI: 10.1091/mbc.E19-07-0387	NA	tissue staining (1:10,000)

Drosophila husbandry

Drosophila melanogaster was cultured using standard techniques at 25°C (unless otherwise noted). For Gal80^{ts} experiments, crosses were maintained at 18°C and moved to 29°C for the duration specified in each experiment.

Generating *crb*-mutant somatic mosaic clones

To generate *crb*-mutant clones *ywhsFlp; 82BFRT Ubi>RFP/SM6-TM6* females were crossed to either *Nub>Gal4, Utr-GFP/CyOdfdYFP; 82BFRT crb^{1}/TM6, Tb* or *Sqh-GFP; 82BFRT crb^{1}/TM6, Tb* males. The larvae were heat shocked 60-84h after egg laying to generate clones.

Generating *kib*-mutant somatic mosaic clones

To generate *kib*-mutant clones, *ywhsFlp; 82BFRT Ubi>RFP/SM6-TM6* females were crossed to *82BFRT kib^{Del}/TM6, Tb* males. The larvae were heat shocked 48h after egg laying to generate clones.

Osmotic and pharmacological manipulations

Osmotic and pharmacological manipulations were performed as described in Chapter 3 and Chapter 4.

Appendix B

Kibra accumulates in the Z-disc in the larval body wall muscle

The association of Kib with the actomyosin network observed in Chapter 4 and Appendix A raises the question of which component of the network, F-actin or myosin, Kib associates with. One way to address this question is to examine Kib localization in a cell type where F-actin and myosin are organized in manner that allows for such distinction. Unlike an epithelial cell cortex, the sarcomeres of striated muscles have a distinct organization of F-actin, myosin, and the associated components. F-actin bundles are anchored with their growing (barbed) ends at the Z-disc, and their length reaches up to the H-zone from each side (Fig. B1.A). Thus, the H-zone itself is completely devoid of F-actin. In the Z-disc, different F-actin associated proteins are localized, including the capping proteins and alpha-actinin (Germain et al., 2022). The Z-disc is also the point of mechanotransduction in the sarcomere, where proteins such as titin and different LIM-domain proteins reside.

The Hippo pathway was recently shown to regulate flight muscle growth in Drosophila (Kaya-Çopur et al., 2021). Therefore, I decided to examine the localization of endogenous Kib::GFP in the body wall muscles of late third instar larvae. Strikingly, when imaged together with an F-actin marker ChMCA, Kib::GFP accumulated in the Z-disc of the sarcomeres (Fig. B.1B-B''), though Kib expression appeared extremely low. To better visualize Kib localization in the sarcomeres, I fixed and stained filleted cuticles of third instar larvae expressing Ubi>Kib-GFP with an anti-GFP antibody and Phalloidin. As with endogenous Kib, Ubi>Kib-GFP appeared enriched in the Z-disc (Fig. B.1C-C''). These observations suggest that Kib may be associated with F-actin or mechanosensitive components in the sarcomere.

Figure B.1: Kib is associated with the Z-disc in the Drosophila larval sarcomere

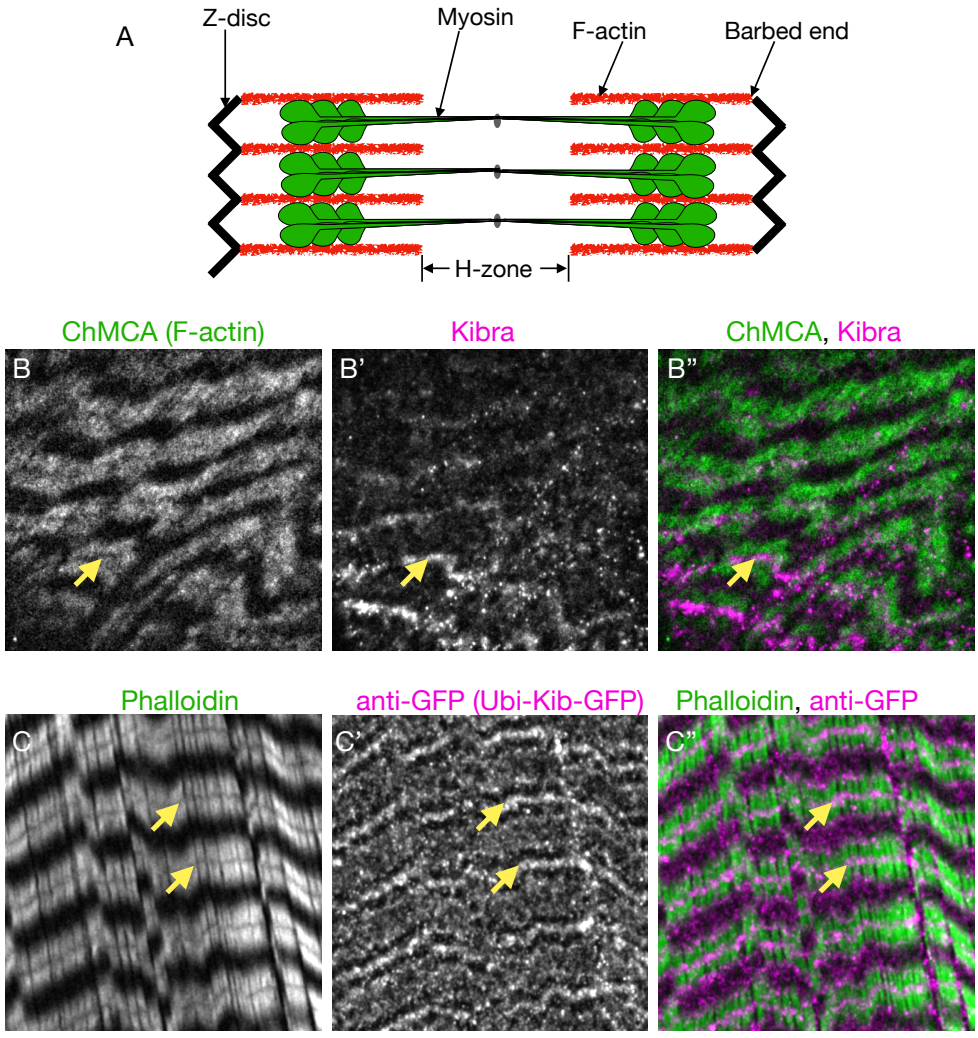

A) A simplified cartoon of a sarcomere. Note that the structures are not shown to scale.
B-B'') Live image of the Drosophila 3d instar larval cuticle muscle showing that endogenous Kib::GFP accumulates in the Z-disc (yellow arrow) of the sarcomere.
C-C'') Drosophila 3d instar larval cuticle prep stained with anti-GFP antibody (Kib) and phalloidin shows that Kib is enriched in the sarcomere Z-disc (yellow arrows).

The role of Kib in the muscles is unknown, and my initial goal was to find an actomyosin associated component that Kib could potentially associate with in the wing imaginal disc. Common F-actin associated proteins that are expressed in the muscle and epithelial cells include alpha-actinin (actn) and capping proteins a and b (cpa, cpb). Indeed, the capping proteins are known to regulate growth via the Hippo pathway (Fernandez et al., 2011). Therefore, I depleted cpa and actn in the wing imaginal disc and examined the effect on Kib abundance and localization. However, loss of cpa or actn did not have any detectible effect on Kib (Fig. B.2A-B').

The observations in this Appendix could lead to a future investigation of cytoskeletal or mechanosensitive proteins associated with Kib. One idea is to conduct a candidate RNAi screen against other components expressed both in the muscles and wing imaginal disc. Alternatively, one could investigate the role of Kib in muscle growth and development.

Figure B.2: Loss of the capping protein A or alpha-actinin has no detectible effect on Kib abundance or localization

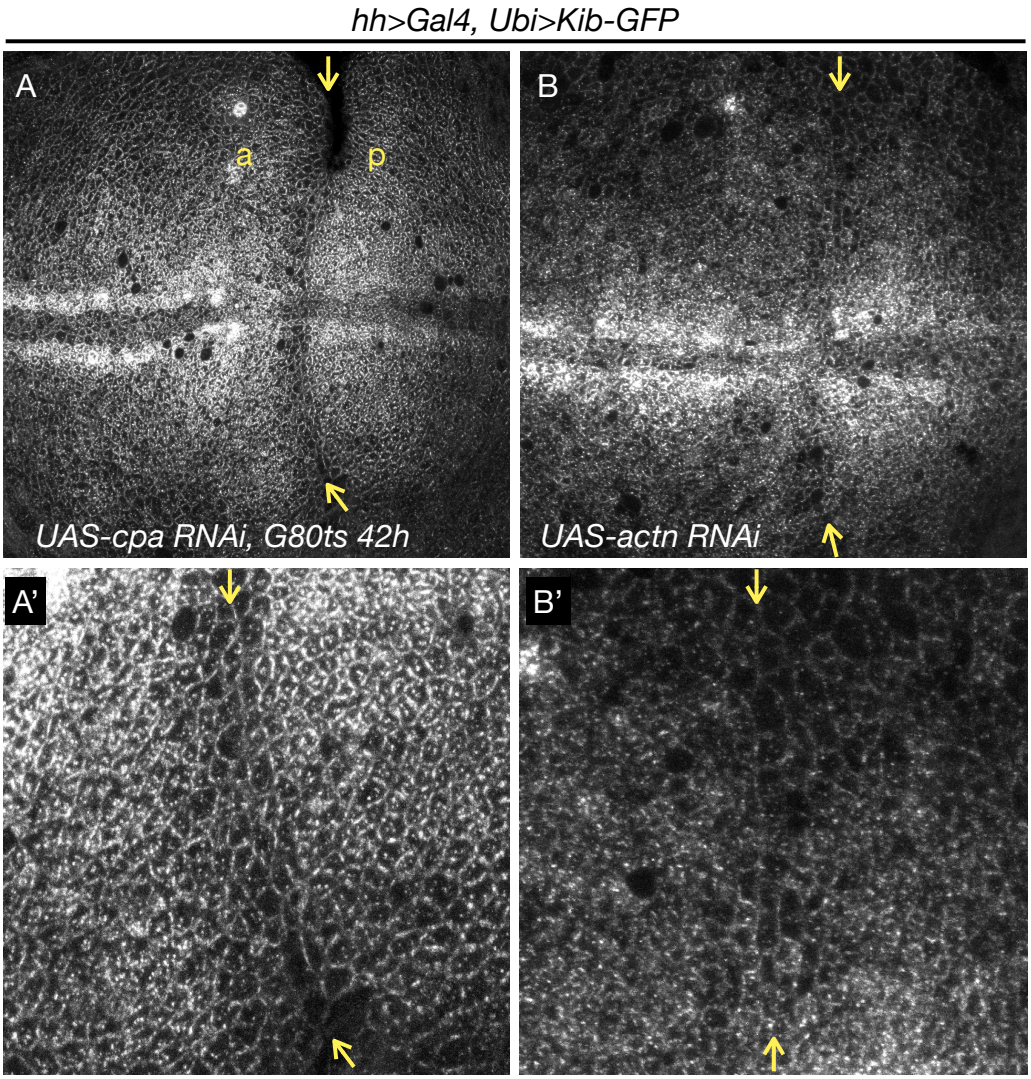

A-A') Transient depletion of cpa in the posterior compartment of the wing imaginal disc using *hh>Gal4* and *Gal80^{ts}* has no effect on Kib abundance or localization. Yellow arrows mark the anterior-posterior (a-p) boundary.
B-B') Depletion of actn in the posterior compartment using *hh>Gal4* has no effect on Kib.

Methods

Table B.1. Reagents

Reagent type (species) or resource	Designation	Source or reference	Identifiers	Additional information
genetic reagent (*D. melanogaster*)	*Ubi>Kib-GFP*	10.7554/eLife.62326		
genetic reagent (*D. melanogaster*)	*Kib::GFP*	10.1016/j.devcel.2017.02.004		
genetic reagent (*D. melanogaster*)	*sChMCA*	Bloomington Drosophila Stock Center	BL35520	
genetic reagent (*D. melanogaster*)	*Actn RNAi*	Bloomington Drosophila Stock Center	BL34874	
genetic reagent (*D. melanogaster*)	*Cpa RNAi*	Bloomington Drosophila Stock Center	BL41685	
antibody	anti-GFP (Guinea pig polyclonal)	DOI: 10.1091/mbc.E19-07-0387	NA	tissue staining (1:10,000)

Drosophila husbandry

Drosophila melanogaster was cultured using standard techniques at 25°C (unless otherwise noted). For Gal80^{ts} experiments, crosses were maintained at 18°C and moved to 29°C for the duration specified in each experiment.

Larval fillet preparation and staining

Wandering third instar larvae were dissected in PBS on Sylgard dishes and pinned down using 0.1 mm Insect Pins (FST #26002–10). Samples were then fixed for 30 min using 4% paraformaldehyde in PBS. After fixation samples were washed three times, 15 min each, in PBS supplemented with 0.01% Saponin. Samples were then blocked for 1 hr in PSN (PBS, 0.01% Saponin, 1% Normal Goat Serum), and then incubated in primary antibodies overnight at 4°C. On the second day, the larval preps were rinsed with PBS three times and washed in PSN for 30 min. After the wash, the preps were stained with the secondary antibodies for 3h at room temperature. All larval washes and antibody incubations were performed with mild agitation on a nutator.

Appendix C

Kibra and myosin dynamics during the *Drosophila* mesoderm invagination

Our work in Chapter 4 demonstrates that apicomedial Kibra (Kib) localization is dependent on actomyosin dynamics. Apicomedial myosin activity has been extensively studied in the context of the early gastrulation in the *Drosophila* embryo, the process known as the ventral furrow (VF) formation (Martin et al., 2009; Heer and Martin, 2017). In this process, the expression of two transcription factors, *twist* and *snail*, leads to the activation of Rho1 GTPase, and Rho1 promotes pulsatile medial myosin activity that ultimately drives the invagination of these cells via apical constriction. Because much of what is known about apicomedial myosin dynamics has been characterized in this system, I asked if the correlation of Kib dynamics with the medial actomyosin network I observe in the wing imaginal disc also occurs during the VF formation.

To examine the dynamics of Kib and myosin during the VF formation, I imaged embryos expressing Ubi>Kib-GFP and Sqh-mKate2 at the onset of gastrulation. Although I have also examined the dynamics of endogenous Kib and confirmed that it behaves similarly to Ubi>Kib-GFP, these data are not included here for the following reasons: 1) maternally-deposited Kib appears to be expressed at very low levels at this stage, and 2) I was only able to look at Kib::GFP/+ embryos, which resulted in a very low signal.

Prior to gastrulation, both Kib and myosin appear to be mostly diffuse on the ventral side (Fig. C.1A). However, concomitant with the initiation of pulsatile myosin activity, Kib punctae are seen to also accumulate at the apicomedial cortex (Figs. C.1A'-A''). Examination of Kib and myosin dynamics in a single cell over the course of a single pulse reveals that individual Kib "clusters" initially appear at the cortex, followed by the accumulation of medial myosin which leads to further coalescence of Kib clusters (Fig. C.1B). The duration of the myosin pulse I

Figure C.1: Kib dynamics in the Drosophila ventral furrow correlate with myosin

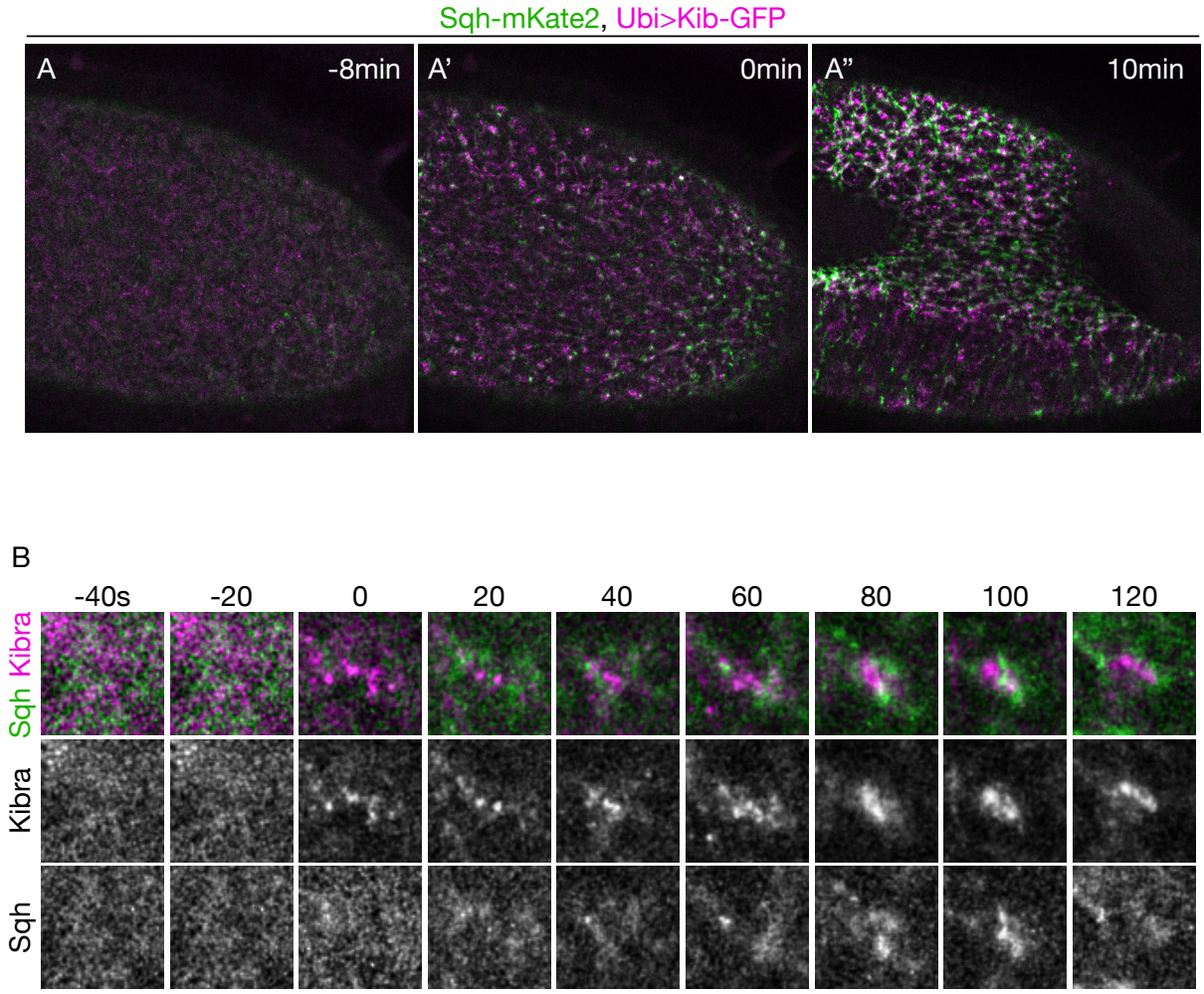

A-A'') Stills from a movie showing that medial Kib appears together with medial myosin pulses during the ventral furrow invagination
B) Stills of a single cell during ventral furrow invagination showing that medial Kib punctae appear to precede myosin accumulation, coalesce at the peak of the myosin pulse, and persist after myosin pulse dissipates.

observed (~80s) is comparable to what has been reported previously (Martin et al., 2009). Interestingly, coalesced Kib punctae persisted after myosin dissipation (Fig. C.1B).

These observations strengthen our findings described in Chapter 4 that myosin dynamics regulate Kib medial localization and raise several intriguing exploratory directions. First, the observation that medial Kib punctae precede the apparent medial myosin accumulation suggest that Kib may associate with an upstream activator of myosin. It would be interesting to observe how Kib dynamics are affected upon inhibiting pulsatile myosin activity, such as in embryos mutant for or depleted of *twist/snail* or under inhibition of Rho kinase activity with Y-27632 injection. Second, only a few Kib binding partners have been uncovered to date (mostly Hippo pathway components). Unbiased protein-protein interaction analysis of Kib, such as affinity purification and mass spectrometry (AP-MS), have been hindered by the fact that the tissue where Kib has been mostly characterized, the wing imaginal disc, is challenging to extract in sufficient quantities for protein purification. My observations that Kib is associated with the actomyosin network in the Drosophila embryo suggests that it should be possible to perform AP-MS on Kib purified from the Drosophila embryos, which can yield sufficient protein concentrations (Yang et al., 2017), to identify potential cytoskeletal components associated with Kib. Third, the function of Kib in the embryonic stages of Drosophila development is not known. My preliminary results (not shown in this dissertation) indicate that maternal/zygotic *kibra* mutant embryos do not survive to larval stages. Future work can be focused on examining if loss of Kib has any effects on actomyosin dynamics during the VF formation or other processes.

Methods

Table C.1. Reagents

Reagent type (species) or resource	Designation	Source or reference	Identifiers	Additional information
genetic reagent (*D. melanogaster*)	*Ubi>Kib-GFP*	10.7554/eLife.62326		
genetic reagent (*D. melanogaster*)	*Sqh-3XmKate2*	10.1038/nature22041		

Drosophila husbandry

Drosophila melanogaster was cultured using standard techniques at 25°C (unless otherwise noted). A stable line with the following genotype was used: Sqh-3XmKate2/CyodfdYFP; Ubi>Kib-GFP/TM6, Tb, Hu.

Embryo collection and live imaging

Flies were grown in bottles and cultured for 4 days after eclosure prior to embryo collections. Embryos were collected for 1h in a small collection cage on temperature-equilibrated apple juice plates with a spot of yeast paste at 25°C. After 1h collection, adults were removed, and the plate with embryos was incubated for additional 2h. Then, embryos were dechorionated with 30% bleach solution for 3 min, rinsed with dH_2O, aligned on an apple juice agar pad, and mounted on a coverslip with embryo glue (adhesive from double-sided tape dissolved in heptane) with the

ventral side facing the coverslip. The cover slip was attached via petroleum jelly to a metal cover slip with a hole in the center. Embryos were covered with halocarbon oil 200 and imaged on an inverted Zeiss LSM880 laser scanning confocal microscope equipped with a GaAsP spectral detector. Images were acquired every 20s until the completion of the VF.

REFERENCES

Aegerter-Wilmsen, T., Aegerter, C.M., Hafen, E., and Basler, K. (2007). Model for the regulation of size in the wing imaginal disc of Drosophila. Mechanisms of Development *124*, 318–326. https://doi.org/10.1016/j.mod.2006.12.005.

Aegerter-Wilmsen, T., Heimlicher, M.B., Smith, A.C., de Reuille, P.B., Smith, R.S., Aegerter, C.M., and Basler, K. (2012). Integrating force-sensing and signaling pathways in a model for the regulation of wing imaginal disc size. Development *139*, 3221–3231. https://doi.org/10.1242/dev.082800.

Aerne, B.L., Gailite, I., Sims, D., and Tapon, N. (2015). Hippo Stabilises Its Adaptor Salvador by Antagonising the HECT Ubiquitin Ligase Herc4. PLOS ONE *10*, e0131113. https://doi.org/10.1371/journal.pone.0131113.

Affolter, M., and Basler, K. (2007). The Decapentaplegic morphogen gradient: from pattern formation to growth regulation. Nat Rev Genet *8*, 663–674. https://doi.org/10.1038/nrg2166.

Alégot, H., Markosian, C., Rauskolb, C., Yang, J., Kirichenko, E., Wang, Y.-C., and Irvine, K.D. (2019). Recruitment of Jub by α-catenin promotes Yki activity and *Drosophila* wing growth. Journal of Cell Science *132*, jcs222018. https://doi.org/10.1242/jcs.222018.

Alexandre, C., Baena-Lopez, A., and Vincent, J.-P. (2014). Patterning and growth control by membrane-tethered Wingless. Nature *505*, 180–185. https://doi.org/10.1038/nature12879.

Anderson, C.A., Kovar, D.R., Gardel, M.L., and Winkelman, J.D. (2021). LIM domain proteins in cell mechanobiology. Cytoskeleton *78*, 303–311. https://doi.org/10.1002/cm.21677.

Aragona, M., Panciera, T., Manfrin, A., Giulitti, S., Michielin, F., Elvassore, N., Dupont, S., and Piccolo, S. (2013). A Mechanical Checkpoint Controls Multicellular Growth through YAP/TAZ Regulation by Actin-Processing Factors. Cell *154*, 1047–1059. https://doi.org/10.1016/j.cell.2013.07.042.

Badouel, C., Gardano, L., Amin, N., Garg, A., Rosenfeld, R., Le Bihan, T., and McNeill, H. (2009). The FERM-Domain Protein Expanded Regulates Hippo Pathway Activity via Direct Interactions with the Transcriptional Activator Yorkie. Developmental Cell *16*, 411–420. https://doi.org/10.1016/j.devcel.2009.01.010.

Baena-Lopez, L.A., Franch-Marro, X., and Vincent, J.-P. (2009). Wingless Promotes Proliferative Growth in a Gradient-Independent Manner. Sci. Signal. *2*. https://doi.org/10.1126/scisignal.2000360.

Baonza, A., and Freeman, M. (2005). Control of Cell Proliferation in the Drosophila Eye by Notch Signaling. Developmental Cell *8*, 529–539. https://doi.org/10.1016/j.devcel.2005.01.019.

Baonza, A., and Garcia-Bellido, A. (2000). Notch signaling directly controls cell proliferation in the Drosophila wing disc. Proc. Natl. Acad. Sci. U.S.A. *97*, 2609–2614. https://doi.org/10.1073/pnas.040576497.

Bardin, A.J., Visintin, R., and Amon, A. (2000). A Mechanism for Coupling Exit from Mitosis to Partitioning of the Nucleus. Cell *102*, 21–31. https://doi.org/10.1016/S0092-8674(00)00007-6.

Barrio, L., and Milán, M. (2017). Boundary Dpp promotes growth of medial and lateral regions of the Drosophila wing. ELife *6*, e22013. https://doi.org/10.7554/eLife.22013.

Basler, K. (1994). Compartment boundaries and the control of Drosophila limb pattern by hedgehog protein. *368*, 7. .

Baumgartner, R., Poernbacher, I., Buser, N., Hafen, E., and Stocker, H. (2010). The WW Domain Protein Kibra Acts Upstream of Hippo in Drosophila. Developmental Cell *18*, 309–316. https://doi.org/10.1016/j.devcel.2009.12.013.

Bayraktar, J., Zygmunt, D., and Carthew, R.W. (2006). Par-1 kinase establishes cell polarity and functions in Notch signaling in the *Drosophila* embryo. Journal of Cell Science *119*, 711–721. https://doi.org/10.1242/jcs.02789.

Bennett, F.C., and Harvey, K.F. (2006). Fat Cadherin Modulates Organ Size in Drosophila via the Salvador/Warts/Hippo Signaling Pathway. Current Biology *16*, 2101–2110. https://doi.org/10.1016/j.cub.2006.09.045.

Benton, R., and Johnston, D.St. (2003). A Conserved Oligomerization Domain in Drosophila Bazooka/PAR-3 Is Important for Apical Localization and Epithelial Polarity. Current Biology *13*, 1330–1334. https://doi.org/10.1016/S0960-9822(03)00508-6.

Benton, R., and St Johnston, D. (2003). Drosophila PAR-1 and 14-3-3 inhibit Bazooka/PAR-3 to establish complementary cortical domains in polarized cells. Cell *115*, 691–704. .

Boedigheimer, M., and Laughon, A. (1993). expanded: a gene involved in the control of cell proliferation in imaginal discs. Development *118*, 1291–1301. .

Boedigheimer, M.J., Nguyen, K.P., and Bryant, P.J. (1997). Expanded functions in the apical cell domain to regulate the growth rate of imaginal discs. Developmental Genetics *20*, 103–110. https://doi.org/10.1002/(SICI)1520-6408(1997)20:2<103::AID-DVG3>3.0.CO;2-B.

Boggiano, J.C., Vanderzalm, P.J., and Fehon, R.G. (2011). Tao-1 Phosphorylates Hippo/MST Kinases to Regulate the Hippo-Salvador-Warts Tumor Suppressor Pathway. Developmental Cell *21*, 888–895. https://doi.org/10.1016/j.devcel.2011.08.028.

Booth, A.J.R., Blanchard, G.B., Adams, R.J., and Röper, K. (2014). A Dynamic Microtubule Cytoskeleton Directs Medial Actomyosin Function during Tube Formation. Developmental Cell *29*, 562–576. https://doi.org/10.1016/j.devcel.2014.03.023.

Bosch, J.A., Sumabat, T.M., Hafezi, Y., Pellock, B.J., Gandhi, K.D., and Hariharan, I.K. (2014). The Drosophila F-box protein Fbxl7 binds to the protocadherin Fat and regulates Dachs localization and Hippo signaling. ELife *3*, e03383. https://doi.org/10.7554/eLife.03383.

Boulant, S., Kural, C., Zeeh, J.-C., Ubelmann, F., and Kirchhausen, T. (2011). Actin dynamics counteract membrane tension during clathrin-mediated endocytosis. Nat Cell Biol *13*, 1124–1131. https://doi.org/10.1038/ncb2307.

Bretscher, A., Edwards, K., and Fehon, R.G. (2002). ERM proteins and merlin: integrators at the cell cortex. Nature Reviews Molecular Cell Biology *3*, 586–599. https://doi.org/10.1038/nrm882.

Brittle, A., Thomas, C., and Strutt, D. (2012). Planar Polarity Specification through Asymmetric Subcellular Localization of Fat and Dachsous. Current Biology *22*, 907–914. https://doi.org/10.1016/j.cub.2012.03.053.

Bryant, P.J., and Levinson, P. (1985). Intrinsic Growth Control in the lmaginal Primordia of Drosophila, and the Autonomous Action of a Lethal Mutation Causing Overgrowth. Developmental Biology *107*, 355–363. https://doi.org/10.1016/ 0012-1606(85)90317-3.

Bryant, P.J., Huettner, B., Held, L.I., Ryerse, J., and Szidonya, J. (1988). Mutations at the fat locus interfere with cell proliferation control and epithelial morphogenesis in Drosophila. Developmental Biology *129*, 541–554. https://doi.org/10.1016/0012-1606(88)90399-5.

Bugaj, L.J., Choksi, A.T., Mesuda, C.K., Kane, R.S., and Schaffer, D.V. (2013). Optogenetic protein clustering and signaling activation in mammalian cells. Nature Methods *10*, 249–252. https://doi.org/10.1038/nmeth.2360.

Bui, D.A., Lee, W., White, A.E., Harper, J.W., Schackmann, R.C.J., Overholtzer, M., Selfors, L.M., and Brugge, J.S. (2016). Cytokinesis involves a nontranscriptional function of the Hippo pathway effector YAP. Sci. Signal. *9*, ra23–ra23. https://doi.org/10.1126/scisignal.aaa9227.

Büther, K., Plaas, C., Barnekow, A., and Kremerskothen, J. (2004). KIBRA is a novel substrate for protein kinase Cζ. Biochemical and Biophysical Research Communications *317*, 703–707. https://doi.org/10.1016/j.bbrc.2004.03.107.

Callus, B.A., Verhagen, A.M., and Vaux, D.L. (2006). Association of mammalian sterile twenty kinases, Mst1 and Mst2, with hSalvador via C-terminal coiled-coil domains, leads to its stabilization and phosphorylation. FEBS Journal *273*, 4264–4276. https://doi.org/10.1111/j.1742-4658.2006.05427.x.

Cao, L., Wang, P., Gao, Y., Lin, X., Wang, F., and Wu, S. (2014). Ubiquitin E3 ligase dSmurf is essential for Wts protein turnover and Hippo signaling. Biochemical and Biophysical Research Communications *454*, 167–171. https://doi.org/10.1016/j.bbrc.2014.10.058.

Chakraborty, S., Njah, K., Pobbati, A.V., Lim, Y.B., Raju, A., Lakshmanan, M., Tergaonkar, V., Lim, C.T., and Hong, W. (2017). Agrin as a Mechanotransduction Signal Regulating YAP

through the Hippo Pathway. Cell Reports *18*, 2464–2479. https://doi.org/10.1016/j.celrep.2017.02.041.

Chang, Y., and Dickinson, D.J. (2022). A particle size threshold governs diffusion and segregation of PAR-3 during cell polarization. Cell Reports *39*, 110652. https://doi.org/10.1016/j.celrep.2022.110652.

Chen, C.-L., Gajewski, K.M., Hamaratoglu, F., Bossuyt, W., Sansores-Garcia, L., Tao, C., and Halder, G. (2010). The apical-basal cell polarity determinant Crumbs regulates Hippo signaling in Drosophila. Proceedings of the National Academy of Sciences *107*, 15810–15815. https://doi.org/10.1073/pnas.1004060107.

Chen, X., Chen, Y., and Dong, J. (2016). MST2 phosphorylation at serine 385 in mitosis inhibits its tumor suppressing activity. Cellular Signalling *28*, 1826–1832. https://doi.org/10.1016/j.cellsig.2016.08.013.

Chia, W., Somers, W.G., and Wang, H. (2008). Drosophila neuroblast asymmetric divisions: cell cycle regulators, asymmetric protein localization, and tumorigenesis. Journal of Cell Biology *180*, 267–272. https://doi.org/10.1083/jcb.200708159.

Chinthalapudi, K., Mandati, V., Zheng, J., Sharff, A.J., Bricogne, G., Griffin, P.R., Kissil, J., and Izard, T. (2018). Lipid binding promotes the open conformation and tumor-suppressive activity of neurofibromin 2. Nature Communications *9*. https://doi.org/10.1038/s41467-018-03648-4.

Cho, E., Feng, Y., Rauskolb, C., Maitra, S., Fehon, R., and Irvine, K.D. (2006). Delineation of a Fat tumor suppressor pathway. Nat Genet *38*, 1142–1150. https://doi.org/10.1038/ng1887.

Cho, Y.S., Li, S., Wang, X., Zhu, J., Zhuo, S., Han, Y., Yue, T., Yang, Y., and Jiang, J. (2020). CDK7 regulates organ size and tumor growth by safeguarding the Hippo pathway effector Yki/Yap/Taz in the nucleus. Genes Dev. *34*, 53–71. https://doi.org/10.1101/gad.333146.119.

Chung, H.-L., Augustine, G.J., and Choi, K.-W. (2016). Drosophila Schip1 Links Expanded and Tao-1 to Regulate Hippo Signaling. Developmental Cell *36*, 511–524. https://doi.org/10.1016/j.devcel.2016.02.004.

Corbalan-Garcia, S., and Gómez-Fernández, J.C. (2014). Signaling through C2 domains: More than one lipid target. Biochimica et Biophysica Acta (BBA) - Biomembranes *1838*, 1536–1547. https://doi.org/10.1016/j.bbamem.2014.01.008.

Darnat, P., Burg, A., Sallé, J., Lacoste, J., Louvet-Vallée, S., Gho, M., and Audibert, A. (2022). Cortical Cyclin A controls spindle orientation during asymmetric cell divisions in Drosophila. Nat Commun *13*, 2723. https://doi.org/10.1038/s41467-022-30182-1.

Dawes, A.T., and Munro, E.M. (2011). PAR-3 Oligomerization May Provide an Actin-Independent Mechanism to Maintain Distinct Par Protein Domains in the Early Caenorhabditis elegans Embryo. Biophysical Journal *101*, 1412–1422. https://doi.org/10.1016/j.bpj.2011.07.030.

Deng, H., Wang, W., Yu, J., Zheng, Y., Qing, Y., and Pan, D. (2015). Spectrin regulates Hippo signaling by modulating cortical actomyosin activity. ELife *4*, e06567. https://doi.org/10.7554/eLife.06567.

Deng, H., Yang, L., Wen, P., Lei, H., Blount, P., and Pan, D. (2020). Spectrin couples cell shape, cortical tension, and Hippo signaling in retinal epithelial morphogenesis. Journal of Cell Biology *219*, e201907018. https://doi.org/10.1083/jcb.201907018.

Dewey, E.B., Sanchez, D., and Johnston, C.A. (2015). Warts Phosphorylates Mud to Promote Pins-Mediated Mitotic Spindle Orientation in Drosophila , Independent of Yorkie. Current Biology *25*, 2751–2762. https://doi.org/10.1016/j.cub.2015.09.025.

Di Ciano, C., Nie, Z., Szászi, K., Lewis, A., Uruno, T., Zhan, X., Rotstein, O.D., Mak, A., and Kapus, A. (2002). Osmotic stress-induced remodeling of the cortical cytoskeleton. American Journal of Physiology-Cell Physiology *283*, C850–C865. https://doi.org/10.1152/ajpcell.00018.2002.

Dickinson, D.J., Schwager, F., Pintard, L., Gotta, M., and Goldstein, B. (2017). A Single-Cell Biochemistry Approach Reveals PAR Complex Dynamics during Cell Polarization. Developmental Cell *42*, 416-434.e11. https://doi.org/10.1016/j.devcel.2017.07.024.

Ding, R., Weynans, K., Bossing, T., Barros, C.S., and Berger, C. (2016). The Hippo signalling pathway maintains quiescence in Drosophila neural stem cells. Nat Commun *7*, 10510. https://doi.org/10.1038/ncomms10510.

Diz-Muñoz, A., Thurley, K., Chintamen, S., Altschuler, S.J., Wu, L.F., Fletcher, D.A., and Weiner, O.D. (2016). Membrane Tension Acts Through PLD2 and mTORC2 to Limit Actin Network Assembly During Neutrophil Migration. PLoS Biol *14*, e1002474. https://doi.org/10.1371/journal.pbio.1002474.

Doe, C.Q. (2008). Neural stem cells: balancing self-renewal with differentiation. Development *135*, 1575–1587. https://doi.org/10.1242/dev.014977.

Doerflinger, H., Benton, R., Shulman, J.M., and St Johnston, D. (2003). The role of PAR-1 in regulating the polarised microtubule cytoskeleton in the Drosophila follicular epithelium. Development *130*, 3965–3975. https://doi.org/10.1242/dev.00616.

Doerflinger, H., Zimyanin, V., and St Johnston, D. (2021). The Drosophila anterior-posterior axis is polarized by asymmetric myosin activation. Current Biology S0960982221015487. https://doi.org/10.1016/j.cub.2021.11.024.

Duda, M., Kirkland, N.J., Khalilgharibi, N., Tozluoglu, M., Yuen, A.C., Carpi, N., Bove, A., Piel, M., Charras, G., Baum, B., et al. (2019). Polarization of Myosin II Refines Tissue Material Properties to Buffer Mechanical Stress. Developmental Cell *48*, 245-260.e7. https://doi.org/10.1016/j.devcel.2018.12.020.

Duman-Scheel, M., Weng, L., Xin, S., and Du, W. (2002). Hedgehog regulates cell growth and proliferation by inducing Cyclin D and Cyclin E. Nature *417*, 299–304. https://doi.org/10.1038/417299a.

Dupont, S., Morsut, L., Aragona, M., Enzo, E., Giulitti, S., Cordenonsi, M., Zanconato, F., Le Digabel, J., Forcato, M., Bicciato, S., et al. (2011). Role of YAP/TAZ in mechanotransduction. Nature *474*, 179–183. https://doi.org/10.1038/nature10137.

Dustin, M.L., and Groves, J.T. (2012). Receptor Signaling Clusters in the Immune Synapse. Annual Review of Biophysics *41*, 543–556. https://doi.org/10.1146/annurev-biophys-042910-155238.

Dutta, S., Mana-Capelli, S., Paramasivam, M., Dasgupta, I., Cirka, H., Billiar, K., and McCollum, D. (2017). TRIP6 inhibits Hippo signaling in response to tension at adherens junctions. EMBO Reports e201744777. https://doi.org/10.15252/embr.201744777.

Fehon, R.G., Kooh, P.J., Rebay, I., Regan, C.L., Xu, T., Muskavitch, M.A.T., and Artavanis-Tsakonas, S. (1990). Molecular interactions between the protein products of the neurogenic loci Notch and Delta, two EGF-homologous genes in Drosophila. Cell *61*, 523–534. https://doi.org/10.1016/0092-8674(90)90534-L.

Feng, Y., and Irvine, K.D. (2009). Processing and phosphorylation of the Fat receptor. Proc. Natl. Acad. Sci. U.S.A. *106*, 11989–11994. https://doi.org/10.1073/pnas.0811540106.

Fernandez, B.G., Gaspar, P., Bras-Pereira, C., Jezowska, B., Rebelo, S.R., and Janody, F. (2011a). Actin-Capping Protein and the Hippo pathway regulate F-actin and tissue growth in Drosophila. Development *138*, 2337–2346. https://doi.org/10.1242/dev.063545.

Fernandez, B.G., Gaspar, P., Bras-Pereira, C., Jezowska, B., Rebelo, S.R., and Janody, F. (2011b). Actin-Capping Protein and the Hippo pathway regulate F-actin and tissue growth in Drosophila. Development *138*, 2337–2346. https://doi.org/10.1242/dev.063545.

Fernandez-Gonzalez, R., and Zallen, J.A. (2011). Oscillatory behaviors and hierarchical assembly of contractile structures in intercalating cells. Phys. Biol. *8*, 045005. https://doi.org/10.1088/1478-3975/8/4/045005.

Fiore, A.P.Z.P., Rodrigues, A.M., Ribeiro-Filho, H.V., Manucci, A.C., de Freitas Ribeiro, P., Botelho, M.C.S., Vogel, C., Lopes-de-Oliveira, P.S., Pagano, M., and Bruni-Cardoso, A. (2022). Extracellular matrix stiffness regulates degradation of MST2 via SCF βTrCP. Biochimica et Biophysica Acta (BBA) - General Subjects *1866*, 130238. https://doi.org/10.1016/j.bbagen.2022.130238.

Fletcher, G.C., Elbediwy, A., Khanal, I., Ribeiro, P.S., Tapon, N., and Thompson, B.J. (2015a). The Spectrin cytoskeleton regulates the Hippo signalling pathway. The EMBO Journal *34*, 940–954. https://doi.org/10.15252/embj.201489642.

Fletcher, G.C., Elbediwy, A., Khanal, I., Ribeiro, P.S., Tapon, N., and Thompson, B.J. (2015b). The Spectrin cytoskeleton regulates the Hippo signalling pathway. The EMBO Journal *34*, 940–954. https://doi.org/10.15252/embj.201489642.

Flores-Benitez, D., and Knust, E. (2015). Crumbs is an essential regulator of cytoskeletal dynamics and cell-cell adhesion during dorsal closure in Drosophila. ELife *4*, e07398. https://doi.org/10.7554/eLife.07398.

Fomicheva, M., Tross, E.M., and Macara, I.G. (2020). Polarity proteins in oncogenesis. Current Opinion in Cell Biology *62*, 26–30. https://doi.org/10.1016/j.ceb.2019.07.016.

Forest, E., Logeay, R., Géminard, C., Kantar, D., Frayssinoux, F., Heron-Milhavet, L., and Djiane, A. (2018). The apical scaffold big bang binds to spectrins and regulates the growth of *Drosophila melanogaster* wing discs. The Journal of Cell Biology jcb.201705107. https://doi.org/10.1083/jcb.201705107.

Formstecher, E., Aresta, S., Collura, V., Hamburger, A., Meil, A., Trehin, A., Reverdy, C., Betin, V., Maire, S., and Brun, C. (2005). Protein interaction mapping: a Drosophila case study. Genome Research *15*, 376–384. .

Fulford, A., Tapon, N., and Ribeiro, P.S. (2018). Upstairs, downstairs: spatial regulation of Hippo signalling. Current Opinion in Cell Biology *51*, 22–32. https://doi.org/10.1016/j.ceb.2017.10.006.

Fulford, A.D., Holder, M.V., Frith, D., Snijders, A.P., Tapon, N., and Ribeiro, P.S. (2019). Casein kinase 1 family proteins promote Slimb-dependent Expanded degradation. ELife *8*, e46592. https://doi.org/10.7554/eLife.46592.

Garcia De Las Bayonas, A., Philippe, J.-M., Lellouch, A.C., and Lecuit, T. (2019). Distinct RhoGEFs Activate Apical and Junctional Contractility under Control of G Proteins during Epithelial Morphogenesis. Current Biology *29*, 3370-3385.e7. https://doi.org/10.1016/j.cub.2019.08.017.

Gavilan, H.S., Kulikauskas, R.M., Gutmann, D.H., and Fehon, R.G. (2014). In Vivo Functional Analysis of the Human NF2 Tumor Suppressor Gene in Drosophila. PLoS ONE *9*, e90853. https://doi.org/10.1371/journal.pone.0090853.

Genevet, A., Wehr, M.C., Brain, R., Thompson, B.J., and Tapon, N. (2010). Kibra Is a Regulator of the Salvador/Warts/Hippo Signaling Network. Developmental Cell *18*, 300–308. https://doi.org/10.1016/j.devcel.2009.12.011.

Germain, P., Delalande, A., and Pichon, C. (2022). Role of Muscle LIM Protein in Mechanotransduction Process. IJMS *23*, 9785. https://doi.org/10.3390/ijms23179785.

Gibson, D.G., Young, L., Chuang, R.-Y., Venter, J.C., Hutchison, C.A., and Smith, H.O. (2009). Enzymatic assembly of DNA molecules up to several hundred kilobases. Nat Methods *6*, 343–345. https://doi.org/10.1038/nmeth.1318.

Giraldez, A.J., and Cohen, S.M. (2003). Wingless and Notch signaling provide cell survival cues and control cell proliferation during wing development. Development *130*, 6533–6543. https://doi.org/10.1242/dev.00904.

Go, M.J., Eastman, D.S., and Artavanis-Tsakonas, S. (1998). Cell proliferation control by Notch signaling in Drosophila development. Development *125*, 2031–2040. https://doi.org/10.1242/dev.125.11.2031.

Goehring, N.W., Trong, P.K., Bois, J.S., Chowdhury, D., Nicola, E.M., Hyman, A.A., and Grill, S.W. (2011). Polarization of PAR Proteins by Advective Triggering of a Pattern-Forming System. Science *334*, 1137–1141. https://doi.org/10.1126/science.1208619.

Grzeschik, N.A., Parsons, L.M., Allott, M.L., Harvey, K.F., and Richardson, H.E. (2010). Lgl, aPKC, and Crumbs Regulate the Salvador/Warts/Hippo Pathway through Two Distinct Mechanisms. Current Biology *20*, 573–581. https://doi.org/10.1016/j.cub.2010.01.055.

Guilak, F., Erickson, G.R., and Ting-Beall, H.P. (2002). The Effects of Osmotic Stress on the Viscoelastic and Physical Properties of Articular Chondrocytes. Biophysical Journal *82*, 720–727. https://doi.org/10.1016/S0006-3495(02)75434-9.

Guo, S., and Kemphues, K.J. (1996). A non-muscle myosin required for embryonic polarity in Caenorhabditis elegans. Nature *382*, 455–458. https://doi.org/10.1038/382455a0.

Guo, C., Tommasi, S., Liu, L., Yee, J.-K., Dammann, R., and Pfeifer, G.P. (2007). RASSF1A Is Part of a Complex Similar to the Drosophila Hippo/Salvador/Lats Tumor-Suppressor Network. Current Biology *17*, 700–705. https://doi.org/10.1016/j.cub.2007.02.055.

Guruharsha, K.G., Rual, J.-F., Zhai, B., Mintseris, J., Vaidya, P., Vaidya, N., Beekman, C., Wong, C., Rhee, D.Y., Cenaj, O., et al. (2011). A Protein Complex Network of Drosophila melanogaster. Cell *147*, 690–703. https://doi.org/10.1016/j.cell.2011.08.047.

Guss, K.A., Benson, M., Gubitosi, N., Brondell, K., Broadie, K., and Skeath, J.B. (2013). Expression and function of scalloped during *Drosophila* development: Expression and Function of *Drosophila* Scalloped. Dev. Dyn. *242*, 874–885. https://doi.org/10.1002/dvdy.23942.

Halaoui, R., and McCaffrey, L. (2015). Rewiring cell polarity signaling in cancer. Oncogene *34*, 939–950. https://doi.org/10.1038/onc.2014.59.

Hamaratoglu, F., Willecke, M., Kango-Singh, M., Nolo, R., Hyun, E., Tao, C., Jafar-Nejad, H., and Halder, G. (2006). The tumour-suppressor genes NF2/Merlin and Expanded act through Hippo signalling to regulate cell proliferation and apoptosis. Nature Cell Biology *8*, 27–36. https://doi.org/10.1038/ncb1339.

Han, K. (1996). An efficient DDAB-mediated transfection of Drosophila S2 cells. Nucleic Acids Research *24*, 4362–4363. https://doi.org/10.1093/nar/24.21.4362.

Hannaford, M., Loyer, N., Tonelli, F., Zoltner, M., and Januschke, J. (2019). A chemical-genetics approach to study the role of atypical protein kinase C in *Drosophila*. Development dev.170589. https://doi.org/10.1242/dev.170589.

Hariharan, I.K. (2015). Organ Size Control: Lessons from Drosophila. Developmental Cell *34*, 255–265. https://doi.org/10.1016/j.devcel.2015.07.012.

Harrison, R.G. (1924). Some Unexpected Results of the Heteroplastic Transplantation of Limbs. Proc. Natl. Acad. Sci. U.S.A. *10*, 69–74. https://doi.org/10.1073/pnas.10.2.69.

Hart, M., Concordet, J.-P., Lassot, I., Albert, I., del los Santos, R., Durand, H., Perret, C., Rubinfeld, B., Margottin, F., Benarous, R., et al. (1999). The F-box protein β-TrCP associates with phosphorylated β-catenin and regulates its activity in the cell. Current Biology *9*, 207–211. https://doi.org/10.1016/S0960-9822(99)80091-8.

Hartman, N.C., and Groves, J.T. (2011). Signaling clusters in the cell membrane. Current Opinion in Cell Biology *23*, 370–376. https://doi.org/10.1016/j.ceb.2011.05.003.

Harumoto, T., Ito, M., Shimada, Y., Kobayashi, T.J., Ueda, H.R., Lu, B., and Uemura, T. (2010). Atypical Cadherins Dachsous and Fat Control Dynamics of Noncentrosomal Microtubules in Planar Cell Polarity. Developmental Cell *19*, 389–401. https://doi.org/10.1016/j.devcel.2010.08.004.

Harvey, K.F., Pfleger, C.M., and Hariharan, I.K. (2003a). The Drosophila Mst Ortholog, hippo, Restricts Growth and Cell Proliferation and Promotes Apoptosis. Cell *114*, 457–467. https://doi.org/10.1016/S0092-8674(03)00557-9.

Harvey, K.F., Pfleger, C.M., and Hariharan, I.K. (2003b). The Drosophila Mst Ortholog, hippo, Restricts Growth and Cell Proliferation and Promotes Apoptosis. Cell *114*, 457–467. https://doi.org/10.1016/S0092-8674(03)00557-9.

Heer, N.C., and Martin, A.C. (2017). Tension, contraction and tissue morphogenesis. Development *144*, 4249–4260. https://doi.org/10.1242/dev.151282.

Hergovich, A., and Hemmings, B.A. (2012). Hippo signalling in the G2/M cell cycle phase: Lessons learned from the yeast MEN and SIN pathways. Seminars in Cell & Developmental Biology *23*, 794–802. https://doi.org/10.1016/j.semcdb.2012.04.001.

Hergovich, A., Kohler, R.S., Schmitz, D., Vichalkovski, A., Cornils, H., and Hemmings, B.A. (2009). The MST1 and hMOB1 Tumor Suppressors Control Human Centrosome Duplication by Regulating NDR Kinase Phosphorylation. Current Biology *19*, 1692–1702. https://doi.org/10.1016/j.cub.2009.09.020.

Hirate, Y., Hirahara, S., Inoue, K., Suzuki, A., Alarcon, V.B., Akimoto, K., Hirai, T., Hara, T., Adachi, M., Chida, K., et al. (2013). Polarity-Dependent Distribution of Angiomotin Localizes Hippo Signaling in Preimplantation Embryos. Current Biology *23*, 1181–1194. https://doi.org/10.1016/j.cub.2013.05.014.

Homem, C.C.F., and Peifer, M. (2008). Diaphanous regulates myosin and adherens junctions to control cell contractility and protrusive behavior during morphogenesis. Development *135*, 1005–1018. https://doi.org/10.1242/dev.016337.

Hotz, M., Leisner, C., Chen, D., Manatschal, C., Wegleiter, T., Ouellet, J., Lindstrom, D., Gottschling, D.E., Vogel, J., and Barral, Y. (2012). Spindle Pole Bodies Exploit the Mitotic Exit Network in Metaphase to Drive Their Age-Dependent Segregation. Cell *148*, 958–972. https://doi.org/10.1016/j.cell.2012.01.041.

Huang, H.-L., Wang, S., Yin, M.-X., Dong, L., Wang, C., Wu, W., Lu, Y., Feng, M., Dai, C., Guo, X., et al. (2013). Par-1 Regulates Tissue Growth by Influencing Hippo Phosphorylation Status and Hippo-Salvador Association. PLoS Biology *11*, e1001620. https://doi.org/10.1371/journal.pbio.1001620.

Huang, J., Wu, S., Barrera, J., Matthews, K., and Pan, D. (2005). The Hippo Signaling Pathway Coordinately Regulates Cell Proliferation and Apoptosis by Inactivating Yorkie, the Drosophila Homolog of YAP. Cell *122*, 421–434. https://doi.org/10.1016/j.cell.2005.06.007.

Hufnagel, L., Teleman, A.A., Rouault, H., Cohen, S.M., and Shraiman, B.I. (2007). On the mechanism of wing size determination in fly development. Proc. Natl. Acad. Sci. U.S.A. *104*, 3835–3840. https://doi.org/10.1073/pnas.0607134104.

Ibar, C., Kirichenko, E., Keepers, B., Enners, E., Fleisch, K., and Irvine, K.D. (2018). Tension-dependent regulation of mammalian Hippo signaling through LIMD1. J Cell Sci *131*, jcs214700. https://doi.org/10.1242/jcs.214700.

Ingham, P.W. (1998). Transducing Hedgehog: the story so far. The EMBO Journal *17*, 3505–3511. https://doi.org/10.1093/emboj/17.13.3505.

Jaspersen, S.L., Charles, J.F., Tinker-Kulberg, R.L., and Morgan, D.O. (1998). A Late Mitotic Regulatory Network Controlling Cyclin Destruction in *Saccharomyces cerevisiae*. MBoC *9*, 2803–2817. https://doi.org/10.1091/mbc.9.10.2803.

Jensen, S., Geymonat, M., Johnson, A.L., Segal, M., and Johnston, L.H. (2002). Spatial regulation of the guanine nucleotide exchange factor Lte1 in *Saccharomyces cerevisiae*. Journal of Cell Science *115*, 4977–4991. https://doi.org/10.1242/jcs.00189.

Ji, M., Yang, S., Chen, Y., Xiao, L., Zhang, L., and Dong, J. (2012). Phospho-regulation of KIBRA by CDK1 and CDC14 phosphatase controls cell-cycle progression. Biochemical Journal *447*, 93–102. https://doi.org/10.1042/BJ20120751.

Jia, J., Zhang, W., Wang, B., Trinko, R., and Jiang, J. (2003). The Drosophila Ste20 family kinase dMST functions as a tumor suppressor by restricting cell proliferation and promoting apoptosis. Genes & Development *17*, 2514–2519. https://doi.org/10.1101/gad.1134003.

Jiang, J., and Struhl, G. (1998). Regulation of the Hedgehog and Wingless signalling pathways by the F-box/WD40-repeat protein Slimb. Nature *391*, 493–496. https://doi.org/10.1038/35154.

Jiang, T., and Harris, T.J.C. (2019). Par-1 controls the composition and growth of cortical actin caps during Drosophila embryo cleavage. Journal of Cell Biology *218*, 4195–4214. https://doi.org/10.1083/jcb.201903152.

Jin, A., Neufeld, T.P., and Choe, J. (2015). Kibra and aPKC regulate starvation-induced autophagy in Drosophila. Biochemical and Biophysical Research Communications *468*, 1–7. https://doi.org/10.1016/j.bbrc.2015.11.011.

Johnson, D.I. (1999). Cdc42: An Essential Rho-Type GTPase Controlling Eukaryotic Cell Polarity. Microbiol Mol Biol Rev *63*, 54–105. https://doi.org/10.1128/MMBR.63.1.54-105.1999.

Johnston, C.A., Hirono, K., Prehoda, K.E., and Doe, C.Q. (2009). Identification of an Aurora-A/PinsLINKER/ Dlg Spindle Orientation Pathway using Induced Cell Polarity in S2 Cells. Cell *138*, 1150–1163. https://doi.org/10.1016/j.cell.2009.07.041.

Justice, R.W., Zilian, O., Woods, D.F., Noll, M., and Bryant, P.J. (1995). The Drosophila tumor suppressor gene warts encodes a homolog of human myotonic dystrophy kinase and is required for the control of cell shape and proliferation. Genes & Development *9*, 534–546. .

Kango-Singh, M. (2002). Shar-pei mediates cell proliferation arrest during imaginal disc growth in Drosophila. Development *129*, 5719–5730. https://doi.org/10.1242/dev.00168.

Kaya-Çopur, A., Marchiano, F., Hein, M.Y., Alpern, D., Russeil, J., Luis, N.M., Mann, M., Deplancke, B., Habermann, B.H., and Schnorrer, F. (2021). The Hippo pathway controls myofibril assembly and muscle fiber growth by regulating sarcomeric gene expression. ELife *10*, e63726. https://doi.org/10.7554/eLife.63726.

Keder, A., Rives-Quinto, N., Aerne, B.L., Franco, M., Tapon, N., and Carmena, A. (2015). The Hippo Pathway Core Cassette Regulates Asymmetric Cell Division. Current Biology *25*, 2739–2750. https://doi.org/10.1016/j.cub.2015.08.064.

Kemphues, K.J., Priess, J.R., Morton, D.G., and Cheng, N. (1988). Identification of genes required for cytoplasmic localization in early C. elegans embryos. Cell *52*, 311–320. https://doi.org/10.1016/S0092-8674(88)80024-2.

Kissil, J.L., Johnson, K.C., Eckman, M.S., and Jacks, T. (2002). Merlin Phosphorylation by p21-activated Kinase 2 and Effects of Phosphorylation on Merlin Localization. Journal of Biological Chemistry *277*, 10394–10399. https://doi.org/10.1074/jbc.M200083200.

Klueg, K.M., Alvarado, D., Muskavitch, M.A.T., and Duffy, J.B. (2002). Creation of a GAL4/UAS-coupled inducible gene expression system for use indrosophila cultured cell lines. Genesis *34*, 119–122. https://doi.org/10.1002/gene.10148.

Koontz, L.M., Liu-Chittenden, Y., Yin, F., Zheng, Y., Yu, J., Huang, B., Chen, Q., Wu, S., and Pan, D. (2013a). The Hippo Effector Yorkie Controls Normal Tissue Growth by Antagonizing Scalloped-Mediated Default Repression. Developmental Cell *25*, 388–401. https://doi.org/10.1016/j.devcel.2013.04.021.

Koontz, L.M., Liu-Chittenden, Y., Yin, F., Zheng, Y., Yu, J., Huang, B., Chen, Q., Wu, S., and Pan, D. (2013b). The Hippo Effector Yorkie Controls Normal Tissue Growth by Antagonizing Scalloped-Mediated Default Repression. Developmental Cell *25*, 388–401. https://doi.org/10.1016/j.devcel.2013.04.021.

Korinek, W.S., Copeland, M.J., Chaudhuri, A., and Chant, J. (2000). Molecular Linkage Underlying Microtubule Orientation Toward Cortical Sites in Yeast. Science *287*, 2257–2259. https://doi.org/10.1126/science.287.5461.2257.

Krueger, D., Pallares Cartes, C., Makaske, T., and De Renzis, S. (2020). βH-spectrin is required for ratcheting apical pulsatile constrictions during tissue invagination. EMBO Rep *21*. https://doi.org/10.15252/embr.201949858.

Kwan, J., Sczaniecka, A., Arash, E.H., Nguyen, L., Chen, C.-C., Ratkovic, S., Klezovitch, O., Attisano, L., McNeill, H., and Emili, A. (2016). DLG5 connects cell polarity and Hippo signaling protein networks by linking PAR-1 with MST1/2. Genes & Development *30*, 2696–2709. .

Lacey, K.R., Jackson, P.K., and Stearns, T. (1999). Cyclin-dependent kinase control of centrosome duplication. Proc. Natl. Acad. Sci. U.S.A. *96*, 2817–2822. https://doi.org/10.1073/pnas.96.6.2817.

Lai, E.C. (2004). Notch signaling: control of cell communication and cell fate. Development *131*, 965–973. https://doi.org/10.1242/dev.01074.

Lai, Z.-C., Wei, X., Shimizu, T., Ramos, E., Rohrbaugh, M., Nikolaidis, N., Ho, L.-L., and Li, Y. (2005). Control of Cell Proliferation and Apoptosis by Mob as Tumor Suppressor, Mats. Cell *120*, 675–685. https://doi.org/10.1016/j.cell.2004.12.036.

LaJeunesse, D.R., McCartney, B.M., and Fehon, R.G. (1998). Structural analysis of Drosophila merlin reveals functional domains important for growth control and subcellular localization. The Journal of Cell Biology *141*, 1589–1599. .

Lang, C.F., and Munro, E. (2017). The PAR proteins: from molecular circuits to dynamic self-stabilizing cell polarity. Development *144*, 3405–3416. https://doi.org/10.1242/dev.139063.

Lecuit, T., Lenne, P.-F., and Munro, E. (2011). Force Generation, Transmission, and Integration during Cell and Tissue Morphogenesis. Annu. Rev. Cell Dev. Biol. *27*, 157–184. https://doi.org/10.1146/annurev-cellbio-100109-104027.

Lee, L., Tirnauer, J.S., Li, J., Schuyler, S.C., Liu, J.Y., and Pellman, D. (2000). Positioning of the Mitotic Spindle by a Cortical-Microtubule Capture Mechanism. Science *287*, 2260–2262. https://doi.org/10.1126/science.287.5461.2260.

Lee, S., Wang, J.-W., Yu, W., and Lu, B. (2012). Phospho-dependent ubiquitination and degradation of PAR-1 regulates synaptic morphology and tau-mediated Aβ toxicity in Drosophila. Nat Commun *3*, 1312. https://doi.org/10.1038/ncomms2278.

LeGoff, L., Rouault, H., and Lecuit, T. (2013). A global pattern of mechanical stress polarizes cell divisions and cell shape in the growing *Drosophila* wing disc. Development *140*, 4051–4059. https://doi.org/10.1242/dev.090878.

Lehner, C.F., and O'Farrell, P.H. (1989). Expression and function of Drosophila cyclin a during embryonic cell cycle progression. Cell *56*, 957–968. https://doi.org/10.1016/0092-8674(89)90629-6.

Lei, Q.-Y., Zhang, H., Zhao, B., Zha, Z.-Y., Bai, F., Pei, X.-H., Zhao, S., Xiong, Y., and Guan, K.-L. (2008). TAZ Promotes Cell Proliferation and Epithelial-Mesenchymal Transition and Is Inhibited by the Hippo Pathway. Mol Cell Biol *28*, 2426–2436. https://doi.org/10.1128/MCB.01874-07.

Leterrier, C., and Pullarkat, P.A. (2022). Mechanical role of the submembrane spectrin scaffold in red blood cells and neurons. Journal of Cell Science *135*, jcs259356. https://doi.org/10.1242/jcs.259356.

Leung, C.Y., and Zernicka-Goetz, M. (2013). Angiomotin prevents pluripotent lineage differentiation in mouse embryos via Hippo pathway-dependent and -independent mechanisms. Nat Commun *4*, 2251. https://doi.org/10.1038/ncomms3251.

Lin, Z., Xie, R., Guan, K., and Zhang, M. (2020). A WW Tandem-Mediated Dimerization Mode of SAV1 Essential for Hippo Signaling. Cell Reports *32*, 108118. https://doi.org/10.1016/j.celrep.2020.108118.

Ling, C., Zheng, Y., Yin, F., Yu, J., Huang, J., Hong, Y., Wu, S., and Pan, D. (2010). The apical transmembrane protein Crumbs functions as a tumor suppressor that regulates Hippo signaling by binding to Expanded. Proceedings of the National Academy of Sciences *107*, 10532–10537. https://doi.org/10.1073/pnas.1004279107.

Liu, C.-Y., Zha, Z.-Y., Zhou, X., Zhang, H., Huang, W., Zhao, D., Li, T., Chan, S.W., Lim, C.J., Hong, W., et al. (2010a). The Hippo Tumor Pathway Promotes TAZ Degradation by Phosphorylating a Phosphodegron and Recruiting the SCFβ-TrCP E3 Ligase. Journal of Biological Chemistry *285*, 37159–37169. https://doi.org/10.1074/jbc.M110.152942.

Liu, T., Rohn, J.L., Picone, R., Kunda, P., and Baum, B. (2010b). Tao-1 is a negative regulator of microtubule plus-end growth. Journal of Cell Science *123*, 2708–2716. https://doi.org/10.1242/jcs.068726.

López-Gay, J.M., Nunley, H., Spencer, M., di Pietro, F., Guirao, B., Bosveld, F., Markova, O., Gaugue, I., Pelletier, S., Lubensky, D.K., et al. (2020). Apical stress fibers enable a scaling between cell mechanical response and area in epithelial tissue. Science *370*, eabb2169. https://doi.org/10.1126/science.abb2169.

Lucas, E.P., Khanal, I., Gaspar, P., Fletcher, G.C., Polesello, C., Tapon, N., and Thompson, B.J. (2013). The Hippo pathway polarizes the actin cytoskeleton during collective migration of *Drosophila* border cells. J Cell Biol *201*, 875–885. https://doi.org/10.1083/jcb.201210073.

Luo, J., Wang, H., Kang, D., Guo, X., Wan, P., Wang, D., and Chen, J. (2016). Dlg5 maintains apical polarity by promoting membrane localization of Crumbs during Drosophila oogenesis. Scientific Reports *6*. https://doi.org/10.1038/srep26553.

Ly, P.T., Tan, Y.S., Koe, C.T., Zhang, Y., Xie, G., Endow, S., Deng, W.-M., Yu, F., and Wang, H. (2019a). CRL4Mahj E3 ubiquitin ligase promotes neural stem cell reactivation. PLoS Biol *17*, e3000276. https://doi.org/10.1371/journal.pbio.3000276.

Ly, P.T., Tan, Y.S., Koe, C.T., Zhang, Y., Xie, G., Endow, S., Deng, W.-M., Yu, F., and Wang, H. (2019b). CRL4Mahj E3 ubiquitin ligase promotes neural stem cell reactivation. PLOS Biology *17*, 27. .

Ma, X., Guo, X., Richardson, H.E., Xu, T., and Xue, L. (2018). POSH regulates Hippo signaling through ubiquitin-mediated expanded degradation. Proceedings of the National Academy of Sciences 201715165. https://doi.org/10.1073/pnas.1715165115.

Mah, A.S., Jang, J., and Deshaies, R.J. (2001). Protein kinase Cdc15 activates the Dbf2-Mob1 kinase complex. Proceedings of the National Academy of Sciences *98*, 7325–7330. https://doi.org/10.1073/pnas.141098998.

Maitra, S., Kulikauskas, R.M., Gavilan, H., and Fehon, R.G. (2006). The Tumor Suppressors Merlin and Expanded Function Cooperatively to Modulate Receptor Endocytosis and Signaling. Current Biology *16*, 702–709. https://doi.org/10.1016/j.cub.2006.02.063.

Majumder, P., Aranjuez, G., Amick, J., and McDonald, J.A. (2012). Par-1 Controls Myosin-II Activity through Myosin Phosphatase to Regulate Border Cell Migration. Current Biology *22*, 363–372. https://doi.org/10.1016/j.cub.2012.01.037.

Mana-Capelli, S., Paramasivam, M., Dutta, S., and McCollum, D. (2014). Angiomotins link F-actin architecture to Hippo pathway signaling. Molecular Biology of the Cell *25*, 1676–1685. .

Manning, S.A., Kroeger, B., and Harvey, K.F. (2020). The regulation of Yorkie, YAP and TAZ: new insights into the Hippo pathway. Development *147*, dev179069. https://doi.org/10.1242/dev.179069.

Mao, Y. (2006). Dachs: an unconventional myosin that functions downstream of Fat to regulate growth, affinity and gene expression in Drosophila. Development *133*, 2539–2551. https://doi.org/10.1242/dev.02427.

Mao, Y., Tournier, A.L., Hoppe, A., Kester, L., Thompson, B.J., and Tapon, N. (2013). Differential proliferation rates generate patterns of mechanical tension that orient tissue growth. EMBO J *32*, 2790–2803. https://doi.org/10.1038/emboj.2013.197.

Mardin, B.R., Lange, C., Baxter, J.E., Hardy, T., Scholz, S.R., Fry, A.M., and Schiebel, E. (2010). Components of the Hippo pathway cooperate with Nek2 kinase to regulate centrosome disjunction. Nat Cell Biol *12*, 1166–1176. https://doi.org/10.1038/ncb2120.

Martin, A.C., Kaschube, M., and Wieschaus, E.F. (2009). Pulsed contractions of an actin–myosin network drive apical constriction. Nature *457*, 495–499. https://doi.org/10.1038/nature07522.

Matakatsu, H., and Blair, S.S. (2004). Interactions between Fat and Dachsous and the regulation of planar cell polarity in the *Drosophila wing*. Development *131*, 3785–3794. https://doi.org/10.1242/dev.01254.

Matakatsu, H., and Blair, S.S. (2012). Separating planar cell polarity and Hippo pathway activities of the protocadherins Fat and Dachsous. Development *139*, 1498–1508. https://doi.org/10.1242/dev.070367.

Matakatsu, H., Blair, S.S., and Fehon, R.G. (2017). The palmitoyltransferase Approximated promotes growth via the Hippo pathway by palmitoylation of Fat. Journal of Cell Biology *216*, 265–277. https://doi.org/10.1083/jcb.201609094.

McCartney, B.M., and Fehon, R.G. (1996). Distinct cellular and subcellular patterns of expression imply distinct functions for the Drosophila homologues of moesin and the neurofibromatosis 2 tumor suppressor, merlin. The Journal of Cell Biology *133*, 843–852. https://doi.org/10.1083/jcb.133.4.843.

McCartney, B.M., Kulikauskas, R.M., LaJeunesse, D.R., and Fehon, R.G. (2000). The neurofibromatosis-2 homologue, Merlin, and the tumor suppressor expanded function together in Drosophila to regulate cell proliferation and differentiation. Development *127*, 1315–1324. .

Metcalf, D. (1963). The autonomous behaviour of normal thymus grafts. Aust J Exp Biol Med Sci *41*, 437–447. https://doi.org/10.1038/icb.1963.64.

Metcalf, D. (1964). Restricted growth capacity of multiple spleen grafts. Transplantation *2*, 387–392. https://doi.org/10.1097/00007890-196405000-00008.

Milán, M., Campuzano, S., and García-Bellido, A. (1996). Cell cycling and patterned cell proliferation in the wing primordium of Drosophila. Proc. Natl. Acad. Sci. U.S.A. *93*, 640–645. https://doi.org/10.1073/pnas.93.2.640.

Misra, J.R., and Irvine, K.D. (2016). Vamana Couples Fat Signaling to the Hippo Pathway. Developmental Cell *39*, 254–266. https://doi.org/10.1016/j.devcel.2016.09.017.

Misra, J.R., and Irvine, K.D. (2018). The Hippo Signaling Network and its Biological Functions. 23. .

Misra, J.R., and Irvine, K.D. (2019). Early girl is a novel component of the Fat signaling pathway. PLoS Genet *15*, e1007955. https://doi.org/10.1371/journal.pgen.1007955.

Mitonaka, T., Muramatsu, Y., Sugiyama, S., Mizuno, T., and Nishida, Y. (2007). Essential roles of myosin phosphatase in the maintenance of epithelial cell integrity of Drosophila imaginal disc cells. Developmental Biology *309*, 78–86. https://doi.org/10.1016/j.ydbio.2007.06.021.

Mohl, D.A., Huddleston, M.J., Collingwood, T.S., Annan, R.S., and Deshaies, R.J. (2009). Dbf2–Mob1 drives relocalization of protein phosphatase Cdc14 to the cytoplasm during exit from mitosis. Journal of Cell Biology *184*, 527–539. https://doi.org/10.1083/jcb.200812022.

Moleirinho, S., Hoxha, S., Mandati, V., Curtale, G., Troutman, S., Ehmer, U., and Kissil, J.L. (2017). Regulation of localization and function of the transcriptional co-activator YAP by angiomotin. ELife *6*, e23966. https://doi.org/10.7554/eLife.23966.

Morais-de-Sá, E., Mirouse, V., and St Johnston, D. (2010). aPKC Phosphorylation of Bazooka Defines the Apical/Lateral Border in Drosophila Epithelial Cells. Cell *141*, 509–523. https://doi.org/10.1016/j.cell.2010.02.040.

Morais-de-Sá, E., Vega-Rioja, A., Trovisco, V., and St Johnston, D. (2013). Oskar Is Targeted for Degradation by the Sequential Action of Par-1, GSK-3, and the SCF-Slimb Ubiquitin Ligase. Developmental Cell *26*, 303–314. https://doi.org/10.1016/j.devcel.2013.06.011.

Morisaki, T., Hirota, T., Iida, S., Marumoto, T., Hara, T., Nishiyama, Y., Kawasuzi, M., Hiraoka, T., Mimori, T., Araki, N., et al. (2002). WARTS tumor suppressor is phosphorylated by Cdc2/cyclin B at spindle poles during mitosis. FEBS Letters *529*, 319–324. https://doi.org/10.1016/S0014-5793(02)03360-4.

Morrison, H., Sherman, L.S., Legg, J., Banine, F., Isacke, C., Haipek, C.A., Gutmann, D.H., Ponta, H., and Herrlich, P. (2001). The NF2 tumor suppressor gene product, merlin, mediates contact inhibition of growth through interactions with CD44. Genes & Development *15*, 968–980. .

Munjal, A., Philippe, J.-M., Munro, E., and Lecuit, T. (2015). A self-organized biomechanical network drives shape changes during tissue morphogenesis. Nature *524*, 351–355. https://doi.org/10.1038/nature14603.

Munro, E., Nance, J., and Priess, J.R. (2004). Cortical Flows Powered by Asymmetrical Contraction Transport PAR Proteins to Establish and Maintain Anterior-Posterior Polarity in the Early C. elegans Embryo. Developmental Cell *7*, 413–424. https://doi.org/10.1016/j.devcel.2004.08.001.

Nechiporuk, T., Klezovitch, O., Nguyen, L., and Vasioukhin, V. (2013). Dlg5 maintains apical aPKC and regulates progenitor differentiation during lung morphogenesis. Developmental Biology *377*, 375–384. https://doi.org/10.1016/j.ydbio.2013.02.019.

Neufeld, T.P., de la Cruz, A.F.A., Johnston, L.A., and Edgar, B.A. (1998). Coordination of Growth and Cell Division in the Drosophila Wing. Cell *93*, 1183–1193. https://doi.org/10.1016/S0092-8674(00)81462-2.

Nishiyama, Y., Hirota, T., Morisaki, T., Hara, T., Marumoto, T., Iida, S., Makino, K., Yamamoto, H., Hiraoka, T., Kitamura, N., et al. (1999). A human homolog of Drosophila warts tumor suppressor, h-warts, localized to mitotic apparatus and specifically phosphorylated during mitosis. FEBS Letters *459*, 159–165. https://doi.org/10.1016/S0014-5793(99)01224-7.

Nolo, R., Morrison, C.M., Tao, C., Zhang, X., and Halder, G. (2006). The bantam MicroRNA Is a Target of the Hippo Tumor-Suppressor Pathway. Current Biology *16*, 1895–1904. https://doi.org/10.1016/j.cub.2006.08.057.

Oh, H., and Irvine, K.D. (2008). In vivo regulation of Yorkie phosphorylation and localization. Development *135*, 1081–1088. https://doi.org/10.1242/dev.015255.

Oh, H., and Irvine, K.D. (2009). In vivo analysis of Yorkie phosphorylation sites. Oncogene *28*, 1916–1927. https://doi.org/10.1038/onc.2009.43.

Okada, T., Lopez-Lago, M., and Giancotti, F.G. (2005). Merlin/ *NF-2* mediates contact inhibition of growth by suppressing recruitment of Rac to the plasma membrane. The Journal of Cell Biology *171*, 361–371. https://doi.org/10.1083/jcb.200503165.

Oon, C.H., and Prehoda, K.E. (2021). Phases of cortical actomyosin dynamics coupled to the neuroblast polarity cycle. Cell Biology 11. https://doi.org/10.7554/eLife.66574.

Pan, Y., Heemskerk, I., Ibar, C., Shraiman, B.I., and Irvine, K.D. (2016). Differential growth triggers mechanical feedback that elevates Hippo signaling. Proceedings of the National Academy of Sciences *113*, E6974–E6983. https://doi.org/oskar.

Pan, Y., Alégot, H., Rauskolb, C., and Irvine, K.D. (2018). The dynamics of Hippo signaling during *Drosophila* wing development. Development *145*, dev165712. https://doi.org/10.1242/dev.165712.

Paszek, M.J., Zahir, N., Johnson, K.R., Lakins, J.N., Rozenberg, G.I., Gefen, A., Reinhart-King, C.A., Margulies, S.S., Dembo, M., Boettiger, D., et al. (2005). Tensional homeostasis and the malignant phenotype. Cancer Cell *8*, 241–254. https://doi.org/10.1016/j.ccr.2005.08.010.

Pereira, G., and Schiebel, E. (2005). Kin4 Kinase Delays Mitotic Exit in Response to Spindle Alignment Defects. Molecular Cell *19*, 209–221. https://doi.org/10.1016/j.molcel.2005.05.030.

Perrimon, N., and McMahon, A.P. (1999). Negative Feedback Mechanisms and Their Roles during Pattern Formation. Cell *97*, 13–16. https://doi.org/10.1016/S0092-8674(00)80710-2.

Phillips, J.E., Santos, M., Konchwala, M., Xing, C., and Pan, D. (2022). Genome editing in the unicellular holozoan Capsaspora owczarzaki suggests a premetazoan role for the Hippo pathway in multicellular morphogenesis. ELife *11*, e77598. https://doi.org/10.7554/eLife.77598.

Pietuch, A., Brückner, B.R., and Janshoff, A. (2013). Membrane tension homeostasis of epithelial cells through surface area regulation in response to osmotic stress. Biochimica et Biophysica Acta (BBA) - Molecular Cell Research *1833*, 712–722. https://doi.org/10.1016/j.bbamcr.2012.11.006.

Poernbacher, I., Baumgartner, R., Marada, S.K., Edwards, K., and Stocker, H. (2012a). Drosophila Pez Acts in Hippo Signaling to Restrict Intestinal Stem Cell Proliferation. Current Biology *22*, 389–396. https://doi.org/10.1016/j.cub.2012.01.019.

Poernbacher, I., Baumgartner, R., Marada, S.K., Edwards, K., and Stocker, H. (2012b). Drosophila Pez Acts in Hippo Signaling to Restrict Intestinal Stem Cell Proliferation. Current Biology *22*, 389–396. https://doi.org/10.1016/j.cub.2012.01.019.

Polesello, C., Huelsmann, S., Brown, N.H., and Tapon, N. (2006). The Drosophila RASSF Homolog Antagonizes the Hippo Pathway. Current Biology *16*, 2459–2465. https://doi.org/10.1016/j.cub.2006.10.060.

Poon, C.L.C., Lin, J.I., Zhang, X., and Harvey, K.F. (2011). The Sterile 20-like Kinase Tao-1 Controls Tissue Growth by Regulating the Salvador-Warts-Hippo Pathway. Developmental Cell *21*, 896–906. https://doi.org/10.1016/j.devcel.2011.09.012.

Poon, C.L.C., Mitchell, K.A., Kondo, S., Cheng, L.Y., and Harvey, K.F. (2016). The Hippo Pathway Regulates Neuroblasts and Brain Size in Drosophila melanogaster. Current Biology *26*, 1034–1042. https://doi.org/10.1016/j.cub.2016.02.009.

Prehoda, K.E. (2009). Polarization of Drosophila Neuroblasts During Asymmetric Division. Cold Spring Harbor Perspectives in Biology *1*, a001388–a001388. https://doi.org/10.1101/cshperspect.a001388.

Rape, M. (2018). Ubiquitylation at the crossroads of development and disease. Nat Rev Mol Cell Biol *19*, 59–70. https://doi.org/10.1038/nrm.2017.83.

Rauskolb, C., Pan, G., Reddy, B.V.V.G., Oh, H., and Irvine, K.D. (2011). Zyxin Links Fat Signaling to the Hippo Pathway. PLoS Biol *9*, e1000624. https://doi.org/10.1371/journal.pbio.1000624.

Rauskolb, C., Sun, S., Sun, G., Pan, Y., and Irvine, K.D. (2014). Cytoskeletal Tension Inhibits Hippo Signaling through an Ajuba-Warts Complex. Cell *158*, 143–156. https://doi.org/10.1016/j.cell.2014.05.035.

Rauskolb, C., Cervantes, E., Madere, F., and Irvine, K.D. (2019). Organization and function of tension-dependent complexes at adherens junctions. Journal of Cell Science *132*, jcs224063. https://doi.org/10.1242/jcs.224063.

Razzell, W., Bustillo, M.E., and Zallen, J.A. (2018). The force-sensitive protein Ajuba regulates cell adhesion during epithelial morphogenesis. The Journal of Cell Biology jcb.201801171. https://doi.org/10.1083/jcb.201801171.

Rebay, I., Fleming, R.J., Fehon, R.G., Cherbas, L., Cherbas, P., and Artavanis-Tsakonas, S. (1991). Specific EGF repeats of Notch mediate interactions with Delta and serrate: Implications for notch as a multifunctional receptor. Cell *67*, 687–699. https://doi.org/10.1016/0092-8674(91)90064-6.

Restrepo, S., Zartman, J.J., and Basler, K. (2016). Cultivation and Live Imaging of Drosophila Imaginal Discs. In Drosophila, C. Dahmann, ed. (New York, NY: Springer New York), pp. 203–213.

Ribeiro, P., Holder, M., Frith, D., Snijders, A.P., and Tapon, N. (2014). Crumbs promotes expanded recognition and degradation by the SCFSlimb/ -TrCP ubiquitin ligase. Proceedings of the National Academy of Sciences *111*, E1980–E1989. https://doi.org/10.1073/pnas.1315508111.

Ribeiro, P.S., Josué, F., Wepf, A., Wehr, M.C., Rinner, O., Kelly, G., Tapon, N., and Gstaiger, M. (2010). Combined Functional Genomic and Proteomic Approaches Identify a PP2A Complex as a Negative Regulator of Hippo Signaling. Molecular Cell *39*, 521–534. https://doi.org/10.1016/j.molcel.2010.08.002.

Robinson, B.S., Huang, J., Hong, Y., and Moberg, K.H. (2010). Crumbs Regulates Salvador/Warts/Hippo Signaling in Drosophila via the FERM-Domain Protein Expanded. Current Biology *20*, 582–590. https://doi.org/10.1016/j.cub.2010.03.019.

Rodrigues-Campos, M., and Thompson, B.J. (2014). The ubiquitin ligase FbxL7 regulates the Dachsous-Fat-Dachs system in Drosophila. Development *141*, 4098–4103. https://doi.org/10.1242/dev.113498.

Roffay, C., Molinard, G., Kim, K., Urbanska, M., Andrade, V., Barbarasa, V., Nowak, P., Mercier, V., García-Calvo, J., Matile, S., et al. (2021). Passive coupling of membrane tension and cell volume during active response of cells to osmosis. Proc Natl Acad Sci USA *118*, e2103228118. https://doi.org/10.1073/pnas.2103228118.

Rogers, G.C., Rusan, N.M., Roberts, D.M., Peifer, M., and Rogers, S.L. (2009). The SCFSlimb ubiquitin ligase regulates Plk4/Sak levels to block centriole reduplication. The Journal of Cell Biology *184*, 225–239. https://doi.org/10.1083/jcb.200808049.

Romanova-Michaelides, M., Hadjivasiliou, Z., Aguilar-Hidalgo, D., Basagiannis, D., Seum, C., Dubois, M., Jülicher, F., and Gonzalez-Gaitan, M. (2022). Morphogen gradient scaling by recycling of intracellular Dpp. Nature *602*, 287–293. https://doi.org/10.1038/s41586-021-04346-w.

Rørth, P. (1998). Gal4 in the Drosophila female germline. Mechanisms of Development *78*, 113–118. https://doi.org/10.1016/S0925-4773(98)00157-9.

Ruberte, E., Marty, T., Nellen, D., Affolter, M., and Basler, K. (1995). An absolute requirement for both the type II and type I receptors, punt and thick veins, for Dpp signaling in vivo. Cell *80*, 889–897. https://doi.org/10.1016/0092-8674(95)90292-9.

Salis, P., Payre, F., Valenti, P., Bazellieres, E., Le Bivic, A., and Mottola, G. (2017). Crumbs, Moesin and Yurt regulate junctional stability and dynamics for a proper morphogenesis of the Drosophila pupal wing epithelium. Sci Rep *7*, 16778. https://doi.org/10.1038/s41598-017-15272-1.

Sansores-Garcia, L., Bossuyt, W., Wada, K.-I., Yonemura, S., Tao, C., Sasaki, H., and Halder, G. (2011). Modulating F-actin organization induces organ growth by affecting the Hippo pathway. The EMBO Journal *30*, 2325–2335. .

Sarpal, R., Yan, V., Kazakova, L., Sheppard, L., Yu, J.C., Fernandez-Gonzalez, R., and Tepass, U. (2019). Role of α-Catenin and its mechanosensing properties in regulating Hippo/YAP-dependent tissue growth. PLoS Genet *15*, e1008454. https://doi.org/10.1371/journal.pgen.1008454.

Scheid, M.P., Schubert, K.M., and Duronio, V. (1999). Regulation of Bad Phosphorylation and Association with Bcl-x $_L$ by the MAPK/Erk Kinase. J. Biol. Chem. *274*, 31108–31113. https://doi.org/10.1074/jbc.274.43.31108.

Schwank, G., and Basler, K. (2010). Regulation of Organ Growth by Morphogen Gradients. Cold Spring Harbor Perspectives in Biology *2*, a001669–a001669. https://doi.org/10.1101/cshperspect.a001669.

Schwank, G., Restrepo, S., and Basler, K. (2008). Growth regulation by Dpp: an essential role for Brinker and a non-essential role for graded signaling levels. Development *135*, 4003–4013. https://doi.org/10.1242/dev.025635.

Sebé-Pedrós, A., Zheng, Y., Ruiz-Trillo, I., and Pan, D. (2012). Premetazoan Origin of the Hippo Signaling Pathway. Cell Reports *1*, 13–20. https://doi.org/10.1016/j.celrep.2011.11.004.

Shraiman, B.I. (2005). Mechanical feedback as a possible regulator of tissue growth. Proceedings of the National Academy of Sciences *102*, 3318–3323. https://doi.org/10.1073/pnas.0404782102.

Silva, E., Tsatskis, Y., Gardano, L., Tapon, N., and McNeill, H. (2006). The Tumor-Suppressor Gene fat Controls Tissue Growth Upstream of Expanded in the Hippo Signaling Pathway. Current Biology *16*, 2081–2089. https://doi.org/10.1016/j.cub.2006.09.004.

Silver, J.T., Wirtz-Peitz, F., Simões, S., Pellikka, M., Yan, D., Binari, R., Nishimura, T., Li, Y., Harris, T.J.C., Perrimon, N., et al. (2019). Apical polarity proteins recruit the RhoGEF Cysts to promote junctional myosin assembly. Journal of Cell Biology *218*, 3397–3414. https://doi.org/10.1083/jcb.201807106.

Singh, A., Saha, T., Begemann, I., Ricker, A., Nüsse, H., Thorn-Seshold, O., Klingauf, J., Galic, M., and Matis, M. (2018). Polarized microtubule dynamics directs cell mechanics and coordinates forces during epithelial morphogenesis. Nature Cell Biology *20*, 1126–1133. https://doi.org/10.1038/s41556-018-0193-1.

Sinha, B., Köster, D., Ruez, R., Gonnord, P., Bastiani, M., Abankwa, D., Stan, R.V., Butler-Browne, G., Vedie, B., Johannes, L., et al. (2011). Cells Respond to Mechanical Stress by Rapid Disassembly of Caveolae. Cell *144*, 402–413. https://doi.org/10.1016/j.cell.2010.12.031.

Skaar, J.R., Pagan, J.K., and Pagano, M. (2013). Mechanisms and function of substrate recruitment by F-box proteins. Nat Rev Mol Cell Biol *14*, 369–381. https://doi.org/10.1038/nrm3582.

Sopko, R., Silva, E., Clayton, L., Gardano, L., Barrios-Rodiles, M., Wrana, J., Varelas, X., Arbouzova, N.I., Shaw, S., Saburi, S., et al. (2009). Phosphorylation of the Tumor Suppressor Fat Is Regulated by Its Ligand Dachsous and the Kinase Discs Overgrown. Current Biology *19*, 1112–1117. https://doi.org/10.1016/j.cub.2009.05.049.

Stelling, J., Sauer, U., Szallasi, Z., Doyle, F.J., and Doyle, J. (2004). Robustness of Cellular Functions. Cell *118*, 675–685. https://doi.org/10.1016/j.cell.2004.09.008.

Stephens, R., Lim, K., Portela, M., Kvansakul, M., Humbert, P.O., and Richardson, H.E. (2018). The Scribble Cell Polarity Module in the Regulation of Cell Signaling in Tissue Development and Tumorigenesis. Journal of Molecular Biology *430*, 3585–3612. https://doi.org/10.1016/j.jmb.2018.01.011.

Stringer, C., Wang, T., Michaelos, M., and Pachitariu, M. (2021). Cellpose: a generalist algorithm for cellular segmentation. Nat Methods *18*, 100–106. https://doi.org/10.1038/s41592-020-01018-x.

Su, T., Ludwig, M.Z., Xu, J., and Fehon, R.G. (2017). Kibra and Merlin Activate the Hippo Pathway Spatially Distinct from and Independent of Expanded. Developmental Cell *40*, 478-490.e3. https://doi.org/10.1016/j.devcel.2017.02.004.

Sun, S., Reddy, B.V.V.G., and Irvine, K.D. (2015). Localization of Hippo signalling complexes and Warts activation in vivo. Nature Communications *6*. https://doi.org/10.1038/ncomms9402.

Swanson, G.J., and Lewis, J. (1982). The timetable of innervation and its control in the chick wing bud. Joournal of Embryology and Experimental Morphology *71*, 121–137. .

Swarup, S., and Verheyen, E.M. (2012). Wnt/Wingless Signaling in Drosophila. Cold Spring Harbor Perspectives in Biology *4*, a007930–a007930. https://doi.org/10.1101/cshperspect.a007930.

Szymaniak, A.D., Mahoney, J.E., Cardoso, W.V., and Varelas, X. (2015). Crumbs3-Mediated Polarity Directs Airway Epithelial Cell Fate through the Hippo Pathway Effector Yap. Developmental Cell *34*, 283–296. https://doi.org/10.1016/j.devcel.2015.06.020.

Tabata, T., and Kornberg, T.B. (1994). Hedgehog Is a Signaling Protein with a Key Role in Patterning Drosophila lmaginal Discs. Cell *76*, 89–102. .

Tao, W., Zhang, S., Turenchalk, G.S., Stewart, R.A., St John, M.A.R., Chen, W., and Xu, T. (1999a). Human homologue of the Drosophila melanogaster lats tumour suppressor modulates CDC2 activity. Nat Genet *21*, 177–181. https://doi.org/10.1038/5960.

Tao, W., Zhang, S., Turenchalk, G.S., Stewart, R.A., St John, M.A.R., Chen, W., and Xu, T. (1999b). Human homologue of the Drosophila melanogaster lats tumour suppressor modulates CDC2 activity. Nat Genet *21*, 177–181. https://doi.org/10.1038/5960.

Tapon, N., Harvey, K.F., Bell, D.W., Wahrer, D.C., Schiripo, T.A., Haber, D.A., and Hariharan, I.K. (2002). Salvador promotes both cell cycle exit and apoptosis in Drosophila and is mutated in human cancer cell lines. Cell *110*, 467–478. .

Tepass, U. (2012a). The Apical Polarity Protein Network in *Drosophila* Epithelial Cells: Regulation of Polarity, Junctions, Morphogenesis, Cell Growth, and Survival. Annual Review of Cell and Developmental Biology *28*, 655–685. https://doi.org/10.1146/annurev-cellbio-092910-154033.

Tepass, U. (2012b). The Apical Polarity Protein Network in Drosophila Epithelial Cells: Regulation of Polarity, Junctions, Morphogenesis, Cell Growth, and Survival. Annual Review of Cell and Developmental Biology *28*, 655–685. https://doi.org/10.1146/annurev-cellbio-092910-154033.

Thompson, B.J., and Cohen, S.M. (2006). The Hippo Pathway Regulates the bantam microRNA to Control Cell Proliferation and Apoptosis in Drosophila. Cell *126*, 767–774. https://doi.org/10.1016/j.cell.2006.07.013.

Tokamov, S.A., Su, T., Ullyot, A., and Fehon, R.G. (2021). Negative feedback couples Hippo pathway activation with Kibra degradation independent of Yorkie-mediated transcription. ELife *10*, e62326. https://doi.org/10.7554/eLife.62326.

Tsoumpekos, G., Nemetschke, L., and Knust, E. (2018). Drosophila Big bang regulates the apical cytocortex and wing growth through junctional tension. Journal of Cell Biology *217*, 1033–1045. https://doi.org/10.1083/jcb.201705104.

Twitty, V.C., and Schwind, J.L. (1931). The growth of eyes and limbs transplanted heteroplastically between two species of Amblystoma. J. Exp. Zool. *59*, 61–86. https://doi.org/10.1002/jez.1400590105.

Udan, R.S., Kango-Singh, M., Nolo, R., Tao, C., and Halder, G. (2003). Hippo promotes proliferation arrest and apoptosis in the Salvador/Warts pathway. Nature Cell Biology *5*, 914–920. https://doi.org/10.1038/ncb1050.

Vasquez, C.G., Tworoger, M., and Martin, A.C. (2014). Dynamic myosin phosphorylation regulates contractile pulses and tissue integrity during epithelial morphogenesis. Journal of Cell Biology *206*, 435–450. https://doi.org/10.1083/jcb.201402004.

Visintin, R., and Amon, A. (2001). Regulation of the Mitotic Exit Protein Kinases Cdc15 and Dbf2. MBoC *12*, 2961–2974. https://doi.org/10.1091/mbc.12.10.2961.

Visintin, R., Craig, K., Hwang, E.S., Prinz, S., Tyers, M., and Amon, A. (1998). The Phosphatase Cdc14 Triggers Mitotic Exit by Reversal of Cdk-Dependent Phosphorylation. Molecular Cell *2*, 709–718. https://doi.org/10.1016/S1097-2765(00)80286-5.

Vollmer, J., Casares, F., and Iber, D. (2017). Growth and size control during development. Open Biol. *7*, 170190. https://doi.org/10.1098/rsob.170190.

Vrabioiu, A.M., and Struhl, G. (2015). Fat/Dachsous Signaling Promotes Drosophila Wing Growth by Regulating the Conformational State of the NDR Kinase Warts. Developmental Cell *35*, 737–749. https://doi.org/10.1016/j.devcel.2015.11.027.

Wada, K.-I., Itoga, K., Okano, T., Yonemura, S., and Sasaki, H. (2011). Hippo pathway regulation by cell morphology and stress fibers. Development *138*, 3907–3914. https://doi.org/10.1242/dev.070987.

van der Walt, S., Schönberger, J.L., Nunez-Iglesias, J., Boulogne, F., Warner, J.D., Yager, N., Gouillart, E., and Yu, T. (2014). scikit-image: image processing in Python. PeerJ *2*, e453. https://doi.org/10.7717/peerj.453.

Wang, S.-C., Low, T.Y.F., Nishimura, Y., Gole, L., Yu, W., and Motegi, F. (2017). Cortical forces and CDC-42 control clustering of PAR proteins for Caenorhabditis elegans embryonic polarization. Nat Cell Biol *19*, 988–995. https://doi.org/10.1038/ncb3577.

Wang, X., Zhang, Y., and Blair, S.S. (2019a). Fat-regulated adaptor protein Dlish binds the growth suppressor Expanded and controls its stability and ubiquitination. Proceedings of the National Academy of Sciences *116*, 1319–1324. https://doi.org/10.1073/pnas.1811891116.

Wang, X., Zhang, Y., and Blair, S.S. (2019b). Fat-regulated adaptor protein Dlish binds the growth suppressor Expanded and controls its stability and ubiquitination. Proceedings of the National Academy of Sciences 201811891. https://doi.org/10.1073/pnas.1811891116.

Wartlick, O., Mumcu, P., Kicheva, A., Bittig, T., Seum, C., Jülicher, F., and González-Gaitán, M. (2011). Dynamics of Dpp Signaling and Proliferation Control. Science *331*, 1154–1159. https://doi.org/10.1126/science.1200037.

Wee, B., Johnston, C.A., Prehoda, K.E., and Doe, C.Q. (2011). Canoe binds RanGTP to promote PinsTPR/Mud-mediated spindle orientation. Journal of Cell Biology *195*, 369–376. https://doi.org/10.1083/jcb.201102130.

Wei, S.-Y., Escudero, L.M., Yu, F., Chang, L.-H., Chen, L.-Y., Ho, Y.-H., Lin, C.-M., Chou, C.-S., Chia, W., Modolell, J., et al. (2005). Echinoid Is a Component of Adherens Junctions That Cooperates with DE-Cadherin to Mediate Cell Adhesion. Developmental Cell *8*, 493–504. https://doi.org/10.1016/j.devcel.2005.03.015.

Wei, X., Shimizu, T., and Lai, Z.-C. (2007). Mob as tumor suppressor is activated by Hippo kinase for growth inhibition in Drosophila. EMBO J *26*, 1772–1781. https://doi.org/10.1038/sj.emboj.7601630.

White, K.A., Grillo-Hill, B.K., Esquivel, M., Peralta, J., Bui, V.N., Chire, I., and Barber, D.L. (2018). β-Catenin is a pH sensor with decreased stability at higher intracellular pH. Journal of Cell Biology *217*, 3965–3976. https://doi.org/10.1083/jcb.201712041.

Wiersdorff, V., Lecuit, T., Cohen, S.M., and Mlodzik, M. (1996). Mad acts downstream of Dpp receptors, revealing a differential requirement for dpp signaling in initiation and propagation of morphogenesis in the Drosophila eye. Development *122*, 2153–2162. .

Winkelman, J.D., Anderson, C.A., Suarez, C., Kovar, D.R., and Gardel, M.L. (2020). Evolutionarily diverse LIM domain-containing proteins bind stressed actin filaments through a conserved mechanism. Proc. Natl. Acad. Sci. U.S.A. *117*, 25532–25542. https://doi.org/10.1073/pnas.2004656117.

Wodarz, A., Ramrath, A., Kuchinke, U., and Knust, E. (1999). Bazooka provides an apical cue for Inscuteable localization in Drosophila neuroblasts. Nature *402*, 544–547. https://doi.org/10.1038/990128.

Wu, S., Huang, J., Dong, J., and Pan, D. (2003). hippo encodes a Ste-20 family protein kinase that restricts cell proliferation and promotes apoptosis in conjunction with salvador and warts. Cell *114*, 445–456. .

Wu, S., Liu, Y., Zheng, Y., Dong, J., and Pan, D. (2008). The TEAD/TEF Family Protein Scalloped Mediates Transcriptional Output of the Hippo Growth-Regulatory Pathway. Developmental Cell *14*, 388–398. https://doi.org/10.1016/j.devcel.2008.01.007.

Xiao, G.-H., Beeser, A., Chernoff, J., and Testa, J.R. (2002). p21-activated Kinase Links Rac/Cdc42 Signaling to Merlin. Journal of Biological Chemistry *277*, 883–886. https://doi.org/10.1074/jbc.C100553200.

Xiao, L., Chen, Y., Ji, M., and Dong, J. (2011a). KIBRA Regulates Hippo Signaling Activity via Interactions with Large Tumor Suppressor Kinases. Journal of Biological Chemistry *286*, 7788–7796. https://doi.org/10.1074/jbc.M110.173468.

Xiao, L., Chen, Y., Ji, M., Volle, D.J., Lewis, R.E., Tsai, M.-Y., and Dong, J. (2011b). KIBRA Protein Phosphorylation Is Regulated by Mitotic Kinase Aurora and Protein Phosphatase 1. Journal of Biological Chemistry *286*, 36304–36315. https://doi.org/10.1074/jbc.M111.246850.

Xu, J., Vanderzalm, P.J., Ludwig, M., Su, T., Tokamov, S.A., and Fehon, R.G. (2018). Yorkie Functions at the Cell Cortex to Promote Myosin Activation in a Non-transcriptional Manner. Developmental Cell *46*, 271-284.e5. https://doi.org/10.1016/j.devcel.2018.06.017.

Xu, J., Su, T., Tokamov, S.A., and Fehon, R.G. (2019). Live Imaging of Hippo Pathway Components in Drosophila Imaginal Discs. In The Hippo Pathway, A. Hergovich, ed. (New York, NY: Springer New York), pp. 53–59.

Xu, T., Wang, W., Zhang, S., Stewart, R.A., and Yu, W. (1995). Identifying tumor suppressors in genetic mosaics: the Drosophila lats gene encodes a putative protein kinase. Development *121*, 1053–1063. .

Yan, Y., Denef, N., Tang, C., and Schupbach, T. (2011). Drosophila PI4KIIIalpha is required in follicle cells for oocyte polarization and Hippo signaling. Development *138*, 1697–1703. https://doi.org/10.1242/dev.059279.

Yang, L., Paul, S., DuBois-Coyne, S., Kyriakakis, P., and Veraksa, A. (2017). Medium-scale Preparation of Drosophila Embryo Extracts for Proteomic Experiments. JoVE 55804. https://doi.org/10.3791/55804.

Yang, S., Zhang, L., Liu, M., Chong, R., Ding, S.-J., Chen, Y., and Dong, J. (2013). CDK1 Phosphorylation of YAP Promotes Mitotic Defects and Cell Motility and Is Essential for Neoplastic Transformation. Cancer Res *73*, 6722–6733. https://doi.org/10.1158/0008-5472.CAN-13-2049.

Yee, W.B., Delaney, P.M., Vanderzalm, P.J., Ramachandran, S., and Fehon, R.G. (2019). The CAF-1 complex couples Hippo pathway target gene expression and DNA replication. MBoC *30*, 2929–2942. https://doi.org/10.1091/mbc.E19-07-0387.

Yi, C., Troutman, S., Fera, D., Stemmer-Rachamimov, A., Avila, J.L., Christian, N., Persson, N.L., Shimono, A., Speicher, D.W., Marmorstein, R., et al. (2011). A Tight Junction-Associated Merlin-Angiomotin Complex Mediates Merlin's Regulation of Mitogenic Signaling and Tumor Suppressive Functions. Cancer Cell *19*, 527–540. https://doi.org/10.1016/j.ccr.2011.02.017.

Yin, F., Yu, J., Zheng, Y., Chen, Q., Zhang, N., and Pan, D. (2013). Spatial Organization of Hippo Signaling at the Plasma Membrane Mediated by the Tumor Suppressor Merlin/NF2. Cell *154*, 1342–1355. https://doi.org/10.1016/j.cell.2013.08.025.

Yoshihama, Y., Sasaki, K., Horikoshi, Y., Suzuki, A., Ohtsuka, T., Hakuno, F., Takahashi, S.-I., Ohno, S., and Chida, K. (2011). KIBRA Suppresses Apical Exocytosis through Inhibition of aPKC Kinase Activity in Epithelial Cells. Current Biology *21*, 705–711. https://doi.org/10.1016/j.cub.2011.03.029.

Yu, F.-X., and Guan, K.-L. (2013). The Hippo pathway: regulators and regulations. Genes & Development *27*, 355–371. https://doi.org/10.1101/gad.210773.112.

Yu, J., and Pan, D. (2018). Validating upstream regulators of Yorkie activity in Hippo signaling through *scalloped* -based genetic epistasis. Development *145*, dev157545. https://doi.org/10.1242/dev.157545.

Yu, F., Morin, X., Cai, Y., Yang, X., and Chia, W. (2000). Analysis of partner of inscuteable, a Novel Player of Drosophila Asymmetric Divisions, Reveals Two Distinct Steps in Inscuteable Apical Localization. Cell *100*, 399–409. https://doi.org/10.1016/S0092-8674(00)80676-5.

Yu, J., Zheng, Y., Dong, J., Klusza, S., Deng, W.-M., and Pan, D. (2010). Kibra Functions as a Tumor Suppressor Protein that Regulates Hippo Signaling in Conjunction with Merlin and Expanded. Developmental Cell *18*, 288–299. https://doi.org/10.1016/j.devcel.2009.12.012.

Yue, T., Tian, A., and Jiang, J. (2012). The Cell Adhesion Molecule Echinoid Functions as a Tumor Suppressor and Upstream Regulator of the Hippo Signaling Pathway. Developmental Cell *22*, 255–267. https://doi.org/10.1016/j.devcel.2011.12.011.

Zhang, L., and Ward, R.E. (2011). Distinct tissue distributions and subcellular localizations of differently phosphorylated forms of the myosin regulatory light chain in Drosophila. Gene Expression Patterns *11*, 93–104. https://doi.org/10.1016/j.gep.2010.09.008.

Zhang, Q., Zhang, L., Wang, B., Ou, C.-Y., Chien, C.-T., and Jiang, J. (2006). A Hedgehog-Induced BTB Protein Modulates Hedgehog Signaling by Degrading Ci/Gli Transcription Factor. Developmental Cell *10*, 719–729. https://doi.org/10.1016/j.devcel.2006.05.004.

Zhang, Y., Wang, X., Matakatsu, H., Fehon, R., and Blair, S.S. (2016). The novel SH3 domain protein Dlish/CG10933 mediates fat signaling in Drosophila by binding and regulating Dachs. ELife *5*, e16624. https://doi.org/10.7554/eLife.16624.

Zhao, B., Wei, X., Li, W., Udan, R.S., Yang, Q., Kim, J., Xie, J., Ikenoue, T., Yu, J., Li, L., et al. (2007). Inactivation of YAP oncoprotein by the Hippo pathway is involved in cell contact inhibition and tissue growth control. Genes Dev. *21*, 2747–2761. https://doi.org/10.1101/gad.1602907.

Zhao, B., Li, L., Tumaneng, K., Wang, C.-Y., and Guan, K.-L. (2010). A coordinated phosphorylation by Lats and CK1 regulates YAP stability through SCF $^{\beta\text{-TRCP}}$. Genes Dev. *24*, 72–85. https://doi.org/10.1101/gad.1843810.

Zheng, N., and Shabek, N. (2017). Ubiquitin Ligases: Structure, Function, and Regulation. Annu. Rev. Biochem. *86*, 129–157. https://doi.org/10.1146/annurev-biochem-060815-014922.

Zheng, Y., and Pan, D. (2019a). The Hippo Signaling Pathway in Development and Disease. Developmental Cell *50*, 264–282. https://doi.org/10.1016/j.devcel.2019.06.003.

Zheng, Y., and Pan, D. (2019b). The Hippo Signaling Pathway in Development and Disease. Developmental Cell *50*, 264–282. https://doi.org/10.1016/j.devcel.2019.06.003.

Zheng, Y., Liu, B., Wang, L., Lei, H., Pulgar Prieto, K.D., and Pan, D. (2017). Homeostatic Control of Hpo/MST Kinase Activity through Autophosphorylation-Dependent Recruitment of the STRIPAK PP2A Phosphatase Complex. Cell Reports *21*, 3612–3623. https://doi.org/10.1016/j.celrep.2017.11.076.

Zhou, P.-J., Xue, W., Peng, J., Wang, Y., Wei, L., Yang, Z., Zhu, H.H., Fang, Y.-X., and Gao, W.-Q. (2017). Elevated expression of Par3 promotes prostate cancer metastasis by forming a Par3/aPKC/KIBRA complex and inactivating the hippo pathway. Journal of Experimental & Clinical Cancer Research *36*. https://doi.org/10.1186/s13046-017-0609-y.